CUCURBIT[n]URIL HOST-GUEST COMPLEXES: THE EFFECTS OF INCLUSION ON THE CHEMICAL REACTIVITY AND SPECTROSCOPIC PROPERTIES OF AROMATIC GUEST MOLECULES

by

RUIBING WANG

A thesis submitted to the Department of Chemistry
in conformity with the requirements for
the degree of Doctor of Philosophy

Queen's University

Kingston, Ontario, Canada

August 2007

DEDICATION

This thesis is dedicated to the memory of my father Guangyou Wang, 1952-1999. Dad, I wish you could be here so we could celebrate and enjoy together the achievement that the thesis represents.

ABSTRACT

This thesis deals primarily with supramolecular chemistry based on cucurbit[*n*]uril (CB[*n*], *n* = 7 and 8) host molecules. The research has been focused on the synthesis and characterization of host-guest complexes CB[*n*] with aromatic guest molecules, and the study of the effects of the host-guest complexation on the chemical reactivity and spectroscopic properties of the included guests, such as their photoreactivity and their UV-visible absorption and emission properties, in aqueous solution.

The [4+4] photodimerization of protonated 2-aminopyridine (APH^+) occurs stereoselectively to give the *anti-trans* product as the result of a preferred orientation of two APH^+ guests in the cavity of CB[7]. The CB[7] host inhibits photohydration in the course of the photoisomerizations of protonated *trans*-1,2-bis(4-pyridyl)ethylene and *trans*-1,2-bis(1-methyl-4-pyridinium)ethylene by including the (4-pyridyl)ethylene portion of the guest, while this is not observed with *trans*-1,2-bis(1-hexyl-4-pyridinium)ethylene, as preferential inclusion of the hexyl groups leaves the vinyl group vulnerable to photohydration. Very strong CB[7] complexation of (*E*)-1-ferrocenyl-2-(1-methyl-4-pyridinium)ethylene completely inhibits the (*E*)→(*Z*) photoisomerization process.

The H/D exchange rates and acidities of the C(2)-proton of cationic imidazolium and thiazolium (including thiamine and thiamine phosphates) carbon acids are decreased

upon their complexation with CB[7]. Inclusion of protonated aromatic amines (and aromatic alcohols) in the cavity CB[7] significantly decreases their ground and excited state acidities, such that the emission is switched from the neutral amine to the protonated amine excited state, resulting in changes in the color of fluorescence. The fluorescence of acridizinium cations can be switched off by the formation of 2:1 complexes with CB[8] and then switched back on again by the addition of CB[7] or a competing guest molecule.

The stabilization of the deep blue color of the 4,4'-bis(dimethylamino)diphenyl carbonium ion, upon complexation of the corresponding carbinol with CB[7], results from a complexation-induced shift in the carbinol/carbonium ion equilibrium. A dramatic purple to blue color change in pinacyanol chloride upon addition of CB[7] is due to a partial breakup of dye aggregates, upon the interactions of the dye with the host molecule. The CB[*n*] complexation-induced emission and/or absorption color switch have the potential to be employed in molecular switches and in chemical sensing.

ACKNOWLEDGEMENT

First and foremost I would like to express my sincere appreciation to my research supervisor, Prof. Donal H. Macartney. It would have been impossible for me to accomplish the work without his kindest guidance, support, encouragement, and patience. I consider it a great privilege to have been his student, and I would like to take this opportunity to offer my deepest gratitude for everything he has done for me and I wish him all the best in the coming years.

I would like to have special thanks to my Ph.D. committee members, Prof. Suning Wang and Prof. Simon Hesp, for their advice on my research and the precious time they have shared with me through my Ph.D. studies. I gratefully thank Dr. Francoise Sauriol for her help on the topic of NMR spectroscopy, and Dr. Bernd Keller and Jessie Sui for their time and help with the MS characterization and interpretation. Prof. Natalie Cann and my buddy Shihao Wang are thanked for their assistance with the computational calculations of the energy-minimized structures that this thesis has dealt with.

I have received great support, love, encouragement and companionship from Lina Yuan in both my personal life and academic study during the past few years. I thank her from the bottom of my heart and wish her very well now and in the future. My colleague Ian Wyman is greatly appreciated for his helpful discussion on my research and the friendship he has offered to me. Saroja Hettiarachchi is also thanked for her

fellowship in the lab. I am also grateful to Annette Keyes for her time and kindness with the paperwork I have been through during the past four years at Queen's.

I thank my mother, Guangfang Cao, and my sister, Ruiling Wang, for their love, and support and encouragement for my study in Canada. Sincere and special thanks go to my beloved wife, Xue Wang, for her unconditional love, continuous support and understanding for what I am doing and what I want to do, and also thank her for her help on formatting the thesis.

Last but not the least, Queen's University and NSERC Canada are acknowledged for funding the research presented in this thesis.

STATEMENT OF ORIGINALITY

All work presented herein was performed by the author under the supervision of Professor Donal H. Macartney at Queen's University, except for the experiments of the kinetic measurements of (*E*)-1-ferrocenyl-2-(1-methyl-4-pyridinium)ethylene cation in the absence and in the presence of cucurbit[7]uril (CB[7]) host molecules, which were carried out by the author and Dr. Donal H. Macartney, the synthesis of the cucurbit[7]uril host molecule, which was carried out by both the author and Lina Yuan, and the energy-minimized structures calculations which were carried out with the assistance of Shihao Wang.

TABLE OF CONTENTS

LIST OF ABBREVIATIONS

IUPAC	International Union of Pure and Applied Chemistry
(*E*)-$BHPE^{2+}$	*trans*-1,2-bis(1-hexyl-4-pyridinyl)ethylene
(*E*)-$BMPE^{2+}$	*trans*-1,2-bis(1-methyl-4-pyridinyl)ethylene
1,8-ANS	1-anilino-8-naphthalene sulfonate
1-AAH^{+}	protonated 1-aminoanthracene
1-$APRH^{+}$	protonated 1-aminopyrene
1-$NTAH^{+}$	protonated 1-aminonaphthalene
2,6-TNS	2-*p*-toluidinylnaphthalene-6-sulfonate
2-AA	2-aminoanthracene
2-AAH^{+}	protonated 2-aminoanthracene
2-$NTAH^{+}$	protonated 2-aminonaphthalene
Å	Ångstrom
AA	aromatic amine
$AADZ^{+}$	9-aminoacridizinium
AAH^{+}	protonated aromatic amine
Ac^{-}	acetate ion
ADZ^{+}	acridizinium
APH^{+}	protonated 2-aminopyridine

BDC^{+}	4,4’-bis(dimethylamino)diphenyl carbonium
$BDCH^{2+}$	protonated 4,4’-bis(dimethylamino)diphenyl carbonium
BDC-OH	4,4’-bis(dimethylamino)diphenyl carbinol
BHP-ethanol	1,2-bis(1-hexyl-4-pyridinyl)ethanol
$BIAD^{2+}$	1,3-bis(4,5-dihydro-1*H*-imidazol-2-yl)adamantane
$BMIX^{2+}$	3,3’-bis(1-methylimidazolium)-*p*-xylene
BMP-ethanol	1,2-bis(1-methyl-4-pyridinyl)ethanol
BP-ethanol	1,2-bis(4-pyridinyl)ethanol
BTX^{2+}	3,3’-bis(thiazolium)-*p*-xylene
CB[n]	cucurbit[n]uril
CD	cyclodextrin
COSY	Correlation Spectroscopy
Cp^{-}	cyclopentadienyl
CT	Charge Transfer
δ	chemical shift
d	doublet
$DADAT^{2+}$	4,8-diamino-3,7-diazatricyclo[4.2.2.$2^{2,5}$]dodeca-3,7,9,11-tetraene
$DIC4^{2+}$	3,3’-bis(1-methylimidazolium)-1,4-butane
$DIC6^{2+}$	3,3’-bis(1-methylimidazolium)-1,6-hexane
$DIC8^{2+}$	3,3’-bis(1-methylimidazolium)-1,8-octane
$dipic^{2-}$	2,6-pyridinedicarboxylate

DMRI	all-*trans* N,N-dimethylretinylideneiminium
DMSO	dimethyl sulfoxide
DNA	Deoxyribonucleic acid
E	molar absorptivity coefficient
ESI-MS	Electrospray Ionization Mass Spectrometry
F	emission intensity
$FcMPE^{+}$	1-ferrocenyl-2-(1-methyl-4-pyridinium)ethylene
FT	Fourier Transformation
G1	Guest 1
G2	Guest 2
Gly	glycine
H	Host
H_2BPE^{2+}	1,2-bis(4-pyridinium)ethylene
HPLC	High Performance Liquid Chromatography
hr	hour
Hz	hertz
I	proton integration
$IC4^{+}$	1-methyl-3-butylimidazolium
$IC6^{+}$	1-methyl-3-hexylimidazolium
$IC8^{+}$	1-methyl-3-octylimidazolium
ILCT	Intraligand Charge Transfer

J	coupling constant
Leu	leucine
λ_{max}	wavelength maximum
M	Molar (mole/litre)
m	multiplet
m.p.	melting point
m/z	mass to charge ratio
$Me_{10}CB[5]$	decamethylcucurbit[5]uril
Me_2DAP^{2+}	2,7-dimethyldiazapyrenium dication
mg	milligram
MHz	megahertz
mL	milliliter
MLCT	Metal-to-Ligand Charge Transfer
mV	millivolt
MV^{2+}	methylviologen (1,1'-dimethyl-4,4'-bipyridinium)
NHC	N-heterocyclic carbene
NHE	Normal Hydrogen Electrode
nm	nanometer
PC	pinacyanol chloride
Phe	phenylalanine
ppm	parts per million

q	quartet
qn	quintet
R	reaction progress or gas constant
S	singlet or second
t	triplet
TH	thiamine hydrochloride
THF	tetrahydrofuran
TM	thiamine monophosphate
TP	thiamine pyrophosphate
Trp	tryptophan
UV	Ultraviolet

LIST OF TABLES

LIST OF FIGURES

Chapter 1

INTRODUCTION

This chapter begins with a general introduction to supramolecular chemistry, and host-guest chemistry and its applications, followed by a brief illustration of several of the most popular macrocyclic host molecules. Thereafter, a detailed introduction to the family of cucurbituril molecules is presented and their functions as supramolecular hosts are discussed.

1.1 Supramolecular Chemistry

Supramolecular chemistry has been defined as simple as "chemistry beyond the molecule" by Nobel Prize laureate Jean-Marie Lehn.[1,2] Whereas traditional molecular chemistry involves atoms connecting together or breaking apart through covalent bonds, supramolecular chemistry deals with noncovalent interactions between molecules.

These include attractive and repulsive intermolecular forces, such as van der Waals forces (including dipole-dipole), hydrophobic interactions, electrostatic interactions, hydrogen bonding, and π-π stacking. Supramolecular chemistry is a highly interdisciplinary research field which covers aspects of chemistry, physics, biology and materials science, as the complex chemical species involved in these areas are often brought together or assembled/organized via intermolecular forces. These intermolecular forces are the glue which holds molecules together and therefore they play crucial roles in building up supramolecular structures. In order to highlight the importance of these intermolecular interactions, the definitions of these forces are generalized below.[3,4]

1.1.1 The Glue of Supramolecular Chemistry: Intermolecular Forces

1.1.1.1 van der Waals Forces

van der Waals interactions are a collective group of long range inductive and dispersive intermolecular forces, which arise from the temporary or permanent polarization of molecules into dipoles (or multipoles).[3] The term "van der Waals" is named after Johannes Diderik van der Waals who is the first scientist to document this type of forces. van der Waals forces are divided into two categories: dispersion forces (also known as London forces) and dipole-dipole interactions, considering that dispersion forces result from the temporary fluctuations of dipoles of molecules and dipole-dipole interactions are attributed to the permanent molecular dipoles. The term "London

forces" is named after Fritz London who first suggested where these forces might come from. These forces between molecules are much weaker than the covalent bonds within molecules, however the total collective contribution to complex formation can be dramatic.

1.1.1.2 Hydrophobic Interactions

Hydrophobic interactions, according to IUPAC terminology,[4] are the tendencies of lipophilic hydrocarbon groups to form intermolecular aggregates in aqueous or other protic media (polar), which often refers to the physical properties of non-polar molecules repelled by an amount of aqueous or protic solvent. This interaction is sometimes driven by the tendency of the protic (polar) solvent molecules to interact with the polar part of the molecules to form the most stable hydrogen-bonded networks. Hydrophobic interactions play very important roles in recognition and folding of biomolecules, e.g. hydrophobic forces are considered to be the major driving forces for the folding of globular proteins in nature.[5] This type of intermolecular force is also very crucial in supramolecular systems, especially in the building up of organic host-guest complexes, e.g. the inclusion of hydrophobic guests (or hydrophobic portions of guest molecules) into the hydrophobic cavities of hosts such as cyclodextrins and cucurbiturils.

1.1.1.3 Electrostatic Interactions

Electrostatic interactions are Coulombic forces between charged species, such as

ion-ion interactions.[3] This type of interaction however, can also occur between ions and molecules with dipole moments, and actually both ion-ion and ion-dipole interactions are electrostatic forces in Nature (please note that dipole-dipole interactions are categorized with van der Waals forces). This type of intermolecular forces can be either attractive or repulsive, depending on the nature of the interacting charges. Two positively-charged species, for example, repel each other, while a positively-charged and a negatively-charged ion are attracted to one another. Electrostatic interactions tend to be relatively strong, and the magnitude of the forces can be estimated from Coulomb's law. They often contribute the most in stabilizing or destabilizing supramolecular complexes and play very important roles in molecular self-assembly and recognition.

1.1.1.4 Hydrogen Bonding

Hydrogen bonding is another type of relatively strong intermolecular force. It is often stronger than van der Waals interactions, but weaker than ion-ion interactions. A hydrogen bond (H-bond) is a special type of attractive interaction (can be considered as a variation of a dipole-dipole interaction or a special type of electrostatic interaction) between an electronegative atom on one molecule (H-acceptor, abbreviated A) and a hydrogen atom covalently bonded to another electronegative atom on another molecule (H-donor, abbreviated D).[3] The hydrogen is attached directly to one of the most electronegative elements such as O or N, causing the hydrogen to acquire a significant amount of positive charge. Each element to which the hydrogen is attached through a

H-bond is not only significantly negative, but also has at least one "active" lone pair so that the polarized hydrogen can strongly attach to the lone pair as if they were co-ordinated. Hydrogen bonding can occur either between molecules (intermolecularly), or within different parts of a single molecule (intramolecularly).[4]

1.1.1.5 π-π Stacking

The term π-π stacking refers to a stacked arrangement of aromatic molecules, which works through interactions between the aromatic portions of these molecules. The most popular example of π-π stackings is found in the DNA double helix, which dramatically stabilize the DNA through vertical consecutive base pair interactions. Stacking has been frequently used in synthetic supramolecular systems,[6] although the nature of the interactions is still a matter of debate. Previous popular explanations for π-π stackings included electron donor-acceptor[7] and solvophobic effects,[8] however, neither of these explanations is completely satisfactory for mapping out the nature of the π-π interactions. It is more and more generally agreed that π-π stackings are electrostatic interactions that are weak in nature.[9] There are generally two types of π-π stacking interactions: face-to-face and edge-to-face. The stackings which stabilizes the double helix in DNA are the face-to-face type. Edge-to-face interactions may be considered as weak forms of hydrogen bonding between the electron-rich π cloud of one aromatic ring and slightly electron-deficient hydrogen atoms of another aromatic ring. Examples of the edge-to-face stackings include the herringbone packing in the crystal structures of a

range of small aromatic hydrocarbons, such as benzene.[10]

Important concepts that have been demonstrated in supramolecular chemistry, based on these non-covalent forces, include molecular self-assembly, molecular recognition, host-guest chemistry, and mechanically-interlocked molecular architectures. These concepts are not independent from each other and are often interrelated to one another. As the research in this thesis mainly involves the principles of host-guest chemistry, the concept of host-guest chemistry and its applications will be introduced in detail next.

1.1.2 Host-Guest Chemistry

1.1.2.1 Definition and Concept

In a general definition of a host-guest complex, we generally consider a molecule (a host, H) binding another molecule (as a guest, G) to produce the so-called "host-guest" complex or supramolecular structure. According to Cram, the host component is generally defined as an organic molecule or ion or aggregate whose binding sites converge in the complex, and the guest component is defined as any molecule or ion whose binding sites diverge in the complex.[9,11] Very often, the host-guest chemistry refers to complexation or molecular recognition between a large molecule or complex (the host) that contains a pocket, and a relatively small molecule (the guest) which is able to sit in the pocket.

The criteria for host-guest complexation are both electronic and spatial complementarities.[12] The basic drawing forces for pulling two species together are

complementary functional groups (or atoms) on the two entities, interacting with each other through intermolecular forces such as hydrogen bonding and ion-ion interactions --- this is called electronic complementary. In other words, electronic complementary requires that binding sites on both host and guest are compatible in terms of their electron density distributions.[3,13] In addition to electronic complementarity, a structural (spatial) complementarity, known as the physical requirement for "lock-and-key" principle,[14] is very necessary in supramolecular host-guest complexation. That is, the host and guest should geometrically fit to each other. For example, two positively-charged species repelling each other can't bind together to form a supramolecular complex (not complementary electronically), and a host molecule with a very small cavity couldn't encapsulate a guest molecule whose size is larger than the host cavity (not complementary spatially). Electronic and structural complementarities have to work collaboratively according to the "lock-and-key" principle.[13,14] Complexation will be most efficient when both the shapes and arrangements of binding sites in host and guest molecules match each other.[15]

1.1.2.2 Classifications of Host Molecules

Host-guest complexes can basically be classified into three general categories: cavitates, tweezer complexes and clathrates, based on the difference of the cavities of host molecules involved in host-guest complexation.

Cavitates are supramolecular host-guest complexes based on cavitands, and cavitands

are natural or synthetic receptors with enforced cavities and open ends, originally defined and then developed by Cram.[11,16] "Enforced cavity" implies a preorganized molecular cavity, and therefore cavitands are often macrocyclic compounds, whilst "open end" requires that the molecular container has at least one open end for the entrance of a guest molecule. The most common examples of cavitands include cyclodextrins, calixarenes, and cucurbiturils. Porphyrins and crown ethers can also be added to this category, considering the fact that they both are macrocyclic hosts with preorganized cavities and open ends. As the cavities of cavitands are preorganized, they often are relatively rigid and have better selectivity/recognition for guest molecules with specific size/shape and electronic complementarities. The complexes of cavitates are often very stable due the fit between "preorganized" cavities and included guests.

Tweezer complexes are host-guest complexes based on molecular tweezers (sometimes referred to as molecular clips) that are noncyclic compounds with open cavities capable of binding guests. The noncyclic open cavities of molecular clips are often flexible, with a lack of binding selectivity, as they can accommodate guest molecules with a variety of sizes. Examples of tweezer complexes are numerous, including complexes based on molecular clips derived from glycoluril.[17,18]

Clathrates are host-guest complexes formed between guests and clathrands that are aggregates of two or more molecules with cavities formed between molecules.[19] Alternatively speaking, a clathrate is a supramolecular architecture comprising of a lattice of a type of molecule (the group of molecules together act as a host, with pockets

in the lattice), with another type of molecule (guest) trapped in the lattice. Clathrates mostly exist in the solid phase or at very high concentration in solution phase, which limits the applications of clathrands as hosts in the intensive study of supramolecular chemistry in solution. Numerous liquid and solid crystals are inclusion complexes of clathrates, some of which have been reviewed in detail.[19,20]

In all three types of supramolecular host-guest complexes, the physical and chemical properties of the guests are often altered upon encapsulation into the cavities of host molecules. Sometimes, controlled complexation-decomplexation can be achieved and novel functionalities, such as switching or shuttling are exhibited in the complexes. Supramolecular host-guest chemistry, therefore, has a high potential to be employed in applications in many areas, such as catalysis, molecular-level switches and machines, sensors, drug delivery, self-assembly for fabrication of functional nanocomposites, and the extraction and separation of mixtures.

1.1.3 Applications and Perspectives

The field of supramolecular host-guest chemistry has become relatively mature since it has been intensively studied for several decades.[1] It has been applied extensively in many areas, and these applications include, but are not limited to, the following topics.

1.1.3.1 Supramolecular Catalysts and Inhibitors

Host molecules can often work as catalysts or inhibitors for selected organic reactions.

The reactants (guest molecules) may be bound by host molecules in such a way that the reactants are pulled together and labile groups are placed in close proximity. The reaction is thus sped up and very often the reaction becomes more selective. For example, the photodimerization of 2-anthracenecarboxlic acid is catalyzed by cyclodextrin host molecules, and both the rate and stereoselectivity are dramatically enhanced.[21] Guest molecules might also be protected from reactions and are therefore stabilized by host molecules upon complexation. Kim *et al.* have demonstrated that a *cis*-stilbene derivative is dramatically stabilized with respect to photoisomerization upon its inclusion into the cavity of cucurbit[7]uril (CB[7]).[22] A second type of supramolecular catalyst can occur, such that the actual reaction catalyst is encapsulated in a host molecule. Potassium permanganate, for example, is pulled (phase transferred) from aqueous solution into non-polar reaction media (giving "purple benzene", for example) by 18-crown-6 to catalyze organic reactions in organic solvent (Figure 1.1).[23]

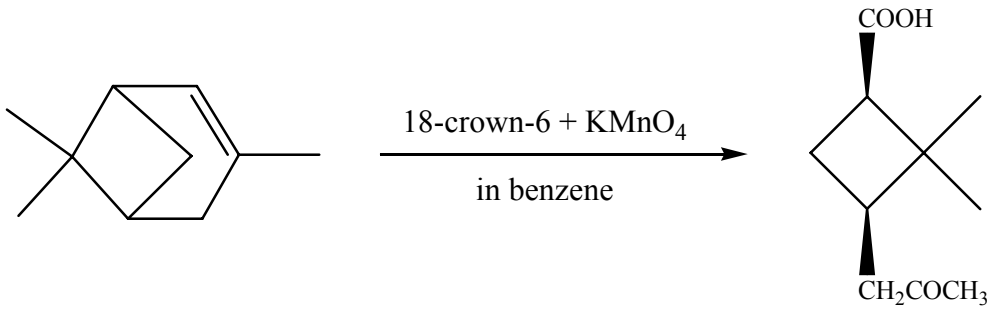

Figure 1.1 Schematic display of an oxidation reaction by 18-crown-6 complexed $KMnO_4$ in an organic solvent ("purple benzene").[23]

1.1.3.2 Molecular Machines

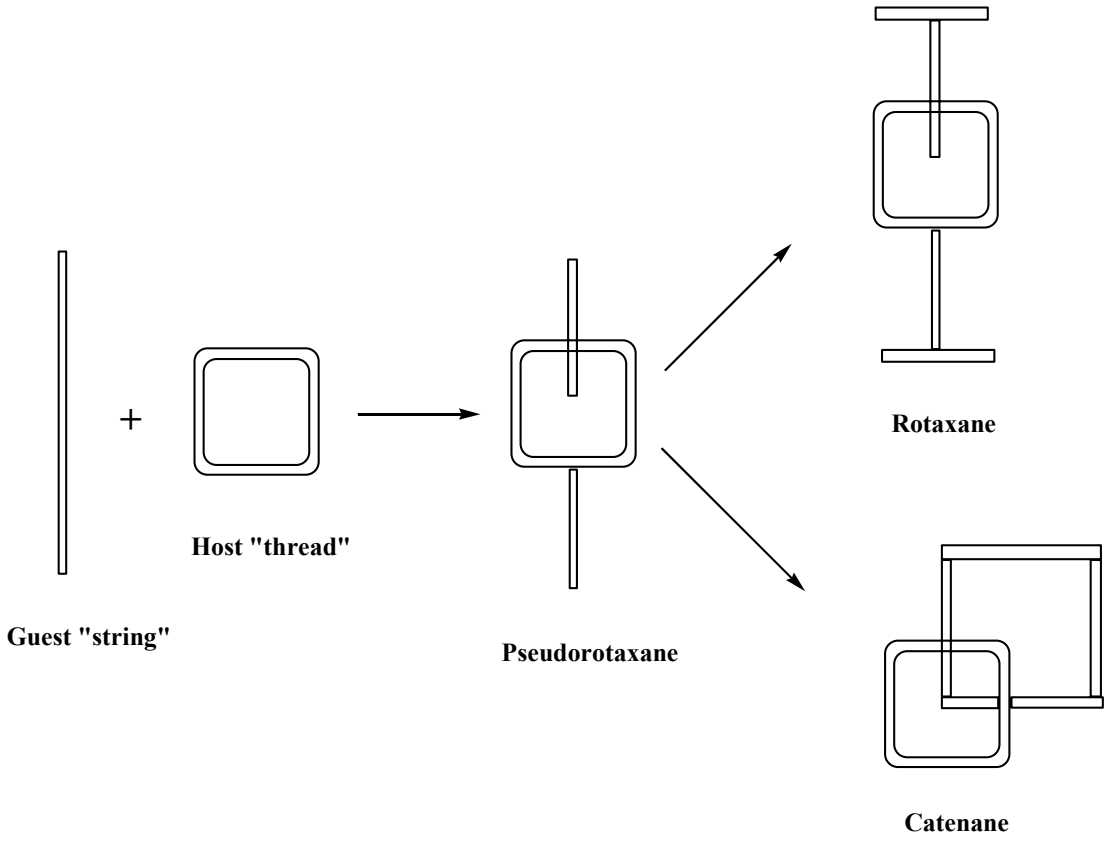

Figure 1.2 Schematic illustration of pseudorotaxane formation and thereafter the preparations of a rotaxane and a catenane.

Before molecular machines are introduced, the basic concepts of rotaxanes, pseudorotaxanes, and catenanes have to be described.[4] A rotaxane is an interlocked molecular architecture in which a dumbbell-shaped molecule is threaded through and enclosed by a macrocyclic ring. The two components are kinetically trapped as the two bulky end-groups (often called stoppers or physical barriers) of the dumbbell are too

large for the macrocyclic ring to dissociate (dethread) from the axile. Rotaxanes without such two bulky ending-groups, in which the macrocyclic ring can slip out of the axle (thread), are termed pseudorotaxanes. A catenane is a mechanically-interlocked molecular complex having two or more interlocked macrocyclic rings connected in a manner of links of chain. The trapped macrocyclic rings can't dissociate from each other without breaking the covalent bonds of the macrocycles. Pseudorotaxanes are frequently necessary precursors to both rotaxanes and catenanes (Figure 1.2).

A molecular-level machine can be defined as an assembly of multiple molecular components (often through supramolecular interactions) designed to perform mechanical movements under the control of an external stimulus.[24] Molecular machines represent the currently smallest mechanically-movable machines. Known examples of molecular machines include nondegenerate rotaxanes, nondegenerate catenanes, as well as controlled threading/dethreading pseudorotaxanes (Figure 1.3). All three components demonstrated in Figure 1.3 are supramolecular complexes based on macrocyclic host molecules. Control of the motions of the components in those systems has been introduced and the machines can often be powered by chemical, electrochemical, or light energy. Controlled machine motion changes result in a change of the chemical/physical properties, which produce a signal that allows the operation of the machine to be monitored. Under these principles, a number of molecular machines have been designed, and artificial molecular machines capable of performing logic operations have already been reported.[24,25]

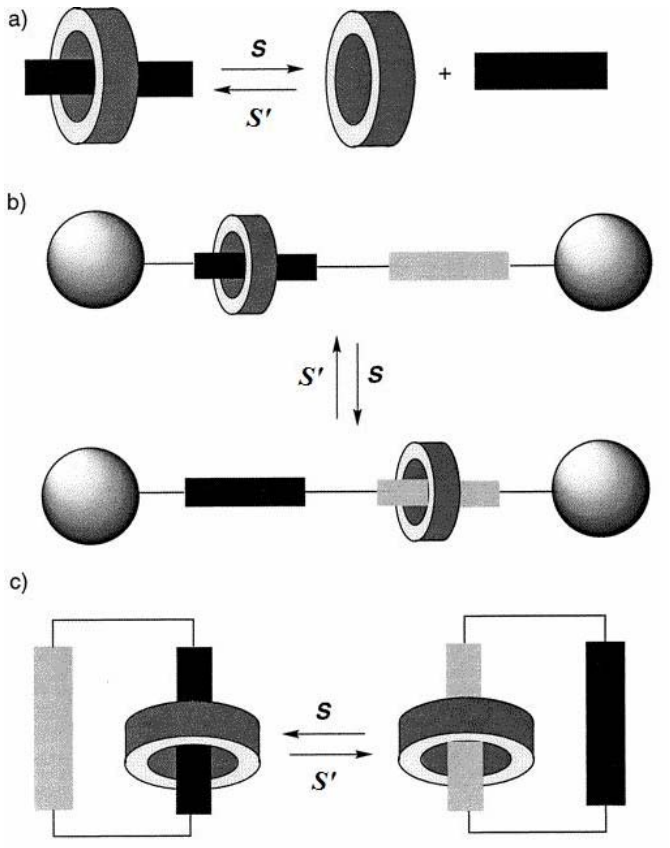

Figure 1.3 Molecular machines based on (a) a pseudorotaxane, (b) a rotaxane, and (c) a catenane. S and S' are the external stimuli.[24]

1.1.3.3 Molecular Sensors

A molecular sensor is a molecule or composite (often molecular receptor) that is able to recognize an analyte to produce a detectable signal.[26] Molecular sensors combine molecular recognition with some form of reporter (or referred to as indicator) so the presence of the guest can be reported by some chemical or physical means.[27] Therefore,

a sensing molecule or a complex often needs to bear a binding site and a reporter group which has electrochemical or spectroscopic properties that can be altered by the proximate host-guest complexation (a receptor-spacer-reporter model, see Figure 1.4).[28]

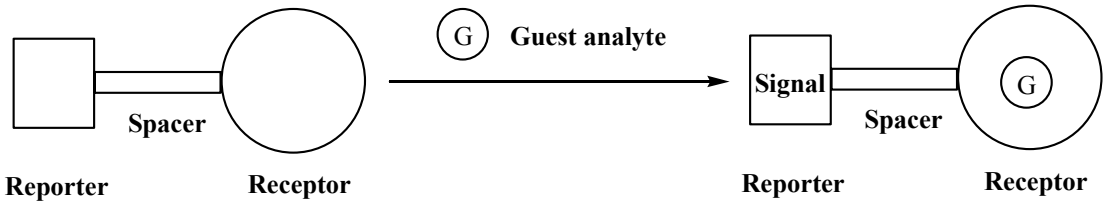

Figure 1.4 Molecular sensor based on a receptor-spacer-reporter model. The reporter senses and reports the presence of guest species complexed by the receptor.

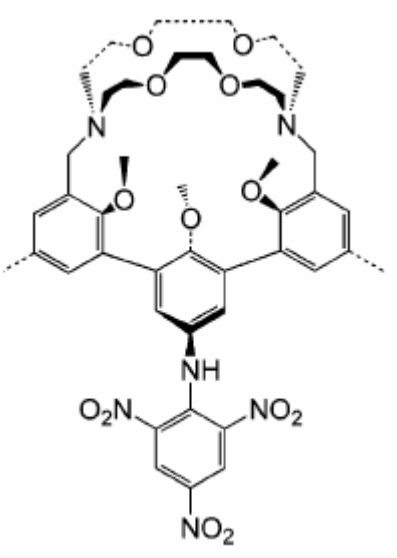

Figure 1.5 The selective complexation of K^+ induces an absorbance change in the attached reporting chromophore group.[29]

One of the first examples of molecular sensors utilizing a macrocyclic receptor was

reported by Cram,[29,30] in which the reporter, a modified crown ether (Figure 1.5), can selectively sense the presence of the potassium ion, and can be used in an analytical assay. A separate reporter is sometimes not required, as the encapsulation of some guests can alter the guest molecule's spectroscopic properties. For example, a simple calix[4]arene host has been employed to sense NO_2/N_2O_4 gas molecules.[31]

With the increasing interest in the design and construction of molecular sensors and the application of the sensing principles into the analytical world, the term "supramolecular analytical chemistry" has been recently introduced by Anslyn to describe the application of molecular sensors to analytical chemistry.[32]

1.1.3.4 Drug Delivery and Controlled Release

The primary purpose of the employment of drug delivery systems is to deliver proper amounts of drug to the targeted site stably, precisely and efficiently,[33] and once the drug is delivered to the site it can ideally be released continually for a prolonged time period and in a controlled manner (such that a high dose doesn't need to be repeated). A drug carrier therefore is playing the role of enhancing stability, water-solubility, and biocompatibility, and releasing drugs in a controlled manner. Some of the macrocyclic host molecules, such as cyclodextrins, are ideal to act in such roles, due to their ability to solubilize, stabilize, and to thread/dethread guest molecules through the formation of inclusion complexes.[34] In order to extend the physiochemical properties and recognition properties of natural cyclodextrins, various cyclodextrin derivatives have

been designed, prepared and tested as novel drug carriers.[35] In addition to cyclodextrins, other macrocyclic molecules, such as parent and derivatized cucurbiturils are also being employed for drug delivery and controlled release.[36] Supramolecular host-guest chemistry has been developed into the medical research area, especially in the pharmaceutical design and drug delivery and controlled release.

1.1.3.5 Separation of Mixtures

One of the most stimulating features of supramolecular host-guest chemistry is guest selectivity, by which the hosts recognize and bind strongly with specific guest species. The complexation selectivity has pushed the utilization of macrocyclic host molecules into various practical separation strategies, such as extraction and chromatography. One of the most important developments in supramolecular-based separations is the incorporation of macrocycles such as crown ethers,[37] cyclodextrins[38] and cucurbiturils[39] into stationary or mobile phases of high performance chromatographic systems.

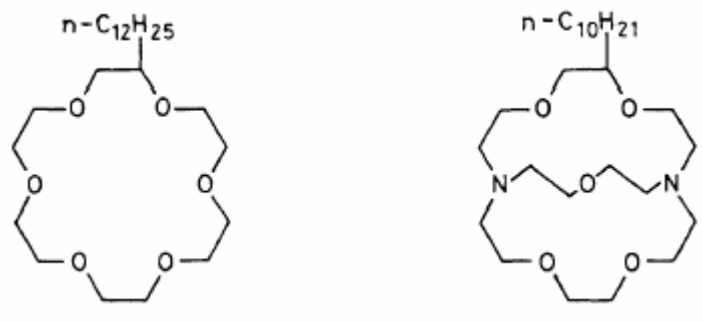

Figure 1.6 The hydrophobic crown ether and cryptand immobilized onto octadecylsilanized silica gel.[40]

One of the pioneering examples for utilizing macrocyclic host molecules into chromatography is that of Kimura and coworkers, who studied the adsorption of hydrophobic crown ethers and cryptands onto octadecylsilanized silica-based reversed-phase HPLC packings (Figure 1.6) for effective separation of alkali metal cations.[40]

1.1.4 Summary and Perspectives

The basic concepts of supramolecular host-guest chemistry, together with examples of its applications in many areas, have been presented briefly in this section. With the focus on intermolecular interactions, supramolecular chemistry has been straying away from traditional chemistry (covalent chemistry), and more and more efforts have been put into the employment of supramolecular principles in biological chemistry, functional devices, nanocomposite construction, and analytical assays. Although supramolecular host-guest chemistry is thought to be a mature research area, it is still a dynamic field and it will help us further understand the self-assembly phenomena in biological systems, fabricate elaborate and sophisticated superstructures and devices, such as molecular machines and robots, and construct nanomedicines and molecular-level surgical devices for medical applications.[13]

Supramolecular host-guest chemistry has been highlighted in this section, in which macrocyclic host molecules are essential and important components. Several of the

most popular macrocyclic hosts are summarized in the next section.

1.2. Macrocyclic Hosts

There are three types of host molecules/composites discussed in the section 1.1.2.2: cavitands, clathrands and tweezers. Only macrocyclic hosts will be introduced here, as the thesis is mainly focused on the study of one of the most popular macrocyclic host molecules, cucurbiturils. There are a number of very popular host molecules in host-guest chemistry, such as crown ethers, cryptands, cyclodextrins, calixarenes, porphyrins, and cucurbiturils.

1.2.1 Crown ethers and Cryptands

Crown ethers are macrocyclic oligomers of ethylene oxide, in the form of $(-CH_2CH_2O-)_n$ with typically $n \geq 4$. The crown ethers have been widely employed by scientists for their capability to strongly solvate cations in organic solvents, since the first publication by Pedersen in 1967.[41] Pedersen, the Nobel laureate of chemistry in 1987, reported the synthesis and metal ion complexation properties of a large number of macrocyclic polyethers (Figure 1.7a).[41] A cation is coordinated by the oxygen atoms in the interior of the ring of a crown ether, and the hydrophobic exterior of the ring renders the complexed cation soluble in organic solvents.[42] The usual "shorthand" designation of crown ethers is m-crown-n where m is equal to the total number of atoms on macrocycle chain and n represents the number of hetero-atoms (usually oxygen) in the

ring. Size-complementarity determines which cation can be solvated by which crown ether, e. g., 18-crown-6 has a high affinity for K^+, 15-crown-5 for Na^+ and 12-crown-4 for Li^+.[42] The ligands can be varied by altering the dimensions and rigidity of the macrocycle and by replacing the oxygen atoms partially or fully with sulfur and nitrogen atoms. In order to have greater affinity toward soft metal ions such as Hg^{2+}, Pd^{2+}, and Cu^{2+}, for example, sulfur atoms are employed to replace oxygen in crown ethers (referred to as a thia-crown ether).[43]

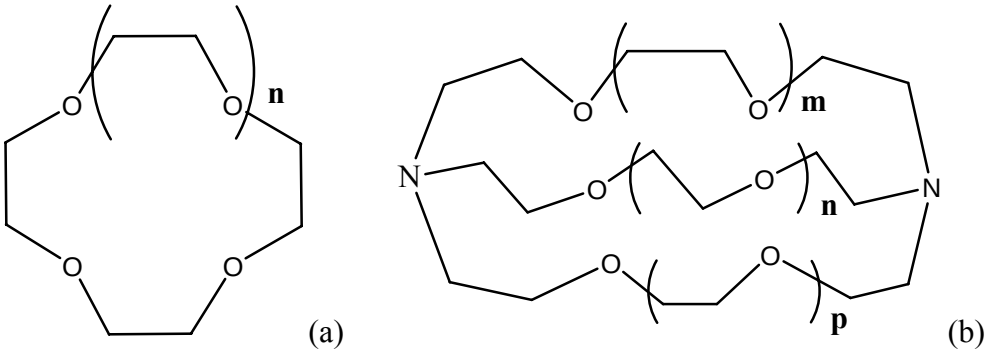

Figure 1.7 a) Representative structure of a parent crown ether (n usually varies from 1 to 4). b) Representative structure of a cryptand with m, n, and p varying from 0 to 2.

In order to increase cation-binding selectivity and affinity, cryptands were designed and synthesized, initially by Lehn and coworkers.[44,45] These cryptands are a family of synthetic bicyclic or polycyclic multidentate host molecules designed to bind a variety of cations. Because of their three dimensional macrocyclic structure (Figure 1.7b) and a *cryptate* effect induced by such a structure, they offer better selectivity and stronger

binding affinities than two dimensional crown ether.[2] Further development has been made for cryptands in order to bind selectively and strongly with anions. Anion cryptates are formed by the protonated polyamines[46] and bind the spherical chloride ion very strongly, and very selectively with respect to bromide and other types of anions, giving the cryptate shown in Figure 1.8.

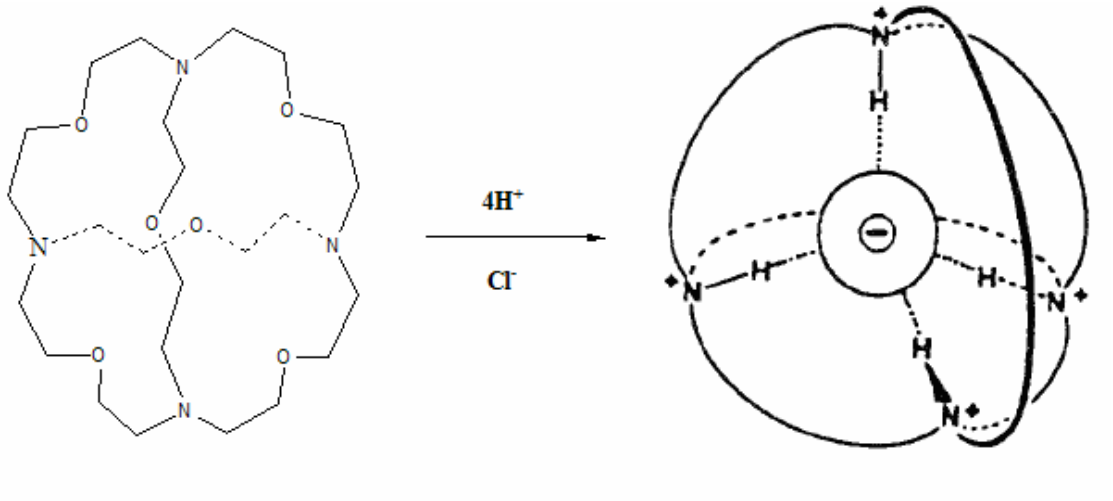

Figure 1.8 Schematic formation of an anion cryptate from a protonated cryptand polyamine and a chloride ion (modified from ref[46]).

1.2.2 Cyclodextrins

Cyclodextrins (CDs) are well-known natural cyclic compounds normally consisting of six to eight glucose units. They are called α-, β-, and γ-cyclodextrin respectively, based on the number of glucose units (Figure 1.9**)**.

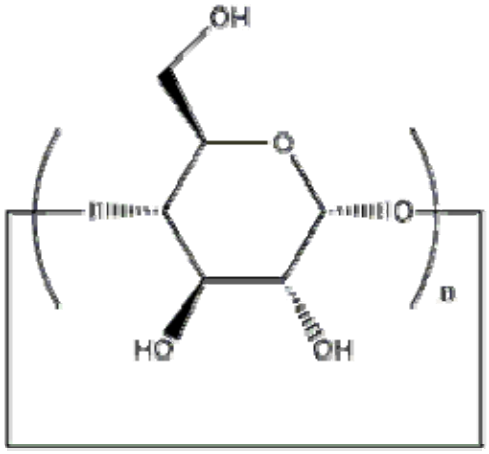

Figure 1.9 Structure of the cyclodextrins with n = 6, 7, and 8, respectively, for α-, β-, and γ-cyclodextrin.

The specific coupling of the glucose monomers in a cyclic manner gives a rigid conical molecular structure with a hydrophobic hollow interior of a specific volume, which can accommodate various organic compounds including nonpolar aliphatic and aromatic molecules, polar amines and acids,[47] neutral metallocenes such as ferrocenes[48] and other organometallic compounds.[49] The driving forces for the cyclodextrin(CD)-guest complexation are mainly attributed to several factors such as van der Waals forces, hydrophobic interactions, electronic effects, and steric factors.[50]

CDs have been widely used in the self-assembly of supramolecular structures, such as the fabrication of pseudorotaxanes, rotaxanes, catenanes and other types of molecular machines.[51,52] Moreover, they have been applied in drug delivery,[34] catalysis of organic reactions,[53] separation techniques[38] and in modulating the absorbance and fluorescence spectra of guest molecules.[54] As a result of their wide range of applications and the

many years of research development, CDs have been intensively employed in industry.[54]

1.2.3 Calixarenes

A calixarene is a cyclic oligomer based on a condensation product of phenols or resorcinols with aldehydes.[55] The word calixarene is derived from the Greek word "*calix*" because this structure of the molecule resembles a vase, and from the word "arene" that refers to the aromatic building block.[56] It forms a cup-like structure when all four aryl groups are oriented in the same direction (the "cone" conformation). Calixarenes have hydrophobic cavities that can hold smaller molecules or ions and aromatic molecules through π-π stackings, and belong to the class of cavitands in host-guest chemistry. The nomenclature of calixarenes is straightforward and involves counting the number of repeating units in the ring and including this number in square brackets between "calix" and "arene". For example, a calix[4]arene has four *para*-substituted phenol units in the cycle while a calix[6]arene has six. A substituent in the *para*-position is often added to the name with a prefix *p*-, as in *p*-*tert*-butylcalix[4]arene.

One characteristic of calixarenes and their derivatives is their diversity in conformation. For example, four basic conformations may be distinguished for a calix[4]arene, differing the relative orientation of the (*endo*) OH and the *p*-substituent, for which Gutsche introduced the names 'cone', 'partial cone', '1,2-alternate' and '1,3-alternate' (Figure 1.10).[55,57] The four hydroxyl groups at the lower rim interact

with each other through hydrogen bonding to stabilize the cone conformation, although the cone conformation is in dynamic equilibrium with the other conformations.

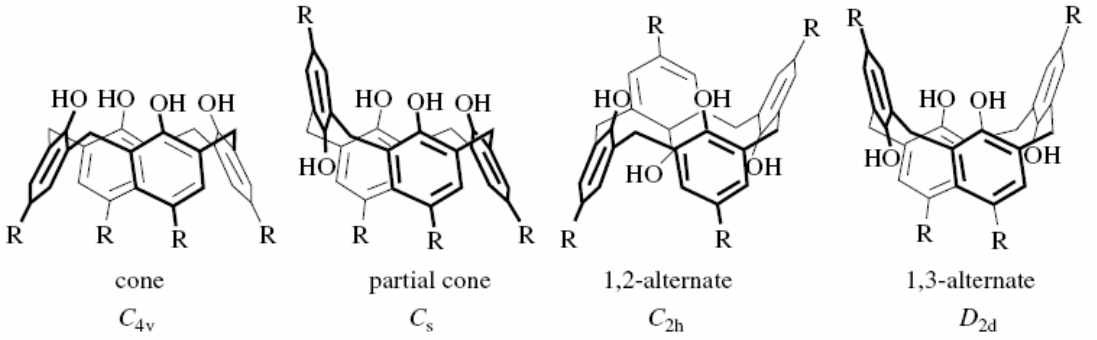

Figure 1.10 Four basic conformations of calix[4]arene with their basic symmetry points groups.[57]

The supramolecular host-guest chemistry of calixarenes has been intensively investigated since the 1970s.[56,58] Calixarenes have been found to be excellent ionophores for metal cations, mainly through cation-π interactions,[59] and good receptors for anions primarily through hydrogen bindings,[60] and therefore, they have been applied to the recognition and sensing selective ions.[61] Very recently, calixarenes have been incorporated into the construction of nanostructures and nanodevices.[62,63]

1.2.4 Porphyrins

Porphyrins are a large class of naturally occurring macrocyclic compounds with many important biological representatives including hemes and chlorophylls,[64] all of

which have in common the porphyrin macrocyclic substructure. The parent compound, known as porphyrin, consists of four pyrrole subunits linked on opposite sides (α position) through four methine bridges (=CH-). The structure of the parent porphyrin macrocycle and the carbon positions are shown in Figure 1.11. The extensive conjugated system makes the compound chromatic, hence the name is *porphyrin*, from the Greek word for purple.[64] Other than natural porphyrins, there are a variety of synthetic porphyrinoid molecules that have been made for various purposes ranging from basic research to functional applications in materials science and biology.[65]

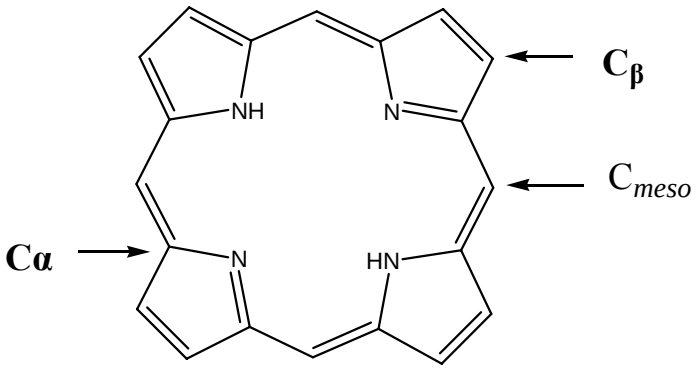

Figure 1.11 The structure of a parent porphyrin.

In the structure of a parent porphyrin (Figure 1.11), if both of the N-H bonds in the porphyrin molecule are ionized, a highly symmetrical dianion is formed in which all four nitrogens become equivalent because of the delocalization of the negative charges.[64] In the dianion all unshared pairs of electrons are directed toward the inside of the macrocyclic cavity. Many ionic metals fit within such a cavity and can be fixed in

space by coordination bonds with the four porphyrin nitrogen atoms.[64] Such compounds have considerable stability and are deeply colored.[66] As a result of their binding properties, porphyrins and metalloporphyrins have been frequently employed in the construction of artificial antenna systems,[67] photosynthetic center mimics,[68] gates and redox switches, and find applications in the fabrication of smart devices and machines.[69]

1.3 Cucurbiturils

The cucurbit[*n*]urils (CB[*n*], where *n* is most commonly 5–8 and 10), a family of cyclic host molecules consisting of *n* paired-methylene bridged glycoluril units, have a fairly rigid hydrophobic cavity of low polarizability, which may be accessed through two carbonyl-lined portals. The name "cucurbituril" is derived from the resemblance of the shape of the molecule with a pumpkin of the family of *Cucurbitaceae*.[70] This group of host molecules has been of particular interest to chemists during the past twenty years, due to their size-tunable properties, and strong and highly selective affinities to guest molecules. As the thesis is mainly involved with the host-guest chemistry of cucurbiturils, the chemistry of the family of host molecules will be discussed in detail.

Although the synthetic reaction of the cucurbituril molecules was reported in 1905, it is not until 1981 that the chemical nature and structure of cucurbit[6]uril (CB[6]) were fully characterized by Mock and coworkers.[70] CB[6] was found to be a remarkably rigid host molecule, with a well-defined internal hydrophobic cavity having a diameter of 5.5 Å, accessible from two polar carbonyl-laced portals. Since 1981, there have been

numerous reports in the literature of the formation of coordination complexes with a range of metal ions, and inclusion complexes with various guest molecules.[71,72] However, unlike the cyclodextrin family, the availability of only one cavity size (and CB[6] is relatively small) until recently had limited the range of guest species that could be encapsulated. The discoveries of CB[5], CB[7], and CB[8] expanded the CB[*n*] family,[73,74] and provided hosts with a wide range of available cavity sizes. The field of CB[*n*] host-guest chemistry has been broadened significantly thereafter. Very recently, free CB[10] was isolated successfully by the Isaacs group,[75] although the complex CB[5]@CB[10] was discovered by Day and coworkers a few years before, in which CB[5] is trapped in the large cavity of CB[10].[76] With the large cavity, CB[10] can encapsulate large or multiple guest molecules, including a calix[4]arene derivative, and therefore CB[10] can further expand the scope of host-guest chemistry of the CB[*n*] family.

A very new addition to the CB[*n*] family are molecules with an inverted glycoluril unit in the structure of regular CB[*n*] (abbreviated *i*-CB[*n*]),[77] and a novel form of CB[10], *nor*-*seco*-CB[10] (abbreviated *ns*-CB[10]).[78] These isomers of CB[*n*] molecules gave a fresh insight on the CB[*n*] formation reaction. Although this thesis focuses on the parent CB[*n*] family, it is worth noting that, in addition to the inverted CB[*n*], many other derivatized CB[*n*] molecules has been synthesized[79-85] and their applications in materials science and biology have been investigated.[86]

With the availability of a diverse set of CB[*n*] molecules, the applications of the CB[*n*]

family have been expanded into numerous areas, such as the design and fabrication of rotaxane and pseudorotaxanes, molecular machines and switches, drug (genes) delivery, water treatment, reaction catalysis and inhibitors, and the recognition of amino acids and peptides. This section will begin by briefly describing the synthesis, structure and physical properties of CB[*n*] molecules, followed by details on their novel host–guest chemistry and applications.

1.3.1 Synthesis, Structures and Chemical and Physical Properties of CB[*n*]

The reaction of glycoluril and excess formaldehyde in the presence of concentrated sulfuric acid or hydrochloric acid at a temperature of around 110 °C produces the macrocyclic CB[*n*] compounds (Figure 1.12) through an acid-catalyzed condensation reaction.

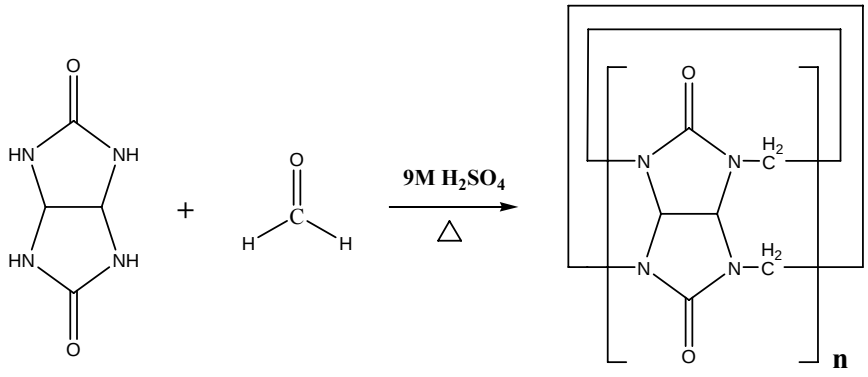

Figure 1.12 Scheme for the synthesis of CB[*n*] (*n* = 5-10).

Originally only CB[6] was isolated and characterized with no other homologues

found.[70,87] In 2000, the research groups of Kim and Day independently isolated the homologues CB[5], CB[7] and CB[8], using a lower synthesis temperature of 75-90 °C.[73,88] While this development dramatically expanded cucurbituril chemistry and has attracted more chemists into this field, the mechanisms of the synthesis and size control still remains to be fully resolved.[73,88] Recently, Isaacs and coworkers successfully isolated free CB[10] from the complex of CB[5]@CB[10] by exchanging the guest of CB[5] with melamine diamine, followed by removal of the new guest through acrylation and intensive washing.[75] Most recently, a more efficient, convenient and practical method of the synthesis of large-scale CB[*n*] mixtures has been patented by Kim and coworkers, in which a microwave-assisted method is employed.[89] The CB[*n*] molecules (*n* = 5, 6, 7, 8 and 10) have been fully characterized by various analytical methods including X-ray crystallography, and they are all readily available through the synthesis and isolation methodologies referred to above.

In the family of CB[*n*], the cavity size increases with the increase in the number (*n*) of repeating units. In Table 1.1, some of the structural parameters are listed for the CB[*n*] molecules. The mean diameter of the internal cavity of CB[*n*] increases from 4.4 (*n* = 5) to around 11 Å (*n* = 10), with a constant height of about 9 Å. The cavity volume increases from 82 $Å^3$ for CB[5] to 870 $Å^3$ for CB[10]. The cavity sizes of CB[6], [7] and [8] are similar to the cyclodextrin analogues, α-, β-, and γ-CD, respectively. In addition, the cavities of CB[5] to CB[8] are relatively rigid, although CB[7] and CB[8] could be distorted by large planar guest molecules, and the cavity of CB[10] is expected

to be relatively flexible due to its large cavity volume.

Table 1.1 Molecular dimensions for CB[*n*] family members.[75,90,91]

	CB[5]	CB[6]	CB[7]	CB[8]	CB[10]
Portal diameter (Å)	2.4	3.9	5.4	6.9	10
Cavity diameter (Å)	4.4	5.8	7.3	8.8	11.7
Height (Å)	9.1	9.1	9.1	9.1	9.1
Volume ($Å^3$)	82	164	279	479	870

One of the potential disadvantages of the CB[*n*] family of host molecules in host-guest chemistry is their relatively poor solubility in common solvents.[91] The solubility of CB[*n*] is very low with the exception of CB[5] and CB[7], which have moderate solubility (around 3×10^{-2} M) in water, comparable with β-CD. The problem of poor solubility of CB[6] was solved by a successful synthesis of more water-soluble derivatives of CB[6], such as cyclohexano-CB[*n*] (*n* = 5 or 6), by Zhao *et al.*,[81] although the water-soluble derivatives have not been widely employed since then. In addition, all of the CB[*n*] homologues are moderately soluble in strongly acidic solution or in aqueous solutions containing alkali metal ions. The latter effect is mainly due to the coordination of metal ions to the carbonyl portals. As a result of its superior water solubility and its relatively large host cavity, able to include such guests as aromatic molecules and ferrocenes, CB[7] has attracted relatively more attention than other CB[*n*]

species during the past few years.[91]

1.3.2 Host-Guest Properties of the Cucurbit[*n*]uril Family

Host-guest interactions have been well studied, leading to fundamental insights into supramolecular chemistry, as was discussed in the previous section. Receptors such as cyclodextrins and calixarenes have been well developed in this field. Recently, intensive interest on host-guest chemistry has been turned to the cucurbituril family (CB[*n*]) due to its rigid structure, wide size range, high binding selectivity, and great thermal stability.

Table 1.2 Examples of guest molecules complexed by CB[*n*] molecules.

CB[*n*]	Typical examples of guest molecules
CB[5]	NH_4^+ and gases such as Kr, Xe, N_2, O_2, Ar, N_2O, NO, CO, CO_2 and CH_4
CB[6]	α,ω-diaminoalkanes, bipyridine derivatives, aromatic compounds, amino acids (and short peptides), and THF.
CB[7]	Adamantanes, naphthalenes, stilbenes, viologens, ferrocenes, aromatic amines and alcohols, and *o*-carborane
CB[8]	Cyclen, cyclam and their metal complexes, fullerene, polyaromatic molecules such as acridizinium, and other metal complexes
CB[10]	CB[5], calix[4]arene, and adamantane derivatives

As briefly mentioned in the previous section, all of the CB[*n*] family members from CB[5] to CB[8], along with CB[10], have a symmetric geometry with two identical polar openings and a hydrophobic cavity. As a result, they all demonstrate specific affinities for guest molecules with complementary charge distributions (mostly positively charged) and size and shape matches. Their varying cavity and portal sizes, however, lead to remarkable molecular recognition properties, differing from one another. Some typical guest molecules for CB[*n*] are listed in the Table 1.2. The complexation properties and examples for each CB[*n*] family member, starting with the parent CB[6], are described below.

1.3.2.1 Cucurbit[6]uril

As macrocyclic hosts with electronegative portals, CB[*n*] molecules are all ideal for binding positive ions at the portals, or including hydrophobic guest molecules with their positive charges complexed by the portals. The pioneering work carried out by Mock and co-workers was exclusively focused on the host-guest chemistry of CB[6], as it was the first CB[*n*] family member to be discovered. They prepared pseudorotaxane complexes using protonated α,ω-diaminoalkane ions in solution.[92] The binding affinities of α,ω-diammoniumalkane cations with different alkyl chain lengths exhibit "alkyl-chain length dependent selectivity", e.g. CB[6] prefers 1,6-diammoniumhexane and 1,5-diammoniumpentane with the respect to 1,4-diammoniumbutane (15-fold) and 1,7-diammoniumheptane (64-fold).[93] The principle of length-dependent selectivity can

be employed to construct molecular switches.[91] More recently, Dearden and coworkers have proved that the diammoniumalkane ions form pseudorotaxanes with the host molecule CB[6] in the gas phase, by using electrospray FT mass spectrometry.[94] In addition to the above-mentioned length-dependent selectivity, shape-dependent selectivity was also demonstrated. The *p*-tolylmethanamine, for example, is encapsulated into the cavity of CB[6], whereas the *o*- and *m*-isomers are not included at all.[90,95]

Table 1.3 Log*K* values for the complexation of metal ions with CB[6] in HCOOH/H_2O (1:1) and with crown ether in water.[96]

Host	Li^+	Na^+	K^+	Rb^+	Ca^{2+}	Sr^{2+}	Ba^{2+}
CB[6]	2.48	3.23	2.79	2.68	2.80	3.18	2.83
18-crown-6	--	0.80	2.03	1.56	<0.5	2.72	3.87

As the carbonyl portals of CB[*n*] are electronegative in nature, it was not surprising that CB[6] binds ammonium, alkali metal, alkaline earth, and transition metal cations in solution.[96-99] Buschmann *et al*. have determined the binding constants for the complexes between CB[6] and several metal cations by calorimetric titrations (Table 1.3).[96] In addition to positively charged organic guests and metal cations, CB[6] was also reported to include neutral guest molecules such as Xe, THF and toluene, mainly through dispersion forces as well as hydrophobic interactions.[100,101] The mechanism

and factors affecting host-guest complexation of CB[6] have been recently studied in detail by Nau and coworkers,[95] in which the kinetics and thermodynamics of binding, as a function of temperature, salt concentration and cation size, were determined. In addition, equilibrium constants, and in many cases the enthalpy and entropy of the binding for many guest molecules including amino acids and dipeptides,[102] aliphatic alcohols, acids and nitriles,[103] and poly(ethylene glycols),[104] have been determined by Buschmann and coworkers.

1.3.2.2 Cucurbit[5]uril

Although the parent CB[5] molecule was discovered and isolated only recently,[73,74,88] its derivative decamethylcucurbit[5]uril (Me_{10}CB[5]) was synthesized in 1992,[79] and its chemistry had been studied before the parent CB[5] was prepared. CB[5] and Me_{10}CB[5] are expected to have rather similar complexation properties, considering the fact that they have identical cavity dimensions. CB[5] has a small cavity with narrow portals, and as a consequence guest complexation has been limited to protons and the ammonium ion, as well as metal cations which are bound only at the portals of CB[5].[74,96,105,106] The encapsulation of neutral guests, such as small gas molecules such as N_2, N_2O, NO, O_2 and Ar, and small solvent molecules such as CH_3OH and CH_3CN were firstly observed by Dearden and Miyahara groups, using electrospray ionization Fourier transform mass spectrometry.[107,108] The gas guest can be "locked" in the cavity by ammonium "lids", and the lids can be removed by competitive binding with

18-crown-6 in the gas phase (Figure 1.13). Most recently, the chloride anion was found to be encapsulated in the cavity of CB[5],[109] which is very unusual because the carbonyls on the portals of CB[*n*] are electronegative in nature.

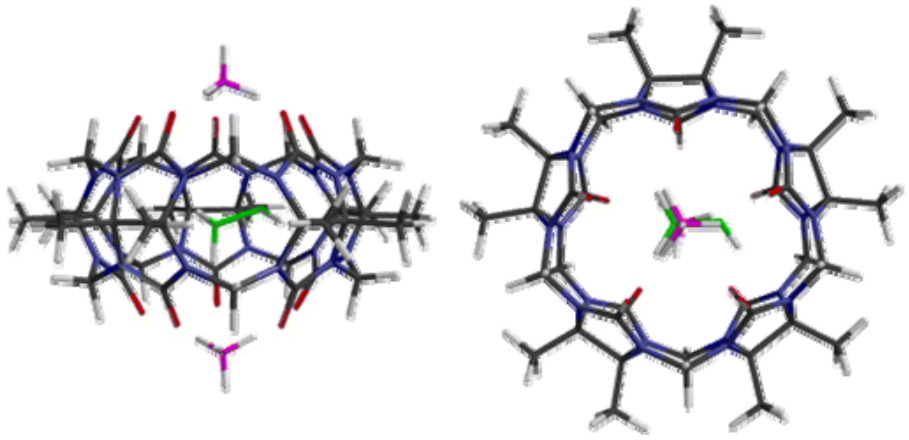

Figure 1.13 Side and top views of MeOH@Me_{10}CB[5] with two NH_4^+ lids.[107]

1.3.2.3 Cucurbit[7]uril

As briefly discussed above, CB[7] has attracted more attention than others in this family during the past few years because of its superior water-solubility and its ability to include aromatic species. CB[7] shares the same characteristic features of CB[6] and CB[5], such as a hydrophobic cavity and twin electronegative portals, however it has a larger cavity size than both CB[6] and CB[5]. It is even slightly more voluminous than its cyclodextrin counterpart β-CD,[91] thus can bind a variety of guest molecules that are larger than those which can be included in the CB[5] and CB[6] cavities. The guests which have been reported as forming complexes with CB[7] include various positively

charged species such as stilbenes,[22] viologen dications,[110,111] protonated aminoadamantanes,[112] protonated polyaromatic amines and 2,7-dimethyldiazapyrenium,[113,114] imidazolium cations,[115] cationic dihydroimidazoles,[116] chiral N-benzyl-1-(1-naphthyl)ethylamines[117] and pyridinium derivatives,[118] and neutral guest molecules such as aromatic alcohols, adamantanes, bicyclooctanes,[90,119] *o*-carborane,[120] and fullerene,[121] and metal complexes such as ferrocene and cobaltocenes derivatives[122,123,124] and others.[36,125]

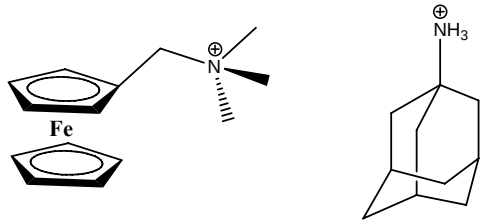

Figure 1.14 Structures of guest molecules which are strongly bound to CB[7]: (trimethylammonio)methylferrocene (left) and protonated 1-aminoadamantane (right)

Among these guest molecules, CB[7] tightly binds ferrocene and its derivative, and protonated 1-aminoadamantane (Figure 1.14) with binding constants in the range of 10^{11} to 10^{12} M^{-1},[112,122,123] which is the strongest complexation ever reported for synthetic receptors in aqueous solution and approaching one of the strongest noncovalent interactions found in Nature, the biotin/streptavidin pair, with $K = 10^{14}$ M^{-1}. This indicates that the strong noncovalent interactions between bio-receptors and substrates in Nature can be replicated by using synthetic receptors. Most recently, Kim and

coworkers have employed the CB[7]/ferrocene derivative pair to replace the biotin/streptavidin pair to immobilize proteins on a solid surface through a non-covalent strategy.[126]

1.3.2.4 Cucurbit[8]uril

Due to the larger cavity than those found in CB[5], CB[6] and CB[7], with similar physical behaviors in many other ways with the other family members, CB[8] selectively binds single large-sized, positively charged guest species such as adamantane derivatives[127] and methylviologen derivatives,[128,129] through ion-dipole and hydrophobic interactions, and encapsulates large-sized neutral compounds such as fullerene,[130] through mainly size-fit and hydrophobic interactions. It is also capable of simultaneously encapsulating two aromatic guest molecules to form 1:2 host-guest complexes with guests such as naphthalene derivatives,[73] acridizinium cations,[131] tetrathiafulvalene,[132] diaminostilbene[133] and cinnamic acids[134,135] through hydrophobic interaction and π-π stacking between guest molecules. CB[8] can also include a hetero-guest pair in the cavity to form 1:1:1 ternary complexes (Figure 1.15), by charge-transfer (CT) interaction between electron-rich and electron-deficient guests, such as methylviologen and 2,6-dihydroxynaphthalene.[136,137] Recognition through such charge-transfer (CT) interactions in the cavity of CB[8] has been employed to control intermolecular back-folding,[138] to fabricate vesicles,[139] to construct a molecular loop lock and a molecular necklace,[140,141] to design molecular and biological sensors,[142-144] and to

switch dendrimer self-assembly.[145] In contrast to the CB[5], CB[6] and CB[7] hosts, the voluminous cavity of CB[8] is even capable of including tetraaza macrocyclic molecules such as cyclen and cyclam to form "macrocycle-within-macrocycle" complexes.[146] Moreover, metal ions can then be encapsulated into the tetraaza macrocycle encapsulated in the CB[8] macrocycle.

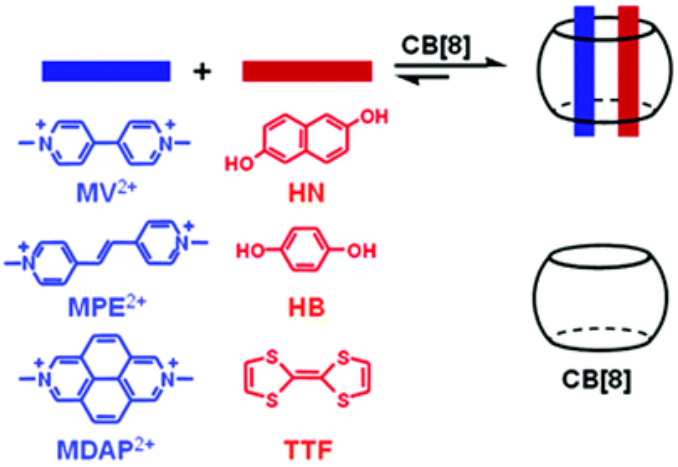

Figure 1.15 Examples of charge-transfer (CT) complexes formed in CB[8].[137]

1.3.2.5 Cucurbit[10]uril (CB[10])

Although CB[10] was discovered a few years ago, it was not until very recently that free CB[10] was isolated successfully by the Isaacs group.[75] Behaving like other family members from CB[5] to CB[8], CB[10] retains the ability to bind a wide variety of chemically and biologically important cationic substances or neutral guest species within its cavity. The vast cavity volume of CB[10] (~870 $Å^3$) allows the macrocycle to form

complexes with large molecules or complexes, such as a calix[4]arene derivative, and the addition of another large guest, adamantanecarboxylic acid, to the macrocycle-within-macrocycle (calix[4]arene-within-CB[8]) leads to the formation of a ternary molecular complex. The addition of free CB[7] can break down the ternary complex, as CB[7] traps the adamantanecarboxylic acid when dissociated from the termolecular complex by including it more strongly in its own cavity.[75] The example above suggests that CB[10] has the potential for formation of even higher order molecular complexes because of its vast cavity.

1.3.3 Applications of Cucurbit[*n*]urils

With their unique structures, wide range of size availability, and remarkable recognition properties, the CB[*n*] family has shown novel host-guest complexation properties with various guest molecules, complexes and composites. The practical use of the CB[*n*] family is therefore diverse and has provided a wide variety of applications ranging from water treatment to catalysis, from drug delivery to molecular machine construction.[91] A brief summary of some of the important applications of CB[*n*] molecules to date, is given below.

1.3.3.1 Cucurbit[*n*]urils as Catalysts and Stabilizers

As described in section 1.1.3.1, it has long been a challenge to develop supramolecular catalysts and stabilizers in the field of supramolecular chemistry. The

CB[*n*] molecules are ideal for these two purposes, as a CB[*n*] can sometimes include two guest molecules simultaneously to form 1:2 host:guest complexes or 1:1:1 ternary complexes. In principle, if the two guest species are reactive towards each other, then pulling the two reactants together into a reaction chamber (the cavity of CB[*n*], in this case) in a specific geometry can potentially catalyze the reaction in a stereoselective way. Secondly, CB[*n*] can form 1:1 inclusion complexes with many guest species and the encapsulation of the guest species in a confined and isolated pocket can often stabilize the molecules from attack by other reactants in the environment, such as oxygen.

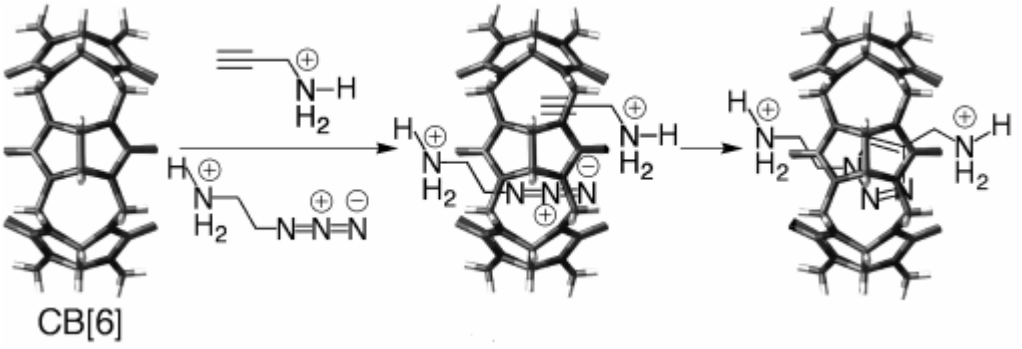

Figure 1.16 Catalysis of a [3+2] dipolar cycloaddition in CB[6].[91]

In the pioneering work carried out by Mock and coworkers, more than twenty years ago, CB[6] was utilized for the first time as a reaction chamber to catalyze a dipolar cycloaddition between azide and an alkyne.[147] Remarkably, compared with the regular bimolecular reaction in the absence of CB[6], the cycloaddition reaction is accelerated by a factor of 10^5 in the presence of CB[6] and high regiospecificity is achieved with only

1,4-disubstituted triazoles being formed (Figure 1.16).[91,147] With the same mechanism, oligotriazoles have been synthesized with catalysis provided by CB[6].[148] Moreover, this principle has been further expanded into the design and construction of molecular rotaxanes and pseudorotaxanes. Tuncel *et al.* reported that CB[6]-catalyzed cycloaddition reaction of azides and terminal acetylenes can be employed to prepare catalytically self-threading polyrotaxanes,[149,150] pseudopolyrotaxanes,[151] rotaxanes, and semirotaxanes.[152]

A few years ago, Kim and coworkers demonstrated that the [2 + 2] photoreaction of a cationic olefinic guest molecule, protonated *trans*-diaminostilbene, may be carried out with a large rate acceleration and high stereoselectivity via the formation of a stable 1:2 host-guest complex with CB[8] in aqueous solution.[133] The major photoreaction product for protonated *trans*-diaminostilbene in the presence of CB[8] upon UV light irradiation is the *syn*-dimer, whereas in the absence of CB[8], the photoisomerization dominates and the major product is protonated *cis*-diaminostilbene. The stereoselectivity comes from the ability of the host to stabilize the inclusion of two guest molecules with a parallel orientation of the olefinic groups in close proximity (Figure 1.17). Recently, using the same principles, the Macartney and Ramamurthy groups independently discovered that irradiation of *trans*-1,2-bis(4-pyridyl)ethylene and *trans*-n-stilbazoles in the presence of CB[8] in aqueous solution leads to mainly *syn* dimers in high yield (*syn:anti*=90%:5%), while in the absence of the host molecules, the corresponding *cis*-isomers and photohydration products were obtained.[153] Pattabiraman

et al. also reported that a variety of cinnamic acid molecules were aligned in a head-head fashion inside the cavity of CB[8] in water so that irradiation of these cinnamic acids in the presence of the templating CB[8] host molecule gives *syn* head-head cyclobutanes in nearly quantitative yields.[134] Wang *et al*. reported that the [4+4]photocycloaddition of protonated 2-aminopyridine inside the cavity of CB[7] leads to exclusively the *anti-trans* dimer, which is also stabilized from the thermal re-aromatization by the encapsulation.[118] In the absence of the template, both a*nti-trans* and *syn-trans* dimers were formed in a ratio of about 4:1.

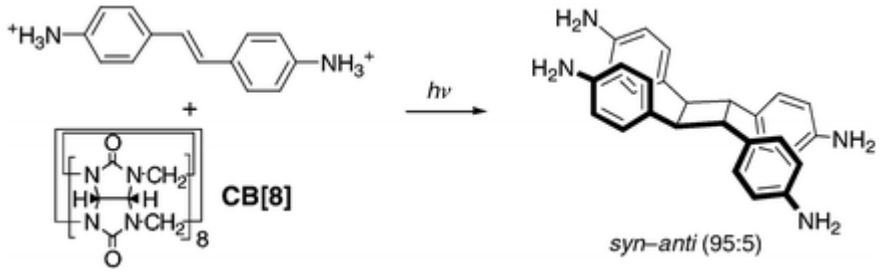

Figure 1.17 CB[8] catalyzed photodimerization.[133]

All of these examples demonstrate that a CB[*n*] with the correct size can act as a reaction "chamber" (or "reactor") in which bimolecular reactions between appropriately designed guest molecules can be facilitated with high regio- and stereoselectivity. In addition to these bimolecular reactions, proper sized CB[*n*] can also catalyze or inhibit unimolecular reactions. The CB[7] catalyzes the *trans*-to-*cis* photoisomerization of protonated diaminostilbene[22] and 1,2-bis(4-pyridyl)ethylene upon irradiation,[154] and

thereafter CB[7] acts as a stabilizer (or inhibitor) to stabilize the *cis*-isomers from otherwise observed thermal or photoisomerizations. Very recently, Macartney and coworkers reported that encapsulation of the (*E*)-1-ferrocenyl-2-(1-methyl-4-pyridinium)ethylene cation by CB[7] is greatly stabilized against (*E*)→(*Z*) photoisomerization in aqueous solution.[123] Similarly, Mohanty *et al.* reported that the CB[7]-complexed dye molecule rhodamine 6G is greatly protected from photobleaching and aggregation in solution.[155]

1.3.3.2 Rotaxanes, Pseudorotaxanes and Other Interlocked Analogues

Both rotaxanes and pseudorotaxanes play important roles in supramolecular chemistry, nanotechnology and the construction of smart materials because of their ability to undergo controllable motion in response to external stimuli.[91] CB[*n*] molecules are capable of playing the roles of molecular beads in the construction of rotaxanes or pseudorotaxanes due to their wheel-like shape and remarkable binding properties. Any host-guest complexes based on CB[*n*] and linear guest molecules in which the guest molecules can freely thread and dethread the cavity can be considered as pseudorotaxanes based on CB[*n*]. The very early pseudorotaxane complexes of CB[*n*] were comprised of alkyldiammonium ligands and CB[6].[156] The first example of the employment of a CB[*n*] in the construction of a rotaxane was reported by Jeon *et al.* about ten years ago.[157] The simple, one-step, high-yield synthesis of a rotaxane involved threading spermine into CB[6], followed by covalently attaching dinitrophenyl

groups to both ends of the spermine unit, to prevent the CB[6] cyclic bead from dethreading (**Figure 1.18**). Similarly, a variety of amide-stopped rotaxanes with CB[6] have been synthesized by Buschmann and coworkers in high yields, by the interfacial condensation of a CB[6]-threaded 1,6-hexanediammonium ion and a CB[6] or CB[5]-threaded spermine ion with various acid and diacid chlorides.[158-161] Coordination of metal complexes such as alkylcobaloxamines has also been employed as stoppers to construct rotaxanes based on CB[6].[162] The metallo-rotaxane was formed in the aqueous solution through the self-assembly of a pre-organized pseudorotaxane of cucurbituril and spermine, with alkylcobaloxime.

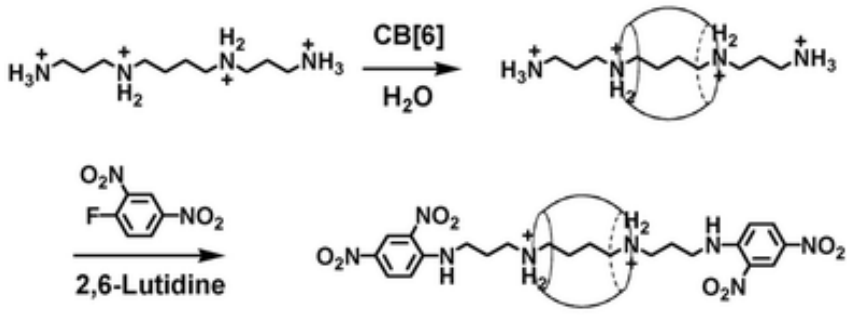

Figure 1.18 One-step synthesis of a rotaxane based on CB[6].[157]

As discussed in the previous section (on the topic of catalysis by CB[*n*]), catalytically self-threading polyrotaxanes (Figure 1.19),[149,150] rotaxanes and semirotaxanes[152] have been prepared in aqueous solution by CB[6]-catalyzed dipolar cycloaddition reaction of azides and terminal acetylenes. These are examples of polyrotaxanes prepared from pre-threaded small guest molecules and host molecules, and thereafter catalytic

cycloadditions. In addition to this method for making polyrotaxanes and polypseudorotaxanes, a variety of polymer backbones and side chains have threaded into CB[6] to prepare pseudo-polyrotaxanes, such as side-chain pseudo-polyrotaxanes using polyacrylamides (diaminobutane side chains),[163] polyviologens[164] and poly-4-vinylpyridine,[165] and main-chain pseudo-polyrotaxane using poly(hexamethyleneimine).[151]

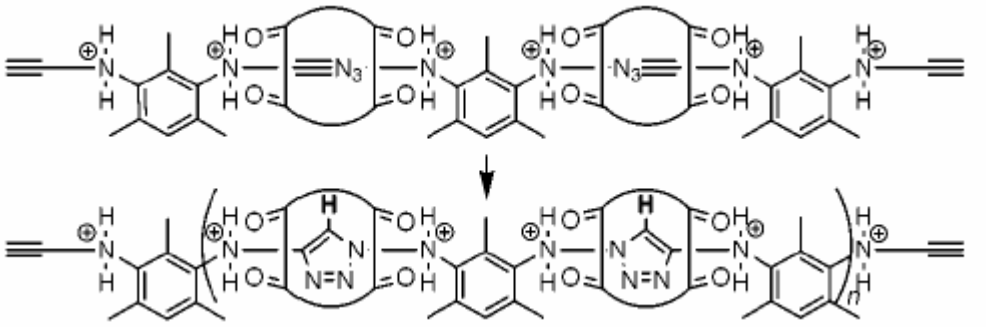

Figure 1.19 Schematic illustration of the preparation of a polyrotaxane through catalytic self-threading.[149]

Dendrimers with terminal or focal groups that are modified with pseudorotaxanes based on CB[*n*] molecules have been reported.[166-169] Kim and coworkers first reported the marriage of CB[*n*] and dendrimers in which they covalently attached diaminobutane units to the terminals of polypropylimine dendrimers, and non-covalently threaded CB[6] onto the diaminobutane periphery to produce pseudorotaxane-terminated dendrimers (Figure 1.20a). Here the physically large and crowd terminal pseudorotaxane units can form a rigid shell at the outer surface of the dendrimer, which can potentially inhibit the

escape of guests trapped in the interior portion of the dendrimer.[166] Kaifer *et al.* reported pseudorotaxanes of CB[7] and dendrimers containing a single guest residue at the focal point, such as viologens,[167] ferrocene[168] and cobaltocenium[169] (Figure 1.20b). Kaifer's work suggested that the nature of the intermolecular forces between the host and the guest may be an important factor in determining the magnitude of dendrimer growth effects on the binding affinity. All of these studies give a picture of a new class of intriguing complexes based on dendrimers and CB[*n*] molecules and provide a novel way of modifying dendrimers exteriorly and interiorly by noncovalent interactions, which might alter their physical properties, such as binding affinities.

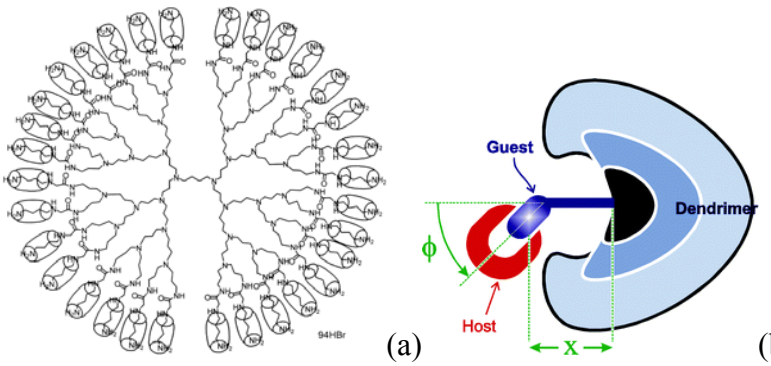

Figure 1.20 A pseudorotaxane-terminated dendrimer (a)[166] and a focal-pseudorotaxane dendrimer (b).[167]

Kim *et al*. have developed a novel strategy to form CB[*n*]-based polyrotaxanes by employing a metal-ion-directed self-assembly.[170] It involves the pre-organization of CB[6] bead and a short linear ligand (string) into a pseudorotaxane, followed by adding

metal ions such as Cu^{2+}, Co^{2+}, Ni^{2+}, Ag^{+}, or Cd^{2+} to link (coordinate) pseudorotaxanes into 1D, 2D (including molecular necklaces) and 3D polyrotaxanes with high structural regularity in the solid state by utilizing coordination chemistry.[170] Many of these structures have been characterized by X-ray crystallography. Short strings that are able to form stable inclusion complexes with CB[6] and to coordinate metal ions using the donor atoms placed at the terminals, such as 3- or 4-pyridylmethyl group attached at both *N*-terminals of diaminobutane or diaminopentane, have been designed.

1.3.3.3 Molecular Machines and Switches

One of the potential applications of mechanically interlocked (rotaxane) or non-interlocked (pseudorotaxane) molecules is to construct molecular-level devices such as molecular machines, as Stoddart *et al.* have demonstrated recently.[171] A molecular switch is one of the most fundamental types of molecular machines that can switch between different states (in this case different binding sites) by appropriate external (chemical, electrochemical or photochemical) stimuli.[91] The very first example of a molecular switch by the employment of CB[*n*] molecules was reported by Mock and coworkers in 1990.[172] The pseudorotaxane-based molecular switch consists of a CB[6] ‘‘bead’’ and a linear triamine ‘‘string’’, $PhNH(CH_2)_6NH(CH_2)_4NH_2$, in which CB[6] shuttles between two alkyl sites along the string by changing the pH value in the solution (Figure 1.21). At a pH below 6.7, which is the pK_a of the anilinium group, the macrocyclic CB[6] resides at the hexyldiammonium site, while at a pH slightly higher

than 6.7, the aniline ammonium is deprotonated and CB[6] moves to the still diprotonated butyldiammonium site, because binding with the monoprotonated diaminohexane is weaker.

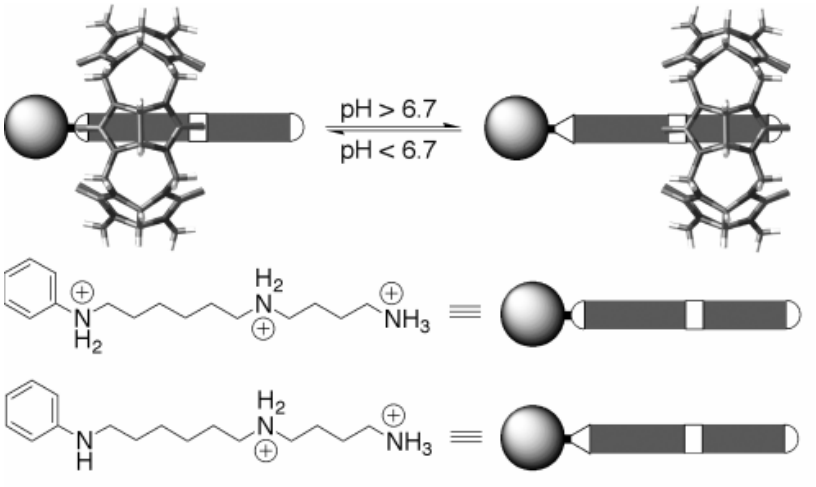

Figure 1.21 CB[6]-based molecule switch.[91]

Similarly, Kim and coworkers designed a pH dependent fluorescent molecular switch based on a CB[6] bead and a fluorenyltriamine string that can sense the sitting position of CB[6] by UV-visible and fluorescence outputs.[173] Another CB[6]-containing bistable [2]rotaxane designed by Kim's group behaves both as a pH and a thermodynamically controlled molecular switch.[174] Other pH-controlled CB[*n*]-based switches include a fluorescent molecular switch,[113] an on/off molecular shuttle,[175] and a pH-driven polymeric switch based on pseudo-polyrotaxanes prepared by catalytic-cycloaddition.[176] A pH-controlled pseudorotaxane on/off switch has been applied in materials surface chemistry.[177] The controllable CB[6] threading/dethreading has the behavior of a

molecular ion-gate on a gold surface at low pH the CB[6] molecules are threaded onto the strings attached on the surface, and a condensed self-assembled-monolayer is formed with external ions having no contact with the gold surface. At high pH, CB[6] molecules are dethreaded from the strings on the surface and the gate is open to external ions again (Figure 1.22). More recently, Kim and coworkers extended this work and have reported a novel pseudopolyrotaxane grown on a gold surface in which the repeating units are linked by host-stabilized charge-transfer interactions between the guest molecules.[178]

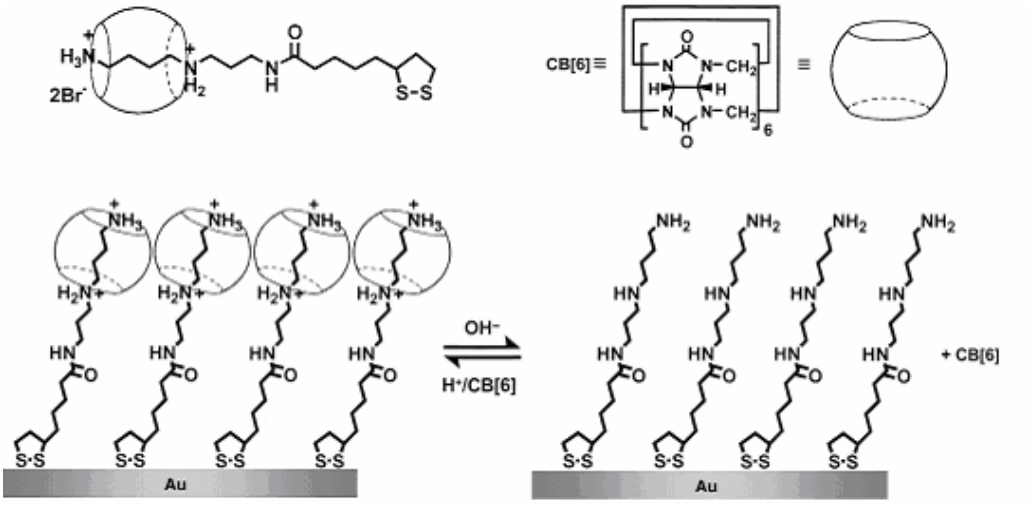

Figure 1.22 An on/off pseudorotaxane applied as an ion-gate on a gold surface.[177]

Other than molecular switches controlled by external chemical stimuli, examples of molecular machines and switches controlled by the means such as photochemical or electrochemical stimuli have also been reported by Kim group[141,179] and Kaifer group.[180]

Kim and coworkers first designed and constructed a novel [2]pseudorotaxane-based molecular machine in which the folding and unfolding of the string can be reversibly controlled by electrochemical and photochemical stimuli.[179] The key feature of the machine-like behavior is the reversible formation of a molecular loop by intramolecular pairing (CT-interaction) of the terminal viologen radical cation units inside CB[8] upon reduction.

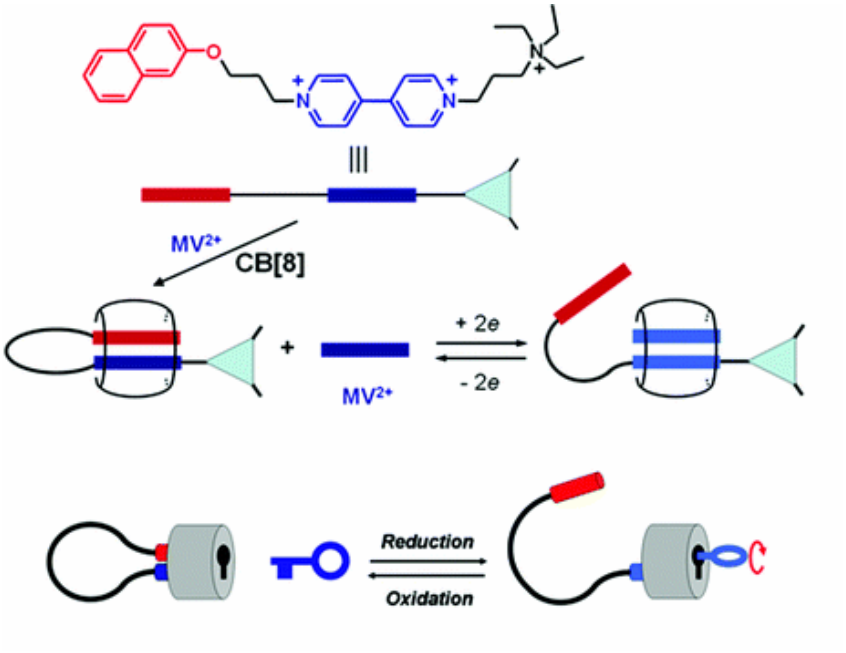

Figure 1.23 Formation of a molecular loop lock and its working mode with a key.[137]

To further extend this molecular loop, a redox-controlled molecular loop lock has been designed, which requires both a key (an external guest) and a redox process to open. In this molecular loop lock, the string contains two active parts (intramolecular CT pair), a viologen unit and a naphthalen-2-yloxy unit. The addition of CB[8] induces the

formation of a 1:1 CT-stabilized complex (loop-shape guest), the lock, while the further addition of another viologen guest, a key, and reduction control, can open the lock (Figure 1.23).[141]

Kaifer reported an electrochemically driven pseudorotaxane switch based on ferrocene containing strings. Upon redox control, the ferrocene unit is oxidized and CB[7] moves to the alkyl ammonium portion from the ferrocene unit (**Figure 1.24**).[180]

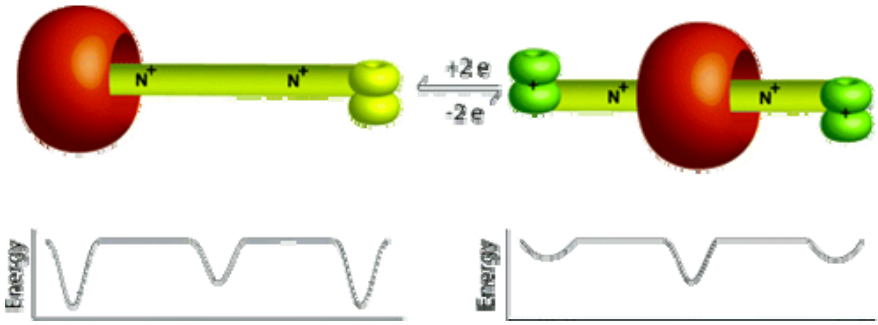

Figure 1.24 Pictorial representation of electrochemical control on the CB[7] binding location (top). Pseudorotaxanes and estimated relative potential energies associated with wheel movement along the axle (bottom).[180]

The potential applications of CB[*n*] in fluorescent color switches and emission intensity switches, controlled by CB[*n*] host threading/dethreading, and fluorescence on/off switches controlled by the binding stoichiometry with CB[*n*] host molecules, have also been demonstrated independently by the Macartney,[113,131] Wagner[181-183] and Nau groups.[184]

1.3.3.4 Molecular Recognition and Sensors

The previously mentioned CB[6] based molecular machine designed by Kim *et al.* can potentially be employed as a fluorescent pH sensor, as the machine displays a pH-sensitive switchable fluorescent output.[173] A few years after the discovery of the CB[*n*] homologues, an elegant design and construction of a CB[8]-based molecular detector was reported by the Kaifer group.[143] They demonstrated the formation of a binary inclusion complex between the 2,7-dimethyldiazapyrenium dication (Me_2DAP^{2+}) and CB[8], which can further include another electron-rich aromatic guest such as catechol or dopamine inside the hydrophobic CB[8] cavity, to form a ternary complex stabilized by charge-transfer interactions between the two guests (Figure 1.25).

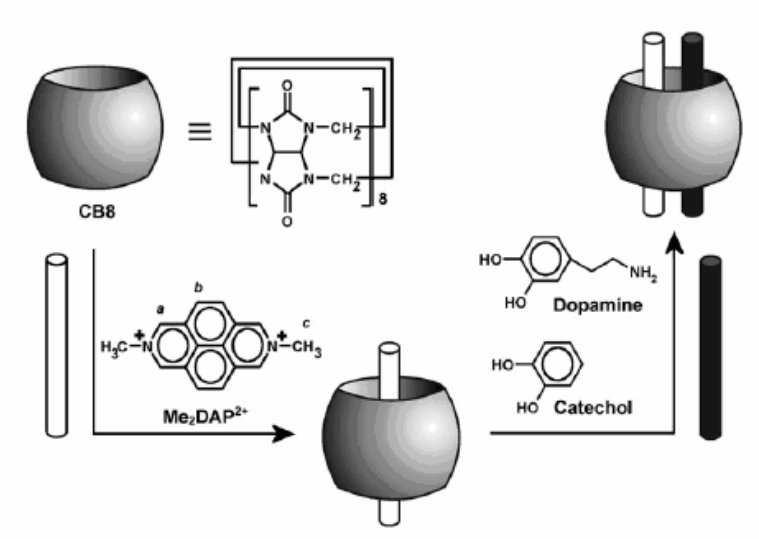

Figure 1.25 Formation of a binary complex, based on CB[8], as a detector to sense catechol and dopamine through ternary complex formation.[143]

As illustrated by Figure 1.25, the ternary complex formation is accompanied by a quench of the fluorescence of Me_2DAP^{2+}. Under these conditions, the CB[8]-based complex has been developed into a novel fluorescence-based molecular sensor to detect catecholamine derivatives,[143] and more recently indole derivatives.[144]

Another novel molecular sensor for the detection of peptides bearing N-terminal tryptophan has been designed using the same principle (CT-interaction based recognition in a CB[8] cavity) by Urbach and coworkers.[142] The idea was originated from previously reported CT-stabilized ternary complexes formation based on methylviologen (MV^{2+}), CB[8], and another electron-donating aromatic species.[138] In the design of this peptide sensor, a 1:1 ratio of MV^{2+} and CB[8] is employed as a detector to further include the tryptophan residue of tryptophan-containing peptides, forming the CT-stabilized ternary complex.

Three tryptophan-containing tripeptides were used to test the detector and the result suggested that a positive charge near the indole in a peptide increases the guest's binding affinity with the MV^{2+}@CB[8] to form a ternary complex. The Trp-Gly-Gly is bound more tightly to MV^{2+}@CB[8] than Gly-Trp-Gly, followed by Gly-Gly-Trp, such that MV^{2+}@CB[8] should bind a N-terminal tryptophan with higher affinity than either the internal or C-terminal tryptophan residue (Figure 1.26). This novel design forms the basis of a specific peptide recognition sensor. This work was further extended by discarding the MV^{2+}, as it was found that the N-terminal aromatic peptides can

themselves form 2:1 inclusion complexes with CB[8].[185] Thus, a sequence-specific recognition of peptides by CB[8] has been achieved, which can be used for the sensing or for the separation of peptides with a specific sequence.

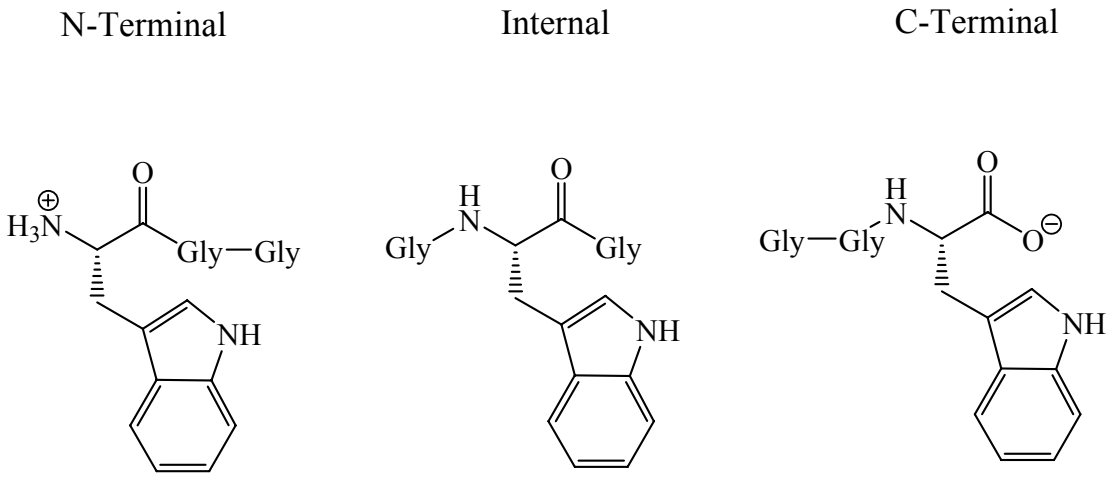

Figure 1.26 Tryptophan-containing tripeptides examined by MV^{2+}@CB[8] (diagram adapted from reference[142]).

Very recently, achiral CB[*n*] molecules were endowed with significant enantiomeric and diastereomeric discrimination by incorporating a strong chiral binder.[186] It has been demonstrated that (S)-2-methylbutylamine (as a strong binder) can be discriminated by two enantiomeric supramolecular hosts, composed of CB[6] and (R)-2-methylpiperazine, with an unprecedented 95% enantioselectivity in aqueous NaCl solution. This is the highest enantioselectivity ever reported for a supramolecular system derived from an achiral host. Similarly, CB[7], with a larger cavity than CB[6], exhibited diastereoselectivities up to 8 times higher for diastereomeric dipeptides, as demonstrated

for L-Phe-L-Leu-NH_3^+ versus L-Phe-D-Leu-NH_3^+.[186]

1.3.3.5 Drug and Gene Delivery

Kim and coworkers have developed a novel prototype of including the host molecule CB[6] into DNA complexes through a non-covalent self-assembly.[187] Because of the dipolar nature for both CB[6] and DNA, they don't bind to each other. However, in this novel strategy Kim *et al*. designed a linker molecule that has two different types of binding sites, an acridine unit and a spermine unit (Figure 1.27). Again, the linking strategy relies on non-covalent assembly between DNA and acridine, and between spermine and CB[6]. Upon addition of the linkers, the ternary complex is formed. Partial DNA protection from cleavage by the restriction enzyme *Ban*II has been observed using this CB[6]-based ternary DNA complex.

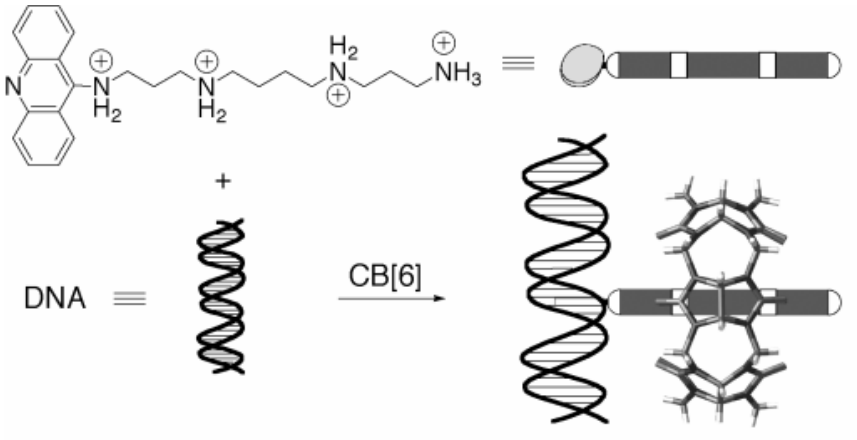

Figure 1.27 Non-covalent self-assembly of CB[6] and DNA through a linker.[91]

To extend this research, Kim and coworkers demonstrated in their recent research that a diaminobutane attached to a dendrimer binds to CB[6] and DNA to form a ternary complex through non-covalent interactions, working as a gene delivery carrier.[188]

It has also been reported that CB[*n*], where *n* = 6 - 8, form complexes with platinum-based complexes (Figure 1.28), which are potential anticancer drugs. This is an important potential application for CB[*n*] as a drug carrier and in controlled release, and a significant feature of this is that the toxicity of the platinum complexes are reduced upon complexation with CB[*n*].[36,125,189,190]

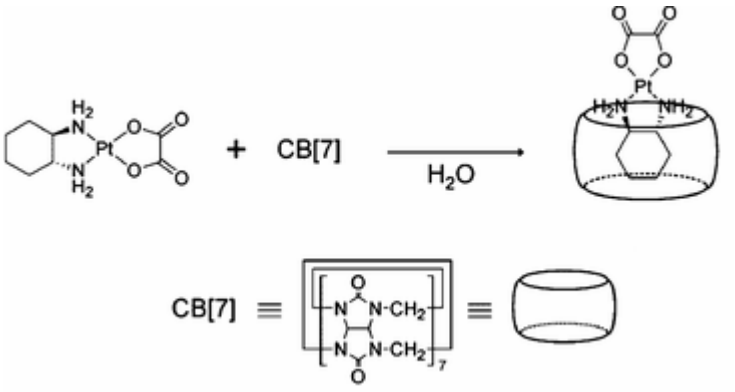

Figure 1.28 Inclusion complex of oxaliplatin in CB[7] in water.[36]

1.3.3.6 Water Treatment

In 1905, CB[6] was applied to the complexation of dye molecules such as congo red and methylene blue, even though the actual structure of CB[6] was unknown.[87,91] Many years later, the capability of CB[6] to remove heavy metals, aromatic substances and

dyes from waste water was intensively studied by the Buschmann[91] and Karcher[191-193] groups independently. The influence of the main parameters governing the sorption of these guest species, such as pH, temperature, salt concentration, has been studied. Before the CB[*n*] family can be used practically in real-world water treatment, some of the major problems, such as attachment of CB[*n*] onto a solid phase for use in fixed-filters and the cost of the CB[*n*] (compared to current methods of dye removal in water treatment) have to be resolved in a economic way.[91] Fortunately, CB[*n*] has now been incorporated onto a solid phase,[39] although the cost of CB[*n*] is still too high for its practical use in water treatment.

1.3.4 Summary and Perspectives

Over 100 years ago, CB[6] was first prepared in the lab of Behrend and coworkers. Not until 76 years later was this molecule fully characterized by Mock *et al.*, and the potential of its being an important host molecule was demonstrated by these pioneers in this field. Elegant research work on CB[6] has been extensively carried out by Kim and coworkers including the synthesis, host-guest chemistry, and applications of CB[6] and derivatives. Joined by other research groups led by Day, Buschmann, Nau, Kaifer, Isaacs, Steinke, Macartney, Fedin, Urbach, Wagner and others, successful research in the last twenty years has expanded the range of homologues, fully or partially solved some of problems such as limited size availability and poor solubility, and demonstrated that cucurbiturils are versatile hosts for fundamental and applied research related to chemistry,

physics, materials science and biochemistry. Applications have been achieved in many areas such as chemical reaction catalysis, waste stream purifications, and drug and gene carriers. Compared to the myriad research reports in the literature on cyclodextrins, the research on cucurbiturils host-guest chemistry and its applications has just started, and significant research opportunities lie ahead with many realistic problems to be addressed in the future. The novel binding properties of CB[*n*] suggest that the CB[*n*] family will likely become important components in the construction of molecular machines and nanostructures and that the CB[*n*] family will play very important roles in biochemical applications.[91]

1.4 Research Aims

With the knowledge of the CB[*n*] family's novel complexation properties and a clear picture of CB[*n*] research in other groups, my research has been focused on the development of new supramolecular host-guest complexes based on CB[*n*], the study of their functional properties, and investigation of the altered physical and chemical properties of guest aromatic molecules induced by CB[*n*] complexation. My main research projects primarily include the following topics.

1) To screen and investigate the application of CB[*n*] in catalyzing or inhibiting chemical reactions, concentrating on the photoisomerization of guest molecules such as 1,2-bis(4-pyridyl)ethylene and its derivatives, and the photodimerization of guest molecules such as protonated 2-aminopyridine (Chapter 2).

2) To study the effect of CB[*n*] complexation on the fluorescence of included guest fluorophores, such as emission color changes of aromatic amines and alcohols, emission intensity changes or fluorescence on/off switching of acridizinium cations upon their complexation with CB[*n*] molecules (Chapter 3).

3) To investigate changes in the acidity of weak carbon acid molecules such as imidazolium and thiazolium cations, upon their complexation with CB[7], through monitoring of their C(2)-H/D exchange rates in the absence and the presence of CB[7] in D_2O (Chapter 4).

4) To study the effect of CB[*n*] complexation on the visible colors of guest molecules through different mechanisms, such as the control of a reaction equilibrium of the 4,4'-bis(dimethylamino)diphenyl carbinol involving two species of different colors, or the control the formation of a monomer/dimer (with different absorbance) equilibrium of the pinacyanol cation upon complexation with CB[7], which have the potential to be applied as a "naked-eye" molecular sensor or visible color switch (Chapter 5).

References

(1) Lehn, J.-M. *Pure Appl. Chem.* **1978**, *50*, 871.

(2) Lehn, J.-M. *Angew. Chem. Int. Ed. Engl.* **1988**, *27*, 89.

(3) Lindoy, L. F.; Atkinson, I. M. *Self-assembly in supramolecular systems* The Royal Society of Chemistry: Cambridge, 2000.

(4) McNaught, A. D.; Wilkinson, A. *Compendium of chemical terminology*; Blackwell Science: Oxford, 1997.

(5) Eriksson, A.; Baase, W.; Zhang, X.; Heinz, D.; Blaber, M.; Baldwin, E.; Matthews, B. *Science* **1992**, *255*, 178.

(6) Claessens, C. G.; Stoddart, J. F. *J. Phys. Org. Chem.* **1997**, *10*, 254.

(7) Morokuma, K. *Acc. Chem. Res.* **1977**, *10*, 294.

(8) Scneider, H.-J.; Philippi, K.; Pohlmann, J. *Angew. Chem. Int. Ed. Engl.* **1984**, *23*, 908.

(9) Steed, J. W.; Atwood, J. L. *Supramolecular Chemistry*; Chichester: New York, 2000.

(10) Curtis, M. D.; Cao, J.; Kampf, J. W. *J. Am. Chem. Soc.* **2004**, *126*, 4318.

(11) Cram, D. J.; Cram, J. M. *Container Molecules and Their Guests*; The Royal Society of Chemistry: Cambridge, 1994.

(12) Cram, D. J. *From Design to Discovery*; ACS: Washington D.C., 1990.

(13) Atwood, J. L.; Steed, J. W. *Encyclopedia of supramolecular chemistry*; M. Dekker: New York, 2004.

(14) Fischer, E. *Ber. Dtsch. Chem. Ges.* **1894**, 2985.

(15) Scheneider, H.-J.; Yatsimirsky, A. *Principles and Methods in Supramolecular Chemistry*; Wiley: Toronto, 2000.

(16) Moran, J. R.; Karbach, S.; Cram, D. J. *J. Am. Chem. Soc.* **1982**, *104*, 5826.

(17) Sijbesma, R. P.; Nolte, R. J. M. *Top. Curr. Chem.* **1995**, *175*, 25.

(18) Rowan, A. E.; Elemans, J. A. A. W.; Nolte, R. J. M. *Acc. Chem. Res.* **1999**, *32*, 995.

(19) MacNicol, D. D.; McKendrick, J. J.; Wilson., D. R. *Chem. Soc. Rev.* **1978**, *7*, 65.

(20) Tsoucaris, G.; Knossow, M.; Green, B. S.; Arad-Yellin, R. *Mol. Cryst. Liq. Cryst.* **1983**, *96*, 181.

(21) Nakamura, A.; Inoue, Y. *J. Am. Chem. Soc.* **2003**, *125*, 966.

(22) Choi, S.; Park, S. H.; Ziganshina, A. Y.; Ko, Y. H.; Lee, J. W.; Kim, K. *Chem. Commun.* **2003**, 2176.

(23) Knipe, A. C. *J. Chem. Educ.* **1976**, 618.

(24) Balzani, V.; Gomez-Lopez, M.; Stoddart, J. F. *Acc. Chem. Res.* **1998**, *31*, 405.

(25) Silva, A. P. d.; McClenaghan, N. D.; McCoy, C. P. In *Molecular Switches*; Feringa, B. L., Ed.; Wiley: Weinheim, 2001, p 339.

(26) Rogers, C. W.; Wolf, M. O. *Coord. Chem. Rev.* **2002**, *233-234*, 341.

(27) Valeur, B.; Leray, I. *Coord. Chem. Rev.* **2000**, *205*, 3.

(28) Beer, P. D.; Gale, A. P.; Smith, D. K. *Supramolecular Chemistry*; Oxford University Press: New York, 1999.

(29) Helgeson, R. C.; Czech, B. P.; Chapoteau, E.; Gebauer, C. R.; Kumar A.; Cram, D. J.

J. Am. Chem. Soc. **1989**, 111, 6339.

(30) Cram, D. J.; Ho, S. P. *J. Am. Chem. Soc.* **1986**, *108*, 2998.

(31) Zyryanov, G. V.; Kang, Y.; Rudkevich, D. M. *J. Am. Chem. Soc.* **2003**, *125*, 2997.

(32) Anslyn, E. V. *J. Org. Chem.* **2007**, *72*, 687.

(33) Buri, P.; Gumma, A. *Drug Targeting*; Elsevier: Amsterdam, 1985.

(34) Uekama, K.; Hirayama, F.; Irie, T. *Chem. Rev.* **1998**, *98*, 2045.

(35) Duchene, D. *New Trends in Cyclodextrins and Derivatives*; Editions de Sante: Paris, 1991.

(36) Jeon, Y. J.; Kim, S. Y.; Ko, Y. H.; Sakamoto, S.; Yamaguchi, K.; Kim, K. *Org. Biomol. Chem.* **2005**, *3*, 2122.

(37) Lamb, J. D.; Smith, R. G. *J. Chrom.* **1991**, 73.

(38) Cserhati, T.; Forgacs, E. *Cyclodextrins in Chromatography*; RSC Loughborough, 2003.

(39) Nagarajan, E. R.; Oh, D. H.; Selvapalam, N.; Ko, Y. H.; Park, K. M.; Kim, K. *Tetrahedron Lett.* **2006**, *47*, 2073.

(40) Kimura, K.; Hayata, E.; Shono, T. *Chem. Commun.* **1984**, 271.

(41) Pedersen, C. J. *J. Am. Chem. Soc.* **1967**, *89*, 7017.

(42) Bradshaw, J. S.; Izatt, R. M. *Acc. Chem. Res.* **1997**, *30*, 338.

(43) Dalley, N. K.; Smith, J. S.; Larsen, S. B.; Matheson, K. L.; Christensen, J. J.; Izatt, R. M. *J. Chem. Soc., Chem. Commun.* **1975**, 84.

(44) Dietrich, B.; Lehn, J.-M.; Sauvage, J.-P. *Tetrahedron Lett.* **1969**, 2885.

(45) Dietrich, B.; Lehn, J.-M.; Sauvage, J.-P. *Tetrahedron Lett.* **1969**, 2889.

(46) Graf, E.; Lehn, J.-M. *J. Am. Chem. Soc.* **1976**, *98*, 6403.

(47) Harada, A. In *Large Ring Molecules*; Semlyen, J. A., Ed.; Wiley: Chichester, 1996.

(48) Harada, A.; Takahashi, S. *J. Chem. Soc., Chem. Commun.* **1984**, 645.

(49) Hapiot, F.; Tilloy, S.; Monflier, E. *Chem. Rev.* **2006**, *106*, 767-781.

(50) Rekharsky, M. V.; Inoue, Y. *Chem. Rev.* **1998**, *98*, 1875.

(51) Harada, A. *Acc. Chem. Res.* **2001**, *34*, 456.

(52) Wenz, G.; Han, B.-H.; Muller, A. *Chem. Rev.* **2006**, *106*, 782.

(53) Takahashi, K. *Chem. Rev.* **1998**, *98*, 2013.

(54) Hedges, A. R. *Chem. Rev.* **1998**, 2035.

(55) Gutsche, C. D. *Calixarenes*; RSC: Cambridge, 1989.

(56) Mandolini, L.; Ungaro, R. *Calixarenes in action*; Imperial College Press: London, 2000.

(57) Boehmer, V. In *Chemistry of Phenols*; Rappoport, Z., Ed.; Wiley: Chichester, 2003; Vol. 2, p 1369.

(58) Gutsche, C. D. *Acc. Chem. Res.* **1983**, *16*, 161.

(59) Lhotak, P.; Shinkai, S. *J. Phys. Org. Chem.* **1997**, *10*, 273.

(60) Lhotak, P. *Top. Curr. Chem.* **2005**, *255*, 65.

(61) Casnati, A.; Sansone, F.; Ungaro, R. *Advances in Supramolecular Chemistry* **2003**, *9*, 163.

(62) Prins, L. J.; Timmerman, P.; Reinhoudt, D. N. *Pure Appl. Chem.* **1998**, *70*, 1459.

(63) Wei, A. *Chem. Commun.* **2006**, 1581.

(64) Smith, K. M. *Porphyrins and Metalloporphyrins*; Elsevier: Amsterdam, 1976.

(65) Jasat, A.; Dolphin, D. *Chem. Rev.* **1997**, *97*, 2267.

(66) Fleischer, E. B. *Acc. Chem. Res.* **1970**, *3*, 105.

(67) Balaban, T. S. *Acc. Chem. Res.* **2005**, *38*, 612.

(68) Maruyama, K.; Osuka, A. *Pure Appl. Chem.* **1990**, *62*, 1511.

(69) Hush, N. S.; Reimers, J. R.; Hall, L. E.; Johnston, L. A.; Crossley, M. J. *Annals of the New York Academy of Sciences* **1998**, *852*, 1.

(70) Freeman, W. A.; Mock, W. L.; Shih, N. Y. *J. Am. Chem. Soc.* **1981**, *103*, 7367.

(71) Mock, W. L. *Supramolecular Chemistry - Host Design and Molecular Recognition* **1995**, *175*, 1.

(72) Mock, W. L. *Top. Curr. Chem.* **1995**, *175*, 1.

(73) Kim, J.; Jung, I. S.; Kim, S. Y.; Lee, E.; Kang, J. K.; Sakamoto, S.; Yamaguchi, K.; Kim, K. *J. Am. Chem. Soc.* **2000**, *122*, 540.

(74) Jansen, K.; Buschmann, H. J.; Wego, A.; Dopp, D.; Mayer, C.; Drexler, H. J.; Holdt, H. J.; Schollmeyer, E. *J. Incl. Phenom. Macrocycl. Chem.* **2001**, *39*, 357.

(75) Liu, S. M.; Zavalij, P. Y.; Isaacs, L. *J. Am. Chem. Soc.* **2005**, *127*, 16798.

(76) Day, A. I.; Blanch, R. J.; Arnold, A. P.; Lorenzo, S.; Lewis, G. R.; Dance, I. *Angew . Chem. Int. Ed. Engl.,* **2001**, *41*, 275.

(77) Isaacs, L.; Park, S. K.; Liu, S. M.; Ko, Y. H.; Selvapalam, N.; Kim, Y.; Kim, H.; Zavalij, P. Y.; Kim, G. H.; Lee, H. S.; Kim, K. *J. Am. Chem. Soc.* **2005**, *127*, 18000.

(78) Huang, W. H.; Liu, S. M.; Zavalij, P. Y.; Isaacs, L. *J. Am. Chem. Soc.* **2006**, *128*, 14744.

(79) Flinn, A.; Hough, G. C.; Stoddart, J. F.; Williams, D. J. *Angew . Chem. Int. Ed. Engl.* **1992**, *31*, 1475.

(80) Sasmal, S.; Sinha, M. K.; Keinan, E. *Org. Lett.* **2004**, *6*, 1225.

(81) Zhao, J. Z.; Kim, H. J.; Oh, J.; Kim, S. Y.; Lee, J. W.; Sakamoto, S.; Yamaguchi, K.; Kim, K. *Angew. Chem. Int. Ed. Engl.* **2001**, *40*, 4233.

(82) Isobe, H.; Sato, S.; Nakamura, E. *Org. Lett.* **2002**, *4*, 1287.

(83) Day, A. I.; Arnold, A. P.; Blanch, R. J. *Molecules* **2003**, *8*, 74.

(84) Zhao, Y. J.; Xue, S. F.; Zhu, Q. J.; Tao, Z.; Zhang, J. X.; Wei, Z. B.; Long, L. S.; Hu, M. L.; Xiao, H. P.; Day, A. I. *Chin. Sci. Bull.* **2004**, *49*, 1111.

(85) Jon, S. Y.; Selvapalam, N.; Oh, D. H.; Kang, J. K.; Kim, S. Y.; Jeon, Y. J.; Lee, J. W.; Kim, K. *J. Am. Chem. Soc.* **2003**, *125*, 10186.

(86) Kim, K.; Selvapalam, N.; Ko, Y. H.; Park, K. M.; Kim, D.; Kim, J. *Chem. Soc. Rev.* **2007**, *36*, 267.

(87) Behrend, R.; Meyer, E.; Rusche, F. *Justus Liebigs Ann. Chem.* **1905**, *339*, 1.

(88) Day, A.; Arnold, A. P.; Blanch, R. J.; Snushall, B. *J. Org. Chem.* **2001**, *66*, 8094.

(89) Kim, K.; Samal, S.; Kumar, R. N.; Selvapalam, N.; Oh, D. H.; PCT: US, 2005; Vol. WO05/103053.

(90) Lee, J. W.; Samal, S.; Selvapalam, N.; Kim, H. J.; Kim, K. *Acc. Chem. Res.* **2003**, *36*, 621.

(91) Lagona, J.; Mukhopadhyay, P.; Chakrabarti, S.; Isaacs, L. *Angew. Chem. Int. Ed. Engl.* **2005**, *44*, 4844.

(92) Mock, W. L.; Shih, N. Y. *J. Org. Chem.* **1986**, *51*, 4440.

(93) Mock, W. L. In *Comprehensive Supramolecular Chemistry*; Vogtle, F., Ed.; Pergamon: Oxford, 1996; Vol. 2, p 477.

(94) Zhang, H. Z.; Paulsen, E. S.; Walker, K. A.; Krakowiak, K. E.; Dearden, D. V. *J. Am. Chem. Soc.* **2003**, *125*, 9284.

(95) Marquez, C.; Hudgins, R. R.; Nau, W. M. *J. Am. Chem. Soc.* **2004**, *126*, 5806.

(96) Buschmann, H. J.; Cleve, E.; Jansen, K.; Wego, A.; Schollmeyer, E. *J. Incl. Phenom. Macrocyc. Chem.* **2001**, *40*, 117.

(97) Buschmann, H. J.; Cleve, E.; Schollmeyer, E. *Inorg. Chim. Acta* **1992**, *193*, 93.

(98) Hoffmann, R.; Knoche, W.; Fenn, C.; Buschmann, H. J. *J. Chem. Soc. Faraday Trans.* **1994**, *90*, 1507.

(99) Buschmann, H. J.; Jansen, K.; Meschke, C.; Schollmeyer, E. *J. Solution Chem.* **1998**, *27*, 135.

(100) El Haouaj, M.; Luhmer, M.; Ko, Y. H.; Kim, K.; Bartik, K. *J. Chem. Soc. Perkin Trans. 2* **2001**, 804.

(101) El Haouaj, M.; Ko, Y. H.; Luhmer, M.; Kim, K.; Bartik, K. *J. Chem. Soc. Perkin Trans. 2* **2001**, 2104.

(102) Buschmann, H. J.; Schollmeyer, E.; Mutihac, L. *Thermochim. Acta* **2003**, *399*, 203.

(103) Buschmann, H. J.; Jansen, K.; Schollmeyer, E. *Thermochim. Acta* **2000**, *346*, 33.

(104) Buschmann, H. J.; Jansen, K.; Schollmeyer, E. *J. Incl. Phenom. Macrocycl. Chem.* **2000**, *37*, 231.

(105) Buschmann, H. J.; Cleve, E.; Jansen, K.; Schollmeyer, E. *Anal. Chim. Acta* **2001**, *437*, 157.

(106) Zhang, G. L.; Xu, Z. Q.; Xue, S. F.; Zhu, Q. J.; Tao, Z. *Chin. J. Inorg. Chem.* **2003**, *19*, 655.

(107) Kellersberger, K. A.; Anderson, J. D.; Ward, S. M.; Krakowiak, K. E.; Dearden, D. V. *J. Am. Chem. Soc.* **2001**, *123*, 11316.

(108) Miyahara, Y.; Abe, K.; Inazu, T. *Angew . Chem. Int. Ed. Engl.,* **2002**, *41*, 3020.

(109) Liu, J. X.; Long, L. S.; Huang, R. B.; Zheng, L. S. *Cryst. Growth Des.* **2006**, *6*, 2611.

(110) Kim, H. J.; Jeon, W. S.; Ko, Y. H.; Kim, K. *Proc. Natl. Acad. Sci. USA* **2002**, *99*, 5007.

(111) Ong, W.; Gomez-Kaifer, M.; Kaifer, A. E. *Org. Lett.* **2002**, *4*, 1791.

(112) Liu, S. M.; Ruspic, C.; Mukhopadhyay, P.; Chakrabarti, S.; Zavalij, P. Y.; Isaacs, L. *J. Am. Chem. Soc.* **2005**, *127*, 15959.

(113) Wang, R.; Yuan, L.; Macartney, D. H. *Chem. Commun.* **2005**, 5867.

(114) Sindelar, V.; Cejas, M. A.; Raymo, F. M.; Kaifer, A. E. *New J. Chem.* **2005**, *29*, 280.

(115) Wang, R. B.; Yuan, L. N.; Macartney, D. H. *Chem. Commun.* **2006**, 2908.

(116) Hettiarachchi, D. S. N.; Macartney, D. H. *Can. J. Chem.* **2006**, *84*, 905.

(117) Yuan, L.; Wang, R.; Macartney, D. H. *Tetrahedron: Asymmetry* **2007**, *18*, 483.

(118) Wang, R.; Yuan, L.; Macartney, D. H. *J. Org. Chem.* **2006**, *71*, 1237.

(119) Mukhopadhyay, P.; Wu, A.; Isaacs, L. *J. Org. Chem.* **2004**, *69*, 6157.

(120) Blanch, R. J.; Sleeman, A. J.; White, T. J.; Arnold, A. P.; Day, A. I. *Nano Lett.* **2002**, *2*, 147.

(121) Constabel, F.; Geckeler, K. E. *Fuller. Nanotub. Carbon Nanostruct.* **2004**, *12*, 811.

(122) Jeon, W. S.; Moon, K.; Park, S. H.; Chun, H.; Ko, Y. H.; Lee, J. Y.; Lee, E. S.; Samal, S.; Selvapalam, N.; Rekharsky, M. V.; Sindelar, V.; Sobransingh, D.; Inoue, Y.; Kaifer, A. E.; Kim, K. *J. Am. Chem. Soc.* **2005**, *127*, 12984.

(123) Wang, R.; Yuan, L.; Macartney, D. H. *Organometallics* **2006**, *25*, 1820.

(124) Ong, W.; Kaifer, A. E. *Organometallics* **2003**, *22*, 4181.

(125) Wheate, N. J.; Day, A. I.; Blanch, R. J.; Arnold, A. P.; Cullinane, C.; Collins, J. G. *Chem. Commun.* **2004**, 1424.

(126) Hwang, I.; Baek, K.; Jung, M.; Kim, Y.; Park, K. M.; Lee, D.-W.; Selvapalam, N.; Kim, K. *J. Am. Chem. Soc.* **2007**, *129*, 4170.

(127) Yang, S. L.; Xue, S. F.; Zhu, Q. J.; Tao, Z.; Zhang, J. X.; Zhou, X. *Chin. J. Org. Chem.* **2005**, *25*, 427.

(128) Jeon, W. S.; Kim, H. J.; Lee, C.; Kim, K. *Chem. Commun.* **2002**, 1828.

(129) Sun, S. G.; Zhang, R.; Andersson, S.; Pan, J. X.; Akermark, B.; Sun, L. C. *Chem.*

Commun. **2006**, 4195.

(130) Jiang, G. C.; Li, G. T. *J. Photochem. Photobiol. B-Biol.* **2006**, *85*, 223.

(131) Wang, R.; Yuan, L.; Ihmels, H.; Macartney, D. H. *Eur. J. Chem.* **2007**, 13, 6468.

(132) Ziganshina, A. Y.; Ko, Y. H.; Jeon, W. S.; Kim, K. *Chem. Commun.* **2004**, 806.

(133) Jon, S. Y.; Ko, Y. H.; Park, S. H.; Kim, H. J.; Kim, K. *Chem. Commun.* **2001**, 1938.

(134) Pattabiraman, M.; Kaanumalle, L. S.; Natarajan, A.; Ramamurthy, V. *Langmuir* **2006**, *22*, 7605.

(135) Pattabiraman, M.; Natarajan, A.; Kaanumalle, L. S.; Ramamurthy, V. *Org. Lett.* **2005**, *7*, 529.

(136) Kim, H. J.; Heo, J.; Jeon, W. S.; Lee, E.; Kim, J.; Sakamoto, S.; Yamaguchi, K.; Kim, K. *Angew. Chem. Int. Ed. Engl.* **2001**, *40*, 1526.

(137) Ko, Y. H.; Kim, E.; Hwang, I.; Kim, K. *Chem. Commun.* **2007**, *In press*.

(138) Lee, J. W.; Kim, K.; Choi, S.; Ko, Y. H.; Sakamoto, S.; Yamaguchi, K.; Kim, K. *Chem. Commun.* **2002**, 2692.

(139) Jeon, Y. J.; Bharadwaj, P. K.; Choi, S. W.; Lee, J. W.; Kim, K. *Angew. Chem. Int. Ed.* **2002**, *41*, 4474.

(140) Ko, Y. H.; Kim, K.; Kang, J. K.; Chun, H.; Lee, J. W.; Sakamoto, S.; Yamaguchi, K.; Fettinger, J. C.; Kim, K. *J. Am. Chem. Soc.* **2004**, *126*, 1932.

(141) Jeon, W. S.; Kim, E.; Ko, Y. H.; Hwang, I. H.; Lee, J. W.; Kim, S. Y.; Kim, H. J.; Kim, K. *Angew. Chem. Int. Ed. Engl.* **2005**, *44*, 87.

(142) Bush, M. E.; Bouley, N. D.; Urbach, A. R. *J. Am. Chem. Soc.* **2005**, *127*, 14511.

(143) Sindelar, V.; Cejas, M. A.; Raymo, F. M.; Chen, W. Z.; Parker, S. E.; Kaifer, A. E. *Chem. Eur. J.* **2005**, *11*, 7054.

(144) Ling, Y.; Wang, W.; Kaifer, A. E. *Chem. Commun.* **2007**, 610.

(145) Wang, W.; Kaifer, A. E. *Angew. Chem. Int. Ed. Engl.* **2006**, *45*, 7042.

(146) Kim, S. Y.; Jung, I. S.; Lee, E.; Kim, J.; Sakamoto, S.; Yamaguchi, K.; Kim, K. *Angew. Chem. Int. Ed. Engl.* **2001**, *40*, 2119.

(147) Mock, W. L.; Irra, T. A.; Wepsiec, J. P.; Manimaran, T. L. *J. Org. Chem.* **1983**, *48*, 3619.

(148) Krasia, T. C.; Steinke, J. H. G. *Chem. Commun.* **2002**, 22.

(149) Tuncel, D.; Steinke, J. H. G. *Chem. Commun.* **1999**, 1509.

(150) Tuncel, D.; Steinke, J. H. G. *Macromolecules* **2004**, *37*, 288.

(151) Tuncel, D.; Steinke, J. H. G. *Chem. Commun.* **2001**, 253.

(152) Tuncel, D.; Steinke, J. H. G. *Chem. Commun.* **2002**, 496.

(153) Pattabiraman, M.; Natarajan, A.; Kaliappan, R.; Mague, J. T.; Ramamurthy, V. *Chem. Commun.* **2005**, 4542.

(154) Wang, R.; Yuan, L.; Macartney, D. H. *Can. J. Chem.* **2007**, 13, 6468.

(155) Mohanty, J.; Nau, W. M. *Angew. Chem. Int. Ed. Engl.* **2005**, *44*, 3750.

(156) Mock, W. L.; Shih, N. Y. *J. Am. Chem. Soc.* **1988**, *110*, 4706.

(157) Jeon, Y. M.; Whang, D.; Kim, J.; Kim, K. *Chem. Lett.* **1996**, 503.

(158) Meschke, C.; Buschmann, H. J.; Schollmeyer, E. *Macromol. Rapid Commun.*

1998, *19*, 59.

(159) Meschke, C.; Buschmann, H. J.; Schollmeyer, E. *Polymer* **1999**, *40*, 945.

(160) Buschmann, H. J.; Wego, A.; Schollmeyer, E.; Dopp, D. *Supramol. Chem.* **2000**, *11*, 225.

(161) Wego, A.; Jansen, K.; Buschmann, H. J.; Schollmeyer, E.; Dopp, D. *J. Incl. Phenom. Macro. Chem.* **2002**, *43*, 201.

(162) He, X. Y.; Li, G.; Chen, H. L. *Inorg. Chem. Commun.* **2002**, *5*, 633.

(163) Tan, Y. B.; Choi, S. W.; Lee, J. W.; Ko, Y. H.; Kim, K. *Macromolecules* **2002**, *35*, 7161.

(164) Choi, S.; Lee, J. W.; Ko, Y. H.; Kim, K. *Macromolecules* **2002**, *35*, 3526.

(165) Hou, Z. S.; Tan, Y. B.; Zhou, Q. F. *Polymer* **2006**, *47*, 5267.

(166) Lee, J. W.; Ko, Y. H.; Park, S. H.; Yamaguchi, K.; Kim, K. *Angew. Chem. Int. Ed. Engl.* **2001**, *40*, 746.

(167) Ong, W.; Kaifer, A. E. *Angew. Chem. Int. Ed. Engl.* **2003**, *42*, 2164.

(168) Sobransingh, D.; Kaifer, A. E. *Chem. Commun.* **2005**, 5071.

(169) Sobransingh, D.; Kaifer, A. E. *Langmuir* **2006**, *22*, 10540.

(170) Kim, K. *Chem. Soc. Rev.* **2002**, *31*, 96.

(171) Balzani, V.; Credi, A.; Raymo, F. M.; Stoddart, J. F. *Angew. Chem. Int. Ed.* **2000**, *39*, 3348.

(172) Mock, W. L.; Pierpont, J. *J. Chem. Soc. Chem. Commun.* **1990**, 1509.

(173) Jun, S. I.; Lee, J. W.; Sakamoto, S.; Yamaguchi, K.; Kim, K. *Tetrahedron Lett.*

2000, *41*, 471.

(174) Lee, J. W.; Kim, K. P.; Kim, K. *Chem. Commun.* **2001**, 1042.

(175) Sindelar, V.; Silvi, S.; Kaifer, A. E. *Chem. Commun.* **2006**, 2185.

(176) Tuncel, D.; Tiftik, H. B.; Salih, B. *J. Mater. Chem.* **2006**, *16*, 3291.

(177) Kim, K.; Jeon, W. S.; Kang, J. K.; Lee, J. W.; Jon, S. Y.; Kim, T.; Kim, K. *Angew. Chem. Int. Ed. Engl.* **2003**, *42*, 2293.

(178) Kim, K.; Kim, D.; Lee, J. W.; Ko, Y. H.; Kim, K. *Chem. Commun.* **2004**, 848.

(179) Jeon, W. S.; Ziganshina, A. Y.; Lee, J. W.; Ko, Y. H.; Kang, J. K.; Lee, C.; Kim, K. *Angew. Chem. Int. Ed. Engl.* **2003**, *42*, 4097.

(180) Sobransingh, D.; Kaifer, A. E. *Org. Lett.* **2006**, *8*, 3247.

(181) Wagner, B. D.; Fitzpatrick, S. J.; Gill, M. A.; MacRae, A. I.; Stojanovic, N. *Can. J. Chem.* **2001**, *79*, 1101.

(182) Wagner, B. D.; Stojanovic, N.; Day, A. I.; Blanch, R. J. *J. Phys. Chem. B.* **2003**, *107*, 10741.

(183) Rankin, M. A.; Wagner, B. D. *Supramol. Chem.* **2004**, *16*, 513.

(184) Marquez, C.; Nau, W. M. *Angew. Chem. Int. Ed. Engl.* **2001**, *40*, 4387.

(185) Heitmann, L. M.; Taylor, A. B.; Hart, P. J.; Urbach, A. R. *J. Am. Chem. Soc.* **2006**, *128*, 12574.

(186) Rekharsky, M. V.; Yamamura, H.; Inoue, C.; Kawai, M.; Osaka, I.; Arakawa, R.; Shiba, K.; Sato, A.; Ko, Y. H.; Selvapalam, N.; Kim, K.; Inoue, Y. *J. Am. Chem. Soc.* **2006**, *128*, 14871.

(187) Isobe, H.; Tomita, N.; Lee, J. W.; Kim, H. J.; Kim, K.; Nakamura, E. *Angew. Chem. Int. Ed. Engl.* **2000**, *39*, 4257.

(188) Lim, Y. B.; Kim, T.; Lee, J. W.; Kim, S. M.; Kim, H. J.; Kim, K.; Park, J. S. *Bioconjugate Chem.* **2002**, *13*, 1181.

(189) Wheate, N. J.; Buck, D. P.; Day, A. I.; Collins, J. G. *Dalton Trans.* **2006**, 451.

(190) Bali, M. S.; Buck, D. P.; Coe, A. J.; Day, A. I.; Collins, J. G. *Dalton Trans.* **2006**, 5337.

(191) Karcher, S.; Kornmuller, A.; Jekel, M. *Water Sci. Technol.* **1999**, *40*, 425.

(192) Karcher, S.; Kornmuller, A.; Jekel, M. *Water Res.* **2001**, *35*, 3309.

(193) Kornmuller, A.; Karcher, S.; Jekel, M. *Water Res.* **2001**, *35*, 3317.

Chapter 2

CUCURBIT[*n*]URIL MEDIATED PHOTOREACTIONS

This chapter is mainly concerned with the use of cucurbit[n]uril (CB[n]) in mediating organic photoreactions, such as catalyzing or inhibiting photodimerization or photoisomerization processes.

2.1 Introduction

It has been demonstrated in chapter 1 that host molecules can often work as catalysts or inhibitors for selected organic reactions. This chapter will focus on the photoreactions mediated by CB[*n*] host molecules.

Organic photochemical reactions often lead to products virtually inaccessible through thermal reactions, and are therefore very important in modern synthetic chemistry.[1] There are however, three primary challenges remaining in the area of photochemical

reactions. It is difficult to control the regio- or stereoselectivity of many organic photoreactions. Some photoreactions can occur through several routes and often it is very difficult to control the reaction so that it proceeds through a specifically favored pathway. In addition, many substances such as dye molecules, aromatic molecules, and compounds containing vinyl groups are unstable and photoreactive under UV light which creates major problems when storing, transferring or using those chemicals under light. Therefore it still remains a challenge to stabilize these compounds and to inhibit some unwanted photoreactions.

As previously discussed in chapter 1, CB[*n*] has been employed by several other research groups to solve some of the problems addressed above in the area of photochemical reactions.[2-7] Through a few selected examples involving photoreactions, we have demonstrated that the CB[*n*] host family has the capability and potential to catalyze photoreactions with a desired stereoselectivity, such as photodimerization of protonated 2-aminopyridine catalyzed by CB[7] to yield exclusively the *anti-trans* dimer (Figure 2.1).

In a second study, the photoisomerization of protonated (*E*)-1,2-bis(4-pyridyl)ethylene ((*E*)-H_2BPE^{2+}) was favored over a photohydration upon (*E*)-H_2BPE^{2+} encapsulation in the cavity of CB[7] in aqueous solution (Figure 2.2).

Finally, in a study of the inhibition of unwanted photoreactions or other chemical attacks, the photoreaction of (*E*)-1-ferrocenyl-2-(1-methyl-4-pyridinium)ethylene [(*E*)-$FcMPE^+$] was shown to be dramatically inhibited upon inclusion of (*E*)-$FcMPE^+$ in

CB[7] (Figure 2.3).

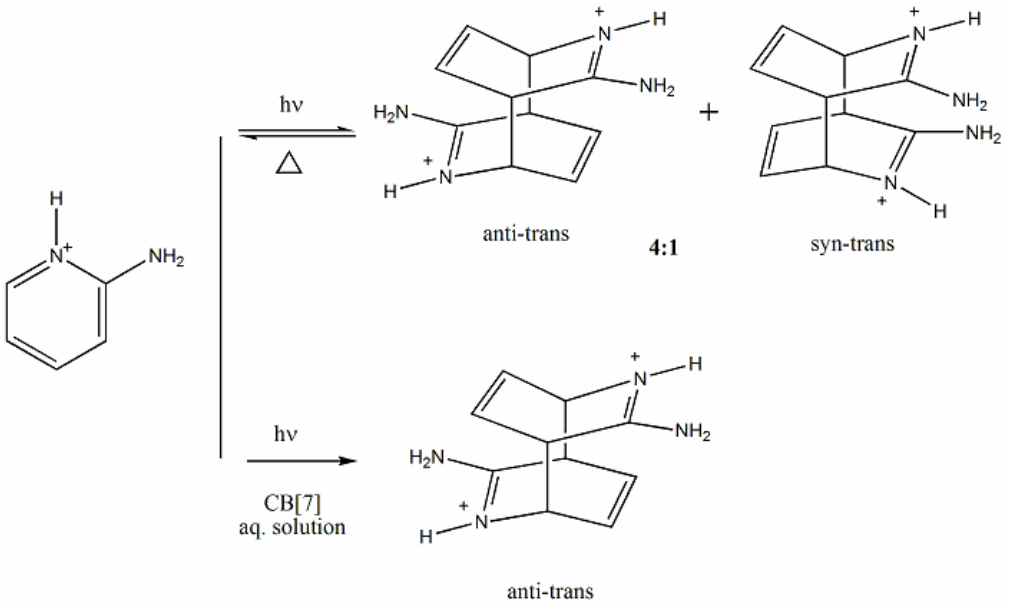

Figure 2.1 Schematic diagram of the CB[7] catalyzed stereoselective photodimerization of protonated 2-aminopyridine.

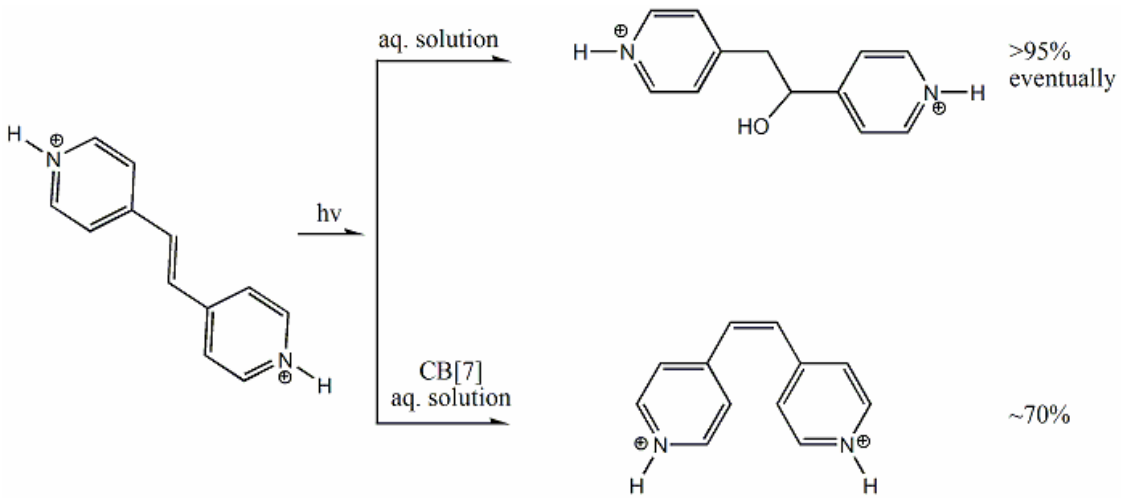

Figure 2.2 Schematic diagram of the CB[7] promoted photoisomerization of (*E*)-H_2BPE^{2+}.

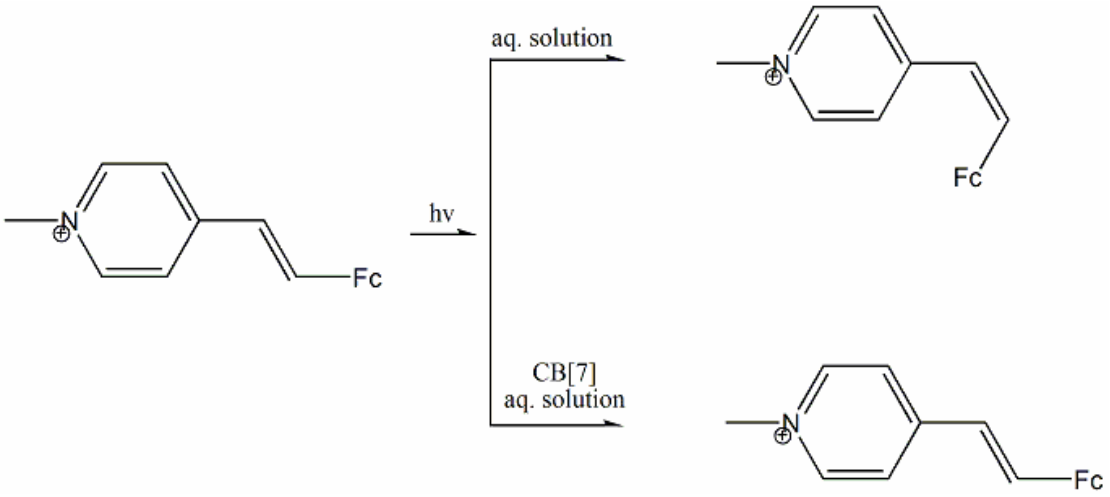

Figure 2.3 Schematic diagram of the CB[7] photoprotection of (*E*)-FcMPE$^+$.

2.2 Experimental

2.2.1 Materials Preparation

The host molecule cucurbit[7]uril and the 1,2-bis(1-alkyl-4-pyridinyl)ethylene guest molecules were synthesized according to modified literature methods, as described below. The oxidant $NH_4[Co(dipic)_2]$ ($dipic^{2-}$ = 2,6-pyridinedicarboxylate) was synthesized by Dr. J. A. Imonigie using a literature method.[8] The (*E*)-FcMPE$^+$ solutions used for cyclic voltammetry and kinetics experiments were prepared by anion exchange (Dowex (1-X8)) of the I^- ion by Cl^-.

All other chemicals involved in this project were purchased and used as received.

2.2.1.1 Cucurbit[7]uril

The CB[7] macrocyclic compound was prepared by using modified method of Day *et al*.[9] Briefly, 10 g glycoluril (70 mmol) and 4.22 g paraformaldehyde (140 mmol) were mixed thoroughly, and then ice-cold concentrated HCl (14.2 mL) was added to the powdered mixture, and stirred vigorously to get a gel-like mixture. The gel mixture was then heated slowly to 100 °C and kept at this temperature for about 20 hours, and thereafter the mixture was cooled down to room temperature. The remaining solid in the mixture was removed by filtration. The filtrate was concentrated to one fourth of its original volume and 5 mL of water was added to give a cloudy solution again, which was filtered again to remove any solid. Approximately 35 mL of methanol was added to the remaining filtrate, and then stirred overnight to give a precipitate which was collected by vacuum filtration. The off-white crude product was dissolved in 100 mL of hot 20% aqueous glycerol, heated and stirred for 30 minutes to give a relatively clear solution. A white precipitate was produced by addition of cold methanol, and was collected by vacuum filtration, and then washed several times with methanol to remove glycerol. The product was dried overnight in vacuum oven to give a white powder. Yield: 2.70 g, 25%. ^{1}H NMR (400 MHz, D_2O): δ 5.73 (d, J = 15.4 Hz, 14H), 5.48 (s, 14H), 4.19 (d, J = 15.4 Hz, 14H) ppm. ESI-MS: m/z = 1186 $(M+Na)^+$, calculated 1186.

2.2.1.2 1,2-bis(1-alkyl-4-pyridinyl)ethylene dihalides

Trans-1,2-bis(1-methyl-4-pyridinyl)ethylene diiodide ([(*E*)-BMPE]I_2) was

synthesized by a modification of the literature method for the syntheses of alkylated viologens.[10] *Trans*-1,2-bis(4-pyridyl)ethylene (0.46 g, 2.5 mmol) and iodomethane (0.7 mL, 10 mmol) were added to 10 mL of acetonitrile and refluxed for one day. An orange colored precipitate was filtered and washed sequentially by 5 mL of chloroform, 10 mL of acetone and 5 mL of ether, and then dried in a vacuum oven. Yield: 1.0 g, 86%. ^{1}H NMR (400 MHz, D_2O): δ 8.67 (d, J = 5.4 Hz, 4H), 8.12 (d, J = 5.4 Hz, 4H), 7.76 (s, 2H), 4.27 (s, 6H) ppm. ESI-MS: m/z = 212.4 $(M-2I)^+$, calculated 212.3.

The complex based on a 1:1 stoichiometry of (*E*)-$BMPE^{2+}$ and CB[7] was prepared by mixing equimolar amounts of the guest and host in D_2O (for NMR spectroscopy) or in water (for photochemical reactions or ESI-MS). ^{1}H NMR (400 MHz, D_2O): δ 8.49 (broad s, 4H), 7.64 (broad s, 4H), 6.92 (s, 2H), 4.31 (s, 6H) ppm. ESI-MS: m/z = 1375.8 $(M-2I)^+$, calculated 1374.5; 687.5 $(M-2I)^{2+}$, calculated 687.3.

Trans-1,2-bis(1-hexyl-4-pyridinyl)ethylene dibromide ([(*E*)-BHPE]Br_2) was synthesized using the same method as described above. *Trans*-1,2-bis(4-pyridyl)ethylene (0.91 g, 5.0 mmol) and 1-bromohexane (5.7 mL, 40 mmol) were added into 15 mL of acetonitrile and refluxed for two days. A yellow precipitate was filtered and sequentially washed by 5 mL of hot chloroform, 20 mL of acetone and 5 mL of ether, and then dried in a vacuum oven. Yield: 2.1 g, 82%. ^{1}H NMR (400 MHz, D_2O): δ 8.73 (d, J = 5.0 Hz, 4H), 8.12 (d, J = 5.0 Hz, 4H), 7.77 (s, 2H), 4.49 (t, J = 6.2 Hz, 4H), 1.92 (m, 4H), 1.22 (m, 12H), 0.75 (t, J = 6.2 Hz, 6H) ppm. ESI-MS: m/z = 351.6 $(M-Br)^+$, calculated 352.0; 176.5 $(M-2Br)^{2+}$, calculated 176.2.

The complex based on a 1:2 stoichiometry of (*E*)-BHPE^{2+} and CB[7] was prepared by mixing 1:2 molar ratio of the guest and host molecules in D_2O (for NMR spectroscopy) or in water (for photochemical reactions and ESI-MS). ^{1}H NMR (400 MHz, D_2O): δ 8.66 (d, *J* = 4.8 Hz, 4H), 8.15 (d, *J* = 4.8 Hz, 4H), 7.78 (s, 2H), 4.28 (broad, 4H), 1.69 (broad, 4H), 1.04 (broad, 12H), 0.55 (broad, 6H) ppm. ESI-MS: *m/z* = 1514.1 $(M-Br)^+$, calculated 1514.6; 757.7 $(M-2Br)^{2+}$, calculated 757.3.

2.2.1.3 Photodimer of 2-Aminopyridine

Both of the photodimers of the protonated 2-aminopyridine (APH^+), *anti-trans*- and *syn-trans*-4,8-diamino-3,7-diazatricyclo[4.2.2.2^{2,5}]dodeca-3,7,9,11-tetraene ($DADAT^{2+}$), were prepared from a photoirradiation of a APH^+ sample D_2O in the NMR tube under 365 nm UV light.[11,12]

Anti-trans-$DADAT^{2+}$. ^{1}H NMR (400 MHz, D_2O/DCl): δ 6.82 (t, *J* = 7 Hz, H5', 2H), 6.28 (t, *J* = 7 Hz, H4', 2H), 4.56 (dd, *J* = 9.7 Hz, 7 Hz, H6', 2H), 3.98 (t, *J* = 7 Hz, H3', 2H) ppm. ESI-MS *m/z* = 189.2 $[M+H]^+$. *Syn-trans*-$DADAT^{2+}$: ^{1}H NMR (400 MHz, D_2O/DCl) δ 6.40 (t, H5", 2H), 6.26 (t, H4", 2H), 4.61 (t, H6", 2H), 3.95 (t, H3", 2H) ppm. ESI-MS *m/z* = 189.2 $[M+H]^+$.

The *anti-trans*-$DADAT^{2+}$@CB[7] complex was prepared by a photoirradiation of $(APH)_2^{2+}$@CB[7] (2:1 molar ratio of APH^+ and CB[7]) sample in D_2O in an NMR tube with the irradiation of 365 nm UV light. ^{1}H NMR (400 MHz, D_2O) δ 6.29 (t, *J* = 7.2 Hz, H5', 2H), 5.66 (t, H4", 2H), 3.68 (t, *J* = 8.1 Hz, H6", 2H), 2.92 (t, *J* = 8.1 Hz, H3", 2H),

5.68 (d, CH_2 of CB[7], 14H), 5.55 (s, CH of CB[7], 14H), 4.26 (d, CH of CB[7], 14H) ppm; ESI-MS *m/z* = 676.4 $[M+2H]^{2+}$.

2.2.2 Methods and Instrumentation

The 1D ^{1}H NMR and 2D COSY spectra were measured on a Bruker AV-400M NMR spectrometer. The ESI-MS spectra were acquired on a Waters 2Q Single Quadrupole MS spectrometer equipped with an ESI/APcI multiprobe. The UV-visible spectra were acquired on a Hewlett Packard 8452A diode array UV-visible spectrometer using quartz cells with a 1.00 cm path length.

All of the modeled structures of the host-guest complexes involved in this project were computed by energy-minimizations using Gaussian 03 (Revision C.02) programs[13] run on the computing facilities of the High Performance Virtual Computing Laboratory (HPVCL) at Queen's University. The structures of the complexes were originally constructed using ChemDraw and Chem3D (ChemOffice 7.0, CambridgeSoft) programs and thereafter imported into Gaussian 03. The basis set used for the calculations was HF/3-21G**.

Cyclic voltammograms were collected using a Bioanalytical Systems CV-1B cyclic voltammeter, with a glassy carbon working electrode, a platinum auxiliary electrode, and a Ag/ AgCl reference electrode.

The kinetic experiments were performed on an Applied Photophysics SV-MX17 stopped-flow spectrophotometer. The electron-transfer reactions between (*E*)-$FcMPE^+$

(1.0×10^{-4} M) and $Co(dipic)^{2-}$ (1.0×10^{-3} M) were carried out in aqueous solution containing 0.10 M NaCl at 25.0 ± 0.1 °C, maintained by an external water bath. The second-order rate constants were determined from five to six replicate traces.

The photo-irradiation light source was Spectroline hand-held UV lamp (longer wavelength: 365 nm). All photoreactions were carried out in solutions in the dark. Digital images of the colored solutions of $FcMPE^+$ with and without CB[7] host molecules before and after UV light irradiation were taken by using a Sony DSC-P71 camera.

2.2.3 Host-Guest Stability Constant Determination

2.2.3.1 Quantitative ^{1}H NMR Titrations

This quantitative ^{1}H NMR titration method for determination of a host-guest binding constant is applicable when the exchange rate between free and bound guest is fast in ^{1}H NMR timescale. For an aqueous solution (D_2O) containing equimolar amounts of CB[7] and the guest molecule G, if the total concentration of the CB[7] (bound and unbound) is c, then it follows that the total concentration of the guest G (bound and unbound) is also c (equations 2.1 and 2.2).[14] A represents the complex G@CB[7].

$$[CB[7]] + [A] = c \quad (2.1)$$

$$[G] + [A] = c \quad (2.2)$$

If x is the equilibrium concentration ([A]) of A, then $K_a = [A]/[CB[7]][G] = x/(c - x)^2$.

For a given proton in G, the observed chemical shift (δ_o) is related to the corresponding chemical shift (δ_p) in free G and the limiting chemical shift (δ_A) of the 1:1 complex A by equation 2.3, and rearrangement gives equation 2.4.

$$\delta_o = (c\text{-}x)*\delta_p /c + x*\delta_A/c \quad (2.3)$$

$$x/c = (\delta_o - \delta_p)/(\delta_A\text{-}\delta_p) \quad (2.4)$$

If Δ and Δ_0 are defined by equations 2.5 and 2.6, respectively, then x in equation 2.4 can be rewritten in terms of Δ and Δ_0 as shown in equation 2.7.

$$\Delta = \delta_o - \delta_p \quad (2.5)$$

$$\Delta_0 = \delta_A - \delta_p \quad (2.6)$$

$$x = c(\Delta/\Delta_0) \quad (2.7)$$

Although Δ can be determined directly from the ^{1}H NMR spectra, Δ_0 however, is unknown since δ_A can't be determined by the ^{1}H NMR experiment of 1:1 molar ratio of guest-host complex. Substituting x from equation 2.7 into $K_a = x/(c - x)^2$ affords equation 2.8, which relates K_a to c, Δ and Δ_0,

$$K_a[c - c(\Delta/\Delta_0)]^2 = c(\Delta/\Delta_0) \quad (2.8)$$

Rearrangement of equation 2.8 gives equation 2.9

$$\Delta = \Delta_0 - (\Delta/c)^{1/2}(\Delta_0/K_a)^{1/2} \quad (2.9)$$

K_a can be determined from the slope of a plot of Δ against $(\Delta/c)^{1/2}$ through ^{1}H NMR dilution experiments.

2.2.3.2 Competitive ^{1}H NMR Titrations

The competitive ^{1}H NMR method is practically useful to determine binding constants for strong host-guest complexation.[15] The ^{1}H NMR competition experiments were performed on a 400 MHz NMR spectrometer and the temperature was maintained at 298 K with a temperature control module. Each sample contained CB[7] and an excess of the two competitive guests. The resonances corresponding to bound and free guests in non-overlapping regions of the spectrum were integrated, which allowed for the determination of the concentration of the free guests and the two host-guest complexes. Equations 2.10-2.11 define the thermodynamics of the host-guest and competition experiments. Substitution of the various concentrations measured by ^{1}H NMR into eq. 2.12 yielded a value of K_{rel}. The unknown binding constant K_{G2} can be acquired using the eq. 2.13 based on the K_{rel} values (determined from 2.12) and the reference K_{G1} value determined by UV/visible or ^{1}H NMR titration method.[15]

$$\text{CB[n]} + \text{G1} \overset{K_{G1}}{\rightleftharpoons} \text{G1@CB[n]} \tag{2.10}$$

$$\text{CB[n]} + \text{G2} \overset{K_{G2}}{\rightleftharpoons} \text{G2@CB[n]} \tag{2.11}$$

$$K_{rel} = K_{G2}/K_{G1} = ([\text{G2@CB[n]}][\text{G1}])/([\text{G1@CB[n]}][\text{G2}]) \tag{2.12}$$

$$K_{G2} = (K_{G1})(K_{rel}) \tag{2.13}$$

2.3 Results and Discussion

2.3.1 CB[7] Catalyzed Photodimerization of 2-Aminopyridine

We investigated the inclusion of protonated 2-aminopyridine (APH^+) by CB[7] and a highly stereoselective [4+4] photodimerization of APH^+ to *anti-trans* $DADAT^{2+}$ catalyzed by the host molecule. In addition, we have observed that the stability of otherwise unstable *anti-trans*-$DADAT^{2+}$ is dramatically enhanced when encapsulated in CB[7], and the dimer does not rearomatize to the APH^+ monomer under ambient conditions (Figure 2.4).

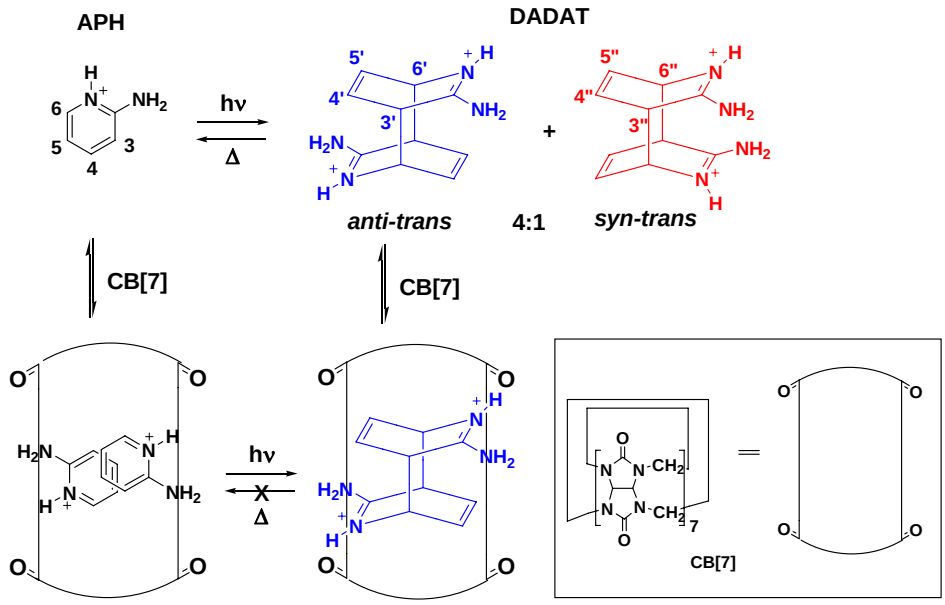

Figure 2.4 Schematic diagram of the CB[7]-catalyzed photodimerization of protonated 2-aminopyridine, with the proton labeling indicated.

2.3.1.1 Complex Formation Between CB[7] and 2-Aminopyridine

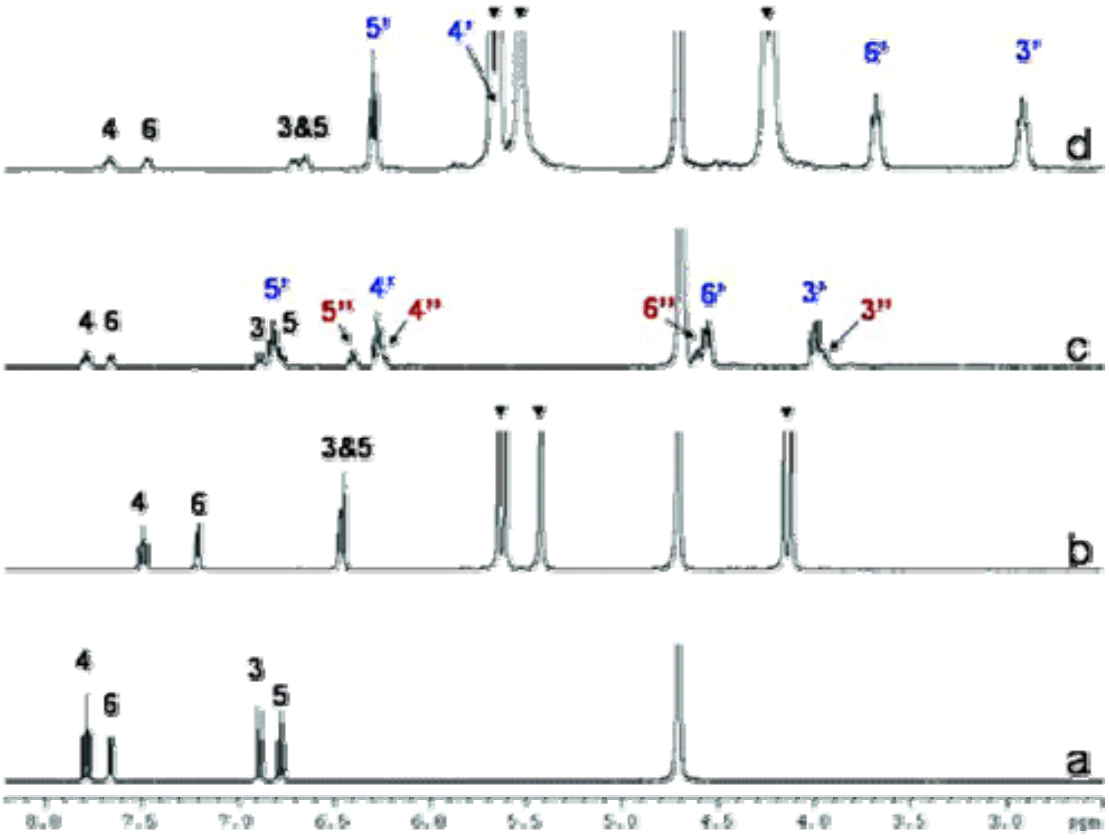

Figure 2.5 ^{1}H NMR spectra (D_2O) of APH^+ before (a) and after (c) 21 hours of 365 nm irradiation and of $(APH)_2^{2+}$@CB[7] before (b) and after (d) 21 hours of 365 nm irradiation (proton labeling given in Scheme 1, CB[7] peaks (▼)).

The complexation between CB[7] and guest molecule APH^+ was investigated first. CB[7] exhibits superior solubility in aqueous solution to the other CB[*n*] molecules, and its complexation properties therefore, have been extensively studied. It has been well known that it is unable to simultaneously encapsulate two larger aromatic molecules,

such as stilbenes. We have found, however, that a smaller cationic aromatic guest, APH^+, may rapidly (upon mixing) form very stable 1:1 and 2:1 complexes with CB[7] in aqueous solution, as indicated by ^1H NMR and ESI-MS spectra. The complexation induced limiting upfield shifts of the APH^+ resonances (Figure 2.5b) in the presence of excess CB[7] are 0.7 ppm for protons 4 and 5 and 1.1 ppm for protons 3 and 6, which suggests that the majority of guest molecules are included in the hydrophobic cavity of the CB[7] host molecule. The ESI-MS spectrum contains doubly-charged peaks at *m/z* = 629 and 676, consistent with both 1:1 and 2:1 guest-host complexes. The stoichiometry of 2:1 guest-host complexes has been further confirmed by a Job's plot of chemical shift changes from a continuous variation ^1H NMR titration.

2.3.1.2 CB[7] Catalyzes Stereoselective Photodimerization

The [4+4] photochemical dimerization of APH^+ to 4,8-diamino-3,7-diazatricyclo[4.2.2.$2^{2,5}$]dodeca-3,7,9,11-tetraene ($DADAT^{2+}$), in acidic aqueous solution, was first reported nearly a half century ago.[11,12] The crystallized photodimer in the original study was assigned to be the *anti*-*trans*-$DATAT^{2+}$ isomer of the four potential stereoisomers. The investigated templating effect of CB[7] here represents its first ever employment in a stereoselective photodimerization of aromatic molecules. UV irradiation of an aqueous solution of the $(APH)_2^{2+}$@CB[7] complex at 365 nm for 21 hours gives exclusively the *anti*-*trans*-$DADAT^{2+}$, with a yield of up to 90% conversion without any side products (Figure 2.5d), which is significantly higher

than the previously reported yield.[11]

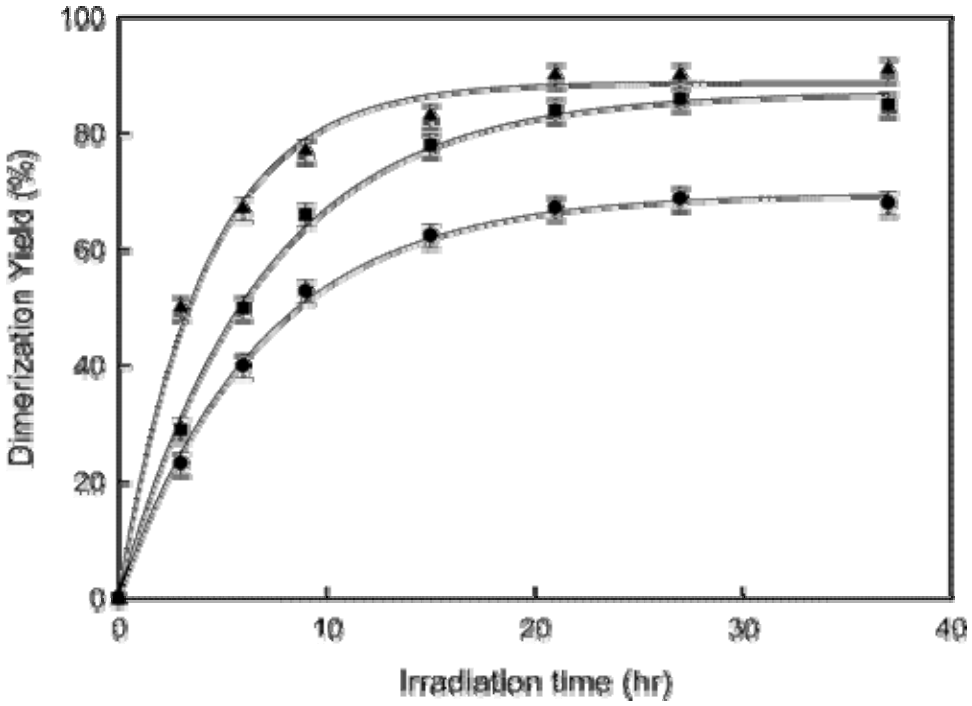

Figure 2.6 The dimer yields (based on one experiment) as a function of irradiation time for APH^+ photodimerization in the presence of CB[7] (triangles: *anti-trans* dimer) and in the absence of CB[7] (squares: both *anti-trans* and *syn-trans* dimers; and circles: *anti-trans* dimer only).

For comparison purposes, we repeated the APH^+ photodimerization in the absence of CB[7] and observed (by ^{1}H NMR, Figure 2.5c) after 21 hours of irradiation a 4:1 ratio of the *anti-trans* and *syn-trans* isomers (Figure 2.4) as identified by ^{1}H and 2D COSY NMR. The theoretically possible *anti-cis* and *syn-cis* isomers do not appear to be formed in solution, likely because of the Coulombic repulsions between the positively charged

pyridinium nitrogens. The yields of the photodimer isomers as a function of irradiation time (Figure 2.6) were evaluated from integrations of their respective ^{1}H NMR resonances. The high stereoselectivity may be related to the *anti*-*trans* alignment of the two APH^+ molecules in the CB[7] cavity or by the portals, stabilized by cation-dipole and hydrogen-bonding interactions. The results (Figure 2.6) also indicate that the photodimerization is somewhat faster in the presence of CB[7] (3 h *vs* 6 h in the absence of CB[7] for 50% conversion to a dimer). With CB[7] present, the unidentifiable side products seen in the ^{1}H NMR spectra after prolonged irradiation of APH^+ without CB[7] were not observed.

2.3.1.3 Photodimer Product Stabilized by CB[7]

The $DADAT^{2+}$ dimer undergoes spontaneous rearomatization back to the APH^+ monomer very slowly at room temperature, or quickly by adding base.[11,12] In this study, the *anti*-*trans*-$DADAT^{2+}$ encapsulated in CB[7] does not undergo rearomatization at room temperature but does do so upon addition of base to the solution, which presumably deprotonates the guest, releasing it from its stabilizing environment. Although the mechanism of the thermal rearomatization of $DADAT^{2+}$ to APH^+ is not clear yet, stabilization of otherwise unstable photochemical products by means of supramolecular encapsulation in host containers has precedence.[16-19] It has also been mentioned in the previous chapter that CB[7] has also been recently employed to stabilize *cis*-stilbene derivatives[7] and fluorescent rhodamines.[4] The observed behavior in the

$APH^+/DADAT^{2+}$ system may be useful in the design of pH/photochemically controlled on/off switchable (reversible) photodimerization, because in switch design both states need to be stable.

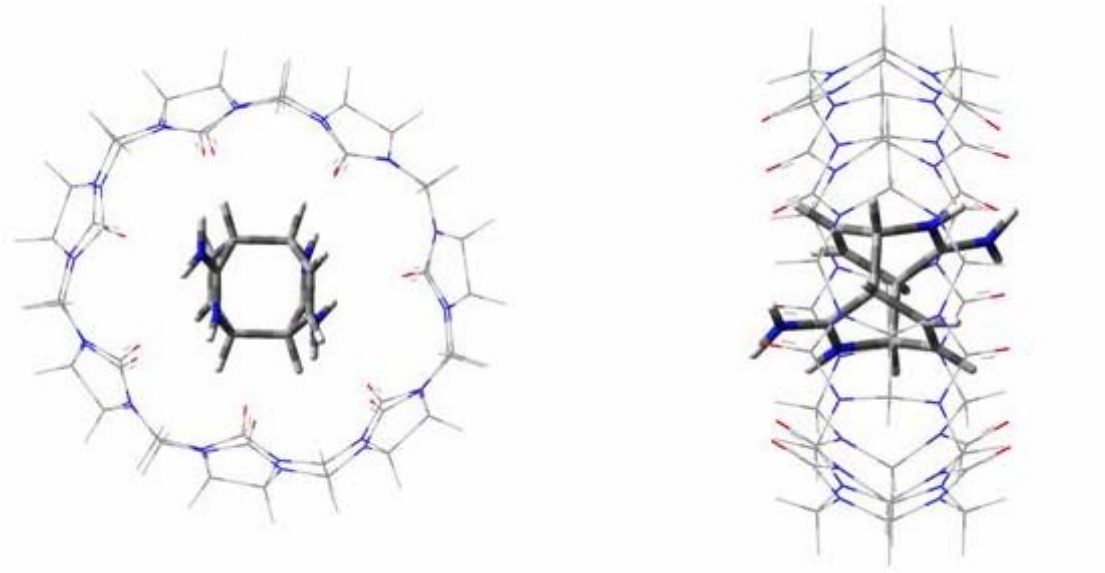

Figure 2.7 Energy-minimized structures of *anti-trans*-$DADAT^{2+}$@CB[7] in the gas phase (HF/3-21G** basis set). The $DADAT^{2+}$ is indicated by the tube-type structure, and the CB[7] is indicated by the wireframe-type structure.

The stabilization of the *anti-trans* photodimer in the CB[7] cavity, with $K_{CB} = (8 \pm 2) \times 10^5\ M^{-1}$ determined by ^1H NMR dilution experiments (the method is described in the experimental section), relies on multiple noncovalent hydrophobic, cation-dipole, and hydrogen-bonding interactions. An energy-minimized structure of the *anti-trans*-$DADAT^{2+}$@CB[7] complex by *ab initio* calculations is shown in Figure 2.7. The photodimer is held tightly in the cavity of CB[7], with several hydrogen-bonding

interactions between the amine hydrogens and the portal oxygens at each end of the cavity. The orientation of the dimer in the CB[7] cavity is consistent with the magnitudes of the upfield shifts in the ^{1}H NMR resonances of the alkene and bridgehead protons (Figure 2.5d).

We have demonstrated that the [4+4] photodimerization of protonated 2-aminopyridine within a 2:1 guest-host complex with CB[7] is highly stereoselective, producing exclusively the *anti*-*trans*-DADAT^{2+} isomer and protecting the dimer from thermal rearomatization. This result, for the first time, has demonstrated the potential application of CB[7] in mediating stereoselective photodimerizations of small aromatic molecules in aqueous solution.

2.3.2 CB[7] Mediated Photoreactions of *trans*-1,2-bis(4-pyridyl)ethylene and Its Derivatives

We have investigated the CB[7] mediated photoreactions of protonated *trans*-1,2-bis(4-pyridyl)ethylene ((*E*)-H_2BPE^{2+}) and its derivatives to demonstrate the potential of CB[7] to control the outcome of a photoreaction, specifically, to direct a photoreaction to proceed through a selective route. Upon complexation by CB[7], the (*E*)-H_2BPE^{2+} guest molecule selectively favors photoisomerization over the otherwise dominant photohydration reaction in aqueous solution. The mediations of the photoreactions of two 1,2-bis(1-alkyl-4-pyridinyl)ethylene dications have also been studied for comparison, in order to understand the mechanism of CB[7] mediation.

2.3.2.1 Host-Guest Complexation Between CB[7] and (*E*)-H_2BPE^{2+}

Protonated *trans*-1,2-bis(4-pyridyl)ethylene ((E)-H_2BPE^{2+}) forms a stable 1:1 host-guest complex with CB[7] as indicated by ^{1}H NMR spectroscopy and a Job's plot. The ^{1}H NMR resonances for the pyridyl and ethylene protons exhibited upfield shifts upon the formation of the complex (Figure 2.8**)** indicating that they are located in the cavity of CB[7]. The Job's plot, based on a UV-visible continuous variation method, further suggests that the binding stoichiometry is simply 1:1 (Figure 2.9). The host-guest interactions are presumably the hydrophobic interactions taking place in the cavity, with ion-dipole and hydrogen bonding interactions dominating at the host portals. The ESI-MS spectrum has a doubly-charged peak at m/z = 673.8, also indicative of the formation of a 1:1 complex.

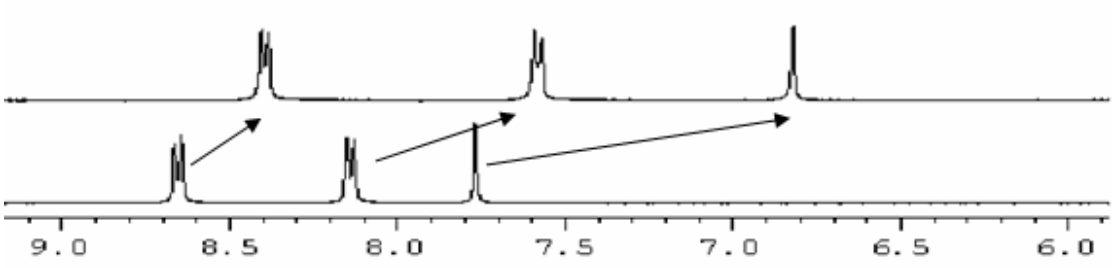

Figure 2.8 ^{1}H NMR spectra (400 MHz, DCl/D_2O) of (*E*)-H_2BPE^{2+} in the absence (bottom) and in the presence (top) of 1.1 equivalents of CB[7].

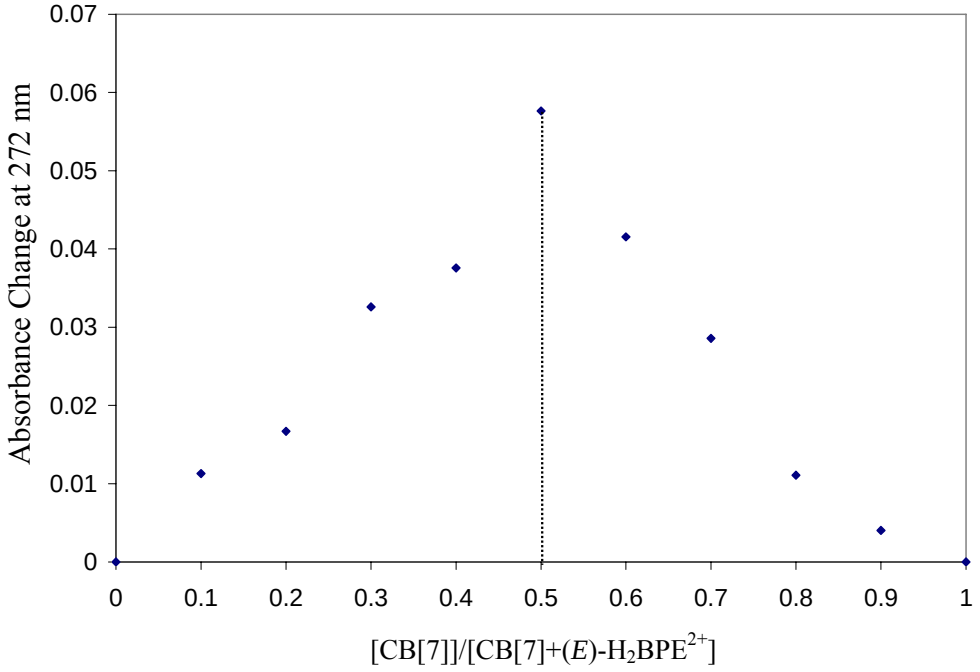

Figure 2.9 Job's plot for the (*E*)-H_2BPE^{2+}@CB[7] complex at 272 nm. This is plotted from a continuous titration of (*E*)-H_2BPE^{2+} with CB[7] by keeping [CB[7]]+[(*E*)-H_2BPE^{2+}] = 5.5×10^{-5} M.

2.3.2.2 CB[7] mediation: Photoisomerization Replaces Photohydration

With the knowledge of the 1:1 complex formation between protonated (*E*)-H_2BPE^{2+} and CB[7], the photoreactions were further investigated in the absence and in the presence of CB[7]. It is well known that photohydration reaction competes strongly with photoisomerization reaction for (*E*)-H_2BPE^{2+} in aqueous solution.[20,21] The presence of water molecules, therefore, often prevents the desired photoisomerization or

photodimerization reactions for (*E*)-H_2BPE^{2+} and its alkylated derivatives.

Table 2.1 Distribution of the photoreaction products after the UV (365 nm) irradiation of protonated (*E*)-H_2BPE^{2+} in aqueous solution in the absence and in the presence of 1.2 equivalents of CB[7] (the yields are based on ^{1}H NMR integration. The concentration of the guest is 0.0136 M).

	Time (hour)	Photoisomerization		Photoaddition BP-ethanol
		(*E*)-H_2BPE^{2+}	(*Z*)-H_2BPE^{2+}	
(*E*)-H_2BPE^{2+} Photoreaction in the absence of CB[7]	0.5	70%	9%	21%
	1.0	43%	16%	41%
	2.0	11%	14%	75%
	3.0	5%	7%	88%
	4.5	0	0	>95%
(*E*)-H_2BPE^{2+} Photoreaction in the presence of CB[7]	0.5	77%	23%	0
	1.0	64%	36%	0
	2.0	48%	52%	0
	3.0	39%	60%	1%
	4.5	~ 28%	~ 69%	2%

The time-resolved product distribution during the photoreaction of (E)-H_2BPE^{2+} has been investigated for the first time (Table 2.1). Similar to the results reported before,[5] the eventual major product of (*E*)-H_2BPE^{2+} photoreaction without CB[7] was the

hydration product BP-ethanol (Figure 2.2). Even without CB[7], the photoisomerization occurred and the (*Z*)-isomer was produced at a yield of up to 16% after one hour irradiation, although all isomers were eventually photohydrolyzed to BP-ethanol.

In the presence of CB[7], the (*Z*)-H_2BPE^{2+} was essentially the only product after 4 hours of irradiation, with a yield of up to 70%. Further irradiation, however, produced BP-ethanol and other unidentifiable products. The presence of CB[7], therefore, has changed the photoreaction's pathways with the help of CB[7], such that the photoisomerization of (*E*)-H_2BPE^{2+} dominates over the otherwise dominant photohydration. The reason for this selection might be that (*E*)-H_2BPE^{2+}, upon encapsulation by CB[7], was physically protected by CB[7] from water attack in aqueous solution. Interestingly, the photoisomerization product, (*Z*)-H_2BPE^{2+}, remains in the cavity of CB[7], which also protects the (*Z*)-H_2BPE^{2+} from being photohydrated.

The greater amount of the (*Z*)-H_2BPE^{2+}@CB[7] isomer at equilibrium might be due to a higher affinity of CB[7] towards (*Z*)-H_2BPE^{2+}. In another words, the isomer with higher binding affinity towards host is favored more in the photoisomerization.[22,23] The possible higher binding affinity for CB[7] with (*Z*)-H_2BPE^{2+} may be explained by the shape and symmetry suitability since both *Z* and *E* isomers of H_2BPE^{2+} have totally same size and charge complementarities with CB[7] (cation-dipole interactions), as shown by the energy-minimized structures of the two complexes (Figure 2.10). Both two positive charges on the C-shaped (*Z*)-H_2BPE^{2+} are closer to the negatively carbonyl portals than

those of (*E*)-H_2BPE^{2+}, which makes the cation-dipole interactions of (*Z*)-H_2BPE^{2+} with CB[7] stronger than that of (*E*)-H_2BPE^{2+}. In addition, the proximity of the hydrogens on the nitrogen to the carbonyl oxygens also allows for the stronger hydrogen bonding. Therefore, the (*Z*)-H_2BPE^{2+} might have a higher binding affinity with CB[7] than (*E*)-H_2BPE^{2+}, which has contributed to the efficient catalysis of (*E*)→(*Z*) photoisomerization.

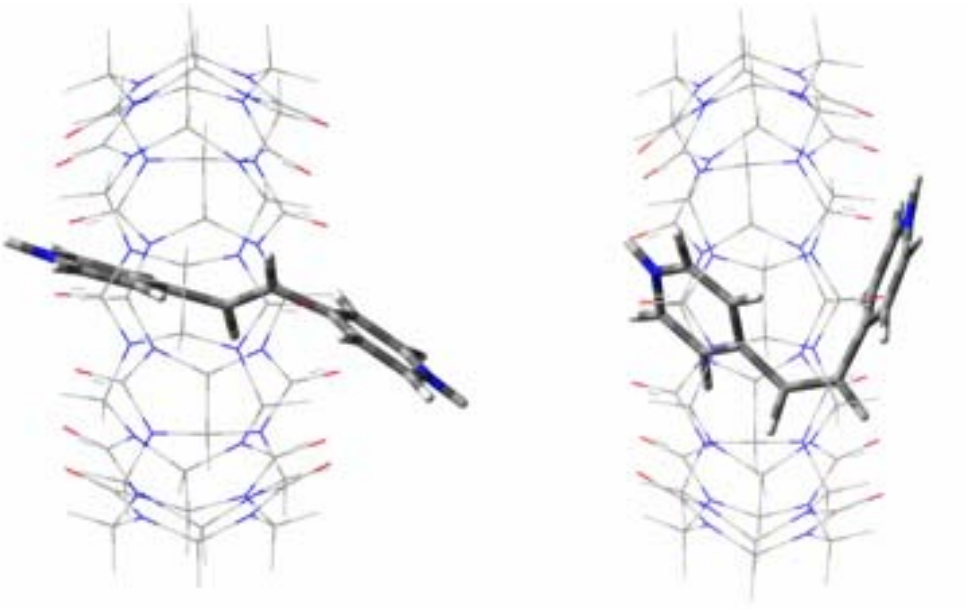

Figure 2.10 Energy-minimized structures of **a)** (*E*)-H_2BPE^{2+}@CB[7] (left) and **b)** (*Z*)-H_2BPE^{2+}@CB[7] (right) in the gas phase (HF/3-21G** basis set).

2.3.2.3 Comparison of CB[7] Mediation on Photoreactions of BPE Derivatives

The effect of CB[7] on the photoreactions of 1,2-bis(1-methyl-4-pyridinyl)ethylene, (*E*)-$BMPE^{2+}$, was investigated by the same methods for a comparison with the reactions of (*E*)-H_2BPE^{2+}. As observed with (*E*)-H_2BPE^{2+}, (*E*)-$BMPE^{2+}$ compound forms 1:1 host-guest inclusion complex as demonstrated by ^{1}H NMR spectroscopy and a Job's plot (Figures 2.11 and 2.12). The upfield shift of the pyridine and ethylene resonances in the ^{1}H NMR spectra indicates that the bis(4-pyridinyl)ethylene unit has been encapsulated in the hydrophobic cavity of CB[7], and the slight downfield shift of the methyl proton resonance is a result of the deshielding effect from carbonyl portals. A UV-visible Job's plot also strongly supports the 1:1 complex formation.

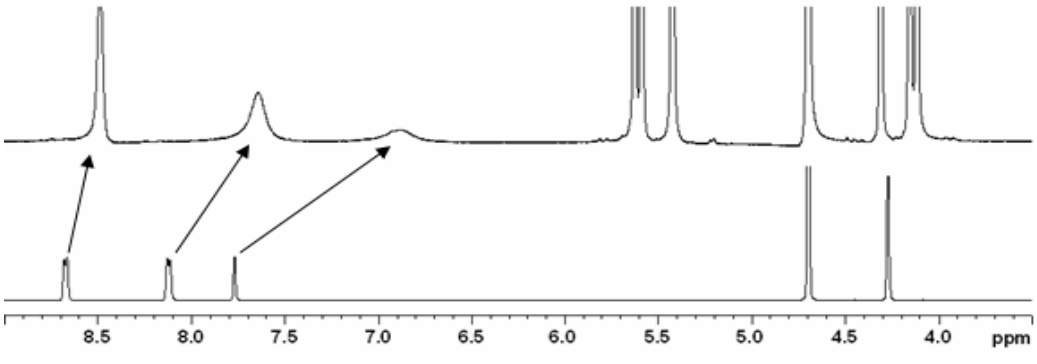

Figure 2.11 ^{1}H NMR spectra (400 MHz, D_2O) of (*E*)-$BMPE^{2+}$ in the absence and in the presence of 1.2 equivalents of CB[7].

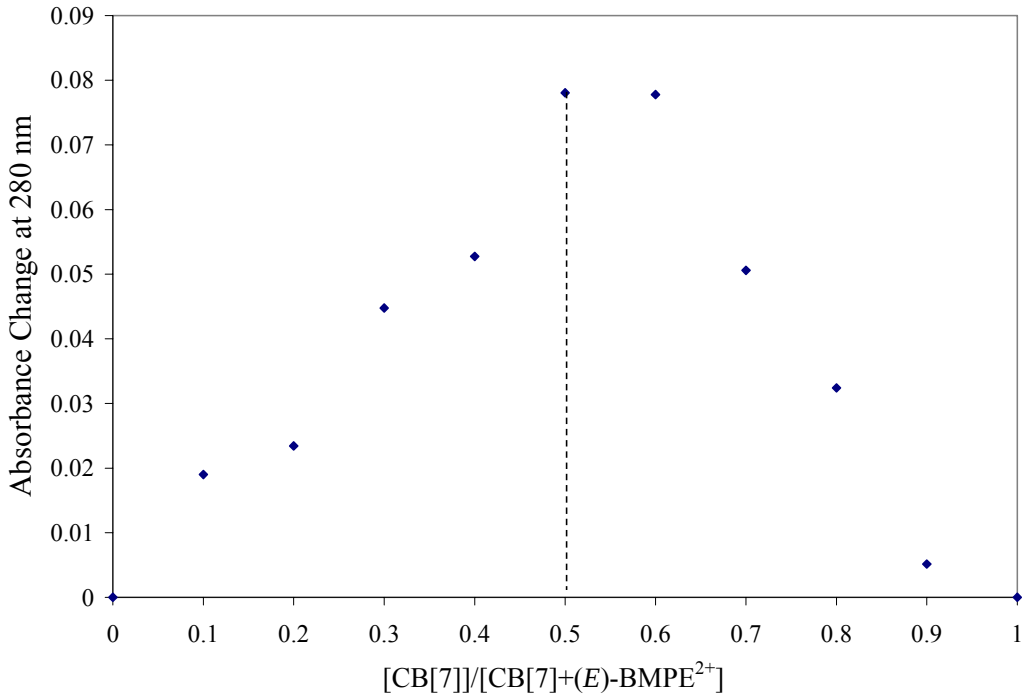

Figure 2.12 Job's plot for the (*E*)-BMPE^{2+}@CB[7] complex at 280 nm, from a continuous variation titration of protonated (*E*)-BMPE^{2+} with CB[7] by keeping [CB[7]]+[(*E*)-BMPE^{2+}] = 5.5×10^{-5} M.

We expected to see similar effect CB[7] plays on this photoreaction with that of (*E*)-BPE^{2+}. To our surprise, contrary to (*E*)-BPE^{2+}, the (*E*)-BMPE^{2+} was moderately stabilized by complexation of CB[7] (Table 2.2). In the absence of CB[7], the major photoproduct was BMP-ethanol, though the (*Z*)-BMPE^{2+} was produced at a yield of up to 11% after one hour of irradiation, similar to the case of (*E*)-BPE^{2+}. In the presence of CB[7], the (*E*)-BMPE^{2+} was moderately preserved even after two hours irradiation, and further irradiation still maintained the majority of (*E*)-BMPE^{2+}. Some unidentifiable products (due to the broad bands and resonance overlaps in the ^{1}H NMR spectra) are

presumably mainly BMP-ethanol.

Table 2.2 Distribution of the photoreaction products after the UV (365 nm) irradiation of aqueous (*E*)-BMPE^{2+} ($2I^-$) solution in the absence and in the presence of 1.2 equivalent of CB[7] (the yields are based on ^{1}H NMR integration. The concentration of guest is 0.0107 M).

	Time (hour)	Photoisomerization		BMP-ethanol
		(E)-BMPE^{2+}	(Z)-BMPE^{2+}	
(E)-BMPE^{2+} Photoreaction in the absence of CB[7]	0.5	51%	10%	39%
	1.0	25%	11%	64%
	1.5	0	5%	95%
	2.0	0	<1%	>95%
(E)-BMPE^{2+} Photoreaction in the presence of CB[7]	0.5	63%	37%	
	1.0	52%	47%	
	1.5	51%	48%	
	2.0	51%	48%	

Since the isomer with higher binding affinity towards the host is favored in photoisomerization, the CB[7] selection of (*E*)-BMPE^{2+} over (*Z*)-BMPE^{2+} might be attributed to the higher binding between CB[7] and (*E*)-BMPE^{2+}. As shown by Figure 2.13, relatively bulky methyl groups of (*Z*)-BMPE^{2+} experience more steric hindrance with carbonyl portals of CB[7] than those of (*E*)-BMPE^{2+}.

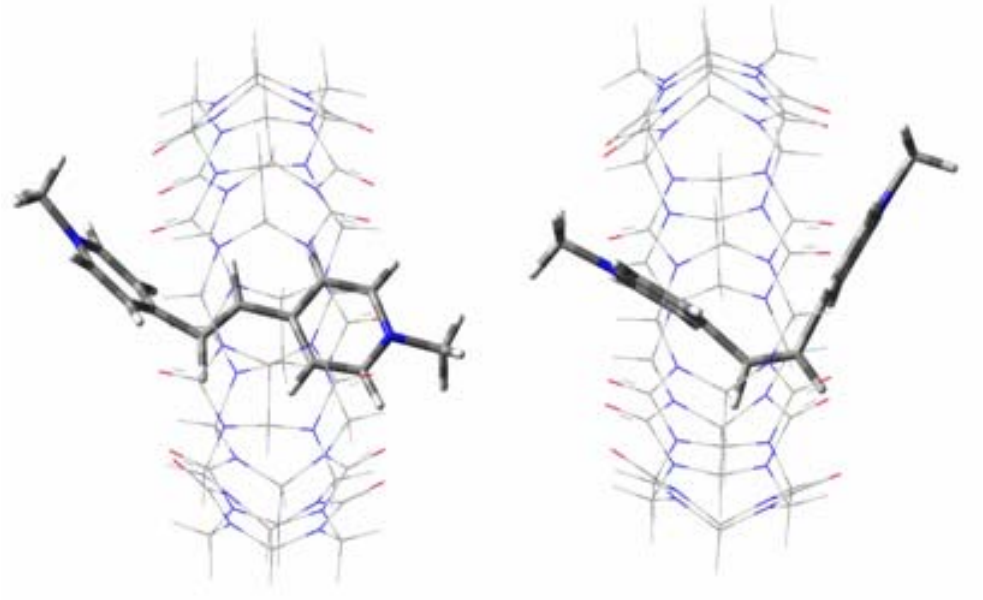

Figure 2.13 Energy-minimized structures of **a)** (*E*)-BMPE^{2+}@CB[7] (left) and **b)** (*Z*)-BMPE^{2+}@CB[7] (right) in the gas phase (HF/3-21G** basis set).

In order to further compare the alkyl substituent's effect on complexation and CB[7]-mediated photoreactions, we employed the more bulky dihexylated derivative, (*E*)-BHPE^{2+}. To our surprise again, the photohydration product was the major product for (*E*)-BHPE^{2+}, even upon the complexation of CB[7] (Table 2.3). It seems that CB[7] complexation had little effect on the photoreactions of (*E*)-BHPE^{2+}, based on the eventual products. When we examined the distribution of the photoproducts during photoirradiation, it was found however, that the photoreaction of (*E*)-BHPE^{2+} was slowed down in the presence of CB[7].

Table 2.3 Distribution of the photoreaction products after the UV (365 nm) irradiation of an aqueous solution of (*E*)-BHPE^{2+}, in the absence and in the presence of 1.2 equivalents of CB[7] (the yields are based on ^{1}H NMR integration). The concentration of the guest is 0.0100 M).

	Time (hour)	Photoisomerization		BHP-ethanol
		(*E*)-BHPE^{2+}	(*Z*)-BHPE^{2+}	
(*E*)-BHPE^{2+} Photoreaction in the absence of CB[7]	0.5	27%	13%	60%
	1.0	2%	6%	92%
	1.5	<1%	2%	~ 97%
(*E*)-BHPE^{2+} Photoreaction in the presence of CB[7]	0.5	61%	13%	26%
	1.0	29%	16%	55%
	1.5	22%	13%	65%
	2.0	9%	<1%	~ 90%

The unexpected results may be primarily attributed to the site of binding between (*E*)-BHPE^{2+} and CB[7] as revealed by ^{1}H NMR spectroscopy (Figure 2.14). The hexyl groups, rather than the bis(4-pyridinyl)ethylene portion, were included in the cavity of CB[7], as the resonances of the hexyl protons are moved upfield, which is solid evidence of hexyl encapsulation in the cavity of CB[7].

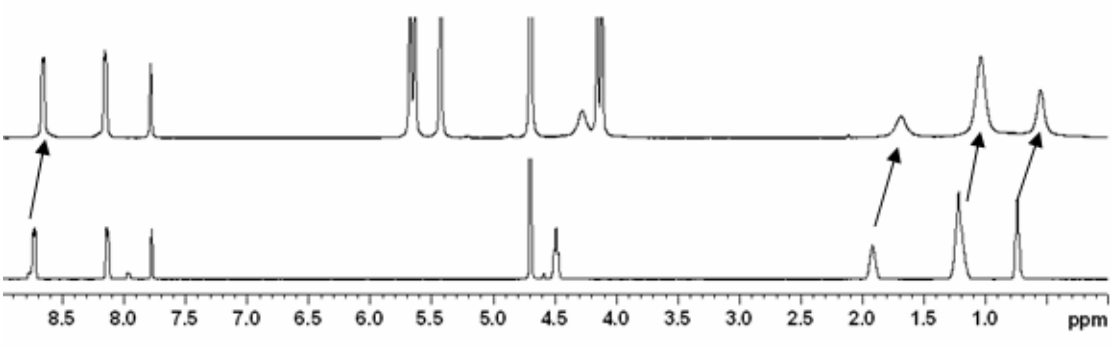

Figure 2.14 ^{1}H NMR spectra (400 MHz, D_2O) of (*E*)-BHPE^{2+} in the absence and in the presence of 1.2 equivalents of CB[7].

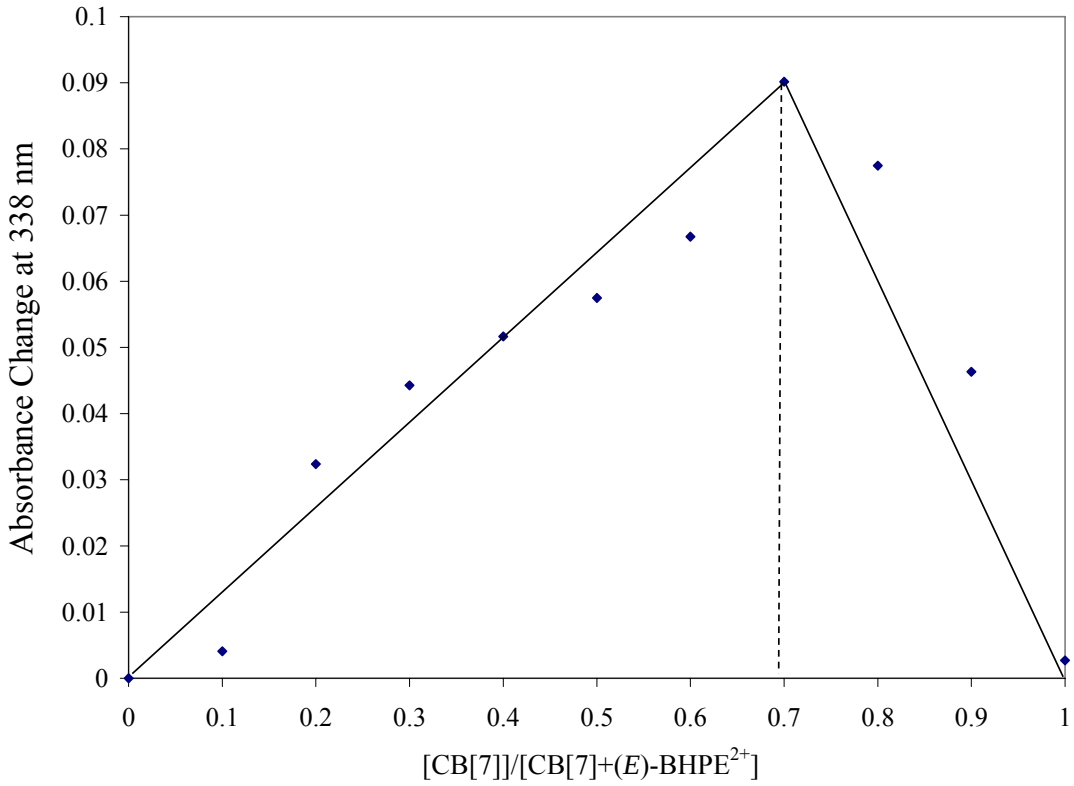

Figure 2.15 Job's plot for the (*E*)-BHPE^{2+}@CB[7] complex at 338 nm, from a continuous variation titration of (*E*)-BHPE^{2+} with CB[7], keeping [CB[7]]+[(*E*)-BHPE^{2+}] = 5.5×10^{-5} M.

By adding more CB[7], a 1:2 guest-host complex was formed (Job's plot, Figure 2.15). The switching of the binding site of CB[7] from the bis(4-pyridinyl)ethylene portion to the alkyl portion is similar to a previous report of CB[7] binding mode selectivity for a series of dialkyl-4,4'-bipyridium (viologen) dicationic guests.[10] The switching of the binding site of CB[7] from viologen portion to alkyl group portion occurs when the linear alkyl group is longer than a propyl chain. When the CB[7] binds exclusively to the hexyl groups in our case, the ethylene group is not effectively protected from the aqueous environment and photohydration.

With the three compounds investigated, CB[7] has demonstrated the ability to mediate photochemical reactions, specifically to favor a pathway of photoreaction through specific binding modes.

2.3.3 CB[7] Stabilization of a Ferrocenylethylene

The investigations of the effect of CB[7] on mediating the photoisomerization of molecules containing vinyl groups has been extended to the substituted ferrocene, (*E*)-1-ferrocenyl-2-(1-methyl-4-pyridinium)ethylene ((*E*)-FcMPE$^+$). This stemmed from our research interest in the employment of CB[7] to mediate photoreactions of vinyl-containing species and the fact that ferrocenes and CB[7] form very stable complexes (the most stable non-covalent interactions found for an artificial host-guest complex).[24] A previous report on the photoreactivity of (*E*)-FcMPE$^+$ demonstrated that (*E*)→(*Z*) photoisomerization of (*E*)-FcMPE$^+$ occurs upon photoirradiation,[25] similar to

other stilbene or stilbazole derivatives. We have observed that the inclusion of the (*E*)-FcMPE$^+$ cation by CB[7] significantly enhances its stability with respect to its photochemical isomerization and chemical oxidation in aqueous solution.

2.3.3.1 Complexation Between CB[7] and (*E*)-FcMPE$^+$

The encapsulation of (*E*)-FcMPE$^+$ inside the cavity of CB[7] to form a (*E*)-FcMPE$^+$@CB[7] inclusion complex in aqueous solution has been established by ^{1}H NMR and UV-visible spectroscopy, ESI-MS spectrometry, and cyclic voltammetry, as well as from kinetic measurements of an outer-sphere electron-transfer reaction. In the presence of one equivalent of CB[7], the resonances for the ethylene protons (H_4 and H_5) and the protons of the two cyclopentadienyl rings in the ^{1}H NMR spectrum of its inclusion complex (Figure 2.16) have moved upfield from those of the free guest, indicative of their positioning within the cavity of CB[7]. The resonance of one of the two pyridine proton resonances (H_3) moved downfield, while the other pyridine proton resonance (H_2), along with the methyl proton (H_1) resonance, exhibited no chemical shift change. This behavior indicates that the *N*-methylpyridinium group is situated outside of the cavity of CB[7], as the downfield shift of one pyridine proton resonance may be attributed to the deshielding effect of the carbonyl-rimmed portal of CB[7]. Therefore, on the basis of the ^{1}H NMR characterization, the ferrocenylethylene portion of (*E*)-FcMPE$^+$ is encapsulated in the cavity of CB[7].

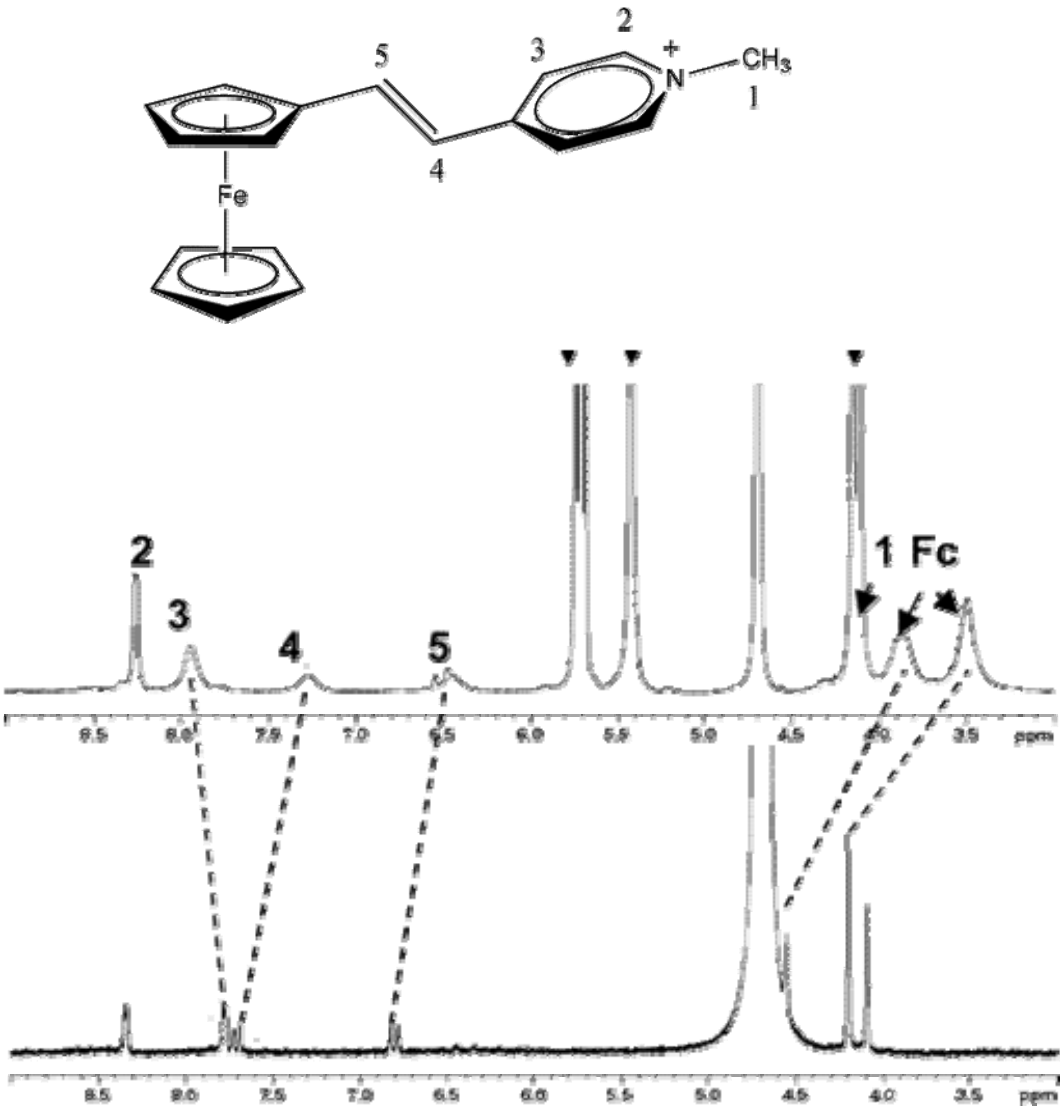

Figure 2.16 **(a)** Structure of (*E*)-FcMPE$^+$ with proton numbering; **(b)** ^{1}H NMR spectra (400 MHz, D_2O) of (*E*)-FcMPE$^+$ in the absence (bottom) and the presence (top) of one equivalent of CB[7]. Resonances labeled with black inverted triangles correspond to protons of the CB[7] host.

The exchange rate between bound and free (*E*)-FcMPE$^+$ is slow on the ^{1}H NMR timescale (400 MHz) at room temperature, as the resonances of free and bound ligands

were distinguishable in the ^{1}H NMR spectrum when less than one equivalent of CB[7] was added. The asymmetry of the orientation of the guest inclusion in the CB[7] cavity is also reflected in the separation of the two resonances for the symmetry-related methylene protons on the exterior of the CB[7], into pairs of doublets.

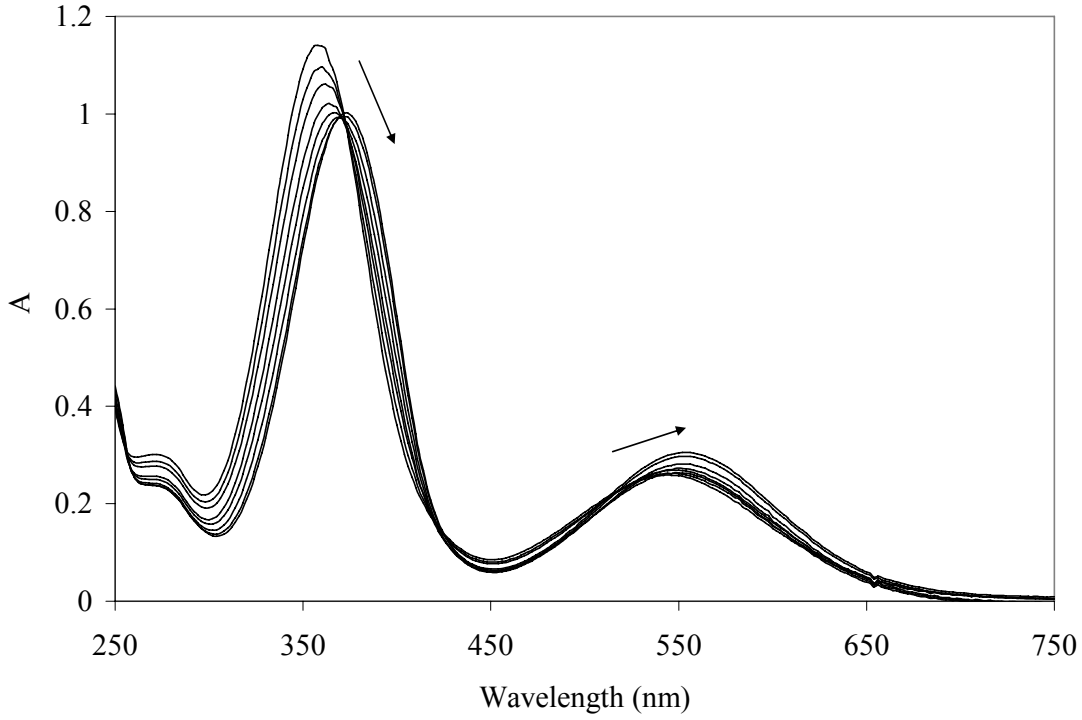

Figure 2.17 UV-visible spectra of aqueous (*E*)-FcMPE$^+$ (50 μM) in the presence of various concentrations of CB[7] (from 0 to 70 μM in the arrow direction).

The UV-visible spectrum of the (*E*)-FcMPE$^+$ cation (Figure 2.17) has peaks with λ_{max} values of 356 nm, due to an intraligand charge transfer (ILCT) from the cyclopentadienyl ring to the pyridinium group, and 546 nm, a Fe(II) to pyridinium metal-to-ligand charge transfer (MLCT) transition.[25,26] Upon addition of CB[7], there are bathochromic shifts

in both peaks to 372 and 554 nm, respectively, with the shorter wavelength peak decreasing in intensity and the longer wavelength peak increasing in intensity. These bathochromic shifts and intensity change upon inclusion of the ferrocenyl portion of the cation in the CB[7] are consistent with the solvatochromism observed previously for this complex.[25] While only the ferrocenyl portion of the cation is included in the CB[7] cavity, this portion contains the donor sites for both the ILCT (Cp^- ring) and MLCT (Fe(II)) transitions.

The 1:1 stoichiometry of the (*E*)-FcMPE$^+$@CB[7] inclusion complex was also established by a Job's plot (based on the continuous variation method) employing UV-visible spectroscopy and by the ESI-MS spectrum, which showed the singly charged peak at m/z = 1466 for the (*E*)-FcMPE$^+$@CB[7] inclusion complex. It was not possible to calculate the binding constant directly from UV-visible spectrophotometric titrations of (*E*)-FcMPE$^+$ with CB[7] because of the very high value of the binding constant. Instead, a ^{1}H NMR competition experiment of the (*E*)-FcMPE$^+$@CB[7] complex with 1-aminoadamantane, whose binding constant with CB[7] has been reported as $(4.23 \pm 1.00) \times 10^{12}$ M^{-1},[24] was carried out. Using a limiting amount of CB[7], a binding constant of $(1.3 \pm 0.5) \times 10^{12}$ M^{-1} was determined for (*E*)-FcMPE$^+$@CB[7]. This binding constant is comparable to the values determined in the range of 10^{11} to 10^{13} M^{-1} for other cationic guest molecules containing ferrocene unit.[24]

2.3.3.2 CB[7] Inhibited Photoreactions

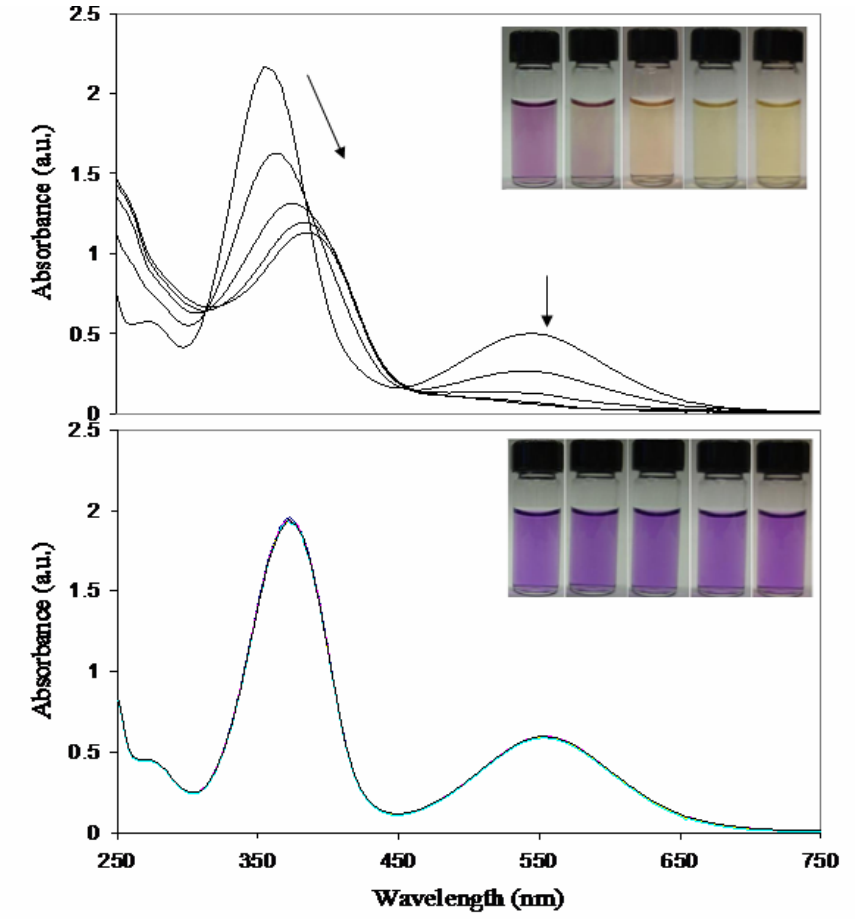

Figure 2.18 Absorbance changes for (*E*)-FcMPE$^+$ in the absence (top) and in the presence (bottom) of 1.2 equivalents of CB[7], recorded after 365 nm irradiation at 5 minutes intervals.

With a knowledge of the large stability constant for the (*E*)-FcMPE$^+$@CB[7] inclusion complex, the effect of CB[7] complexation on the photoreactivity of the (*E*)-FcMPE$^+$ cation in aqueous solution was examined. The (*E*)→(*Z*)

photoisomerization of (*E*)-FcMPE$^+$, which is known to occur upon irradiation at 365 nm,[25] may be monitored by UV-visible spectroscopy (Figure 2.18).

The changes in the spectrum of (*E*)-FcMPE$^+$ upon photoirradiation in the absence of CB[7] are very similar to those previously reported, with the band at 356 nm (ILCT) shifting to 386 nm and a disappearance of the band at 546 nm (MLCT). The reduced intensities of these bands arise from the reduction in conjugation in the *Z* isomer (a consequence of planarity deviation due to the larger steric hindrance of *cis* isomers).[25,27] In contrast, the UV-visible absorbance spectrum of the (*E*)-FcMPE$^+$@CB[7] inclusion complex (1.2 equivalents of CB[7] added), during the same period of photoirradiation (and beyond), showed no changes (Figure 2.18). The photoreactivity of aqueous (*E*)-FcMPE$^+$ is thus dramatically, if not completely, inhibited by CB[7] complexation.

The photostability enhancement in (*E*)-FcMPE$^+$ may be explained by the inclusion orientation of (*E*)-FcMPE$^+$ in the cavity of CB[7], demonstrated by *ab initio* energy-minimized calculations on the structure of the inclusion complex (Figure 2.19). The relatively large ferrocene portion of this molecule fits inside the cavity with the neighboring vinyl group positioned close to the portal of the cavity. This orientation is such that only the *E* isomer can reside in the cavity with only a small steric hindrance between carbonyl portals of CB[7] and the guest pyridine group. In contrast, the *Z* isomer would likely experience a significant steric hindrance between carbonyl groups of CB[7] and the guest pyridine group if the ferrocenylethylene portion were to be included in the CB[7] cavity. The inclusion of a vinyl group in the cavity of CB[7] also serves to

protect it from any other chemical attack, such as photoaddition of water. The overall photoreactivity of (*E*)-FcMPE^{+}, therefore, is highly inhibited, and solutions of the (*E*)-FcMPE^{+}@CB[7] inclusion complex appear to remain unchanged indefinitely on the benchtop under normal light conditions.

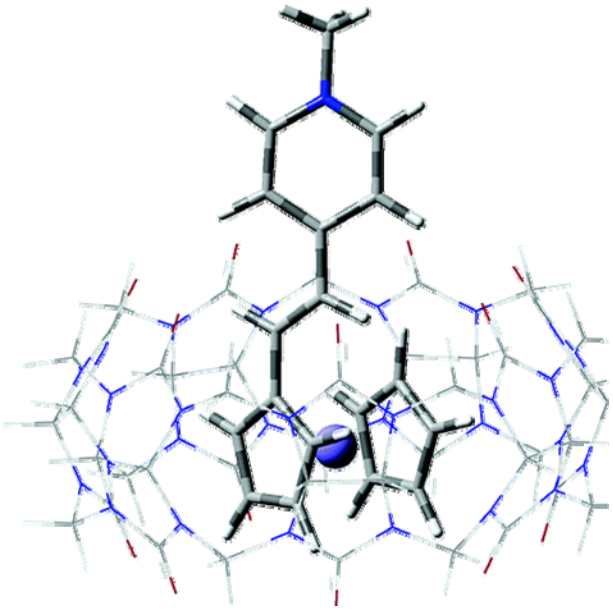

Figure 2.19 Energy-minimized structure of the (*E*)-FcMPE^{+}@CB[7] inclusion complex.

Cyclic voltammetry (CV) was employed to study the redox behavior of (*E*)-FcMPE^{+} in the absence and presence of CB[7]. The presence of 1.2 equivalents of CB[7] resulted in a modest anodic shift (~30 mV) in the position of the corresponding $E_{1/2}$ value for (*E*)-FcMPE$^{2+/+}$ couple (0.53 V *vs* NHE). Larger anodic shifts of >100 mV have been reported for other cationic ferrocenes, such as the

(trimethylammonio)methylferrocene, where the positive charge on the substituent would be located close to the carbonyl portals of CB[7]. Neutral hydroxymethylferrocene[24] and ferrocene[28] itself exhibit much smaller changes of 10 and -22 mV, respectively, upon inclusion in CB[7]. The anodic and cathodic peak currents and reversibility of the waves for (*E*)-FcMPE$^+$@CB[7] also decreased as a result of the host-guest complexation.[24,28,29] The modest anodic shift indicates that the binding constant for the reduced state of ferrocene is only slightly higher than that of the oxidized state of ferrocene. Using $\Delta E_{1/2}$ = 30 mV and the stability constant for the reduced (*E*)-FcMPE$^+$@CB[7] inclusion complex, a value of $K_{CB}^{ox} = 4 \times 10^{11}$ M^{-1} can be estimated ($\Delta E_{1/2} = -(RT/F)\ln(K_{CB}^{ox}/K_{CB}^{red})$) for the oxidized (*E*)-FcMPE$^+$@CB[7] form of the inclusion complex.

2.3.3.3 CB[7] Inhibited Chemical Oxidation

The Macartney group has been involved in the study of the effect of host molecules on the electron transfer reactions of guest metal complexes for the last 15 years.[30-35] As the photostability of (*E*)-FcMPE$^+$ has been dramatically increased upon complexation with CB[7], the redox active ferrocene containing guest molecule is also expected to have a lower oxidation rate upon inclusion into the cavity of CB[7].

The effect of CB[7] inclusion on the rate constant for the chemical oxidation of the (*E*)-FcMPE$^+$ complex was investigated employing Co(dipic)$_2^-$ (dipic^{2-} = 2,6-pyridinedicarboxylate) as the oxidant, as it does not form an inclusion complex with

CB[7]. Using $Co(dipic)_2^-$ in a pseudo-first-order excess (1.0×10^{-3} M) over (*E*)-$FcMPE^+$ (1.0×10^{-4} M), the [CB[7]] was varied up to 2.0×10^{-4} M at 25.0 °C and I = 0.10 M. The second-order rate constant, k_2, decreased linearly with increasing [CB[7]] until a 1:1 ratio of CB[7] and (*E*)-$FcMPE^+$ was present (Figure 2.20), at which point a limiting rate constant was established. The rate constants for the oxidation of (*E*)-$FcMPE^+$ and (*E*)-$FcMPE^+$@CB[7] by $Co(dipic)_2^-$ were determined to be $k_0 = (2.1 \pm 0.1) \times 10^4$ M^{-1} s^{-1} and $k_{CB} = (1.6 \pm 0.1) \times 10^2$ M^{-1} s^{-1}, respectively.

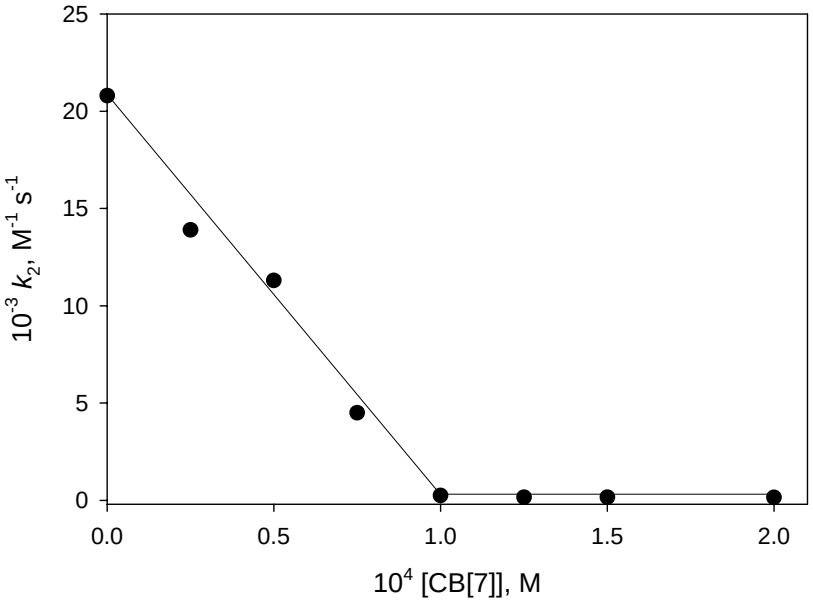

Figure 2.20 Plot of k_2 against [CB[7]] for the reaction of (*E*)-$FcMPE^+$ (1.0×10^{-4} M) with $Co(dipic)_2^-$ (1.0×10^{-3} M) at 25.0 °C (I = 0.10 M (NaCl)).

The decrease in the rate constant for the oxidation of (*E*)-$FcMPE^+$ upon its

inclusion in CB[7] may be attributed to (a) the slight increase in the (*E*)-FcMPE$^{2+/+}$ reduction potential and (b) a steric hindrance of the close approach of the reactants by CB[7] inclusion of the reductant.[35] Similar diminutions in the rate constants for the oxidations of cationic ferrocenes by $Co(dipic)_2^-$ upon their inclusion in cyclodextrins,[30-32] calixarenes[34] and cucurbiturils[35] have been reported and attributed to these thermodynamic and steric factors.

CB[7] has been demonstrated to have the ability to eliminate the photoinstability of (*E*)-FcMPE$^+$ in aqueous solution by supramolecular encapsulation of the ferrocenylethylene portion of the included guest. In addition, the inclusion of the ferrocene in the CB[7] cavity significantly reduces the complex's electron-transfer reactivity. In the same fashion, CB[7] might be able to regulate the reactivity and stability of other ferrocene derivatives through the strong complexation between CB[7] and the ferrocene moiety and/or reactive substituent groups.

2.4 Conclusions

With respect to the three challenges remaining in the area of photochemical reactions discussed in the beginning of this chapter, cucurbit[*n*]uril, specifically CB[7], has been employed to address these challenges for selected photochemical reactions. It has been illustrated by our experimental results that CB[7] can control the stereoselectivity of some organic photoreactions, can favor one of the potential photoreaction routes, and is also able to be employed to inhibit some unwanted photoreactions or other chemical

attack. With the availability of other CB[*n*] family members with different cavity sizes, many other photoreactions can potentially be mediated in a desired way by CB[*n*], which represents one of the most important functions of this family of host molecules.

References

(1) Svoboda, J.; Konig, B. *Chem. Rev.* **2006**, *106*, 5413.

(2) Jon, S. Y.; Ko, Y. H.; Park, S. H.; Kim, H. J.; Kim, K. *Chem. Commun.* **2001**, 1938.

(3) Pattabiraman, M.; Natarajan, A.; Kaanumalle, L. S.; Ramamurthy, V. *Org. Lett.* **2005**, *7*, 529.

(4) Mohanty, J.; Nau, W. M. *Angew. Chem. Int. Ed. Engl.* **2005**, *44*, 3750.

(5) Pattabiraman, M.; Natarajan, A.; Kaliappan, R.; Mague, J. T.; Ramamurthy, V. *Chem. Commun.* **2005**, 4542.

(6) Pattabiraman, M.; Kaanumalle, L. S.; Natarajan, A.; Ramamurthy, V. *Langmuir* **2006**, *22*, 7605.

(7) Choi, S.; Park, S. H.; Ziganshina, A. Y.; Ko, Y. H.; Lee, J. W.; Kim, K. *Chem. Commun.* **2003**, 2176.

(8) Mauk, A. D.; Coyle, C. L.; Bordingnon, E.; Gray, H. B. *J. Am. Chem. Soc.* **1979**, *101*, 5054.

(9) Day, A.; Arnold, A. P.; Blanch, R. J.; Snushall, B. *J. Org. Chem.* **2001**, *66*, 8094.

(10) Moon, K.; Kaifer, A. E. *Org. Lett.* **2004**, *6*, 185.

(11) Taylor, E. C.; Kan, R. O.; Paudler, W. W. *J. Am. Chem. Soc.* **1961**, *83*, 4484.

(12) Taylor, E. C.; Kan, R. O. *J. Am. Chem. Soc.* **1963**, *85*, 776.

(13) Frisch, M. J.; Trucks, G. W.; Schlegel, H. B.; Scuseria, G. E.; Robb, M. A.; Cheeseman, J. R.; Montgomery Jr., J. A.; Vreven, T.; Kudin, N.; Burant, J. C.; Millam, J.

M.; Iyengar, S. S.; Tomasi, J.; Barone, V.; Mennucci, B.; Cossi, M.; Scalmani, G.; Rega, N.; Petersson, G. A.; Nakatsuji, H.; Hada, M.; Ehara, M.; Toyota, K.; Fukuda, R.; Hasegawa, J.; Ishida, M.; Nakajima, T.; Y. Honda, Y.; Kitao, O.; Nakai, H.; Klene, M.; Li, X.; Knox, J. E.; Hratchian, H. P.; Cross, J. B.; Adamo, C.; Jaramillo, J.; Gomperts, R.; Stratmann, R. E.; Yazyev, O.; Austin, A. J.; Cammi, R.; Pomelli, C.; Ochterski, J. W.; Ayala, P. Y.; Morokuma, K.; Voth, G. A.; Salvador, P.; Dannenberg, J. J.; Zakrzewski, V. G.; Dapprich, S.; Daniels, A. D.; Strain, M. C.; Farkas, O.; Malick, D. K.; Rabuck, A. D.; Raghavachari, K.; Foresman, J. B.; Ortiz, J. V.; Cui, Q.; Baboul, A. G.; Clifford, S.; Cioslowski, J.; Stefanov, B. B.; Liu, G.; Liashenko, A.; Piskorz, P.; Komaromi, I.; Martin, R. L.; Fox, D. J.; Keith, T.; Al-Laham, M. A.; Peng, C. Y.; Nanayakkara, A.; Challacombe, M.; Gill, P. M. W.; Johnson, B.; Chen, W.; Wong, M. W.; Gonzalez, C.; Pople, J. A. *Gaussian 03, Revision C.02* Gaussian, Inc., Wallingford, CT, 2004.

(14) Alston, D. R.; Ashton, P. R.; Lilley, T. H.; Stoddart, J. F.; Zarzycki, R. *Carbohydr. Res.* **1989**, *192*, 259.

(15) Liu, S. M.; Ruspic, C.; Mukhopadhyay, P.; Chakrabarti, S.; Zavalij, P. Y.; Isaacs, L. *J. Am. Chem. Soc.* **2005**, *127*, 15959.

(16) Cram, D. J.; Tanner, M. E.; Thomas, R. *Angew. Chem. Int. Ed. Engl.* **1991**, *30*, 1024.

(17) Warmuth, R. *Angew. Chem. Int. Ed. Engl.* **1997**, *36*, 1347.

(18) Warmuth, R. *Chem. Commun.* **1998**, 59.

(19) Kusukawa, T.; Fujita, M. *J. Am. Chem. Soc.* **1999**, *121*, 1397.

(20) McCall, M. T.; Whitten, D. G. *J. Am. Chem. Soc.* **1969**, *91*, 5681.

(21) Happ, J. W.; McCall, M. T.; Whitten, D. G. *J. Am. Chem. Soc.* **1971**, *93*, 5496.

(22) Wulff, G. *Angew. Chem. Int. Ed. Engl.* **1995**, *34*, 1812.

(23) Herrmann, W.; Wehrle, S.; Wenz, G. *Chem. Commun.* **1997**, 1709.

(24) Jeon, W. S.; Moon, K.; Park, S. H.; Chun, H.; Ko, Y. H.; Lee, J. Y.; Lee, E. S.; Samal, S.; Selvapalam, N.; Rekharsky, M. V.; Sindelar, V.; Sobransingh, D.; Inoue, Y.; Kaifer, A. E.; Kim, K. *J. Am. Chem. Soc.* **2005**, *127*, 12984.

(25) Kunkely, H.; Vogler, A. *J. Organomet. Chem.* **2001**, *637-639*, 777.

(26) Marder, S. R.; Perry, J. W.; Tiemann, B. G.; Schaefer, W. P. *Organometallics* **1991**, *10*, 1896.

(27) Goerner, H.; Kuhn, H. J. *Adv. Photochem.* **1995**, *19*, 1.

(28) Ong, W.; Kaifer, A. E. *Organometallics* **2003**, *22*, 4181.

(29) Sobransingh, D.; Kaifer, A. E. *Chem. Commun.* **2005**, 5071.

(30) Imonigie, J. A.; Macartney, D. H. *J. Inclusion Phenom.* **1993**, *15*, 193.

(31) Imonigie, J. A.; Macartney, D. H. *Inorg. Chim. Acta* **1994**, *225*, 51.

(32) Macartney, D. H.; Roszak, A. W.; Smith, K. C. *Inorg. Chim. Acta* **1999**, *291*, 265.

(33) Baer, A. J.; Macartney, D. H. *Inorg. Chem.* **2000**, *39*, 1410.

(34) Imonigie, J. A.; Macartney, D. H. *Inorg. React. Mech.* **2006**, *6*, 161.

(35) Yuan, L.; Macartney, D. H. *J. Phys. Chem. B* **2007**, *111*, in press.

Chapter 3

CUCURBIT[n]URIL MEDIATED FLUORESCENCE OF GUEST FLUOROPHORES

This chapter is mainly concerned with the employment of CB[n] in mediating the fluorescent properties of organic guest fluorophores, such as fluorescent color switches (in the emission wavelength changes) of protonated aromatic amines upon complexation with CB[7], and fluorescence off/on (emission intensity changes) switches of acridizinium guests mediated by both CB[8] and CB[7]. This chapter begins with a brief introduction and short review of host-mediated (especially CB[n]) fluorescence of guest fluorophores, followed by a description of materials preparation, experimental methods and instrumentation, and then the results and discussion of the investigations. Conclusions are drawn at the end to highlight the contributions of this study to the field

of CB[n] chemistry.

3.1 Introduction

It has been briefly introduced in chapter 1 that host molecules can often mediate the fluorescent properties of included guest fluorophores, and this principle is frequently employed to design and construct fluorescent switches and chemical sensors. The study of fluorescence changes of guest molecules upon complexation with nonfluorescent host molecules have been extensively reviewed by Wagner.[1] Many examples presented in this review have demonstrated that inclusion of guest fluorophores into nonfluorescent host molecules often results in significant or moderate changes in its fluorescent properties, including emission color ($\lambda_{F,\max}$), emission intensity (or quantum yield), fluorescent lifetime, and very often photostability enhancement. The fluorescence changes of guest fluorophores upon inclusion in nonfluorescent host molecules are proposed by Wagner and others to be attributed to one or more of three factors.[1] First, the polarity of the microenvironment inside the host cavity is different from that of the bulk medium. Fluorescent property changes have been observed for some polarity-sensitive fluorophores, such as 1-anilino-8-naphthalene sulfonate (1,8-ANS)[2,3] and 2-*p*-toluidinylnaphthalene-6-sulfonate (2,6-TNS)[4] upon their inclusions in host molecules. In addition, there is very often a reduced intramolecular rotational mobility of the guest molecule inside the cavity of the host. This results in a fluorescence enhancement, from the loss of rotational freedom of the fluorophore, such as in the

fluorescence enhancement of a number of benzene derivative upon their inclusions in β-cyclodextrin.[5] Moreover, exposure of the included guest fluorophore to quenchers such as O_2 and other chemicals from the environment is greatly reduced. Rhodamine 6G and other dye molecules, for example, are highly stabilized from photobleaching (frequently caused by photo-oxidation) by CB[7] host molecules.[6,7]

The CB[n] family of host molecules has exhibited unique abilities in mediating guest molecules' fluorescence. The initial work of employing CB[n] molecules in the mediation of guest fluorescence was carried out in the solid state. Both the Buschmann[8] and Wagner[9] groups independently studied the complexation of CB[6] with 1,8-ANS in the solid state and achieved highly fluorescent complexed solids. Buschmann and coworkers suggested that the encapsulation of 1,8-ANS into the nonpolar cavity of CB[6] in the solid state is responsible for the fluorescence light-up,[8] however, Wagner and coworkers discovered a lattice inclusion complex (clathrate) in the crystal structure, instead of a CB[6] cavity-encapsulated complex.[9] In this case, the CB[6] molecules act as spacers to separate 1,8-ANS guest fluorophores from each other in the solid state to prevent their interaction, thus allowing them to fluoresce more efficiently. At a later time, the complex based on 1,8-ANS and a larger member of CB[n] family, CB[7], was investigated by Wagner in solution.[3] A large fluorescence enhancement was discovered for 1,8-ANS in water, upon addition of CB[7]. Again, the internal cavity inclusion of the guest molecules was not envisioned by any means. It was proposed that CB[7] and 1,8-ANS form a 2:1 exclusion host-guest complex (the portals of two CB[7] host

molecules are interacting with one guest molecule externally) in water.[3]

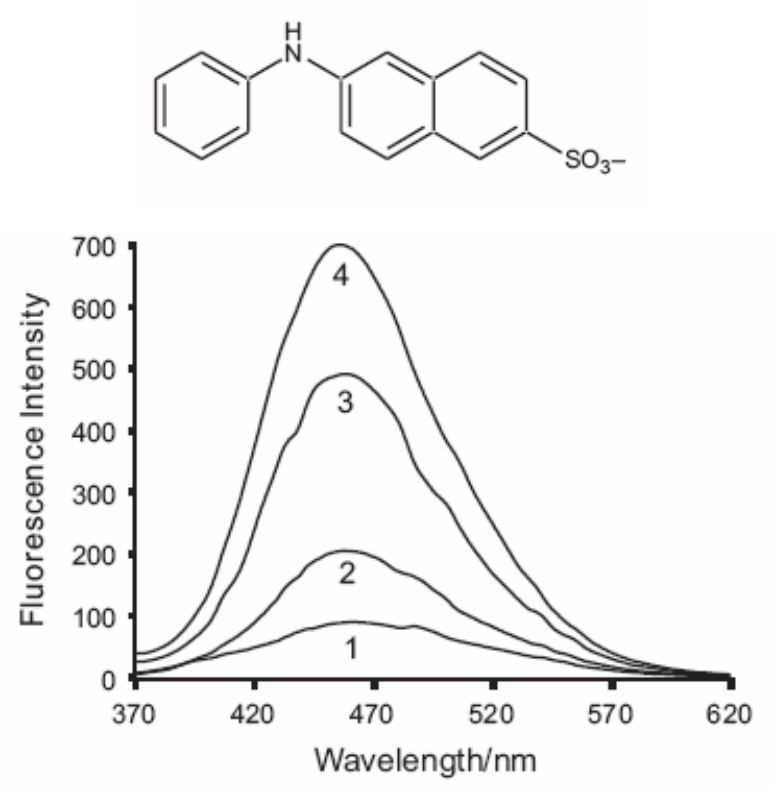

Figure 3.1 **(a)** The structure of 2,6-ANS (top); **(b)** The fluorescence spectrum of 2,6-ANS (2.0×10^{-5} M) in Na_2SO_4 solution (0.20 M) in the presence of: (*1*) 0 mM; (*2*) 4 mM; (*3*) 20 mM; and (*4*) 48 mM CB[6].[10]

An inclusion complex based on CB[n] and guest fluorophores in aqueous solution was firstly reported by Wagner in 2001,[10] in which the fluorescence of 2,6-ANS was found to be dramatically increased upon complexation with CB[6] (Figure 3.1). It was proposed that the aniline portion of 2,6-ANS is included into the cavity of CB[6], with

enhancement occurring through decreased intramolecular rotational freedom of the guest molecule. The replacement of CB[6] with CB[7] for this system gives greater fluorescence enhancement, and the mechanism has been proposed to be the same.[3] Very recently, the same mechanism resulted in a fluorescence increase for the carbendazim guest molecule upon its partial inclusion in the CB[6] cavity.[11]

The fluorescence of curcumin guest molecules has been enhanced as well upon complexation with CB[6] in water, as the fluorescence of this polarity-sensitive guest increases in nonpolar environments and the cavity of CB[6] provides such an environment.[12] Similarly, the nonpolar cavity of CB[7] induces moderate emission shifts, as well as the photostabilization enhancement of included guest fluorophores such as rhodamine 6G and rhodamine 123, as observed by Nau and coworkers.[6,7]

In these briefly reviewed examples, the mediation of the fluorescence of guest molecules by CB[n] can be explained by the previously mentioned three mechanisms (or factors) proposed by Wagner and others.[1] In this chapter, we discuss the fluorescence behaviors of protonated aromatic amines, aromatic alcohols, and the acridizinium (ADZ^+) and 9-aminoacridizinium ($AADZ^+$) cations upon their complexation with CB[n]. We propose two different fluorescence-mediation mechanisms, based on the results of our investigations.

3.2 Experimental

3.2.1 Materials Preparation and Characterization

The host molecule CB[7] was synthesized according to literature methods, as previously described in chapter 2.[13] Acridizinium bromide ([ADZ]Br) and 9-aminoacridizinium bromide ([AADZ]Br) were synthesized and provided by Dr. Heiko Ihmels from the Institute for Organic Chemistry at University of Siegen, Germany.[14] 1-aminoanthracene was crystallized from ethanol before use. All of the other chemicals involved in this project were purchased and used as received.

3.2.2 Methods and Instrumentation

The 1D ^{1}H and 2D COSY NMR spectra were recorded on a Bruker AV-400 MHz NMR spectrometer. The ESI-MS spectra were acquired on a Waters 2Q Single Quadrupole MS spectrometer equipped with an ESI/APcI multiprobe. The UV-visible spectra were acquired on a Hewlett Packard 8452A diode array spectrometer using quartz cells with a 1.00 cm path length. The fluorescence spectra and titrations were all carried out on a Photon Technology International luminescence spectrometer in a dark room.

The modeled structures of the host-guest complexes involved in this project were computed by energy-minimizations using Gaussian 03 (Revision C.02) programs run on the computing facilities of the High Performance Virtual Computing Laboratory (HPVCL) at Queen's University, as described in section 2.2.2 of chapter 2.

Digital images of the fluorescent solutions, with and without host molecules, were taken by using a Sony DSC-P71 camera, under UV light excitation.

3.2.3 Host-Guest Stability Constant Determinations

3.2.3.1 Fluorescence and UV-visible Titrations

One of the important pieces of information on host-guest inclusion systems obtained from fluorescence measurements (fluorescence titrations) is the association constant $K_{CB[n]}$. When the complexation between the host CB[*n*] and a guest molecules is relatively weak, $K_{CB[n]}$ can be acquired by measuring the value of F/F_0 (F is the fluorescence intensity of guest molecules in the presence of various amounts of CB[*n*], whereas F_0 is the fluorescence of free guest molecules) as a function of host concentration (while maintaining guest concentration constant) and the data is fit with the following equation using a nonlinear least-squares procedure.[15]

$$F / F_0 = 1 + (F_\infty / F_0 - 1)\frac{[CB[n]]_0 \times K_{CB[n]}}{1 + [CB[n]]_0 \times K_{CB[n]}} \qquad (3.1)$$

In this equation, F_∞ is the fluorescence of the fully complexed guest fluorophore, *e.g.* at an infinite host concentration, and $[CB[n]]_0$ is the actual host concentration added into the solution of the guest molecule during the titration ($[CB[n]]_f$ is assumed to be approximately equal to $[CB[n]]_0$).

When the complexation is relatively strong (such that $[CB[n]]_f \neq [CB[n]]_0$), equation 3.1 is no longer applicable, and the following equations may be employed to acquire the

stability constant.

$$F / F_0 = \frac{[G]_{total} - [GH] + (F_\infty / F_0)[GH]}{[G]_{total}} \quad (3.2)$$

$$[GH] = \frac{b - \sqrt{b \times b - 4 \times [G]_{total} \times [H]_{total}}}{2} \quad (3.3)$$

$$b = [G]_{total} + [H]_{total} + \frac{1}{K_{CB[n]}} \quad (3.4)$$

In these equations, $[G]_{total}$ is the total concentration of guest molecules, $[H]_{total}$ is the total concentration of host molecules, and [GH] is the concentration of the guest-host complex. The values of F_∞/F_0 can be acquired from the titration spectra, while F/F_0, $[H]_{total}$ and $[G]_{total}$ are known. A fit of the data using equation 3.2 (together with 3.3 and 3.4) yields a value of $K_{CB[n]}$.

For UV-visible titrations, similar to those of fluorescence titrations, the following equation is employed.

$$A = A_0 + (\varepsilon_{GH} - \varepsilon_G) \times [GH] \quad (3.5)$$

In this equation, ε_G is determined from $A_0/[G]_{total}$ (A_0 is the concentration of free guest molecule), while $[H]_{total}$ and $[G]_{total}$ are known. The value of ε_{GH} can be estimated from $A_{limiting}$ (the absorbance of fully complexed guest molecule), and a fit of the data using equation 3.5 (together with 3.3 and 3.4) yields a value of $K_{CB[n]}$.

3.2.3.2 Competitive ^{1}H NMR Titrations

This method has been previously discussed in the section of 2.2.3.2 of chapter 2.

3.2.4 Calculations of p*Ka* and p*Ka** values

3.2.4.1 Ground state p*Ka* measurements

The ground state pK_a values for the AAH^+@CB[7] complex (AAH^+ represents the protonated aromatic amine) in the ground state was estimated by measuring the pH of the solution by adding one half of an equivalent of hydrochloric acid into 25 μM AA@CB[7] (AA is the neutral aromatic amine). Assuming that AA@CB[7] is a relatively strong base (strong proton acceptor), half of the AA@CB[7] is protonated and becomes AAH^+@CB[7], while the other half remains in the unprotonated AA@CB[7] form, according to the following equation.

$$pK_a = pH + \log([AAH^+@CB[7]]/[AA@CB[7]] \quad (3.6)$$

At the point where $[AAH^+@CB[7]] = [AA@CB[7]]$ the pK_a is equal to the measured pH value, which can often by checked by UV-visible spectroscopy.

3.2.4.2 Excited state p*Ka** measurements

The pK_a* value for the excited state AAH^+*@CB[7] complex was initially determined using a Förster cycle,[16] in which the difference in the pK_a between the ground and excited states is related to the change in the emission maxima.

$$pK_a^* = pK_a - 0.625\Delta\nu/T \quad (3.7)$$

In this equation, $\Delta\nu$ is the difference in the emission maxima (cm^{-1}) of the protonated and neutral species, assuming that the entropy change $\Delta S^* - \Delta S^0$ is equal to zero. This calculation is not accurate as $\Delta S^* - \Delta S^0$ is not zero, however, it is quite difficult to correct for this directly because of the host-guest association and dissociation processes. Fortunately, the correction still can be done in a relatively reliable method using dynamic analyses. It has been proposed by Shizuka that for the calculation of the pK_a^* of aromatic amines, the entropy correction can be calculated using the Stokes shift for the compound ΔE_{St} in the following equation.[17]

$$pK_a^* = (pK_a^*)_{FC} + 8.72\Delta E_{St} - 2.64 \quad (3.8)$$

In this equation $(pK_a^*)_{FC}$ is the pK_a^* value calculated from Förster cycle (eq. 3.6). The calculated pK_a^* value can then be compared with the value determined from the fluorescence pH titration.

3.3 Results and Discussion

3.3.1 Fluorescence Switch of Aromatic Amines and Alcohols

We have investigated the effects of the inclusion of protonated aromatic amines: 1- and 2-aminoanthracene (1-AAH^+ and 2-AAH^+), 1- and 2-aminonaphthalene (1-$NTAH^+$

and 2-NTAH$^+$), and 1-aminopyrene (1-APRH$^+$) in acidic aqueous solution, and aromatic alcohols: 1- and 2-naphthol in the cavity of CB[7] in neutral solution, on the guests' fluorescence spectra. An emission maximum switch has been observed for these guest fluorophores upon their complexation with CB[7]. As none of the existing mechanisms described in section 3.1 can explain the fluorescence maximum switch, we have proposed a different explanation. With this guest–host system, the inclusion of a protonated aromatic amine or a neutral aromatic alcohol into the cavity of CB[7] significantly reduces its acidity in both the ground and excited states, which results in the observed emission color switch. This discovery can potentially be employed to design and construct fluorescent molecular switches and molecular sensors.

3.3.1.1 Complexes Formation Between Aromatic Amines and CB[7]

The formation of a 1:1 guest–host complex between 2-AAH$^+$ and CB[7] has been confirmed by electrospray mass spectrometry, ^{1}H NMR spectroscopy, and UV-visible absorbance (Job's plot) and emission spectroscopy. The ^{1}H NMR spectrum of the 1:1 guest–host complex of the 2-AAH$^+$ with CB[7] (Figure 3.2) reveals complexation-induced upfield chemical shifts (0.2 to 1.1 ppm) for the majority of the aromatic guest resonances, consistent with their inclusion in the deshielding hydrophobic cavity of the host. The H5 and H8 protons exhibit slight downfield shifts as they are located in line with the carbonyl groups of the portals, which have been observed to deshield guest protons. The appearances of separate proton resonances for the free and

included guest and host molecules indicate that complexation–decomplexation processes between 2-AAH$^+$ and CB[7] occur at a slow rate on the ^{1}H NMR timescale.

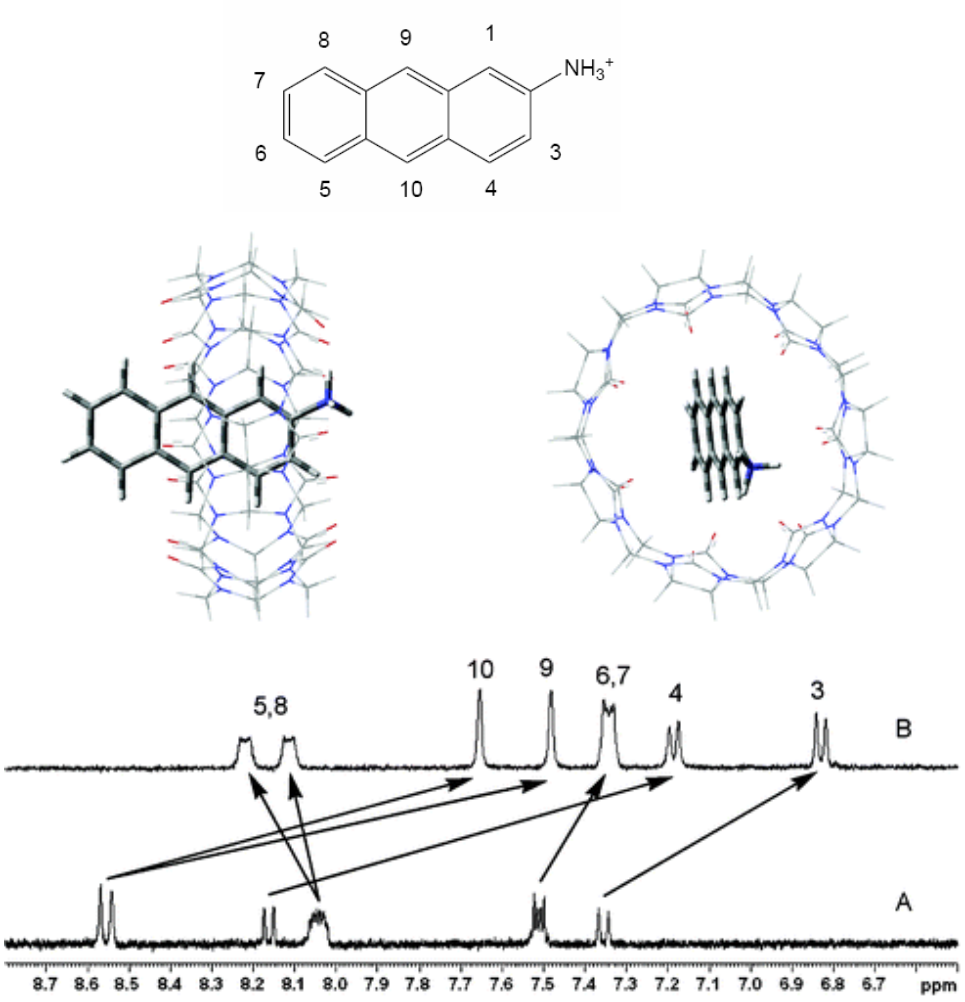

Figure 3.2 **Top**: the structure of protonated 2-aminoanthracene (2-AAH$^+$) with number labeling. **Middle**: two views of the energy-minimized structure of 2-AAH$^+$@CB[7]. **Bottom**: the aromatic region of the ^{1}H NMR spectra of 2-AAH$^+$ (A) and 2-AAH$^+$@CB[7] (B). The H1 proton undergoes deuterium exchange in the D_2O solvent and is not observed.

The effect of inclusion is also seen in the proton resonances for the methylene groups which bridge the glycoluril units in CB[7]. Upon complexation by an asymmetric 2-AAH$^+$ guest, the symmetry-related methylene doublet resonances at 5.64 (protons pointing towards the carbonyl oxygens) and 4.13 ppm are split into pairs of doublets (5.60/5.43 and 4.04/3.93 ppm). This inclusion induced asymmetry generated in the portals of the CB[7] cavity, reminiscent (in the opposite sense) of the splitting of the ^{1}H NMR resonances for symmetry-related protons of symmetrical guests included in the asymmetric cyclodextrin cavities,[18] was also recently reported for the inclusion of cationic substituted ferrocenes in the CB[7] cavity.[19]

An energy-minimized structure of the 2-AAH$^+$@CB[7] complex from *ab initio* calculations (Figure 3.2) is consistent with the NMR results, with two of the three aromatic rings within the CB[7] cavity. The interaction of the ammonium group with the portal oxygens on CB[7] evidently stabilizes the protonated aromatic amine molecule, through H-bonding and cation-dipole interactions.

The UV-visible absorbance spectrum of 2-AAH$^+$ exhibits bathochromic shifts in the transitions in the presence of CB[7], as shown in Figure 3.3, consistent with the solvatochromic behavior reported previously.[20] A spectrophotometric (absorbance and fluorescence) titration of 2-AAH$^+$ with CB[7] provided a stability constant of (8 ± 2) × 10^5 M^{-1} (Figure 3.4) which is similar to the values reported for the inclusion of other cationic aromatic molecules, such as methylviologen ($K_{CB[7]}$ = 2 × 10^5 M^{-1}) in CB[7].[21,22]

Additional evidence supporting the formation of a 1:1 complex between CB[7] and 2-AAH$^+$ is a Job's plot, based on a UV-visible continuous variation method. The absorbance changes most when the molecular ratio of the CB[7] host and the 2-AAH$^+$ guest reaches 1:1.

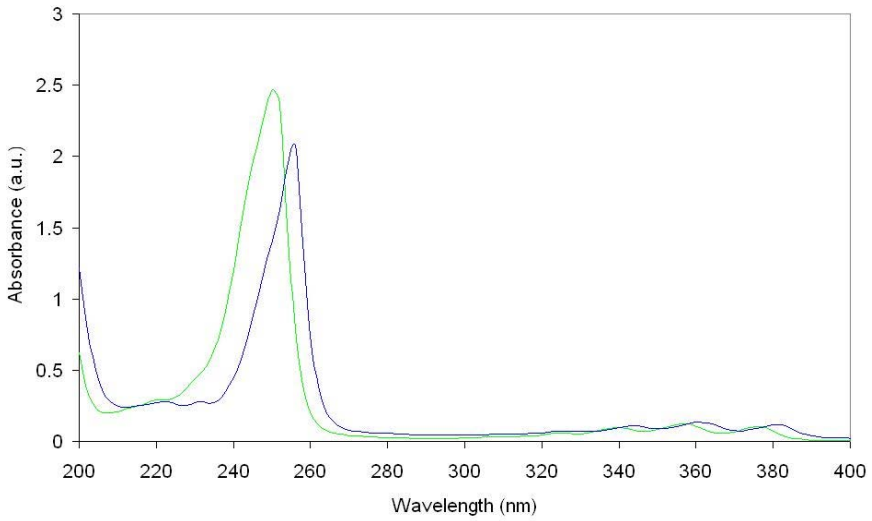

Figure 3.3 The UV-visible absorption spectra of 2-AAH$^+$ (5.0×10^{-5} M) in the absence (green lines) and presence (blue line) of CB[7] (1.0×10^{-4} M) in acidic aqueous solution (pH 1.5).

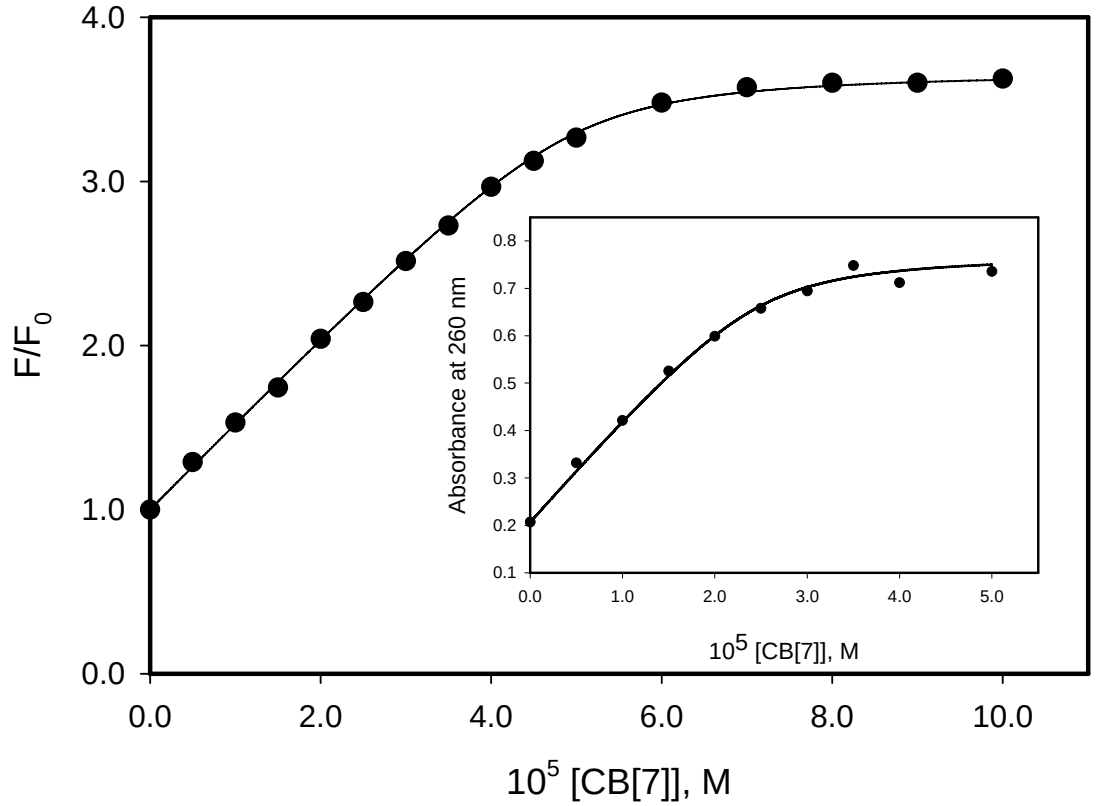

Figure 3.4 The dependence of the fluorescence intensity [(F/F_0), (2-AAH$^+$) = 5.0 × 10^{-5} M] at 412 nm and (inset) the absorbance (2-AAH$^+$ = 2.5 × 10^{-5} M) at 260 nm of 2-AAH$^+$ on the concentration of CB[7] in acidic aqueous solution. The solid lines are fit with a stability constant for 2-AAH$^+$@CB[7] of 8 × 10^5 M^{-1}.

Similarly, all of the other aromatic amines in our investigation, including 1-AAH$^+$, 1-NTAH$^+$, 2-NTAH$^+$ and 1-APRH$^+$, form 1:1 host-guest inclusion complexes with CB[7], which have been confirmed by the same set of characterization techniques such as ESI-MS spectrometry, ^{1}H NMR spectroscopy, and UV-visible absorbance (and Job's plot) and emission spectroscopy, as well as by *ab initio* calculations of energy-minimized

structures (Figure 3.5). As with 2-AAH$^+$, the ^{1}H NMR spectra indicate that a majority of the aromatic portion of these protonated aromatic amines are included in the cavity of CB[7], leaving the positively-charged ammonium group at the portal area to maximize the cation-dipole and hydrogen bonding interactions between the ammonium group and the carbonyl groups of the portal.

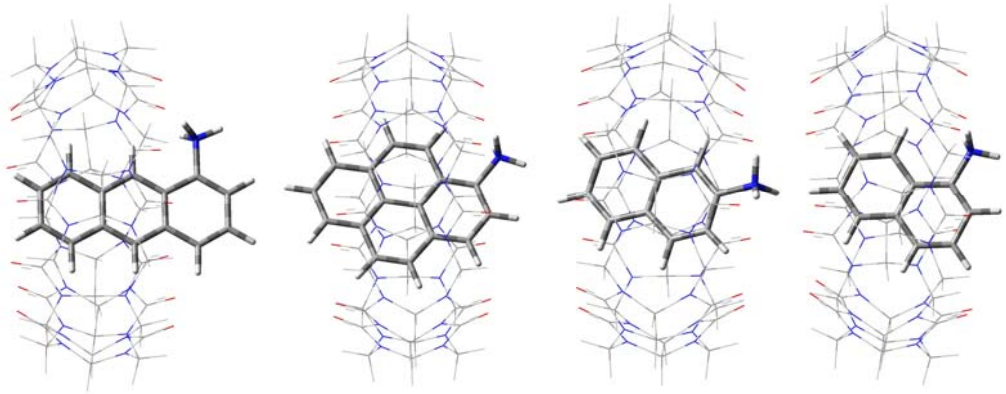

Figure 3.5 Side views of energy-minimized structures of 1-AAH$^+$@CB[7], 1-APRH$^+$@CB[7], 2-NTAH$^+$@CB[7] and 1-NTAH$^+$@CB[7], from left to right.

All of the aromatic amines exhibit bathochromic shifts in the absorption spectra in the presence of the host molecule CB[7], similar to the solvatochromic behavior shown by 2-AAH$^+$. Association constants for these 1:1 host-guest complexes have been determined to be $(7 \pm 1) \times 10^5$ M^{-1} for 1-AAH$^+$@CB[7], $(3 \pm 1) \times 10^5$ M^{-1} for both 1-NTAH$^+$@CB[7] and 2-NTAH$^+$@CB[7], and $(7 \pm 2) \times 10^3$ M^{-1} for 1-APRH$^+$@CB[7] from spectrophotometric titrations of these aromatic amines with CB[7]. As we

expected, the inclusion complexes of CB[7] with the 1- and 2-AAH^+ and 1- and 2-$NTAH^+$ guests are stable and have rather similar stability constants. The much lower stability constant for the 1-$APRH^+$@CB[7] complex, however, may be explained by a poorer size match between the CB[7] cavity and the 1-$APRH^+$ guest. The 1-$APRH^+$ has a large planar polyaromatic structure and significant distortion of CB[7] is required for inclusion of the guest.

3.3.1.2 Fluorescence Switches of Complexes of Aromatic Amines

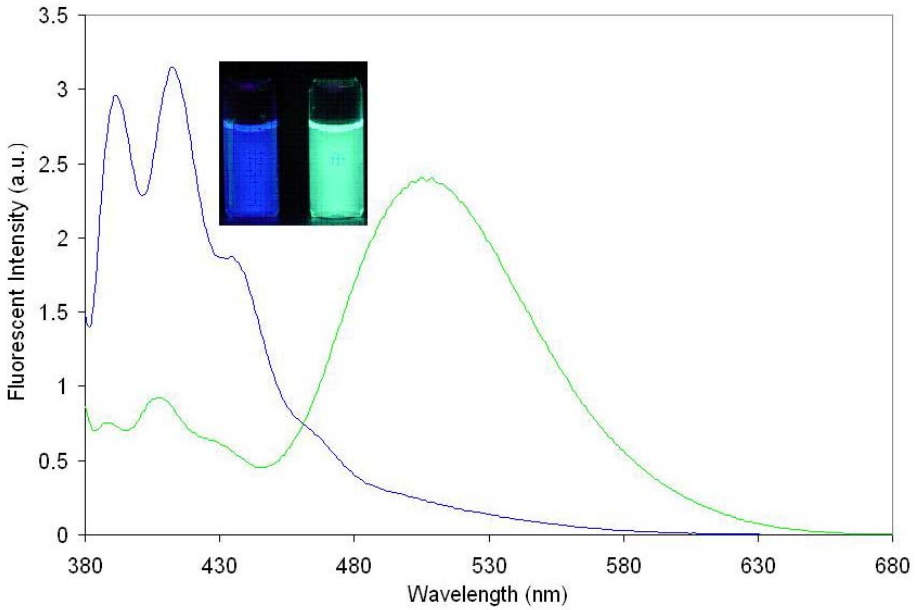

Figure 3.6 Emission (excitation at 342 nm) spectra of 2-aminoanthracene (50 μM 2-AAH^+) in the absence (green lines) and presence (blue lines) of CB[7] (100 μM) in acidic aqueous solution (pH 1.5). Insert pictures are digital images of solutions of 2-AAH^+ in the absence (green) and in the presence (blue) of CB[7].

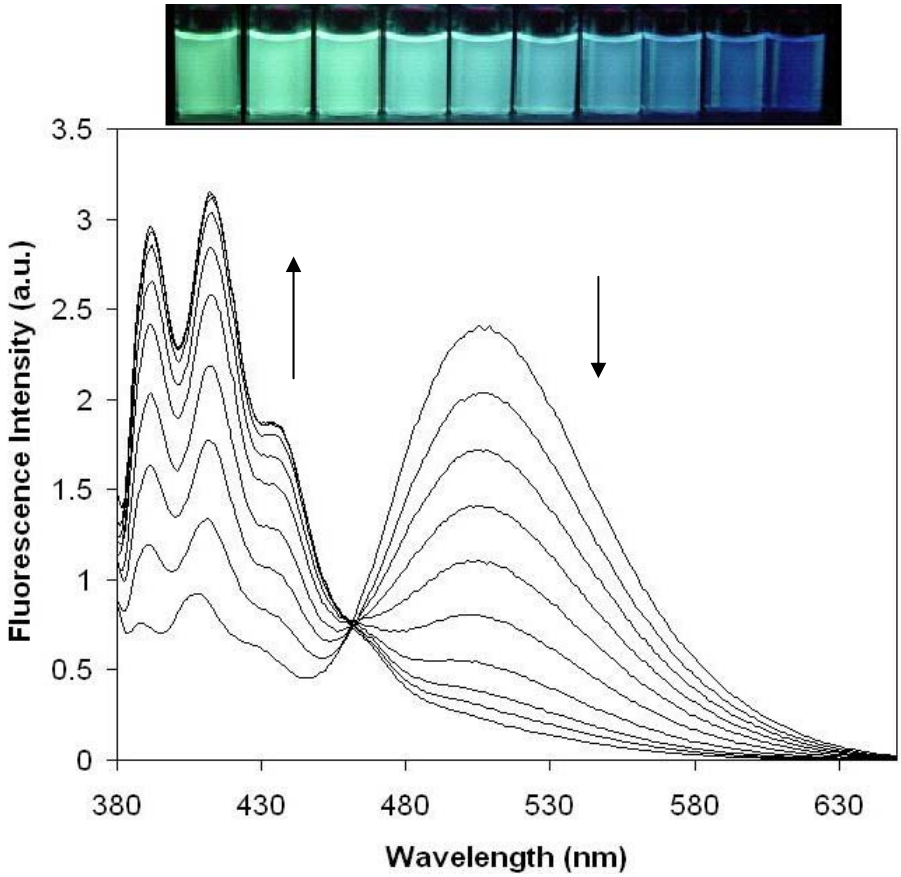

Figure 3.7 **Top**: digital images of the 2-AAH$^+$ solution with different ratios of CB[7] (up to 1.2:1 ratios) under a UV lamp (365 nm wavelength) at [2-AAH$^+$] = 50 μM. **Bottom**: fluorescence spectra (excited at 374 nm) of 2-AAH$^+$ without CB[7] and with various amounts of CB[7].

With a detailed knowledge of the complexation behavior between these protonated aromatic amines and CB[7], the fluorescence of these guest fluorophores in the absence and in the presence of CB[7] host molecules has been studied. In the presence of CB[7],

we observe a switch in the fluorescence of 2-AAH$^+$ from green (emission color of free 2-AAH$^+$) to blue (emission of the complex) emission. Figure 3.6 shows the change in the emission spectrum of 2-AAH$^+$ upon inclusion in CB[7]. The green-to-blue fluorescence switch of 2-AAH$^+$ upon gradual addition of CB[7] host molecule is not a gradual emission maximum green-to-blue shift (λ_{max} movement), but rather a result of the disappearance of the green emission band (to about 10% of its original intensity at 512 nm) and a simultaneous significant enhancement (about four-fold increase in the band at 406 nm) of the second, higher energy blue emission band. Figure 3.7 shows that the fluorescence at 512 nm is suppressed with increasing CB[7] and the fluorescence at about 406 nm is enhanced by complexation of CB[7].

As expected, all of the other aromatic amines in our investigations have demonstrated similar fluorescence switching behavior upon their complexation with CB[7] in acidic solution. Figure 3.8 shows the simultaneous decrease of the emission of the lower energy band and enhancement of the emission of the higher energy band with the addition of CB[7] to the acidic solutions of 1-NTAH$^+$ (the fluorescence at 445 nm is suppressed with increasing CB[7] while the fluorescence at about 335 nm is enhanced by complexation of CB[7]) and 1-APRH$^+$ (the fluorescence at 438 nm is suppressed with increasing CB[7] while the fluorescence at about 370 nm is enhanced by complexation by CB[7]).

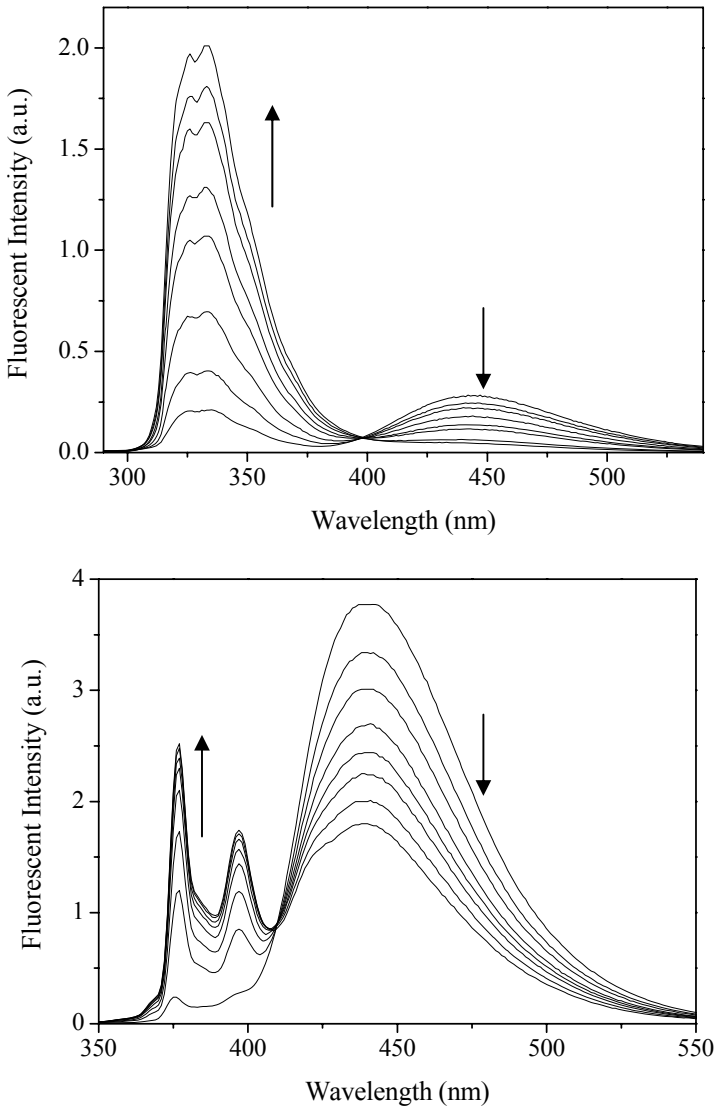

Figure 3.8 **Top**: Fluorescence spectra (excitation at 275 nm) of 1-aminonaphthalene (1-NTAH$^+$) without CB[7] and with various amounts of CB[7] (up to 3:1 ratio of CB[7]:1-NATH$^+$) at pH 1.5. **Bottom**: Fluorescence spectra (excitation at 345 nm) of 1-APRH$^+$ without CB[7] and with various amounts of CB[7] (up to 20:1 ratio of CB[7]:1-APRH$^+$) at pH = 1.5.

The fluorescence emission color switch of guest aromatic amines upon complexation of CB[n] had not been reported before. The mechanism of the host molecule induced emission switch was not immediately clear. In the beginning, we postulated that the emission switch might be induced by the hydrophobic cavity of CB[7]. However, this postulation was excluded after we carried out a comparative study by using another host molecule, β-cyclodextrin, which also has a hydrophobic cavity. In this comparative experiment, very little change in the fluorescence is observed under the same experimental conditions with up to a 10-fold excess of β-cyclodextrin. We considered the fact that the color switch was apparently not a simple shift in the emission maximum from green to blue, but rather a simultaneous higher-energy band emission increase and lower-energy band emission decrease for these aromatic amines, with originally two emission bands (visible in all of the emission spectra of these protonated aromatic amines). A new mechanism for this fluorescence alternation of guest fluorophores (aromatic amines in particular) upon their complexation with CB[7] host molecules, had to be proposed, as none of the existing three mechanisms could explain this novel fluorescence switching.

3.3.1.3 Proposed Mechanism of Fluorescence Switch

After searching the literature, we have found that protonated aromatic amines are known to exhibit dual fluorescent behavior in aqueous solution when the pH is lower than its ground state pK_a and higher than its singlet excited state pK_a*.[20,23,24] This

occurs with 2-AAH$^+$, which fluoresces with blue emission (422, 405, and 387 nm) from 2-AAH$^+$* and green emission (503 nm) from 2-AA*, simultaneously. The pK_a of the ground state 2-AAH$^+$ species has been determined to be 4.0 in water,[23] while the pK_a* value for the singlet excited state has been calculated to be –5.4 in 1:1 water:alcohol.[20,24] As a result of the very low pK_a* of 2-AAH$^+$* (it has been referred to as a photoacid), the major emission is always green in acidic aqueous solution, because the 2-AAH$^+$* is instantaneously deprotonated to 2-AA* at excited state as a result of its super acidity. The excited 2-AA* returns to the ground state 2-AA species by emitting green light before reprotonation.[25-27] Upon complexation with CB[7], the emissions of the guest aromatic amines increase for the higher energy band (from the protonated aromatic amine), and decrease for the lower energy band (from the neutral aromatic amine). This may be attributed to a dramatic decrease in the acidity of the protonated aromatic amines in the excited state, AAH$^+$*, once encapsulated in the cavity of CB[7].

The interaction of the ammonium group with the portal oxygens on CB[7] may result in a change in its acidity in both the ground and excited states. Marquez and Nau have previously reported that CB[6] inclusion of cycloalkylmethylamines increases the pK_a of the protonated ammonium guests by over one pK_a unit.[28] The singlet excited state pK_a* value increases substantially in the AAH$^+$@CB[7] guest–host complex in our investigation. For example, the 2-AAH$^+$@CB[7] has a pK_a* value of 5.2 ± 0.2, estimated from a fluorescence pH titration, compared to its original pK_a* value of -5.4 in the absence of CB[7]. In another words, the acidity of the protonated aromatic amines

(AAH$^+$) in the excited state is dramatically decreased and the ammonium ion is stabilized in excited state upon complexation with CB[7].

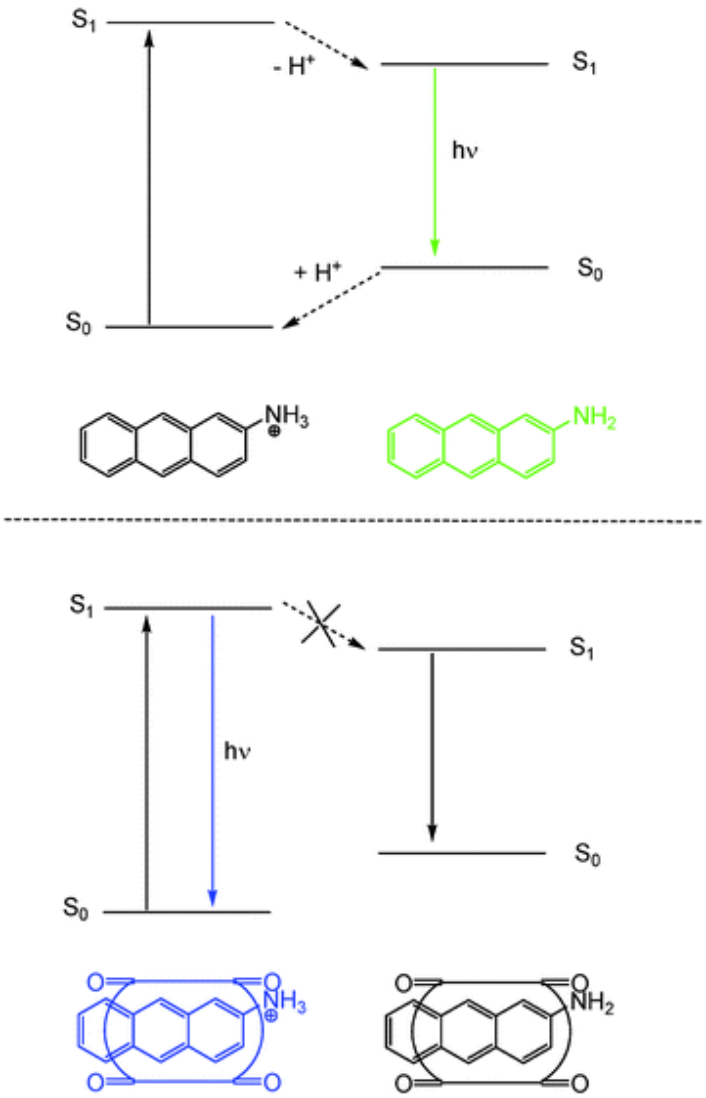

Figure 3.9 Schematic representation of the excitation and emission of 2-AAH$^+$ with and without CB[7] in acidic aqueous solution. The acidity of the excited state of 2-AAH$^+$ (pK_a* = –5.4 ± 1) decreases considerably within the 2-AAH$^+$@CB[7] complex (pK_a* = 5.2 ± 0.2), such that the blue emission dominates (pH < 5.0).

As a result of the increased basicity of the included aromatic amines (AA) in the excited state, emission from the S_1 state of the AAH^+* now occurs prior to deprotonation to AA* in acidic solution. This shuts off the pathway for the green emission, and enhances the blue emission from the included 2-AAH^+* species, in the case of 2-AAH^+@CB[7]. The proposed mechanism for the emission switch is illustrated in Figure 3.9.

3.3.1.4 Fluorescence Switch of Aromatic Alcohols

As aromatic alcohols, such as naphthols, have similar dual fluorescence behavior in neutral aqueous solution, we have extended this research to 1- and 2-naphthol. As expected, the naphthols also demonstrated similar fluorescence switching behavior upon their complexation with CB[7] host molecules.

The inclusion complexation between CB[7] and 1- and 2-naphthol have been confirmed by ^{1}H NMR, UV-visible, fluorescence spectroscopy and *ab initio* calculations of the energy-minimized structures (Figure 3.10). The binding constants have been determined by fluorescence titrations to be $(8 \pm 1) \times 10^4$ M^{-1} and $(4 \pm 1) \times 10^4$ M^{-1} for 1-naphtol and 2-naphthol, respectively, with CB[7].

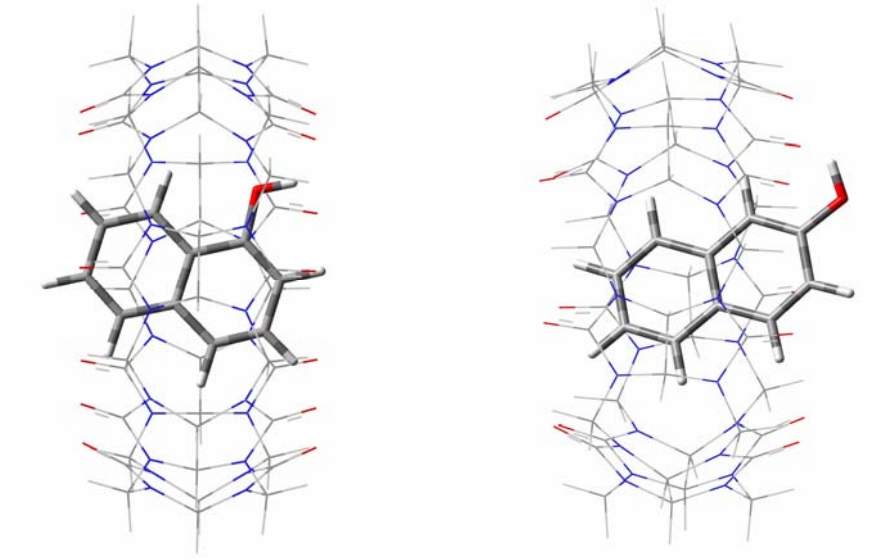

Figure 3.10 The energy-minimized structures of 1-naphthol@CB[7] (left) and 2-naphthol@CB[7] (right) in the gas phase.

The fluorescence switch of naphthols upon complexation has been demonstrated by the addition of CB[7] to solutions of the neutral naphthols. Figure 3.11 demonstrates that the emission of 1-naphthol for the lower-energy band is decreased with a simultaneous emission increase at higher-energy band, upon the guest molecules' complexation with CB[7].

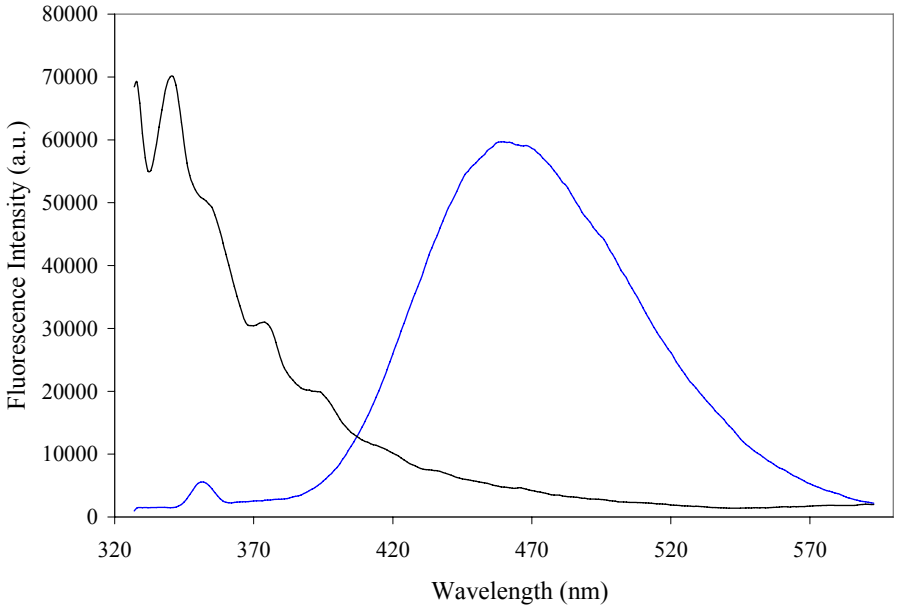

Figure 3.11 Fluorescence spectra of 10 μM 1-naphthol in the absence (blue) and in the presence (black) of the 500 μM CB[7] at neutral pH in aqueous solution (excitation at 310 nm).

The switching mechanism is similar to that of aromatic amines. The complexation of CB[7] stabilizes the neutral hydroxyl group at the portals through hydrogen bonding, so that the deprotonation of naphthols in the excited state becomes difficult. As a consequence, the excited-state deprotonation is inhibited upon guest inclusion in the cavity of CB[7], and the fluorescence from the neutral form of the aromatic alcohol is dramatically enhanced (Figure 3.12).

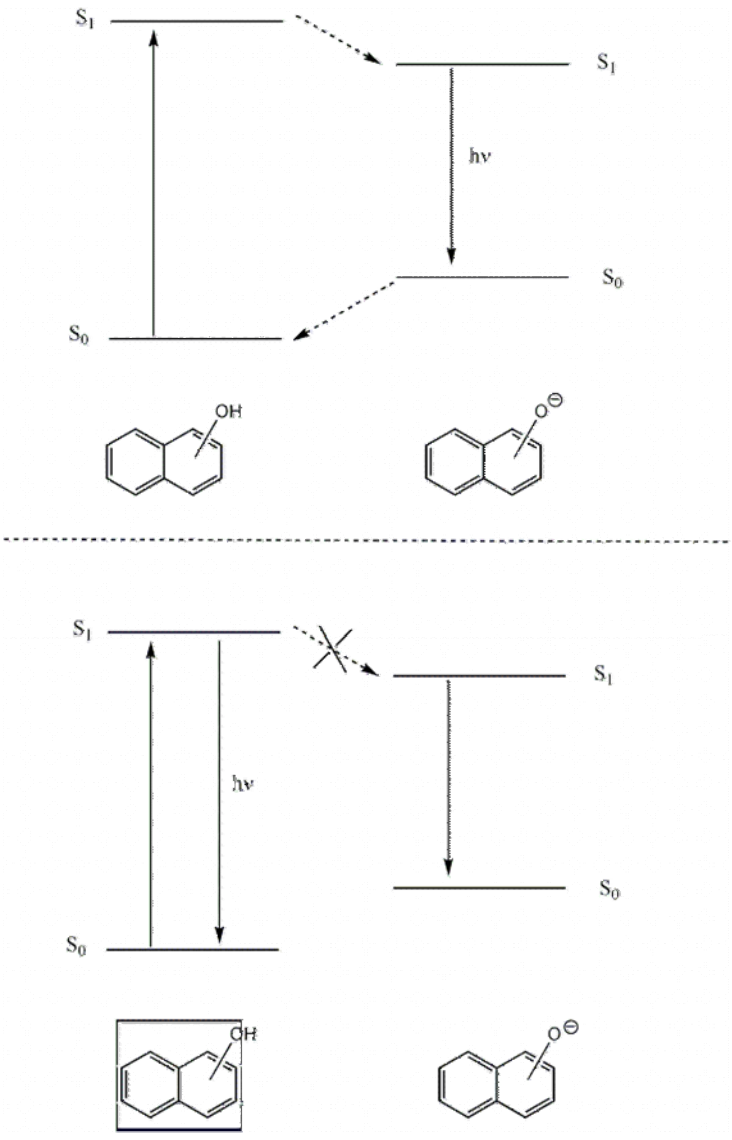

Figure 3.12 Schematic representation of the excitation and emission of naphthols with and without CB[7] in neutral aqueous solutions. The acidity of the excited state of naphthols decreases considerably within the complexes such that the UV emission dominates while the blue emission decreases.

3.3.2 Fluorescence Off/On Switch of Acridizinium/9-Aminoacridizinium

Shortly after our discovery of the fluorescent emission color switch of aromatic amines and alcohols upon their complexation with CB[7] host molecules, the research was extended to a heteroatom-containing aromatic amine, 9-aminoacridizinium ($AADZ^+$). However, an expected fluorescence color switch was not observed at pH around 2. Instead, a substantial fluorescence quenching of the blue emission from the acridizinium cation (ADZ^+) and the green emission from the 9-aminoacridizinium cation ($AADZ^+$), upon their homo-guest pair inclusion in the cavity of CB[8], is observed. The quenched fluorescence is recovered upon the transference of the guests from the 2:1 CB[8] complex to the smaller CB[7] cavity with 1:1 guest-host complex formation. This is the first example of the employment of different sized CB[n] hosts to control fluorescence intensity as the result of the binding stoichiometries between the cyclic hosts and the fluorophore guests.

3.3.2.1 Fluorescence Off/On Switch

Both ADZ^+ and $AADZ^+$ are cyanine dyes with intense color and the propensity for efficient emission properties, which have potential uses as fluorescence probes and as an intercalating and DNA-damaging chromophore.[14,29] Recently, N-aryl-9-amino-substituted acridizinium derivatives were reported as fluorescent “light-up” probes for DNA and protein detection by the Ihmels research group.[30] The acridizinium family of fluorophores, therefore, is popular model for studying both fundamental fluorescent

properties and potential applications in biomolecular detection. We have herein used the acridizinium molecules to construct molecular fluorescence on/off switches with CB[n] molecules.

The fluorescence quenching of the blue (ADZ^+) and green ($AADZ^+$) fluorophores by CB[8] and the subsequent restoration of the emission by CB[7] can be readily observed by the naked eye and are clearly illustrated in the emission spectra (Figure 3.13). The emission band of the $AADZ^+$@CB[7] species (Figure 3.13) exhibits a hypsochromic shift to 495 nm from that of the free $AADZ^+$ at 507 nm. While bathochromic shifts have been observed previously for $AADZ^+$ emission in most organic solvents (508-516 nm),[14,31] the emission maximum for $AADZ^+$ in CH_3CN and CH_3COOH were at 501 and 497 nm, respectively. For ADZ^+, there is no change in the emission maxima between the free guest and the ADZ^+@CB[7]. This suggests that the hypsochromic shift observed for $AADZ^+$@CB[7] is either related to an interaction between the amino group and the carbonyl portal on CB[7] and/or the binding pocket of the host resembles the properties of acetic acid ($E_T(30)$ = 51.7 kcal mol^{-1})[32]. This assumption is in agreement with recent suggestions that the polarity of the CB[7] cavity is comparable to one of ethanol[12] ($E_T(30)$ = 51.9 kcal mol^{-1})[32] or 1-octanol[7] ($E_T(30)$ = 48.3 kcal mol^{-1})[32]. These three solvents have similar $E_T(30)$ values and are consistent with the nature of CB[7], having both a hydrophobic cavity and polar portals, resulting in several specific and non-specific non-covalent interactions contributing to the emission shift.

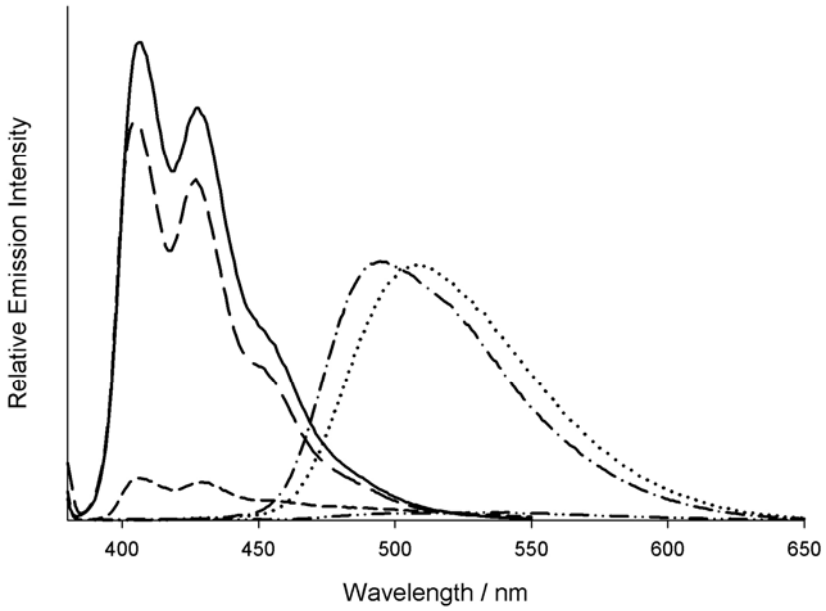

Figure 3.13 Fluorescence spectra in aqueous solution (pH 7) for free ADZ^+ (——) and $AADZ^+$ (•••••), $(ADZ)_2^{2+}$@CB[8] (---)and $(AADZ)_2^{2+}$@CB[8] (-••-) after additions of 1.0 equivalent of CB[8], and ADZ^+@CB[7] (— — —) and $AADZ^+$@CB[7] (-•-) after subsequent additions of 1.2 equivalents of CB[7].

The fluorescence off/on process of the acridizinium guest molecules with the addition of CB[8] and further addition of CB[7] to the solution can be clearly demonstrated by Figure 3.14. A quenching of fluorescence of guest $AADZ^+$ upon its complexation with CB[8], and a nearly complete and instantaneous restoration of the fluorescence upon addition of one equivalent of CB[7] to the solutions of the 1:2 CB[8] host:guest complexes has been observed.

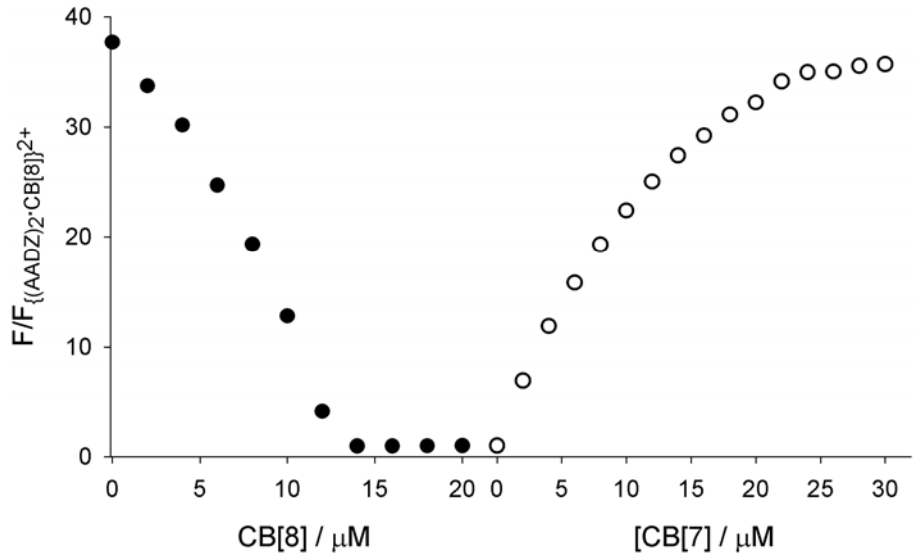

Figure 3.14 Fluorescence titration of $AADZ^+$ (25 μM) with CB[8] (●), followed by CB[7] (○) monitored at 508 nm (pH 7).

In addition to restoring the fluorescence of the guest fluorophore cations by adding CB[7] to the 1:2 fluorophore@CB[8] complex, it should be possible to restore the fluorescence by addition of a competing guest molecule(s) to displace the ADZ^+ or $AADZ^+$ in the cavity of CB[8]. This may be tested by adding a guest which has a high and selective affinity for CB[8]. We have recently found that the 1,3-bis(4,5-dihydro-1*H*-imidazol-2-yl)adamantane dication ($BIAD^{2+}$) binds strongly to CB[8], but much more weakly and through external binding to CB[7].[33] Other dicationic 1,3-disubstituted adamantanes are also reported to have considerably higher stability constants with CB[8] ($K_{CB[8]} \approx 10^{11}$ M^{-1}) compared with CB[7] ($K_{CB[8]} \approx 10^4$ M^{-1}).[34] The addition of $BIAD^{2+}$ to $(ADZ)_2^{2+}$@CB[8] (Figure 3.15) or

$(AADZ)_2^{2+}$@CB[8] results in the restoration of the fluorescence of the liberated fluorophore molecules. The $(ADZ)_2^{2+}$@CB[8] and $(AADZ)_2$@CB[8] type guest-host complexes may therefore act as fluorescence "light-up" probes for other selected nonfluorescent guest molecules.[30,35]

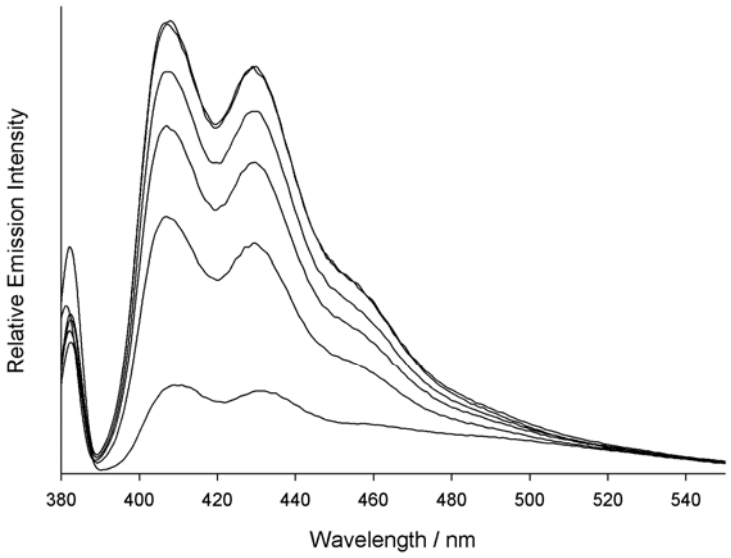

Figure 3.15 Fluorescence titration of $(ADZ)_2^{2+}$@CB[8] (12.5 μM) with, from bottom to top, 1.0, 2.0, 4.0, 6.0, and 8.0 equivalents of $BIAD^{2+}$ in aqueous solution (pH 7).

3.3.2.2 Complexes Formation Between ADZ^+/$AADZ^+$ with CB[7]/CB[8]

The formation of 2:1 guest-host complexes between either ADZ^+ or $AADZ^+$ and CB[8], and 1:1 guest-host complexes between either ADZ^+ or $AADZ^+$ and CB[7] has been confirmed by electrospray mass spectrometry, and ^1H NMR, UV-visible absorbance

(and Job's plots based on UV-visible continuous variation) and emission spectroscopy in aqueous solution, as well as by *ab initio* calculations. The UV-visible spectra of titrations of the $AADZ^+$ and ADZ^+ cations with CB[7] and CB[8] result in hypsochromic shifts in the peaks below 300 nm and bathochromic shifts in the weaker bands above 300 nm.

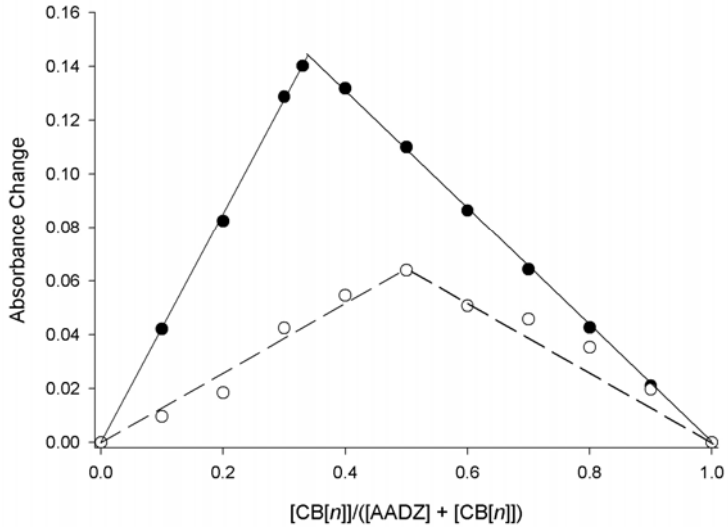

Figure 3.16 Job's plots for the 1:1 $AADZ^+$@CB[7] (○) and 2:1 $(AADZ)_2^{2+}$@CB[8] (●) guest-host complexes from continuous variation titrations monitored at 386 nm.

The Job's plots (Figure 3.16) of the change in the UV-visible absorption spectrum ([CB[*n*]]+[$AADZ^+$] = 50 μM) reached a peak at the ratio of [CB[8]]/([CB[8]]+[$AADZ^+$]) at 0.33 and a maximum at [CB[7]]/([CB[7]]+[AAD^+]) = 0.50. This indicates that the major species in this concentration region is a 1:2 host-guest complex between CB[8] and $AADZ^+$, and a 1:1 complex for CB[7] and $AADZ^+$. The same results of Job's plots

were obtained for the ADZ^+ guest. In addition, the electrospray mass spectra for all four complexes confirmed the respective complex formation.

The stability constants for the 1:1 ADZ^+@CB[7] and $AADZ^+$@CB[7] complexes were too large to be determined from UV-visible or ^{1}H NMR titrations, but could be determined from ^{1}H NMR competitive guest binding studies, using sodium 3-(trimethylsilyl)propionate-2,2,3,3-d_4 ($K_{CB[7]}$ = (1.82 ± 0.22) × 10^7 M^{-1}) as the competing guest.[34] The values of $K_{CB[7]}$ were calculated to be (7.11 ± 0.86) × 10^8 M^{-1} and (4.24 ± 0.51) × 10^8 M^{-1} for the 1:1 ADZ^+@CB[7] and $AADZ^+$@CB[7] complexes, respectively. These stability constants are comparable to the values determined for other cationic aromatic guests, such as 4,4'-bis(4,5-dihydro-1*H*-imidazol-2-yl)biphenyl ($K_{CB[7]}$ = (1.7 ± 0.2) × 10^8 M^{-1})[33] and 2,7-dimethyldiazapyrenium ($K_{CB[7]}$ = (3.81 ± 0.61) × 10^7 M^{-1}),[34] which have been determined from competitive binding experiments.

The lack of change of the absorption spectra of $AADZ^+$ and ADZ^+ after the further addition of CB[8] (upon 0.5 equivalents of CB[8] addition) indicates that the 2:1 guest-host complexes are much more stable than the 1:1 species. This arises from positive cooperativity in the formation of the ternary complexes. The ^{1}H NMR spectra of the 2:1 guest–host complex of ADZ^+ with CB[8] and the 1:1 guest-host complex of ADZ^+ with CB[7] revealed complexation-induced upfield chemical shifts for the majority of the aromatic guest resonances consistent with their inclusions in the shielding hydrophobic cavity. The remainder of the resonances exhibit downfield shifts resulting from the deshielding effect of the portal carbonyl groups of CB[*n*] on the portion of guest

located in the portal. The complexation–decomplexation processes between ADZ^+ and both CB[7] and CB[8] occur at rates which are fast on the ^1H NMR timescale, as there are no separate peaks for free and bound guests. The ^1H NMR spectra of $AADZ^+$ complexes with CB[7] and CB[8] also support the respective 1:1 and 2:1 guest-host complex formation, with guest exchange rates that are slow on the NMR timescale. In the case of $(AADZ)_2^{2+}$@CB[8], the guests exhibit two sets of proton resonances due to the presence of two relative orientation isomers, *anti-trans* and *anti-cis*, in a 5:4 ratio (Figure 3.17).

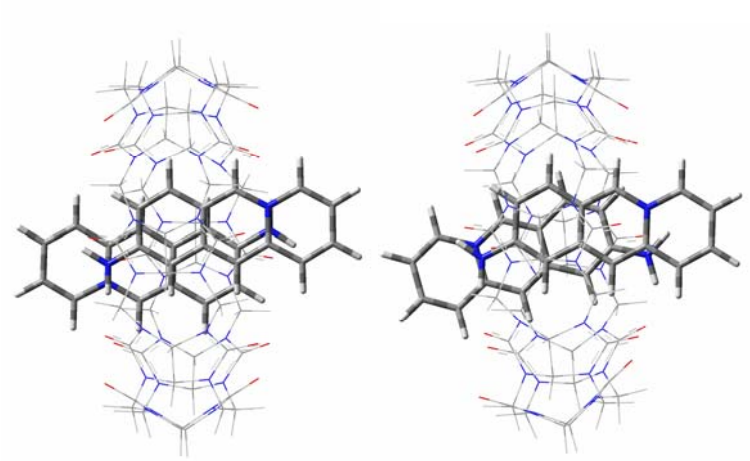

Figure 3.17 The energy-minimized structures of $(AADZ)_2^{2+}$@CB[8], *anti-trans* dimer (left) and *anti-cis* dimer (right).

Both orientations would presumably be also present in the $(ADZ)_2^{2+}$@CB[8], however because of the fast exchange of the guests, only an average of chemical shifts of each orientation is observed for each proton resonance. The relative energies of the gas

phase structures of the two $(guest)_2^{2+}$@CB[8] isomers determined from *ab initio* calculations (Figure 3.17) support the preference for the *anti-trans* configuration. The 2:1 complex in CB[8] is facilitated by stacking of the acridizinium rings. The slower exchange with CB[7] for the $AADZ^+$ guest compared with ADZ^+ may be related to the amino group in the 9-position. Hydrogen bonding interactions between the amine hydrogens of $AADZ^+$ and the carbonyl oxygens in the CB[*n*] portals would enhance the binding of this guest to the cavity (Figure 3.18).

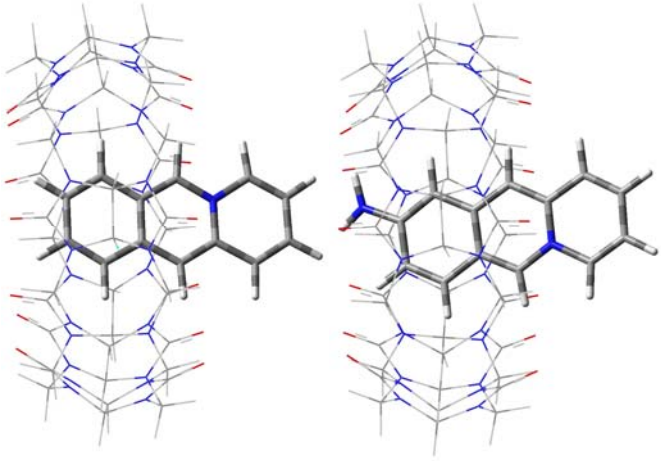

Figure 3.18 The energy-minimized structures of ADZ^+@CB[7] (left) and $AADZ^+$@CB[7] (right).

3.3.2.3 Fluorescence Off/On Switch Mechanism

Again, the fluorescence off/on switch of the acridizinium guest molecules can not be explained by any of the three mechanisms stated in the introduction section of this

chapter. It has been noted that the fluorescence of the guest acridizinium molecules is turned off when two guest molecules are included simultaneously in one cavity of CB[8], and is restored by releasing the dimer from the cavity in the presence of another competitive host (CB[7]) or a competitive guest molecule with stronger binding with CB[8]. Another fact worth noting is that the increased concentration (when it is higher than 10^{-2} M) of these fluorophores resulted in a fluorescence intensity decrease (quench) and a red shift of the emission maximum,[14,31] presumably as a consequence of non-fluorescent (or weak fluorescent) dimer formation at high concentrations of fluorophores.

The fluorescence is quenched, as a result of dimer formation in the cavity of CB[8] (weak fluorescent excimer formation once the dimer is excited). When two molecules are encapsulated in the cavity of CB[8], the concentration of fluorophore is increased to > 1 M in the microenvironment (based on majority of two guests in the 479 $Å^3$ confined CB[8] cavity[36]). The non-fluorescent complex (a non-covalent dimer in the cavity), is therefore assisted by CB[8] in forming at low concentrations of the fluorophores in aqueous solution. The sigmoidal shape of the change in $AADZ^+$ emission with increasing CB[8] concentration (Figure 3.14) is consistent with positive cooperativity[37] in the formation of the 1:2 host:guest complex, with the 1:1 species having a much reduced binding constant and/or not affecting the emission intensity compared to the free $AADZ^+$. The fluorescence is restored when the dimer in the cavity of CB[8] is displaced from the cavity by another competitive guest to form a monomer in the dilute

solution again, or is enticed out of the cavity of CB[8] by another competitive host, to form a stable monomer in the cavity of CB[7]. The proposed fluorescence off/on mechanism controlled by CB[8]/CB[7] can be clearly demonstrated by Figure 3.19.

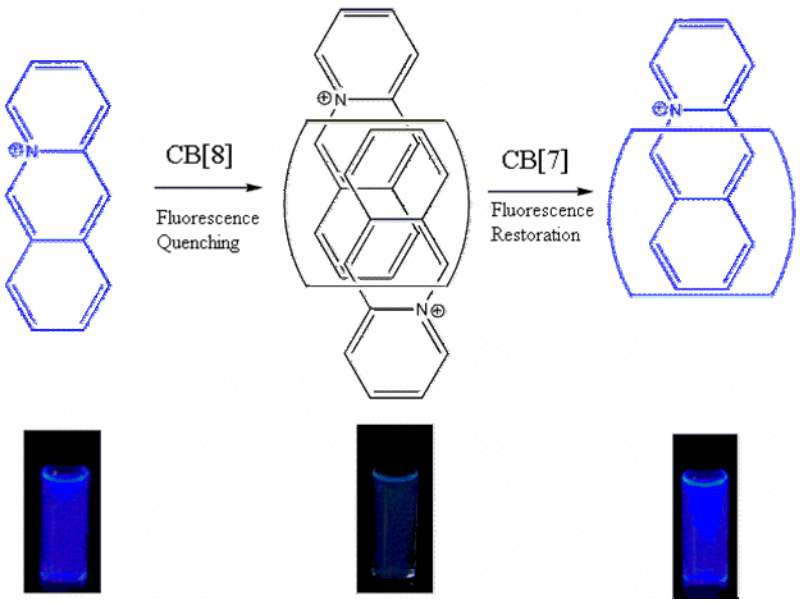

Figure 3.19 Schematic diagram of CB[8]/CB[7] controlled fluorescence-off/on for ADZ^+ (top). The bottom pictures are digital images of fluorophores in aqueous solution before the addition of CB[8] (left), after the addition of CB[8] (central) and upon further addition of CB[7] to the mixture (right) (under hand-held UV-lamp, 365 nm).

The possibility that the fluorescence quenching in the CB[8] cavity could be a result of permanent damage to the fluorophore, e.g. a photoreaction such as photodimerization,[38] may be excluded by the nearly complete and instantaneous

restoration of fluorescence upon addition of one equivalent of CB[7] to the solutions of the 1:2 host:guest complexes (Figures 3.13 and 3.14), as such a photoreaction would be expected to take much longer in both solution and the solid state.[38] In addition to restoring the fluorescence of the guest fluorophore cations by adding CB[7] to the 1:2 dye-CB[8] complex, it has also been demonstrated that a competing nonfluorescent guest molecule(s) can displace the ADZ^+ or $AADZ^+$ in the cavity, and release the free guest fluorophore into the solution.

The fluorescence behaviors of the CB[*n*] complexes demonstrated herein could have applications in supramolecular-controlled fluorescent switches and sensors, such as "light-up" probes and other photonic devices.

3.4 Conclusions

Through this project, we have demonstrated examples of CB[*n*] mediated fluorescence of guest fluorophores, such as an emission color switch of aromatic amines and alcohols, and emission intensity decrease/increase of acridizinium molecules. These changes in the fluorescence properties of guest molecules upon complexation with CB[*n*] host molecules can not be explained by previously proposed mechanisms of similar fluorescence behavior. Two new fluorescent changing mechanisms caused by nonfluorescent CB[*n*] host molecules have been proposed instead in this chapter. The examples demonstrated here might have potential applications in supramolecular-controlled fluorescent switches and sensors.

References

(1) Wagner, B. D. In *Handbook of Photochemistry and Photobiology*; Halwa, S. H., Ed.; American Scientific Publishers: Stevenson Ranch, CA, USA, 2003; Vol. 3, p 1-57.

(2) Cramer, F.; Saenger, W.; Spatz, H.-C. *J. Am. Chem. Soc.* **1967**, *89*, 14.

(3) Wagner, B. D.; Stojanovic, N.; Day, A. I.; Blanch, R. J. *J. Phys. Chem. B.* **2003**, *107*, 10741.

(4) Harada, A.; Furue, M.; Nozakura, S. *Macromolecules* **1977**, *10*, 676.

(5) Hoshino, M.; Imamura, M.; Ikehara, K.; Hama, Y. *J. Phys. Chem.* **1981**, *85*, 1820.

(6) Mohanty, J.; Nau, W. M. *Angew. Chem. Int. Ed. Engl.* **2005**, *44*, 3750.

(7) Nau, W. M.; Mohanty, J. *Int. J. Photoenergy* **2005**, *7*, 133.

(8) Buschmann, H. J.; Wolff, T. *J. Photochem. Photobiol. A* **1999**, *121*, 99.

(9) Wagner, B. D.; MacRae, A. I. *J. Phys. Chem. B.* **1999**, *103*, 10114.

(10) Wagner, B. D.; Fitzpatrick, S. J.; Gill, M. A.; MacRae, A. I.; Stojanovic, N. *Can. J. Chem.* **2001**, *79*, 1101.

(11) Saleh, N.; Al-Rawashdeh, A. A. F. *J. Fluoresc.* **2006**, *16*, 487.

(12) Rankin, M. A.; Wagner, B. D. *Supramol. Chem.* **2004**, *16*, 513.

(13) Day, A.; Arnold, A. P.; Blanch, R. J.; Snushall, B. *J. Org. Chem.* **2001**, *66*, 8094.

(14) Ihmels, H.; Engels, B.; Faulhaber, K.; Lennartz, C. *Chem. Eur. J.* **2000**, *6*, 2854.

(15) de la Pena, A. M.; Salinas, F.; Gomez, M. J.; Acedo, M. I.; Pena, M. S. *J. Incl. Phenom. Mol. Recogn. Chem.* **1993**, *15*, 131.

(16) Förster, T. *Z. Elecktrochem.*, **1950**, *54*, 42.

(17) Tsutsumi, K.; Sekiguchi, S.; Shizuka, H. *J. Chem. Soc., Faraday Trans. 1*, **1982**, *78*, 1087.

(18) Baer, A. J.; Macartney, D. H. *Inorg. Chem.* **2000**, *39*, 1410.

(19) Jeon, W. S.; Moon, K.; Park, S. H.; Chun, H.; Ko, Y. H.; Lee, J. Y.; Lee, E. S.; Samal, S.; Selvapalam, N.; Rekharsky, M. V.; Sindelar, V.; Sobransingh, D.; Inoue, Y.; Kaifer, A. E.; Kim, K. *J. Am. Chem. Soc.* **2005**, *127*, 12984.

(20) Rotkiewicz, K.; Grabowski, Z. R. *Trans. Faraday Soc.* **1969**, *65*, 3263.

(21) Ong, W.; Gomez-Kaifer, M.; Kaifer, A. E. *Org. Lett.* **2002**, *4*, 1791.

(22) Kim, H. J.; Jeon, W. S.; Ko, Y. H.; Kim, K. *Proc. Natl. Acad. Sci. USA* **2002**, *99*, 5007.

(23) Schulman, S. G.; Kovi, P. J.; Torosian, G.; McVeigh, H.; Carter, D. *J. Pharm. Sci.* **1973**, *62*, 1823.

(24) Donckt, E. V.; Porter, G. *Trans. Faraday Soc.* **1968**, *64*, 3218.

(25) Martynov, I. Y.; Demyashkevich, A. B.; Uzhinov, B. M.; Kuz'min, M. G. *Russ. Chem. Rev.* **1977**, *46*, 1.

(26) Arnault, L. G.; Formosinho, S. J. *J. Photochem. Photobiol. A* **1993**, *75*, 1.

(27) Zaitsev, N. K.; Karlsen, A. G.; Glagolev, V. L.; Galashin, A. E.; Alfimov, M. V. *Dokl. Akad. Nauk SSSR* **1990**, *315*, 898.

(28) Marquez, C.; Nau, W. M. *Angew. Chem. Int. Ed. Engl.* **2001**, *40*, 3155.

(29) Bohne, C.; Faulhaber, K.; Giese, B.; Hafner, A.; Hofmann, A.; Ihmels, H.; Kohler,

A. K.; Pera, S.; Schneider, F.; Sheepwash, M. A. L. *J. Am. Chem. Soc.* **2005**, *127*, 76.

(30) Granzhan, A.; Ihmels, H. *Org. Lett.* **2005**, *7*, 5119.

(31) Ihmels, H.; Faulhaber, K.; Sturm, C.; Bringmann, G.; Messer, K.; Gabellini, N.; Vedaldi, D.; Viola, G. *Photochem. Photobiol.* **2001**, *72*, 505.

(32) Reichardt, C. *Chem. Rev.* **1994**, *94*, 2319.

(33) Hettiarachchi, D. S. N.; Macartney, D. H. *Can. J. Chem.* **2006**, *84*, 905.

(34) Liu, S. M.; Ruspic, C.; Mukhopadhyay, P.; Chakrabarti, S.; Zavalij, P. Y.; Isaacs, L. *J. Am. Chem. Soc.* **2005**, *127*, 15959.

(35) Faulhaber, K.; Granzhan, A.; Ihmels, H.; Viola, G. *Pure Appl. Chem.* **2006**, *78*, 2325.

(36) Lagona, J.; Mukhopadhyay, P.; Chakrabarti, S.; Isaacs, L. *Angew. Chem. Int. Ed. Engl.* **2005**, *44*, 4844.

(37) Connors, K. A. *Binding Constants: The Measurement of Molecular Complex Stability*; Wiley: New York, 1987.

(38) Ihmels, H.; Otto, D. *Top. Curr. Chem.* **2005**, *258*, 161.

Chapter 4

INHIBITION OF C(2)-H/D EXCHANGE OF CARBON ACIDS UPON COMPLEXATION WITH CUCURBIT[7]URIL

In the previous chapter, it has been discussed that the acidity of the ground and excited states of protonated aromatic amines and neutral aromatic alcohols decreases (pK_a and pK_a* increases) upon their complexation with CB[7] host molecules. The effect of CB[7] complexation on the acidity of ammonium N-H and hydroxyl O-H groups prompted us to extend this research to even weaker carbon acids (C-H), such as the C(2)-H on imidazolium cations and thiazolium cations. This chapter is focused on the inhibition of C(2)-H/D exchange of such carbon acids upon their complexation with CB[7] host molecules. A brief introduction about carbon acids and previously reported acidity changes will be given, followed by experiment details, and then the results will be

described and discussed in detail. A conclusion is drawn at the end to highlight the functionality of CB[*n*] in altering the acidity of carbon acids, which might be able to be employed to modify guest carbon acids' chemical reactivity, given that they are very popular N-heterocyclic carbene precursors and that C(2)-H deprotonation is often required to produce N-heterocyclic carbenes.

4.1 Introduction

Imidazolium and thiazolium salts have been studied for more than 40 years as models of carbon acids,[1] and for their applications as ionic liquids[2,3] and N-heterocyclic carbene (NHC) precursors.[4-8] Stable nucleophilic NHCs may be formed by deprotonation of the C(2)-proton of the imidazolium and thiazolium cations, evidence of which is the H/D exchange of the proton in D_2O solution. Since the 1950s, the kinetic acidity of imidazolium and thiazolium cations, including H/D exchange rates,[9-14] carbon-proton acidity,[15,16] and carbene precursor stability[4-6] has been of great interest to physical and organic chemists, as the formation of NHCs is often a crucial step in catalytic organic and organometallic reactions.[4-8] The H/D exchange of imidazolium and thiazolium in deuterium oxide solution can be easily monitored by ^{1}H NMR spectroscopy and the first- and second-order rate constants can be acquired from following the integral change of C(2)-H on ^{1}H NMR spectra of the carbon acids. The H/D exchange rate constants and pK_a values for some thiamine and thiazolium cations were investigated comprehensively by Washabaugh and coworkers in late 1980s.[14] Recently, Amyes and coworkers have

carried out detailed measurements of the exchange rate constants for several 1,3-dialkylimidazolium and benzimidazolium cations in D_2O.[12] Very recently, the H/D exchange rate constants for the C(2)-proton of a series of imidazolium cations with alkyl, aryl, and calixarene substituents in CD_3OD containing 3% H_2O have also been reported.[17]

Buncel and coworkers have demonstrated that the lability of the C(2)-proton in aqueous solution is increased by protonation or metalation of imidazoles and thiazoles compared with the neutral substrate.[10] The order of reactivity of C(2)-proton, for most of imidazoles and thiazoles, is generally protonated >> metalated >> neutral form of substrates with the exception of Cr(III) coordination (in the case, reactivity of C(2)-H of metalated form > that of protonated form). Although the protonation/metalation can tune the acidity (or reactivity) of C(2)-proton, this method does require a specific pH environment and/or an addition of metal ions.

The acidity of C(2)-H of imidazolium cations has been observed to decrease in a solvent with a better proton acceptor. A somewhat larger pK_a value for the C(2)-proton on the 1,3-di-*tert*-butylimidazolium cation in DMSO than in THF has been attributed to stronger C-H···O hydrogen bonding in the former solvent.[18] However, tuning the acidity/reactivity of carbon acids without changing the environment (medium) remains a challenge. The effect of supramolecular inclusion of imidazolium and thiazolium cations on the lability and acidity of the C(2)-proton has not previously been investigated. Considering that cucurbituril host molecules have demonstrated versatile complexation properties with various cationic guest molecules and the fact that carbon acids, such as

imidazolium and thiazolium cations, are cationic molecules with good size compatibility to the cucurbituril cavity, the complexation of imidazolium and thiazolium cations with cucurbituril host molecules was investigated and the inhibition of C(2)-H/D exchange of these guest carbon acids upon complexation with CB[7] has been observed. The supramolecular-controlled acidity of imidazolium and thiazolium cations through complexation with CB[7] host molecules is expected to be applicable to control the stability of carbene precursors in aqueous solution and to potentially draw interest in the modification of ionic liquid properties of these salts.

4.2 Experimental

4.2.1 Materials Preparation

The host molecule CB[7] was synthesized according to literature methods, as previously described in Chapter 2.[19] The acetate and phosphate buffer solutions (total buffer concentration of 0.05 M for acetate or 0.02M for phosphate for each kinetic experiment) were prepared by the requisite addition of DCl (Aldrich, 35 wt.% in D_2O) to D_2O solutions of sodium acetate and sodium phosphate (Aldrich), respectively. The ionic strength was adjusted to 0.2 M using NaCl.

Synthesis of 3,3'-Bis(1-methyl-imidazolium)-*p*-xylene dibromide ([B**MIX]Br$_2$)**

3,3'-Bis(1-methyl-imidazolium)-*p*-xylene dibromide ([BMIX]Br_2) was synthesized by

using a modified literature method.[20] Typically 1-methylimidazole (1.0 g, 12 mmol) was mixed with α,α'-dibromo-*p*-xylene (1.58 g, 6 mmol) in 25 ml THF under reflux for about 36 hours to give an off-white precipitate. The crude product was filtered and washed with THF and ether, and dried in a vacuum oven to give white power (yield: 2.4 g, 93%). m.p. 234-236 ºC (dec.). ^{1}H NMR (D_2O, 400 MHz) δ 8.68 (s, 2H), 7.38 (br s, overlapped 8H), 5.34 (s, 4H), 3.80 (s, 6H) ppm. ^{13}C NMR (D_2O, 100 MHz) δ 136.17, 134.60, 129.27, 123.87, 122.29, 52.30 and 35.76 ppm. ESI-MS: *m/z* = 347.1 and 349.1 $(M-Br)^+$; *m/z* = 134 for $(M-2Br)^{2+}$.

Synthesis of alkylated imidazolium salts: The following alkylated imidazolium salts were synthesized by using modified literature method.[20,21]

3,3'-bis(1-methyl-imidazolium)-1,4-butane dibromide ([DIC4]Br_2)

1-methylimidazole (1.0 g, 12 mmol) was mixed with 1,4-dibromobutane (0.71 ml, 6 mmol) in 25 ml anhydrous THF under reflux for about 18 hours. An oily product was layered out of solvent by adding ether and an orange oil product was collected by decanting the upper level liquid out of reaction vessel. It was washed with ether three times, and then dried in vacuum oven (yield: 1.7 g, 75%). ^{1}H NMR (D_2O, 400 MHz) δ 8.63 (s, 2H), 7.36 (d, 2H, *J* = 1.5 Hz), 7.33 (d, 2H, *J* = 1.5 Hz), 4.14 (br, 4H), 3.78 (s, 6H), 1.79 (br, 4H) ppm. ESI-MS: *m/z* = 299.6 and 301.6 $(M-Br)^+$.

3,3'-bis(1-methyl-imidazolium)-1,6-hexane dibromide ([DIC6]Br_2)

1-methylimidazole (0.5 g, 6 mmol) was stirred with 1,6-dibromohexane (0.46 ml, 3 mmol) in 15 ml anhydrous THF under reflux for about 18 hours. After cooling in an ice-water bath, the resulting white precipitate was filtered and washed with THF and ether three times, respectively, and finally dried in a vacuum oven to give a white solid (yield: 0.7 g, 58%). m.p. (26-27 ºC). ^{1}H NMR (D_2O, 400 MHz) δ 8.62 (s, 2H), 7.38 (s, 2H), 7.34 (s, 2H), 4.10 (t, 4H, J = 7.1 Hz), 3.80 (s, 6H), 1.77 (br, 4H); 1.25 (br, 4H) ppm. ESI-MS: m/z = 327.5 and 329.5 $(M\text{-}Br)^+$.

3,3'-bis(1-methyl-imidazolium)-1,8-octane diiodide ([DIC8]I_2)

1-methylimidazole (1.0 g, 12 mmol) was stirred with 1,8-diiodooctane (1.2 ml, 6 mmol) in 25 ml anhydrous THF under reflux for about 18 hours. After cooling in an ice-water bath, the off-white precipitate was filtered and washed with THF and ether three times, respectively, and finally dried in a vacuum oven to give a white solid (yield: 2.8 g, yield 88%). m.p. (92-93 ºC). ^{1}H NMR (D_2O, 400 MHz) δ 8.61 (s, 2H), 7.38 (s, 2H), 7.34 (s, 2H), 4.09 (t, 4H, J= 7.2 Hz), 3.80 (s, 6H), 1.77 (m, 4H), 1.22 (br, 4H) ppm. ESI-MS: m/z = 403.4 $(M\text{-}I)^+$.

1-methyl-3-butyl-imidazolium iodide ([IC4]I)

A solvent-free sonochemical preparation method was used for synthesizing these imidazolium monocation salts.[21] Typically 1-methylimidazole (0.82 ml, 10 mmol) was

mixed with 1-iodobutane (1.26 ml, 11 mmol), and sonicated for 2 hrs. A light yellow oil product was washed with ether three times, and dried in a vacuum oven to give pale yellow oil (yield: 1.5 g, 56%). ^{1}H NMR (D_2O, 400 MHz) δ 8.61 (s, 1H), 7.37 (s, 1H), 7.32 (s, 1H), 4.09 (t, 2H, J = 7.2 Hz), 3.78 (s, 3H), 1.72 (qn, 2H, *J* = 7.1 Hz), 1.21 (qn, 2H, *J* = 7.1 Hz), 0.82 (t, 3H, *J* = 7.3 Hz) ppm. ESI-MS: *m/z* = 138.9 $(M\text{-}I)^+$.

1-methyl-3-hexyl-imidazolium bromide ([IC6]Br)

1-methylimidazole (0.82 ml, 10 mmol) was mixed with 1-bromohexane (1.54 ml, 11 mmol) and sonicated for 4 hrs. A colorless oil product was washed with ether three times and dried in a vacuum oven to give colorless oil (yield: 1.7 g, 69%). ^{1}H NMR (D_2O, 400 MHz) δ 8.60 (s, 1H), 7.37 (d, 1H, *J* = 1.5 Hz), 7.32 (s, 1H, *J* = 1.5 Hz), 4.09 (t, 2H, *J* = 6.9 Hz), 3.79 (s, 3H), 1.76 (qn, 2H, *J* = 6.9 Hz); 1.19 (br, 6H), 0.75 (t, 3H, *J* = 6.9 Hz) ppm. ESI-MS: *m/z* = 167.0 $(M\text{-}Br)^+$.

1-methyl-3-octyl-imidazolium bromide ([IC8]Br)

1-methylimidazole (0.82 ml, 10 mmol) was mixed with 1-bromooctane (1.9 ml, 11 mmol) and sonicated for 5 hrs. A yellow oil product was washed with ether three times and dried in a vacuum oven to give a pale yellow oil product (Yield: 1.5 g, 55%). ^{1}H NMR (D_2O, 400 MHz) δ 8.59 (s, 1H), 7.36 (s, 1H, *J* = 1.6 Hz), 7.32 (s, 1H, *J* = 1.6 Hz), 4.08 (t, 2H, *J* = 7.1 Hz), 3.78 (s, 3H), 1.75 (qn, 2H, *J* = 7.1 Hz), 1.17 (m, 10H), 0.75 (t, 3H, *J* = 6.6 Hz) ppm. ESI-MS: *m/z* = 195.5 $(M\text{-}Br)^+$.

Synthesis of 3,3'-bis-thiazolium-p-xylene dibromide ([BTX]Br_2)

3,3'-bis-thiazolium-p-xylene dibromide was synthesized by using the same method as for the [BMIX]Br_2 synthesis. Thiazole (0.48 g, 5.5 mmol) was mixed with α,α'-dibromo-p-xylene (0.71, 2.7 mmol) in 15 ml THF under reflux for about 24 hours to give a white precipitate. The crude product was filtered and washed with THF and ether, and was further purified by a soxhlet extraction with acetonitrile, and dried in a vacuum oven to give white power (yield: 0.65 g, 55%). ^{1}H NMR (D_2O, 400 MHz) δ 9.91 (s, 2H), 8.21 (s, 2H), 8.11 (s, 2H), 7.45 (s, 4H), 5.71 (s, 4H) ppm. ESI-MS: *m/z* = 325 and 327 $(M-Br)^+$ and *m/z* = 123 $(M-2Br)^{2+}$.

Thiamine hydrochloride, thiamine monophosphate chloride dihydrate, and thiamine pyrophosphate were used as received from Sigma-Aldrich.

4.2.2 Instrumentation and Methods

4.2.2.1 Instrumentation

The 1D ^{1}H NMR spectra were recorded on Bruker AV-400M NMR spectrometer. The ESI-MS spectra were acquired on a Waters 2Q Single Quadrupole MS spectrometer equipped with an ESI/APcI multiprobe. The UV-visible spectra were all acquired on a Hewlett Packard 8452A diode array UV-visible spectrometer using quartz cells with a 1.00 cm path length.

All of the modeled structures of the host-guest complexes involved in this project were computed by energy-minimizations using Gaussian 03 (Revision C.02) programs run on the computing facilities of the High Performance Virtual Computing Laboratory (HPVCL) at Queen's University, as described in section 2.2.2 in chapter 2.

4.2.2.2 Stability Constant Determinations Through Competitive Titrations

The method has been discussed in detail in the section of 2.2.3 of the chapter 2.

4.2.2.3 Kinetics of C(2)-H/D Exchange Monitored by ^{1}H NMR

Representative ^{1}H NMR spectra of the guest carbon acids in the absence and in the presence of CB[7] obtained during the deuterium exchange of the C(2)-proton at different p*D* (p*D* = pH + 0.41)conditions (buffered by DAc/Ac^- or $DPO_4/D_2PO_4^-$, or PO_4^{3-}/DPO_4^{2-} in D_2O, I = 0.2 adjusted with NaCl, 400 MHz NMR) are given below **(**Figure 4.1). Other proton integrals, such as the methylene protons (4H) resonance in $BMIX^{2+}$, were used as an internal reference resonance for attaining the integration of the C(2)-proton. In order to acquire accurate integrals for the C(2)-proton, a relaxation delay, between the pulses, of d_1 = 75 s (> $5T_1$) was used.

First-order rate constants determination by semilogarithmic plots: The proton/deuterium exchange was followed by ^{1}H NMR spectroscopy, as demonstrated in Figure 4.1. Values of the reaction progress, *R*, can be calculated from the integrations of the of C(2)-proton resonances [$(I_{2H})_t$] with an internal reference [$(I_{2H})_0$], at zero time and

time *t*, according to the equation 4.1

$$R = (I_{2H})_t/(I_{2H})_0 \quad (4.1)$$

$$\ln R = -k_{ex}t \quad (4.2)$$

From equation 4.2, the first-order rate constant k_{ex} can be determined from the slope of the linear semilogarithmic plot of reaction progress against reaction time. Therefore, the first-order rate constant k_{ex} values, with and without CB[7], at various p*D* values can be determined.

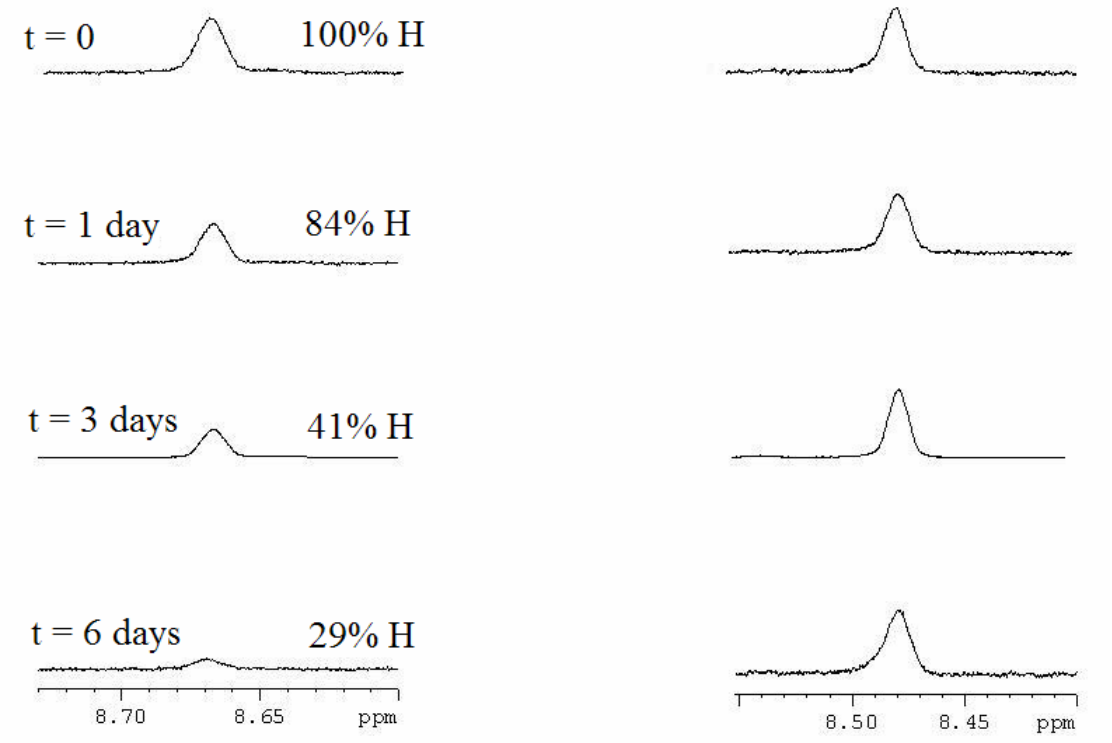

Figure 4.1 Representative ^{1}H NMR spectra (400 MHz) of $BMIX^{2+}$ in the absence (left) and in the presence (right) of 1.1 equivalents of CB[7] obtained during deuterium exchange of C(2)-proton (in D_2O, p*D* = 6.1 buffered by Ac^-/DAc, *I* = 0.2) at 25 ºC.

Determinations of Second-order rate constants: The second-order rate constant, k_{DO}, is calculated from the *y*-axis intercept of the linear fit with a fixed slope of one by plotting logk_{ex} (first-order rate constants) against p*D* values according to the equation 4.3.[11]

$$\log k_{ex} = \log (k_{DO}K_W/\gamma_{OL}) + pD \quad (4.3)$$

The value of pK_W = 14.87 (for deuterated water), and under our experimental conditions the activity correction for deuterium oxide is γ_{OL} = 0.83, estimated from the solvent conditions and ionic strength.[11]

4.3 Results and Discussion

4.3.1 Inhibition of H/D Exchange of Imidazolium Cations Upon Complexation with Cucurbit[7]uril

4.3.1.1 Host-Guest Complexation of Imidazolium Cations with Cucurbit[7]uril

The guest-host interactions of one of the imidazolium cations, $BMIX^{2+}$, with CB[7] was first investigated using ^{1}H NMR spectroscopy in a 0.1 M NaCl D_2O solution. Figure 4.2 shows the appearance of separate proton resonances for free and bound guest molecules in the presence of 0.4 equivalents of CB[7], which indicates that the chemical exchange rate between free guest and CB[7]-complexed guest is slow on the ^{1}H NMR timescale. In the presence of 1.1 equivalents of CB[7] (Figure 4.2), the resonances for the one of the imidazolium ethylene protons (H(4)), the xylyl methylene protons (H(α)),

the aromatic protons (H(2')) and the C(2)-proton in the ^{1}H NMR spectrum of the inclusion complex have moved upfield from those of the free guest, indicative of their positioning within the cavity of CB[7]. The resonance for the methyl protons resonances (H(1)) has moved downfield, while the other imidazolium ethylene resonance (H(5)) exhibited no chemical shift change. This behavior indicates that the methyl group and the ethylene C(5)-H group are likely situated outside of the cavity of CB[7], as the downfield shift of the methyl proton resonance may be attributed to the deshielding effect of the carbonyl-rimmed portal of CB[7].

The 1:1 binding stoichiometry of the $BMIX^{2+}$@CB[7] complex was also revealed by a Job's plot, based on the continuous variation method, by using absorption measurements. It was also supported by the ESI-MS spectrum, which exhibited peaks at *m/z* = 1509 for $[BMIX^{2+}@CB[7]+Br^-]^+$ and 715 for $BMIX^{2+}$@CB[7]. It was not possible to calculate the guest-host stability constant directly from either ^{1}H NMR or UV-visible titrations of $BMIX^{2+}$ with CB[7], owing to its very high value. Instead, a ^{1}H NMR competition experiment was carried out by using a known strong binding guest, the (trimethylammonio)methylferrocene ($FcTMA^+$) cation, as a competitor ($K_{CB[7]}$ = (3.31 ± 0.62) × 10^{11} M^{-1}).[22] Using a limiting amount of CB[7], with $[BMIX^{2+}]>>[FcTMA^+]$, a stability constant of (4.3 ± 0.8) × 10^9 M^{-1} was determined for the $BMIX^{2+}$@CB[7] complex at 25 °C in D_2O. This value is similar to the stability constant of 1.84 x 10^9 M^{-1} reported for the complex between a similar guest, the α,α'-diammonio-*p*-xylene dication, and CB[7].[23]

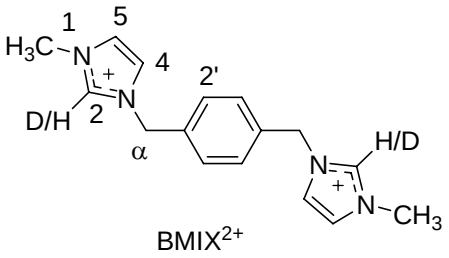

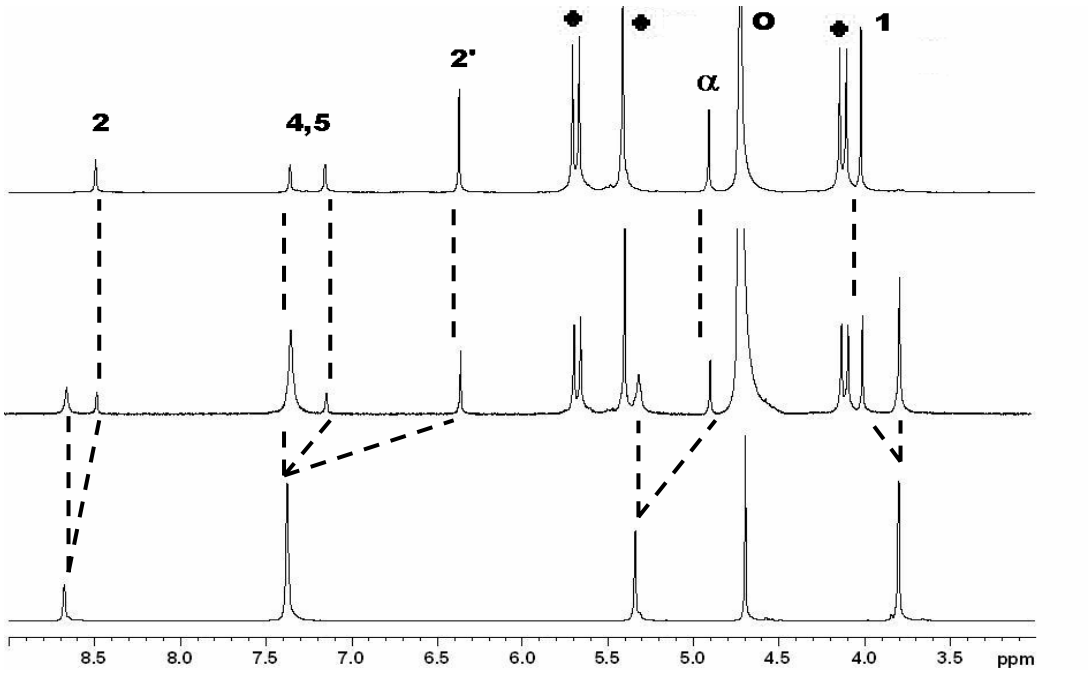

Figure 4.2 Structure of the $BMIX^{2+}$ with proton number labeling (**Top)**; The ^{1}H NMR spectra of the free $BMIX^{2+}$ guest (lower spectrum) and after the addition of 0.4 equivalents of CB[7] (middle) and 1.1 equivalents of CB[7] (upper), with CB[7] protons labelled as (●) and HOD as (○) (**Bottom).**

The strong complexation between CB[7] and the imidazolium dication, $BMIX^{2+}$, prompted us to extend the study to other imidazolium cation guests, a series of alkylated imidazolium cations. The ^{1}H NMR spectra for the complexes support the formation of inclusion complexes with hydrophobic alkyl groups included in the nonpolar cavity of CB[7], and indicate that the exchange rates between the free and CB[7]-bound alkylated imidazolium cations $DIC4^{2+}$, $DIC6^{2+}$, $DIC8^{+}$ and $IC8^{+}$ are all slow, whereas the exchange rates between free and CB[7]-complexed $IC4^{+}$ and $IC6^{+}$ are both fast on the ^{1}H NMR timescale. A representative slow-exchange ^{1}H NMR spectrum (Figure 4.3) shows the appearance of separate proton resonances for free and bound $DIC6^{2+}$ dications in the presence of 0.3 equivalents of CB[7]. In the presence of 1.1 equivalents of CB[7], the three resonances for hexyl protons in the ^{1}H NMR spectrum have moved significantly upfield, indicating that the hexyl group is included in the hydrophobic cavity, while the two ethylene protons and C(2)-proton of its inclusion complex have moved slightly upfield from those of the free guest, indicative of their positions inside the cavity but close to the portals of CB[7]. The resonance of the methyl protons has moved downfield, indicating that the methyl group is likely situated outside of the cavity of CB[7], deshielded by carbonyl groups of the portals.

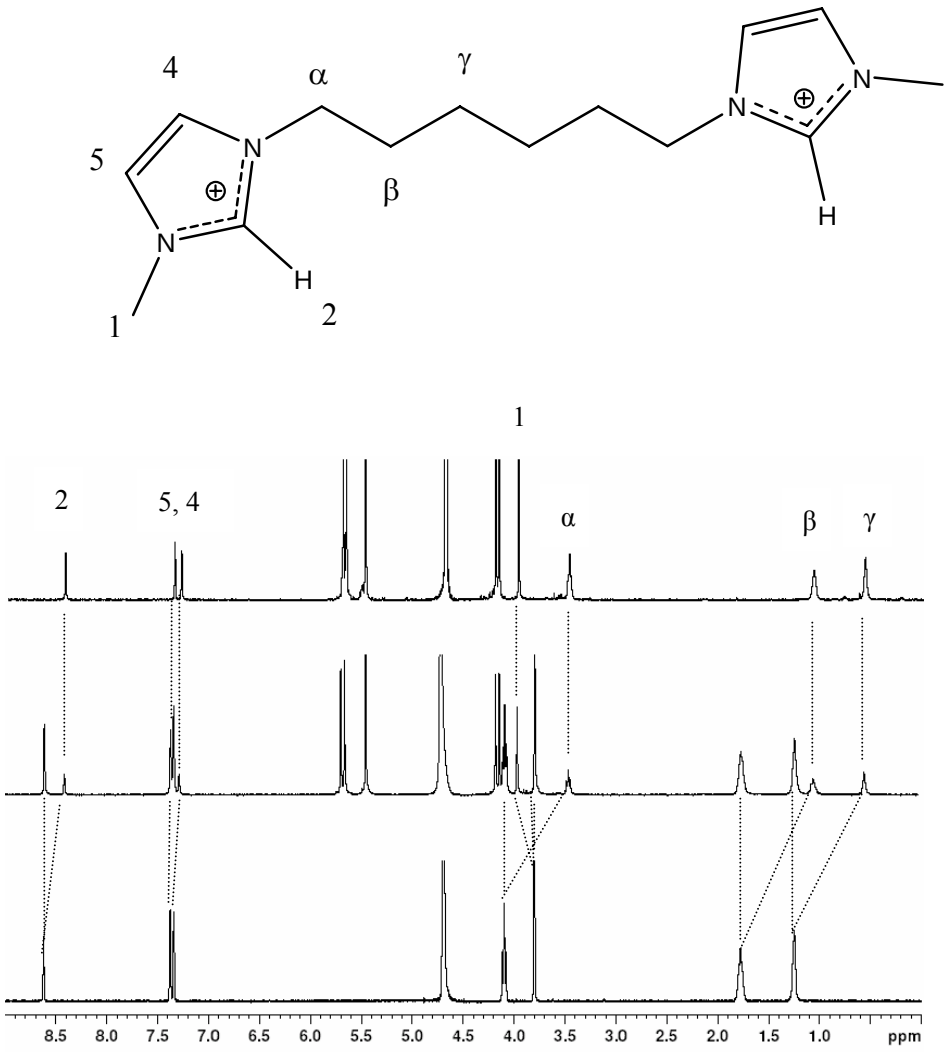

Figure 4.3 The ^{1}H NMR spectra of the free DIC6^{2+} guest (lower spectrum) and after the addition of 0.3 equivalents of CB[7] (middle) and 1.1 equivalents of CB[7] (upper).

A representative fast-exchange ^{1}H NMR spectrum (Figure 4.4) shows only one set of ^{1}H NMR resonances for IC6^{+} in the presence of 0.3 equivalents of CB[7], which is a signature of the fast chemical exchange between free and CB[7]-included IC6^{+} on the NMR timescale. Similar to those of DIC6^{2+}, in the presence of 1.1 equivalents of CB[7], the resonances for hexyl group protons, the two ethylene protons and C(2)-proton on

imidazolium ring of its inclusion complex in the ^{1}H NMR spectrum have moved further upfield from those of free guest, indicating that these groups are likely to be included in the cavity of CB[7]. The resonance of the methyl protons has moved downfield, indicating that the methyl group is likely situated outside of the cavity of CB[7], similar to those of $DIC6^{2+}$.

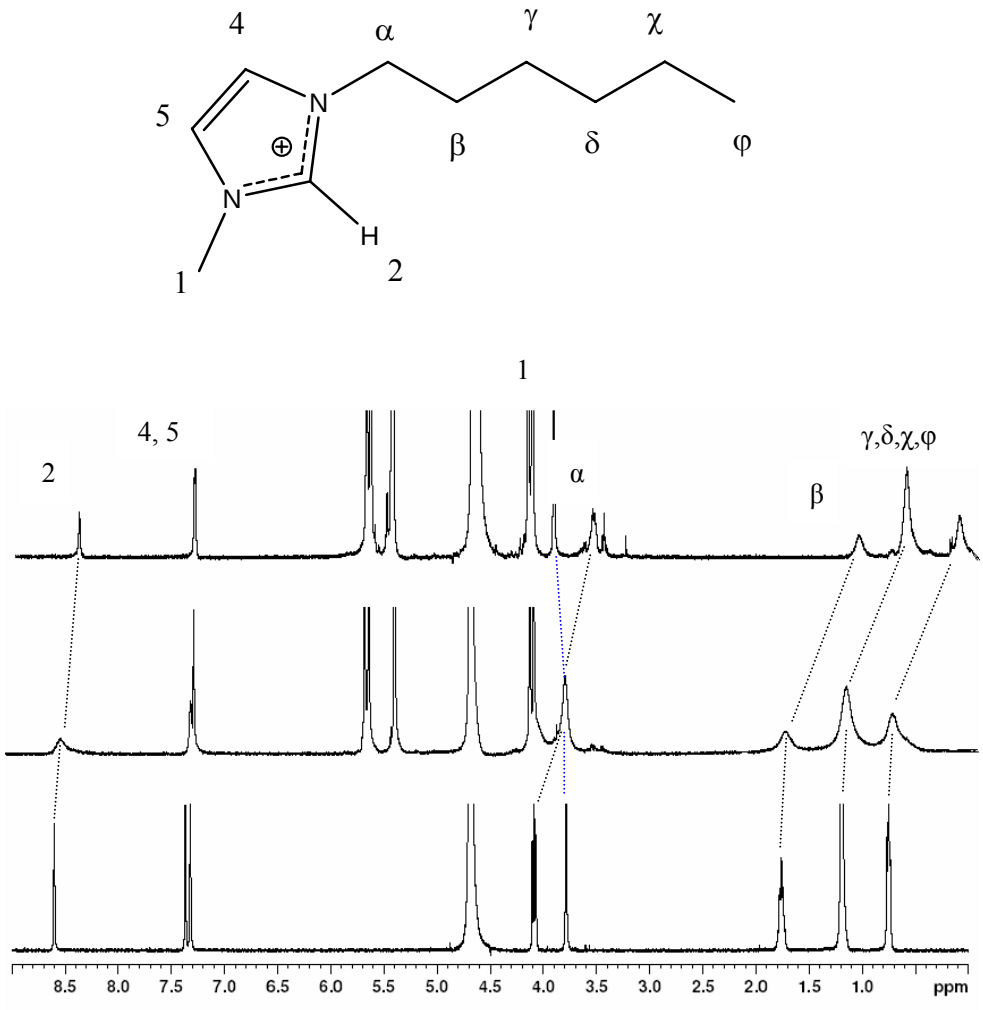

Figure 4.4 The ^{1}H NMR spectra of the free $IC6^+$ guest (lower spectrum) and after the addition of 0.3 equivalents of CB[7] (middle) and 1.1 equivalents of CB[7] (upper).

The ^{1}H NMR spectra support an exclusive 1:1 binding stoichiometry of all these complexes for imidazolium salts and CB[7] . This binding ratio was also revealed by a Job's plot, based on the continuous variation method, by using absorption measurements. It was also supported by the ESI-MS spectra, all of which showed singly and/or doubly charged peaks for the host-guest complexes.

Similar to that of $BMIX^{2+}$, binding constants for these cations with CB[7] have been determined by ^{1}H NMR competition experiments carried out by using a reasonably strong binding guest, 3-(trimethylsilyl)propionic-2,2,3,3-d_4 acid (TMSP), as a competitor whose binding constant with CB[7] (K = (1.82 ± 0.22) × 10^7 M^{-1}) is known.[23] Using a limiting amount of CB[7], a large amount of TMSP, and small amount of the imidazolium cation, the binding constants for $DIC4^{2+}$@CB[7], $DIC6^{2+}$@CB[7], $DIC8^{2+}$@CB[7], $IC4^{+}$@CB[7], $IC6^{+}$@CB[7] and $IC8^{+}$@CB[7] have been determined to be (1.4 ± 0.2) × 10^9 M^{-1}, (1.2 ± 0.2) × 10^{10} M^{-1}, (1.9 ± 0.3) × 10^{10} M^{-1}, (1.0 ± 0.2) × 10^9 M^{-1}, (4.6 ± 0.6) × 10^9 M^{-1} and (2.1 ± 0.3) × 10^9 M^{-1}, respectively. The binding constants for this series of cations with the CB[7] host are not significantly different, which is somewhat surprising as we might expect to see higher binding constants for the bis(imidazolium) cations than those for the mono(imidazolium) cations, as dication would have cation-dipole interactions with both portals of CB[7].

Energy-minimized structures of these imidazolium@CB[7] complexes, from *ab initio* calculations (HF/3-21G** basis set), also support the 1:1 strong complexation and reveal

multipoint C-H···O=C hydrogen bonding contacts between the imidazolium C(2)-proton(s) and portal carbonyl oxygens of CB[7].

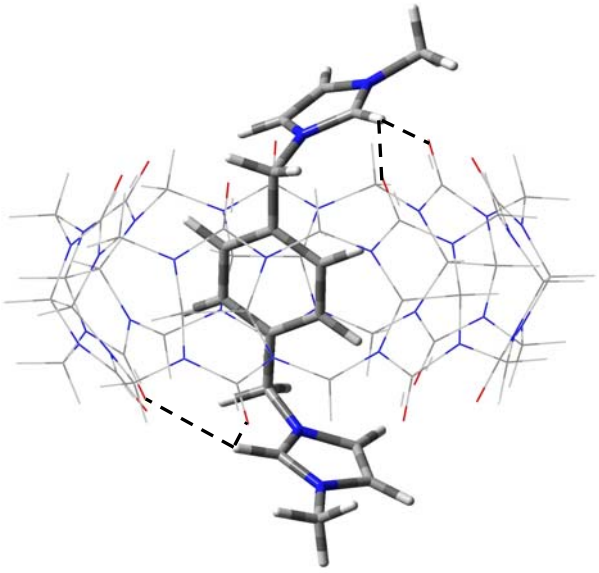

Figure 4.5 An energy-minimized structure of the $BMIX^{2+}$@CB[7] guest-host complex.

Figure 4.5 shows a representative energy-minimized structure to demonstrate the H-bonding at the portals. The distances between the C(2)-hydrogens of $BMIX^{2+}$ and the carbonyl oxygens are 2.43 and 2.46 Å on one portal, and 2.31 and 2.44 Å on the other portal, while the C-H···O bond angles vary from 106° to 146°. The CB[7] host molecule not only acts as a steric barrier (including part of the imidazolium cation), but also a hydrogen bond acceptor for the C(2)-protons, by positioning the guest in the cavity of CB[7] for optimal hydrogen bonding interactions.

A solvent effect resulting in C(2)-H/D exchange inhibition through H-bonding formation has been reported.[18] In addition, we have observed an acidity decrease of

aromatic amines and aromatic alcohols, induced by CB[7] complexation.[24] The C(2)-H/D exchange of this series of imidazolium salts might therefore be expected to be inhibited upon complexation by CB[7] host molecules, with the acidity of these carbon acids decreased (a pK_a increase) upon inclusion.

4.3.1.2 C(2)-H/D Exchange of Imidazolium Cations Monitored by ^{1}H NMR

The exchange of the C(2)-proton of a bis(imidazolium) dication, $BMIX^{2+}$, by deuterium, in buffered D_2O (pD = 5.0 – 8.1) at 25 ˚C and I = 0.2 (adjusted by NaCl) in the absence of CB[7] was followed by ^{1}H NMR spectroscopy. At a pD of 6.1 ($DOAc/OAc^-$ buffer), for example, Figure 4.1 shows that 71% of the C(2)-protons were exchanged by deuterium after six days, while in the presence of 1.1 equivalents of CB[7] no exchange was detected after six days, with only 5% deuterium exchange observed after one month. Only at elevated pD values (8.8 - 10.5) was facile deuterium exchange of the C(2)-protons for the $BMIX^{2+}$@CB[7] complex observed. The first-order rate constants for H/D exchange of the C(2)-proton in the $BMIX^{2+}$ dication in the absence and presence of CB[7] at different pD environments were determined from the plots of reaction progress ln$R$ ($R = I_t/I_o$, where I is the integration of the C(2)-H proton resonance, using Hα as a non-exchanging integration reference) against time (Figure 4.6). From the linearity of the plots it appears that the two imidazolium C(2)-protons exchange independently of one another with similar rate constants.

Under these conditions, the second-order rate constants k_{DO} for the DO^- catalyzed

deuterium exchange can be obtained from a linear fit (fixed slope = 1) to the equation of $\log k_{ex} = \log(k_{DO}K_W/\gamma_{OL}) + pD$ by using the first-order rate constants k_{ex} as a function of the pD value (Figure 4.7).[12] The second-order rate constants for C(2)-proton deuterium exchange were determined from the y-axis intercepts of the linear fits.

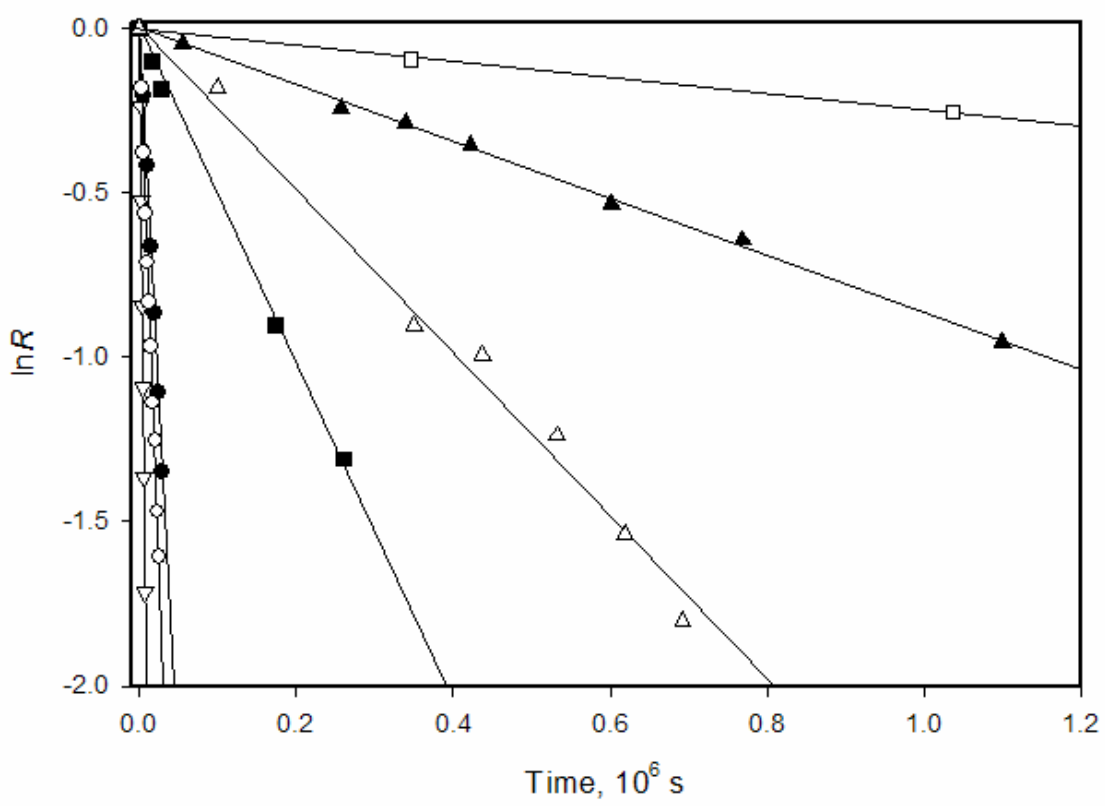

Figure 4.6 Semilogarithmic plot of ln$R$ against time for the C(2)-proton/deuterium exchange for $BMIX^{2+}$ (2 mM) at pD = 5.16 (□, only two points shown), 6.17 (Δ), 7.44 (○), and 8.07 (∇), and for $BMIX^{2+}$@CB[7] (2 mM) at pD = 8.81 (▲), 9.51 (■), and 10.15(●).

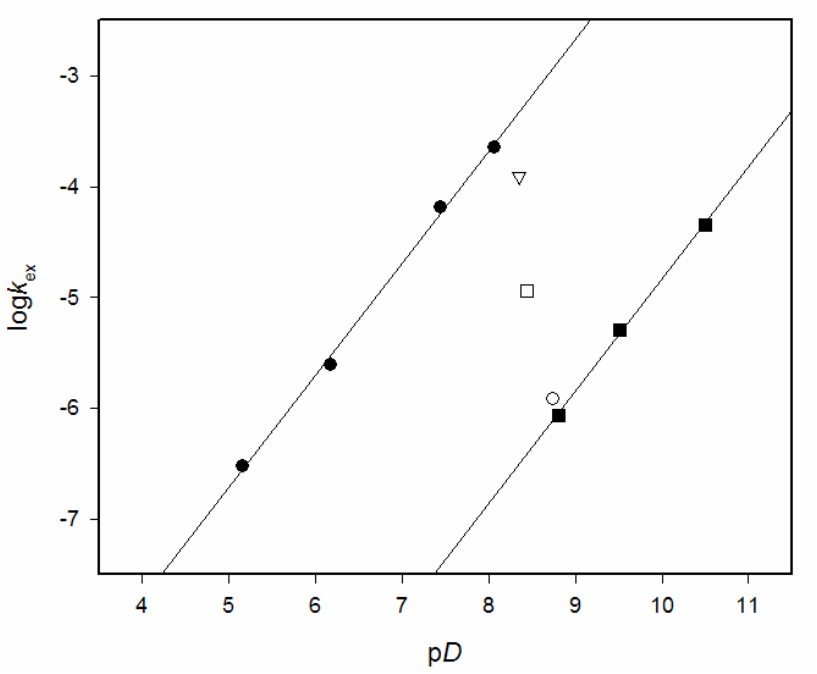

Figure 4.7 Plots of logk_{ex} against pD for the deuterium exchanges of the C(2)-protons on $BMIX^{2+}$ (●, 2 mM) and $BMIX^{2+}$@CB[7] (○, 5 mM; ■, 2mM; □, 1.0 mM; ∇, 0.5 mM) in D_2O at 25 °C.

The value of (1.2 ± 0.1) x 10^3 M^{-1} s^{-1} for $BMIX^{2+}$ in the absence of CB[7] may be compared with the value of 2.47 x 10^2 M^{-1} s^{-1} for 1,3-dimethylimidazolium cation at the same temperature (I = 1.0 M (KCl)).[13] In the presence of CB[7], the exchange rate constant is reduced to 0.9 ± 0.1 M^{-1} s^{-1}, calculated from the linear fit. The pK_a values of the $BMIX^{2+}$ cation in the absence and in the presence of CB[7] were estimated to be 22.3 ± 0.5 and 25.4 ± 0.5, respectively, based on the second-order rate constants k_{DO} and with k_{DO}/k_{HO} = 2.4, $K_W = 10^{-14}$ (for water), and $k_{HOH} = 10^{11}$ s^{-1} for the reverse protonation of the

carbene by solvent water.[12] At lower concentrations of $BMIX^{2+}$@CB[7] (0.5 and 1.0 mM in Figure 4.7), the rates increase as some of the more reactive free $BMIX^{2+}$ is present in solution.

The decreases in the acidity ($\Delta pK_a = 3.1$) and lability of the C(2)-proton is explained by the C-H···O=C hydrogen bond formation upon $BMIX^{2+}$ complexation with CB[7]. Similarly, a somewhat larger pK_a value for the C(2)-proton on the 1,3-di-*tert*-butylimidazolium cation in DMSO than in THF has also been attributed to stronger C-H···O hydrogen bonding in the former solvent, as discussed briefly at the beginning of this chapter.[18] The inhibition of H/D exchange in this system is reminiscent of the well-studied use, in determinations of protein structure and dynamics, of the dependence of amide H/D exchange on H-bonding and exposure of the peptide linkage to the solvent.[25]

Employing the same methodologies, the first-order rate constants, the second-order rate constants and pK_a values for the alkylated imidazolium cations in the absence and in the presence of CB[7] have been evaluated. The deuterium exchange of the C(2)-proton of these cations in buffered D_2O ($pD = 7.5 – 10.5$) at 25 ˚C and $I = 0.2$ (adjusted by NaCl) in the absence or in the presence of CB[7] was also followed by ^1H NMR spectroscopy. The first-order rate constants for the H/D exchange of these imidazolium cations in the absence and in the presence of CB[7] at different p*D* environments were determined from the semilogarithmic plots of reaction progress *R* against time. Under these conditions, the second-order rate constants k_{DO} for DO^- catalyzed deuterium exchange of the

alkylated imidazolium monocations and dications C(2)-proton in the absence and in the presence of CB[7] have been determined from a linear fit (fixed slope = 1) to the equation of log k_{ex} = log ($k_{DO}K_W/\gamma_{OL}$) + pD by using the data of first-order rate constants k_{ex} and pD values (Figure 4.8 shows representative figures).

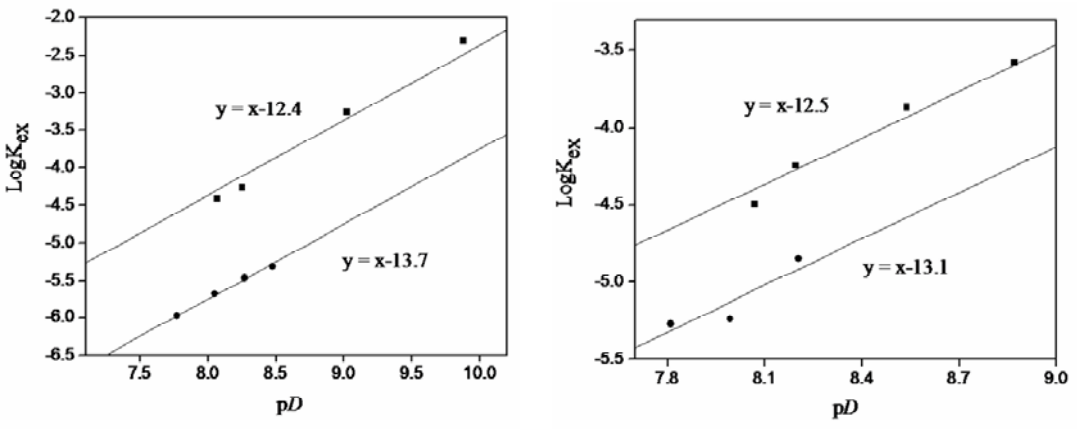

Figure 4.8 Plots of logk_{ex} against pD for the deuterium exchanges of the C(2)-protons on IC6$^+$ (■) and IC6$^+$@CB[7] (●) (**left**), IC8$^+$ (■) and IC8$^+$@CB[7] (●) (**right)** in buffered D_2O at 25 °C.

The values of the determined second-order rate constants of the alkylated imidazolium cations in the absence and in the presence of CB[7] from these linear plots are listed in Table 4.1. Clearly the C(2)-H/D exchange second-order rate constants for all of the imidazolium cations decrease upon complexation with CB[7] host. The carbon acid pK_a values of these imidazolium cations in the absence and in the presence of CB[7] were estimated from the same method and the values are also shown in the table, the pK_a

shifts upon complexation with macrocyclic CB[7] are all determined.

Table 4.1 Second-order rate constants and pK_a values of imidazolium carbon acids in the absence and in the presence of CB[7], and shifts upon complexation.

Imidazolium Cations		k_{DO} (M^{-1} s^{-1})	pK_a	ΔpK_a
$IC4^+$	Without CB[7]	195	23.1	0.4
	With CB[7]	78	23.5	
$DIC4^{2+}$	Without CB[7]	615	22.6	0.7
	With CB[7]	123	23.3	
$IC6^+$	Without CB[7]	245	23.0	1.3
	With CB[7]	12	24.3	
$DIC6^{2+}$	Without CB[7]	498	22.7	1.4
	With CB[7]	20	24.1	
$IC8^+$	Without CB[7]	195	23.1	0.6
	With CB[7]	48	23.7	
$DIC8^{2+}$	Without CB[7]	468	22.7	1
	With CB[7]	48	23.7	

Again, the mechanism of the inhibition of deuterium exchange and acidity decrease for the carbon acid upon complexation has been proposed to be the C─H---O=C

hydrogen bond formation between guest imidazolium C(2)-H and carbonyl oxygens of CB[7]. Therefore, the guest complexation mode and binding geometry might play crucial roles in defining how hydrogen bonding (if it is optimal) may ultimately affect the change of reactivity of the C(2)-proton.

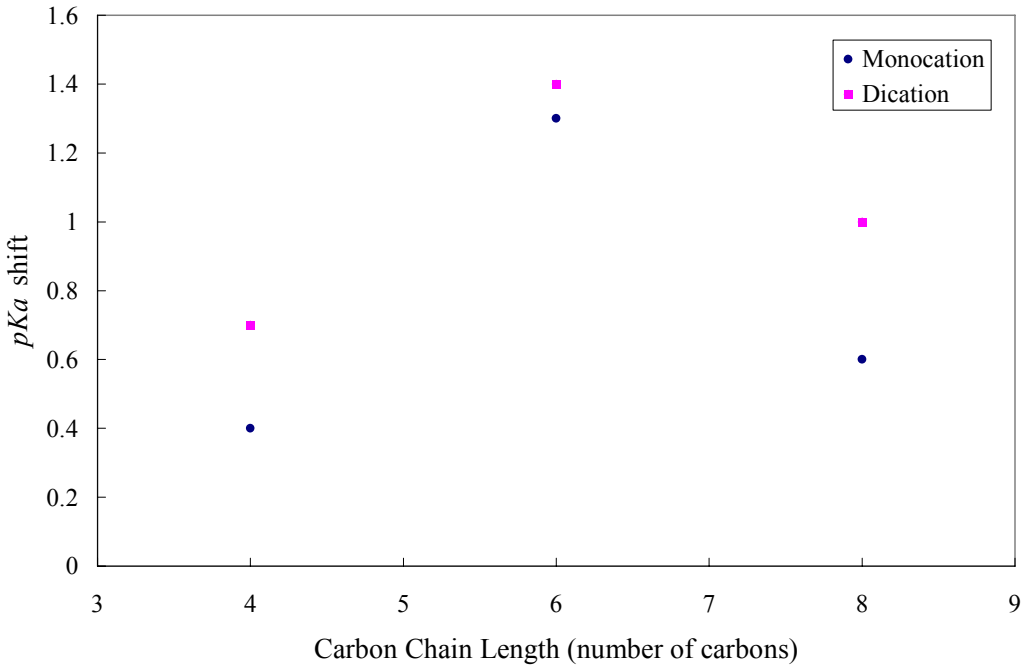

Figure 4.9 Diagram showing the relationship between the alkyl chain length and ΔpK_a for the imidazolium monocations (blue dot) and dications (purple square).

From Table 4.1, it is apparent that the pK_a shifts of all three alkylated bis(imidazolium) dications are larger than their monocation counterparts, which might be attributed to the slightly more stable/optimal binding due to the two relatively bulky imidazolium groups and the two positive charges of the guest with CB[7] through cation-dipole interactions

and size fit. More interestingly, for both the monocations and dications, the imidazolium cations with the hexyl chain ($DIC6^{2+}$ and $IC6^{+}$) have the most significant pK_a shifts (Figure 4.9). This might be attributed to a better binding geometry, resulting in optimal C(2)-H---O=C hydrogen bonding of either of the two imidazolium ring protons with the hexyl chain encapsulated in the cavity of CB[7], compared with those of the imidazolium cations with butyl or octyl chains.

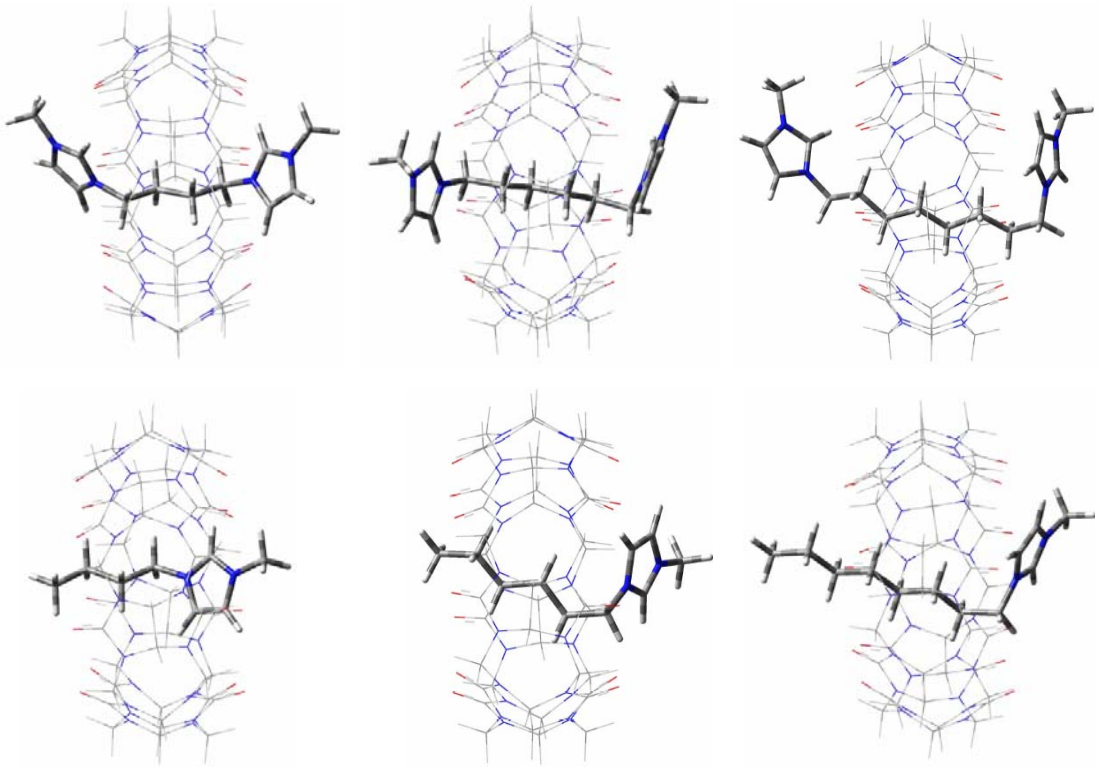

Figure 4.10 Energy-minimized structure of the alkylimidazolium/CB[7] guest-host complexes, $DIC4^{2+}$@CB[7], $DIC6^{2+}$@CB[7], $DIC8^{2+}$@CB[7] (from the left to the right on the top), $IC4^{+}$@CB[7], $IC6^{+}$@CB[7], and $IC8^{+}$@CB[7] (from the left to the right on the bottom).

The energy-minimized structures (Figure 4.10) of the imidazolium-cation/CB[7] complexes provide an indicator of the binding geometry and possible H-bond formations resulting from complexation. For both $IC4^+$ and $DIC4^{2+}$, the C(2)-H is located inside the carbonyl portals, and therefore not in a location for optimal H-bonding. For $IC8^+$ and $DIC8^{2+}$, the C(2)-H is placed out of the portals by the longer octyl chain (longer than the length of the cavity of CB[7]), and again is unable to form optimal H-bonding with the carbonyl oxygens. Only in the case of $IC6^+$ and $DIC6^{2+}$ is the imidazolium ring located adjacent to the carbonyl portals to facilitate the formation of the optimal H-bonding between C(2)-H and carbonyl oxygens of CB[7] portals.

The H-bond lengths and angles acquired from these energy minimized structures may support this assumption. The distances between the C(2)-hydrogens of $IC6^+$ (or $DIC6^{2+}$) and the carbonyl oxygens are all about 2.26 to 2.35 Å, while the C-H···O bond angles vary from 142.3° to 148.8°. The H-bonds between the other alkylated imidazolium cations and CB[7] have either large distances between C(2)-H and the carbonyl oxygens or sharper C-H···O angles.

Compared with the pK_a shifts of the alkylated imidazolium cations, the $BMIX^{2+}$ guest has a significantly larger pK_a decrease upon its complexation with CB[7], although the binding constants for all of these complexes are rather similar. This might be attributed to the optimal length and the rigidity of the hydrophobic xylene linker. Once the xylene group is encapsulated, the two imidazolium rings are anchored to the portals to form

H-bonding interactions between C(2)-proton and CB[7] portal oxygens, and the rigid linker (xylene) is not allowing the imidazolium rings to swing around to break H-bonding, unlike the flexible alkyl groups.

In summary, a series of imidazolium monocations and dications have demonstrated strong complexation with CB[7]. The C(2)-H/D exchange is inhibited and the acidities of these carbon acids are decreased upon their complexation with CB[7]. The attached alkyl chain length of alkylated imidazolium salts plays an important role in determining the binding geometry between the imidazolium rings and CB[7] portals, therefore affecting the C(2)-H reactivity change caused by CB[7] complexation. This research has been extended to another series of carbon acids, the sulphur analogues of imidazolium salts, the thiazolium salts, described next.

4.3.2 Inhibition of H/D Exchange of Thiazolium Cations Upon Complexation with Cucurbit[7]uril

4.3.2.1 Host-Guest Complexation of Thiazolium Cations with Cucurbit[7]uril

The first thiazolium cation to be examined in this study was 3,3'-bis-thiazolium-p-xylene (BTX^{2+}), the sulfur analogue of $BMIX^{2+}$. The guest-host interaction of BTX^{2+} with CB[7] was initially investigated using ^1H NMR spectroscopy in a 0.1 M NaCl-D_2O solution. Figure 4.11 shows the appearance of separate proton resonances for free and bound guest molecules in the presence of 0.4 equivalents of

CB[7], which indicates that the chemical exchange rate between free guest and CB[7]-complexed guest is slow on the ^{1}H NMR timescale, similar to that of the $BMIX^{2+}$ dication.

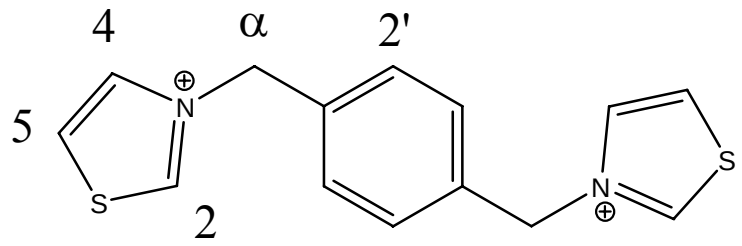

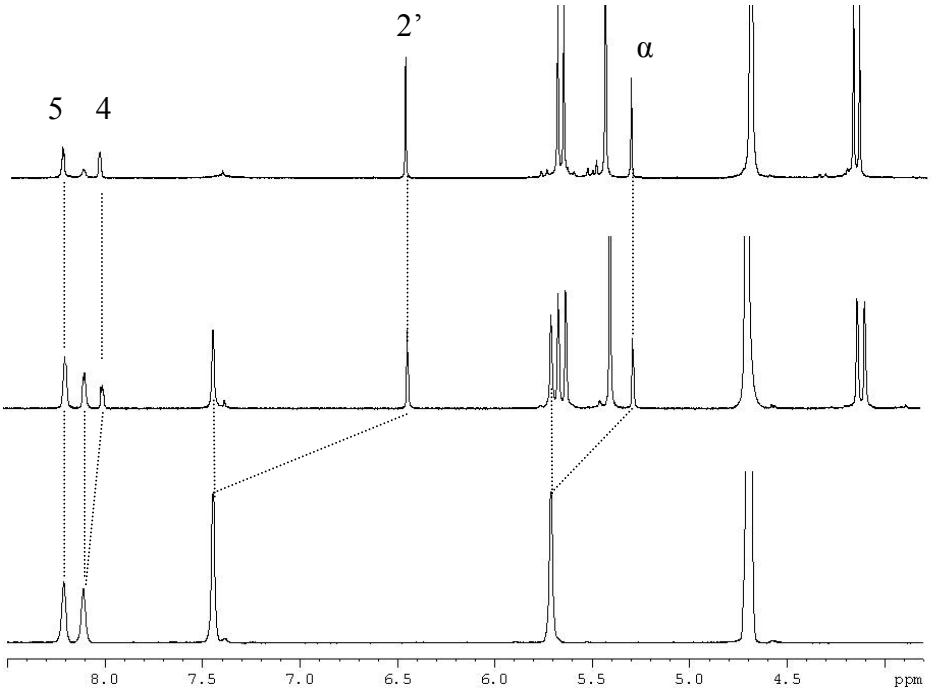

Figure 4.11 The ^{1}H NMR spectra of the free BTX^{2+} guest (lower spectrum) and after the addition of 0.4 equivalents of CB[7] (middle) and 1.1 equivalents of CB[7] (upper).

In the presence of 1.1 equivalents of CB[7], the resonances for the one of the

thiazolium ethylene protons (H(4)), the xylyl methylene protons (H(α)), and the aromatic protons (H(2')) in the ^{1}H NMR spectrum of the inclusion complex have moved upfield from those of the free guest, indicative of their positioning within the cavity of CB[7]. The other thiazolium ethylene resonance (H(5)) and the C(2)-proton (not shown here owning to fast H/D exchange) exhibited no chemical shift change, indicating that the thiazolium ring is most likely located outside of the cavity. The complexation constant was determined to be $K_{CB[7]} = (1.66 \pm 0.31) \times 10^{10}$ M^{-1} by using a similar competitive ^{1}H NMR titration method to that of $BMIX^{2+}$.

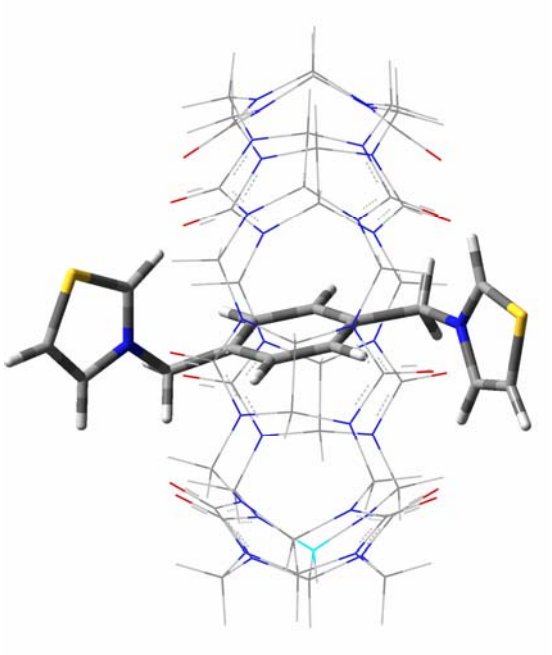

Figure 4.12 Energy-minimized structure (HF/3-21G** basis set) of the BTX^{2+}@CB[7] guest-host complex.

The 1:1 complexation between BTX^{2+} and CB[7] is also indicated by a Job's plot,

based on a UV-visible continuous variation method, and supported by the appearance of a strong doubly charged peak at *m/z* = 718 of the complex BTX^{2+}@CB[7] in the ESI-MS spectrum. The energy-minimized structure, calculated by an *ab initio* method, based on 1:1 complexation (Figure 4.12), providing supplementary evidence that the xylene portion is encapsulated in the cavity and that the two thiazolium rings are located at the portals. Similar to that of $BMIX^{2+}$, the H-bonding interactions between the C(2)-proton and carbonyl oxygens at the portals can be formed through a binding geometry which optimizes the fit according to the size and length of the guest.

The complexation between CB[7] and thiazolium salts have been extended to three thiamine guests, thiamine hydrochloride (Vitamin B1), thiamine monophosphate, and thiamine pyrophosphate. Thiamines have attracted significant interest, as they have novel biological activity, as well as being a common series of thiazolium cations for NHC precursors. As expected, CB[7] forms inclusion complexes with all of these thiamines. However, the binding sites of CB[7] on these guest molecules are different, as affected by the presence of polar phosphate groups on thiamine monophosphate and thiamine pyrophosphate.

Thiamine hydrochloride (TH) forms a 1:1 guest-host complex with CB[7], with the thiazolium-ethanol portion included in the cavity, and leaving the substituted pyrimidine part of the molecule out of the cavity. Figure 4.13 shows that in the presence of 1.1 equivalents of CB[7], the resonances for the ethyl group protons (H(3) and H(4)), the methyl protons on the thiazolium ring (H(1)), the linking methylene protons (H(5)) and

the C(2)-proton in the ^{1}H NMR spectrum of the inclusion complex have moved upfield from those of the free guest, indicative of their positioning within the cavity of CB[7]. The other methyl proton resonance (H(7)) and the aromatic proton on the pyrimidine ring (H(6)) exhibited downfield movement, indicating that the methylated pyrimidine ring is located at the portal of CB[7].

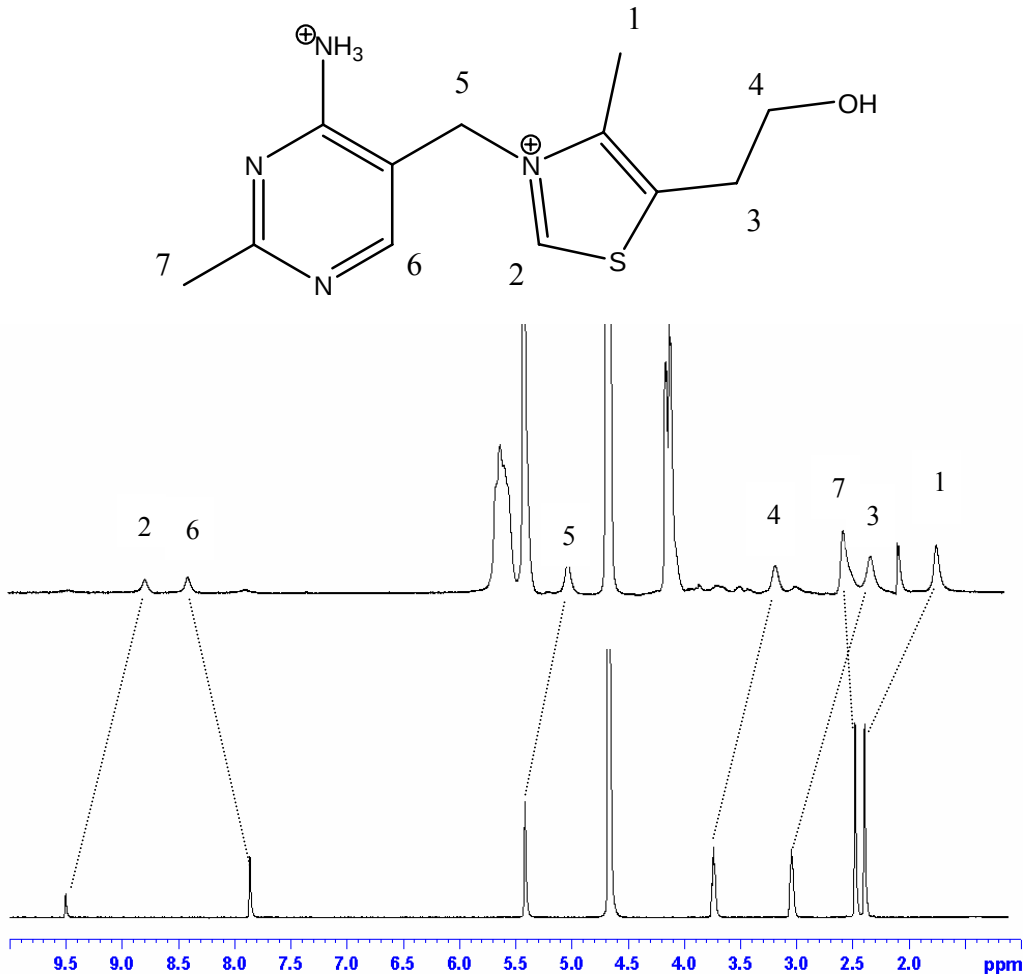

Figure 4.13 The ^{1}H NMR spectra of the free thiamine hydrochloride (TH) guest (lower spectrum) and after the addition of 1.1 equivalents of CB[7] (upper).

The 1:1 complexation between TH and CB[7] is also supported by a Job's plot from a UV-visible continuous variation method and the appearance of a strong singly charged peak at *m/z* = 1428 for the complex of TH^+@CB[7] in the ESI-MS spectrum. The complexation constant was determined to be $K_{CB[7]} = (6.5 \pm 1.0) \times 10^5\ M^{-1}$ from a spectrophotometric titration.

Similar to TH, both thiamine monophosphate (TM) and thiamine phosphate (TP) form 1:1 inclusion complexes with CB[7], supported by ^{1}H NMR and ESI-MS spectra, and *ab initio* structure calculations. However, unlike TH, the substituted pyrimidine ring of TM (and TP) is preferentially bound by CB[7], rather than the thiazolium-ethyl portion, because of the presence of polar (negatively charged) phosphate groups on the ethyl group of TM and TP (shifting the CB[7] over to the pyrimidine side of the guest molecule). The ^{1}H NMR spectra gives the direct evidence for such a binding selectivity. Representative ^{1}H NMR spectra of TM (Figure 4.14) shows that in the presence of 1.1 equivalents of CB[7], the resonances for ethyl group protons (H(3) and H(4)) exhibit very little movement, and methyl protons on thiazolium ring (H(1)) have moved to downfield from those from free guest, indicating that the substituted thiazolium ring is positioned outside of the cavity (at the portal) of CB[7]. The resonances for the linking methylene protons (H(5)), the C(2)-proton, the methyl protons and the aromatic proton on the pyrimidine ring in the ^{1}H NMR spectrum of the inclusion complex have moderately moved upfield from those of the free guest, indicative of their positioning within the cavity of CB[7]. The 1:1 complexations between the TM and TP and the CB[7] host are

also supported by Job's plots and the presence of strong singly charged peak at *m/z* = 1508 for the complex of TM^+@CB[7], and at 1588 for the complex of TP^+@CB[7] in the ESI-MS spectra of the two complexes. The complexation constants for the host-guest complexes of TM and TP with CB[7] were determined to be $K_{CB[7]} = (2.5 \pm 1) \times 10^4\ M^{-1}$ and $K_{CB[7]} = (8.0 \pm 1) \times 10^3\ M^{-1}$, respectively, from spectrophotometric titration methods.

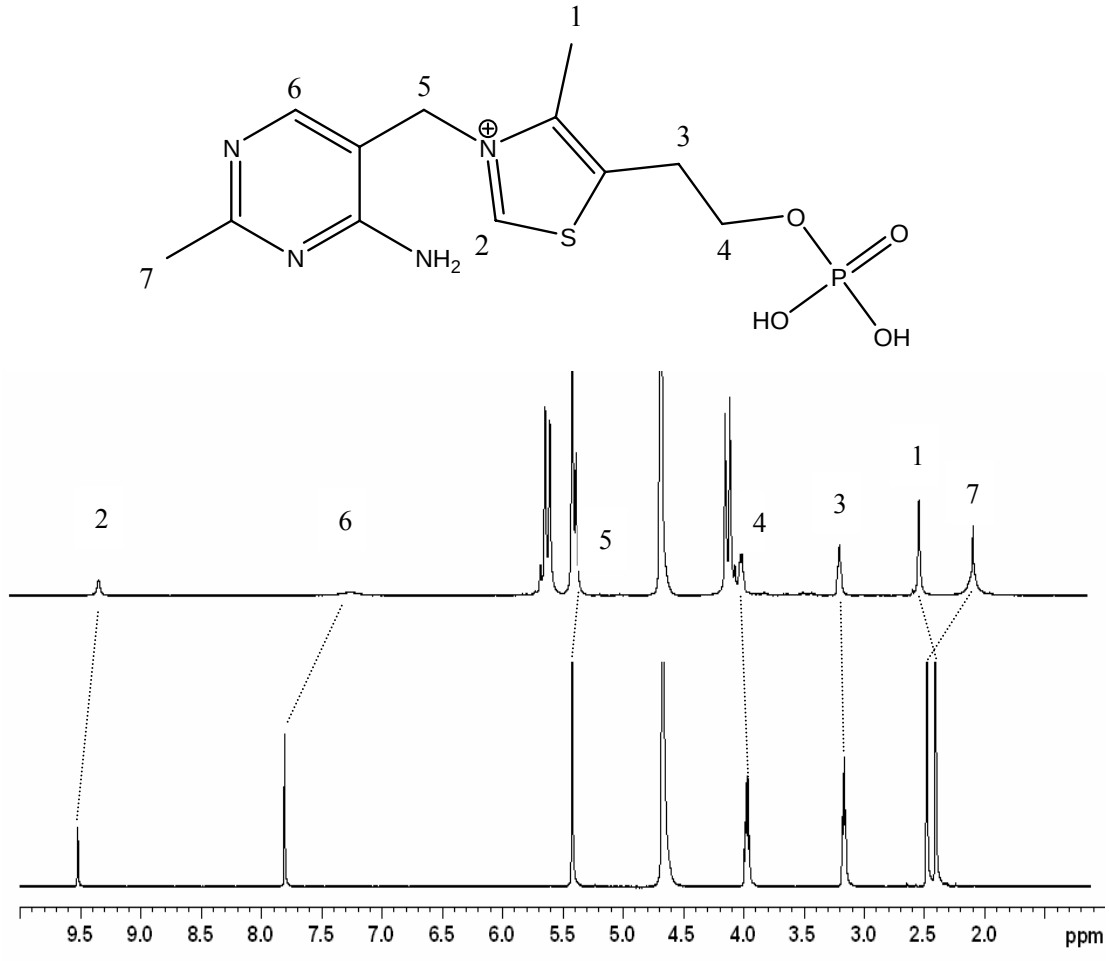

Figure 4.14 The ^1H NMR spectra of the free thiamine monophosphate (TM) guest (lower spectrum) and after the addition of 1.1 equivalents CB[7] (upper).

4.3.2.2 C(2)-H/D Exchange of Thiazolium Cations Monitored by ^{1}H NMR

With the knowledge of the complexations and different binding modes between each of these thiazolium cations and CB[7], the C(2)-H/D exchange of these thiazolium ligands in the absence and in the presence of CB[7] were studied (see representative figures in Figure 4.15). The effect of the respective binding modes towards the inhibition of the C(2)-H/D exchange and the acidities of the C(2)-H protons will be discussed.

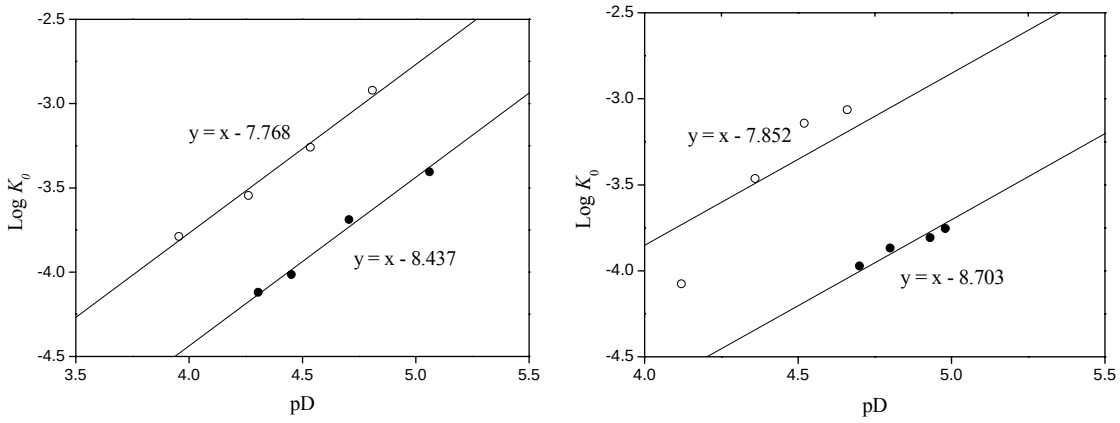

Figure 4.15 Plots of logk_{ex} against p*D* for the deuterium exchanges of the C(2)-protons on BTX^{2+} (o) and BTX^{2+}@CB[7] (●) (**left**), TH (o) and TH@CB[7] (●) (**right)** in buffered D_2O at 25 °C.

The exchange for deuterium on the C(2)-proton of these cations in buffered D_2O (p*D* = 3.0 – 6.0) at 25 ˚C and I = 0.2 (adjusted by NaCl) in the absence or in the presence of CB[7] was followed by ^{1}H NMR spectroscopy (400 MHz). The first-order rate

constants for H/D exchange of these thiazolium cations in the absence and in the presence of CB[7] at different p*D* environments were determined from the semilogarithmic plots of reaction progress *R* against time. Under these conditions, the second-order rate constants k_{DO} for DO^- catalyzed deuterium exchange of the thiazolium cations C(2)-proton in the absence and in the presence of CB[7] can be obtained from a linear fit (fixed slope = 1) to the equation of log k_{ex} = log ($k_{DO}K_W/\gamma_{OL}$) + p*D* by using the data of first-order rate constants k_{ex} and p*D* values (Figure 4.15).

Table 4.2 The pK_a values determined for thiazolium carbon acids in the absence and in the presence of CB[7].

Thiazolium Cations		k_{DO} ($M^{-1}s^{-1}$)	pK_a	ΔpK_a
BTX^{2+}	Without CB[7]	9.8×10^6	18.4	0.7
	With CB[7]	2.1×10^6	19.1	
TH	Without CB[7]	8.7×10^6	18.4	0.9
	With CB[7]	1.2×10^6	19.3	
TM	Without CB[7]	6.4×10^6	18.6	0.3
	With CB[7]	3.2×10^6	18.9	
TP	Without CB[7]	4.3×10^6	18.7	0.4
	With CB[7]	1.9×10^6	19.1	

The values of the second-order rate constants and pK_a values of these thiazolium cations in the absence and in the presence of CB[7], determined from the linear fits of Figure 4.15, are listed in Table 4.2. The pK_a values for all of these free thiazolium cations are in the range of pK_a = 18-19, which are consistent with literature values.[14] It appears that the second order rate constants for C(2)-H/D exchange for all of the thiazolium cations are moderately decreased upon their complexation with CB[7]. The rate constants for both the BTX^{2+} and TH cations in the presence of CB[7] are reduced to about 25% of the original rate constants for these cations in the absence of CB[7], whereas for the thiamines which contain phosphate groups (TM and TP), the rates of C(2)-H/D exchange in the presence of CB[7] are only slowed down to about half of their original rates of the cations in the absence of CB[7].

The pK_a values of the thiazolium cations have moderately shifted by less than 1 pK_a unit, which indicates complexation by CB[7] only moderately decreased the acidity of these thiazolium cations, unlike those of some of the imidazolium cations studied. Moreover, for the three thiamine ligands, the pK_a of thiamine hydrochloride shifted by almost 1 pK_a unit, whereas the pK_a values of the other thiamine phosphate guests shifted less than half a pK_a unit, upon their complexation with CB[7].

The different changes of the second order rate constants, as well as pK_a shifts of the thiamine ligands upon their complexation with CB[7] host molecules, are likely a result of CB[7] binding over different sites of the thiamine ligands and the fact that these complexes have different stability constants. As discussed before, CB[7] binds over the

ethanol portion and most of the thiazolium ring of thiamine strongly, however, it binds the substituted pyrimidine ring of TM and TP through a relatively weaker binding.

The inclusion of the thiamine and ethanol portions of TH might enable a more effective protection of C(2)-H from deuterium exchange, primarily through a better H-bonding interaction between the C(2)-H of the rigid thiazolium ring (mostly included in the cavity) with the carbonyl oxygens of CB[7] (Figure 4.16). The inclusion of the substituted pyrimidine ring of TM (or TP) by CB[7] cavity may provide H-bonding interactions (Figure 4.16), of C(2)-proton with carbonyl oxygens of the portals, however, the thiazolium ring has greater freedom of motion when it is located outside of the cavity.

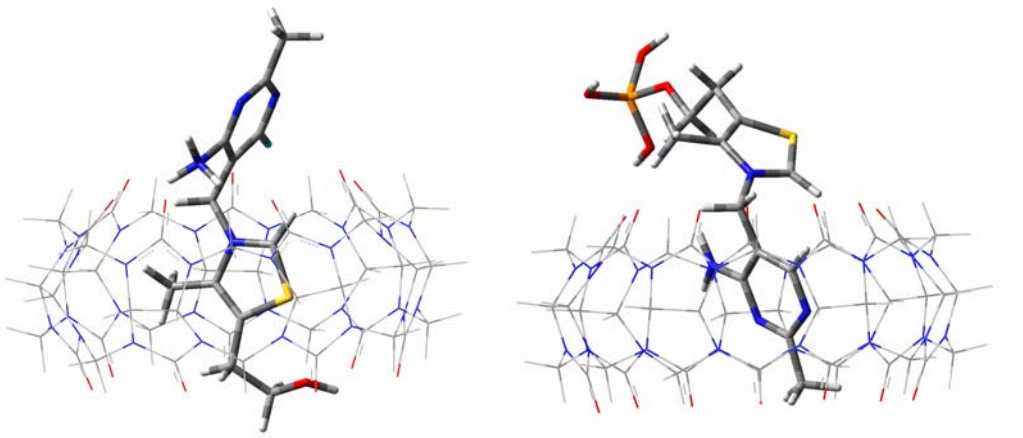

Figure 4.16 Energy-minimized structures of the TH@CB[7] (left) and TM@CB[7] (right) guest-host complexes.

It is noticeable that CB[7] has a more significant effect on decreasing the acidity of imidazolium cations than thiazolium cations through host-guest complexation. The

reason for such a selectivity is not clear yet, although the inhibition of C(2)-H/D exchange for both imidazolium and thiazolium cations is generally proposed to be attributed to hydrogen bonding formation between C(2)-proton and CB[7] portal oxygens through stable guest-host complex formations.

4.4 Conclusions

In summary, a series of imidazolium cations and thiazolium cations have demonstrated strong complexation with CB[7]. The C(2)-H/D exchange reaction is inhibited and the acidities of these carbon acids are decreased upon their complexation with CB[7]. The substituted groups on these cations, such as alkyl chains or phosphate groups, play important roles in the binding site/mode selectivity by the CB[7] host molecules. They affect the complexation geometry between the imidazolium/thiazolium rings and the CB[7] portals and the binding constants, and therefore the C(2)-H/D exchange reactivity. We have demonstrated that through changing the type of carbon acid (between imidazolium and thiazolium), and modifying the imidazolium/thiazolium rings by selective substituents such as phosphate groups and alkyl chains with different chain lengths, we are able to achieve a wide range of carbon acids with different acidities, upon the addition of CB[7] host molecules to solutions of the carbon acids. This guest-host complexation of selective carbon acids has the potential to be employed in controlling the reactivity/stability of a range of imidazolium/thiazolium carbon acids, which are often employed as N-heterocyclic carbene precursors in catalytic organic and

organometallic chemistry.

References

(1) Olofson, A.; Thompson, W. R.; Michelman, J. S. *J. Am. Chem. Soc.* **1964**, *86*, 1865.

(2) Chiappe, C.; Pieraccini, D. *J. Phys. Org. Chem.* **2005**, *18*, 275.

(3) Levillain, J.; Dubant, G.; Abrunhosa, I.; Gulea, M.; Gaumont, A.-C. *Chem. Commun.* **2003**, 2914.

(4) Arduengo, A. J. I. *Acc. Chem. Res.* **1999**, *32*, 913.

(5) Bourissou, D.; Guerret, O.; Gabbaï, F. P.; Bertrand, G. *Chem. Rev.* **2000**, *100*, 39.

(6) Crudden, C. M.; Allen, D. P. *Coord. Chem. Rev.* **2004**, *248*, 2247.

(7) Canal, J. P.; Ramnial, T.; Dickie, D. A.; Clyburne, J. A. C. *Chem. Commun.* **2006**, 1809.

(8) Li, G.-Q.; Dai, L.-X.; You, S.-L. *Chem. Commun.* **2007**, *8*, 852.

(9) Breslow, R. *J. Am. Chem. Soc.* **1957**, *79*, 1762.

(10) Buncel, E.; Clement, O.; Onyido, I. *Acc. Chem. Res.* **2000**, *33*, 672.

(11) Haake, P.; Bausher, L. P.; Miller, W. B. *J. Am. Chem. Soc.* **1969**, *91*, 1113.

(12) Amyes, T. L.; Diver, S. T.; Richard, J. P.; Rivas, F. M.; Toth, K. *J. Am. Chem. Soc.* **2004**, *126*, 4366.

(13) Fahlbusch, T.; Frank, M.; Schatz, J.; Schuhle, D. T. *J. Org. Chem.* **2006**, *71*, 1688.

(14) (a) Washabaugh, M. W.; Jencks, W. P. *Biochemistry* **1988**, *27*, 5044. (b) Washabaugh, M. W.; Jencks, W. P. *J. Am. Chem. Soc.* **1989**, *111*, 674.

(15) Magill, A. M.; Cavell, K. J.; Yates, B. F. *J. Am. Chem. Soc.* **2004**, *126*, 8717.

(16) Haake, P.; Bausher, L. P. *J. Phys. Chem.* **1968**, *72*, 2213.

(17) Handy, S. T.; Okello, M. *J. Org. Chem.* **2005**, *70*, 1915.

(18) Kim, Y.-J.; Streitwieser, A. *J. Am. Chem. Soc.* **2002**, *124*, 5757.

(19) Day, A.; Arnold, A. P.; Blanch, R. J.; Snushall, B. *J. Org. Chem.* **2001**, *66*, 8094.

(20) Wang, J. W.; Xu, F. B.; Li, Q. S.; Song, H. B.; Zhang, Z. Z. *Acta Cryst.* **2005**, *E61*, m367.

(21) Namboodiri, V. V.; Varma, R. S. *Org. Lett.* **2002**, *4*, 3161.

(22) Jeon, W. S.; Moon, K.; Park, S. H.; Chun, H.; Ko, Y. H.; Lee, J. Y.; Lee, E. S.; Samal, S.; Selvapalam, N.; Rekharsky, M. V.; Sindelar, V.; Sobransingh, D.; Inoue, Y.; Kaifer, A. E.; Kim, K. *J. Am. Chem. Soc.* **2005**, *127*, 12984.

(23) Liu, S. M.; Ruspic, C.; Mukhopadhyay, P.; Chakrabarti, S.; Zavalij, P. Y.; Isaacs, L. *J. Am. Chem. Soc.* **2005**, *127*, 15959.

(24) Wang, R.; Yuan, L.; Macartney, D. H. *Chem. Commun.* **2005**, 5867.

(25) Englander, S. W.; Mayne, L.; Bai, Y.; Sosnick, T. R. *Protein Sci.* **1997**, *6*, 1101.

Chapter 5

CUCURBIT[7]URIL MEDIATED VISIBLE COLOR CHANGE OF GUEST DYE MOLECULES

In chapter 3 the ability of CB[*n*] to alter the fluorescent properties of selected guest fluorophores was discussed. In addition to the emission properties, the UV-visible absorption spectra of many guest dye molecules have also been altered by CB[*n*] inclusion. This chapter is focused on significant modifications of the UV-visible absorption spectra of selected guest dye molecules in the presence of CB[*n*], in which the visible colors of these molecules may be changed.

5.1 Introduction

The complex formations between most dye molecules and macrocyclic host

molecules are generally not accompanied by significant changes in the UV-visible absorption spectra of the guest molecules. Very often a moderate UV-visible absorbance change is observable upon guest complexation, similar to those caused by a change in the solvent due to polarity differences.

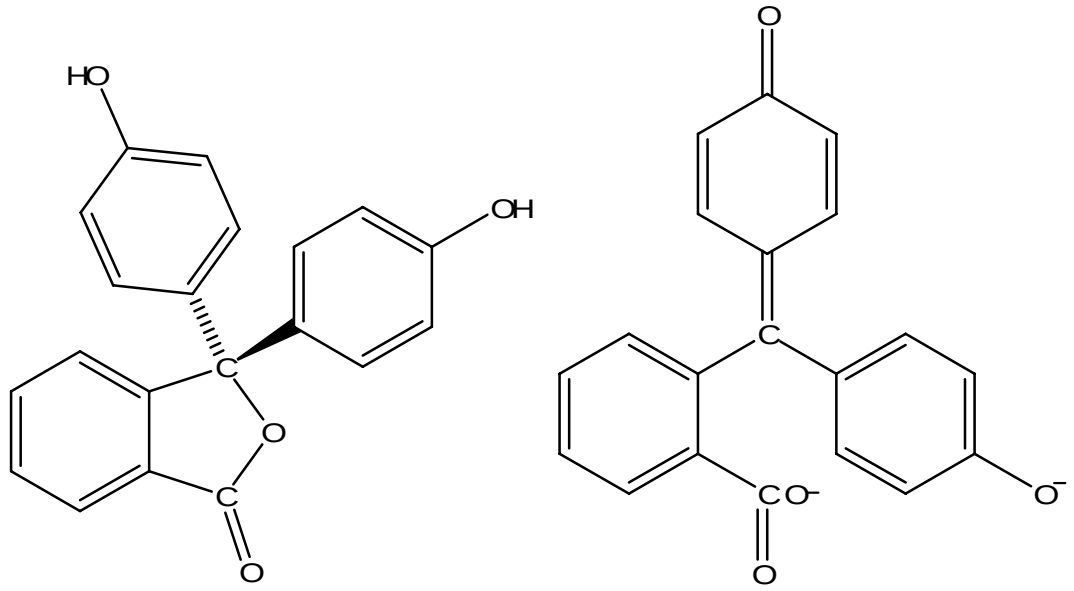

Figure 5.1 The structures of phenolphthalein at neutral pH (left) and at pH 10.5 (right).

A few special cases exhibiting significant spectral changes upon guest complexation have been discovered by employing cyclodextrins.[1-5] A 1:1 guest-host complex is formed between phenolphthalein (Figure 5.1) and β-cyclodextrin at pH 10.5, and the purple solution becomes colorless as the complex formation causes a dramatic increase in the absorption at 440 nm.[1] It has been proposed by Buvari *et al.* that the absorbance change of phenolphthalein at pH 10.5 is attributed to the inclusion of a phenolic ring into

the cavity of β-cyclodextrin through three-site contacts (hydrophobic interactions, hydrogen bonding between the phenolic oxygen and cyclodextrin hydroxyl portals, and the interaction between carboxylate group of the guest and the host hydroxyl groups).[2] The complexation to the cyclodextrin provides hindrance to charge resonance delocalization between the two phenolic rings. In addition, the carboxylate oxygen may be forced to sit close to the central carbon atom of phenolphthalein by the hydroxyl rims of cyclodextrins. These two factors might explain the disappearance of the purple color upon complex formation in alkaline solution.[2]

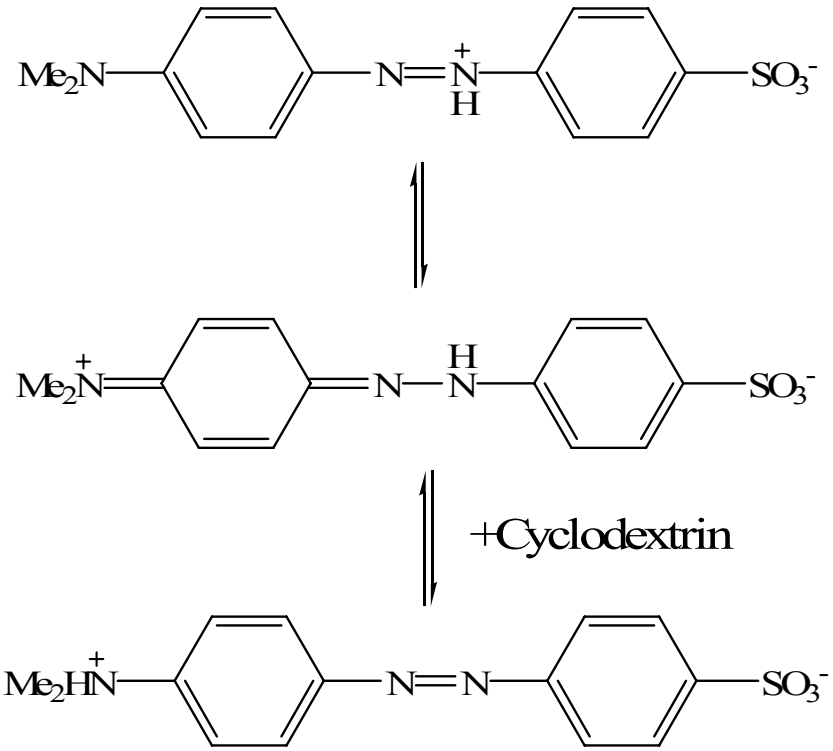

Figure 5.2 Protonated methyl orange equilibrium affected by cyclodextrin complex formation (adapted from reference[3]).

Another example of significant visible color change is the red to colorless switch of azobenzene dye molecules, such as methyl orange, upon complexation with cyclodextrins, which is proposed to be caused by a shift of a tautomeric equilibrium.[3] As shown in Figure 5.2, at low pH the protonated form of methyl orange has three tautomers. Upon complexation with cyclodextrin (α-cyclodextrin works the best), the equilibrium is driven to the formation of the tautomer with a protonated dimethylamino group, presumably because this tautomer, with a proton on the dimethylamino nitrogen, forms the most stable inclusion complex with cyclodextrin. Because of the significant color change of these dye molecules upon cyclodextrin complexation/decomplexation, dye-modified cyclodextrins have been prepared and their applications as molecular indicators (color change upon other guest molecule complexation) have been demonstrated.[4,5]

Unlike cyclodextrins, CB[*n*] has never been reported to dramatically change the visible color of any dye molecule. It has been found that CB[*n*] complexation may induce moderate absorbance spectral changes in the guest molecules, mostly due to the nonpolar characteristics of the cavity of CB[*n*]. The absorption wavelength maximum and intensity for a guest viologen, for example, is depressed moderately upon its complexation with CB[7].[6,7] Inspired by some of the dramatic visible color changes of guest dye molecules caused by cyclodextrin complexation, and considering the fact that visible color of guest dye molecules has never been significantly changed by CB[*n*] host molecules, we have extended the study of CB[*n*] based host-guest complexation to selected guest dye molecules, with a focus on their visible color changes upon their

complexation with CB[*n*] hosts.

Working along this line, we have fortunately discovered significant visible color change of two guest dye molecules, 4,4'-bis(dimethylamino)diphenyl carbinol (BDC-OH) and pinacyanol chloride (PC), upon complexation with CB[7] respectively, and the mechanism for each visible color change has been proposed.

5.2 Experimental

5.2.1 Materials Preparation

The host molecule CB[7] was synthesized according to literature methods, as previously described in Chapter 2.[8] All of the other chemicals involved in this project were purchased from Sigma-Aldrich and used as received.

5.2.2 Methods and Characterization

The 1D ^{1}H NMR spectra were recorded on a Bruker AV-400M NMR spectrometer in D_2O. The ESI-MS spectra were acquired on a Waters 2Q Single Quadrupole MS spectrometer equipped with an ESI/APcI multiprobe. The UV-visible spectra were all acquired from a Hewlett Packard 8452A diode array spectrometer using quartz cells with 1.00 cm path length.

The modeled structures of the host-guest complexes involved in this project were computed by energy-minimizations using Gaussian 03 (Revision C.02) programs run on the computing facilities of the High Performance Virtual Computing Laboratory (HPVCL)

at Queen's University, as described in section 2.2.2 in chapter 2. Digital images of the guest dye solutions with and without host molecules were taken by using a Sony DSC-P71 camera under room light.

5.3 Results and Discussion

5.3.1 Blue Color Enhancement of 4,4'-Bis(dimethylamino)diphenyl Carbinol

5.3.1.1 Host-Guest Complexation and Blue Color Enhancement

The guest-host interaction of 4,4'-bis(dimethylamino)diphenyl carbinol (BDC-OH) with CB[7] was first investigated using ^{1}H NMR spectroscopy in D_2O. Interestingly, the ^{1}H NMR spectrum (the middle spectrum in Figure 5.3) shows the appearance of separate proton resonances for all of the free and bound protons of this guest molecule in the presence of 0.7 equivalents of CB[7], which indicates that the chemical exchange rate between the free guest and the CB[7]-complexed guest is slow on the ^{1}H NMR timescale for this binding mode. Meanwhile, the methyl proton (labeled as H(1)) resonances are noticeably split into three peaks upon addition of 0.7 equivalents of CB[7] (the middle spectrum of Figure 5.3). The downfield shift in the resonance of the methyl group is caused by the inclusion of the aromatic portion of the molecule into the cavity of CB[7], with the carbonyl oxygens deshielding the methyl groups at the portals. The upfield shift of the resonance of the methyl protons might be caused by encapsulation of methyl groups of acetone residue in the hydrophobic cavity of CB[7], and the

complexation/decomplexation rate is fast in ^{1}H NMR timescale, as this particular chemical resonance moved even further upfield upon addition of more CB[7] (Figure 5.3, top spectrum).

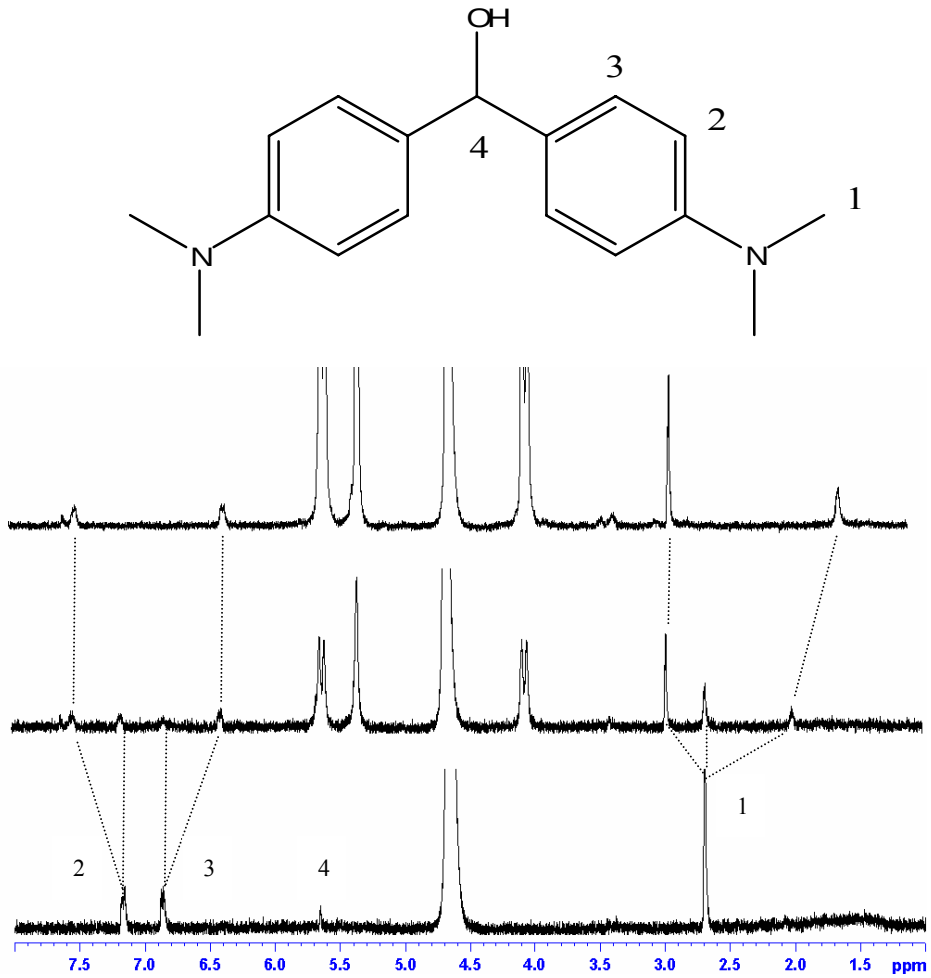

Figure 5.3 Structure of the BDC-OH with proton labeling (**Top)**; The ^{1}H NMR spectra of the free BDC-OH guest (bottom spectrum) and after the addition of 0.7 equivalents of CB[7] (middle) and 1.1 equivalents of CB[7] (upper spectrum) in D_2O (400 MHz) (**Bottom).**

In the presence of 1.1 equivalents of CB[7] (Figure 5.3 top spectrum), the resonance for one of aromatic protons (H(3)) in the ^{1}H NMR spectrum of the inclusion complex have moved upfield from those of the free guest, indicative of its positioning within the cavity of CB[7]. The resonances for the major methyl protons (H(1)) and the other aromatic proton (H(2)) have moved downfield, while the carbinol proton (H(4)) disappeared due to either H/D exchange or overlapping with the proton resonances of the CB[7] host molecule. This behavior indicates that the methyl groups are most likely situated outside of the cavity of CB[7], as the downfield shift of the methyl proton resonance may be attributed to the deshielding effect of the carbonyl-rimmed portal of CB[7], with the aromatic rings encapsulated in the cavity of CB[7].

The 1:1 binding stoichiometry of the BDC-OH@CB[7] complex was revealed by the ESI-MS spectrum (Figure 5.4), which exhibited a peak at *m/z* = 1415 for the 1:1 guest@host complex BDC^{+}@CB[7] (calculated 1415), and also supported by energy-minimized structure *ab initio* calculation. The ESI-MS peak at 1415 is for a complex based on the 4,4'-bis(dimethylamino)diphenyl carbonium ion (BDC^{+}, a carbonium ion after the BDC-OH loses a OH group) and CB[7]. The continuous variation method using absorption spectrometry (Job's plot) could not be employed to determine the binding stoichiometry as the changes in the UV-visible spectrum of the guest dye molecule upon addition with CB[7] are not caused simply by complexation, but mainly induced by a shift in the reaction equilibrium. The reaction equilibrium shift will be discussed in the next section.

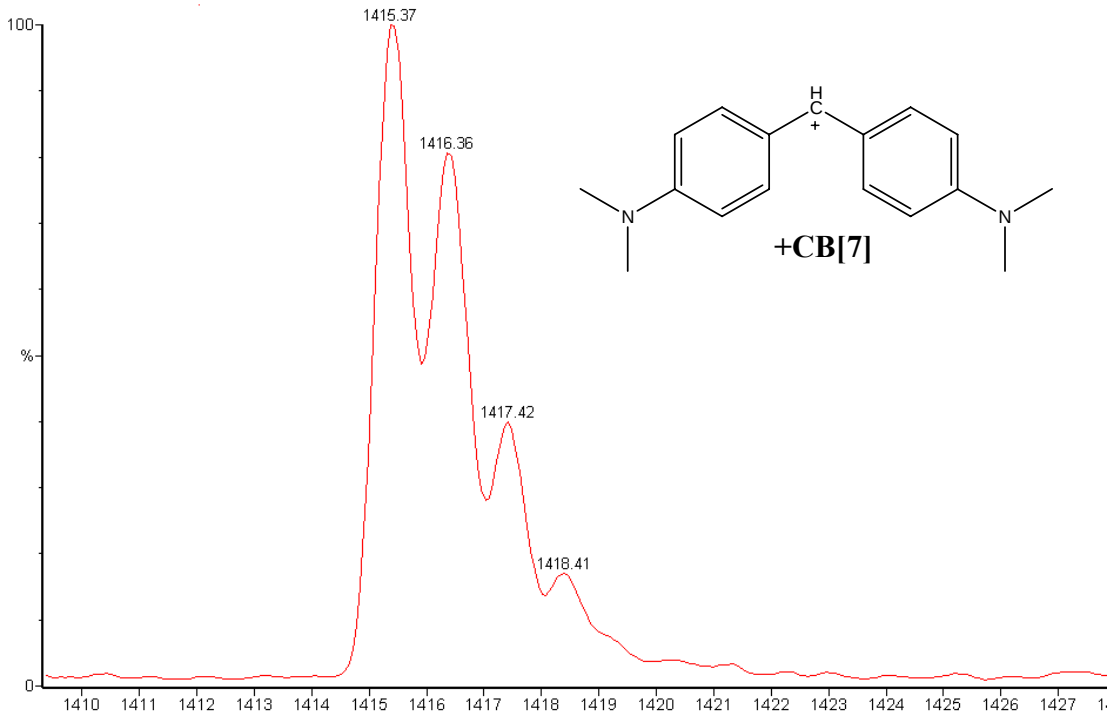

Figure 5.4 ESI-MS spectrum of the complex of BDC^{+}@CB[7] in water.

A significant change of the BDC-OH solution from nearly colorless to a visible blue color, at neutral pH, upon addition of CB[7] host molecules can be easily observed by the naked eye (inset pictures of Figure 5.5). The UV-visible absorption spectra of BDC-OH (10 μM) titrated with CB[7] (up to 100 μM) (Figure 5.5) clearly indicate a significant complexation-induced absorption enhancement at 598 nm, and simultaneously, a dramatic absorption decrease at 258 nm. To our knowledge, the induction of such a significant visible color change of any guest dye molecules by CB[*n*] hosts has not been reported before.

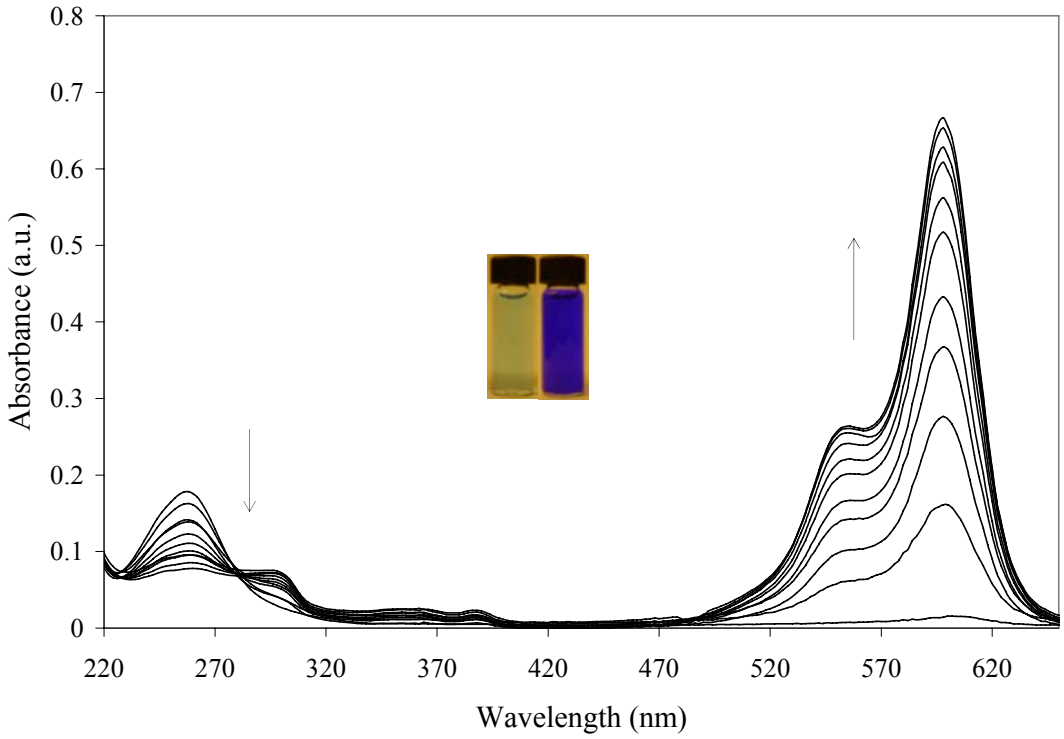

Figure 5.5 UV-visible absorption of BDC-OH (10 μM) at pH 7.1 in the absence and in the presence of various amounts of CB[7] (1:1, 2:1, 3:1, 4:1, 5:1, 6:1, 7:1, 8:1, 9:1 and 10:1 ratios of CB[7]:BDC-OH). **Insert**: Digital images of 10 μM BDC-OH aqueous solution at pH 7.1 without (light blue) and with 100 μM CB[7] (deep blue) under domestic light.

It is worth noting that the absorbance increase in the visible band and a simultaneous decrease in the shorter wavelength UV band are accompanied by very little shift in the wavelength maxima. This might not be caused by a solvent polarity change only (nonpolar cavity of CB[7]), as dissolving BDC-OH in ethanol (with a similar polarity to

the CB[7] cavity)[9] did not produce a blue colored solution. Similar to the mechanism for the color change of methyl orange induced by cyclodextrin complexation,[3] the mechanism of the visible color change of BDC-OH upon complexation with CB[7] might also be explained by a reaction equilibrium shift.

5.3.1.2 Mechanism of Visible Color Change of 4,4'-Bis(dimethylamino)diphenyl Carbinol

A clue to the mechanism of the color change is given by the positive-mode ESI-MS spectrum of the complex of BDC-PH@CB[7] (Figure 5.4) in which there is no $(M+H)^+$ or $(M+Na)^+$ or any of the kind ions observed, instead, a loss of 17 mass units (typical loss of OH group) to give $(M-OH)^+$ (M is the mass for BDC-OH@CB[7]) has been observed. BDC-OH, therefore, has been converted into the blue carbonium ion BDC^+ after its complexation with CB[7] host molecules. A study by Harrison and coworkers indicates that there are primarily three species present in an aqueous solution of BDC-OH in the pH range of 3-6.[10] Only one of the species, BDC^+, has visible blue color (with a strong absorbance at a maximum of around 600 nm) in solution, while the other two species, BDC-OH and $BDCH^{2+}$ are both visibly colorless (Figure 5.6).

They also have reported a pK_{a1} (pK_a of BDC^+) of 4.12, and a pK_{a2} (pK_a of $BDCH^{2+}$) of 5.48 in sodium acetate buffered solution.[10] It has also been demonstrated that an addition of high concentration guanidine hydrochloride (4M) to the acetate buffered BDC-OH solution increased the pK_{a1} value (BDC^+) from 4.12 to 5.55 and decreased the

pK_{a2} value ($BDCH^{2+}$) from 5.48 to 4.70, in such a way that the formation of the blue color BDC^{+} is promoted most at a pH of around 5.1.[10] In other words, the equilibrium was shifted to produce more carbonium ion BDC^{+} by an addition of guanidine hydrochloride, and the absorbance of BDC^{+} at 606 nm was increased about 7 fold.[10] The major species (probably the only species) at a pH higher than 7.0 is BDC-OH , either in sodium acetate buffered aqueous solution or in a buffered solution with an addition of guanidine hydrochloride.[10]

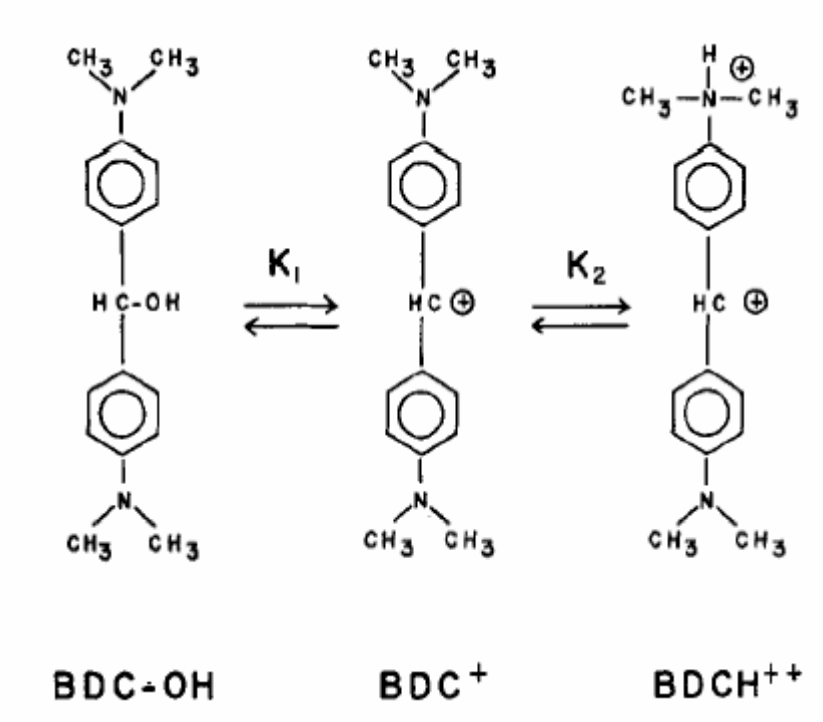

Figure 5.6 Equilibrium among the three species, BDC-OH, BDC^{+} and $BDCH^{2+}$ present in aqueous buffers.[10]

An addition of CB[7] to the BDC-OH solution at pH 7.1 results in an intense blue

color with a 47-fold increase in the absorbance at 598 nm (Figure 5.5). A shift in the equilibrium for BDC-OH/BDC^+ due to complexation by host molecules has not been reported before.

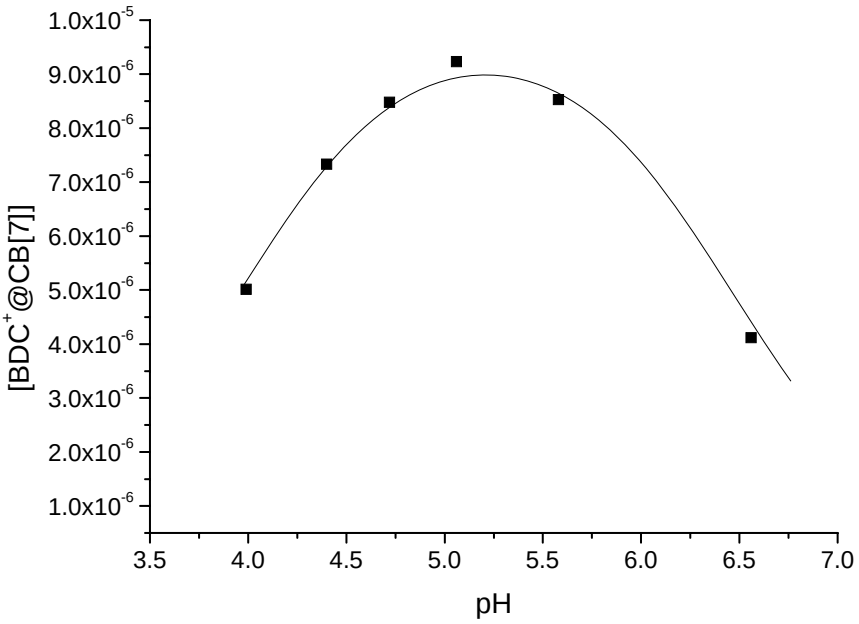

Figure 5.7 Plot of concentration of complexed carbonium cation against pH (black squares) and a nonlinear best fit of equation 5.1 for estimations of the pK_{a1} and pK_{a2} values. $[BDC]_{total}$ = 10 μM in the presence of 100 μM CB[7] in buffered solution.

A pH titration of the BDC-OH@CB[7] complex (buffered by sodium acetate) with the absorbance measured at 598 nm has provided values of pK_{a1} = 6.46 and pK_{a2} = 3.96 in the presence of CB[7], by plotting the concentrations of carbonium ion BDC^+ against the pH of the solution according to the equation 5.1[10] (Figure 5.7). The concentration of the complexed carbonium ion was calculated from the absorbance of the buffered solution at

598 nm at different pH values (pH titration).

$$[BDC^+] = [BDC]_{total}/(1+1/(K_1[H^+])+K_2[H^+]) \quad (5.1)$$

It has been known

$$K_1 = [BDC^+]/([BDC\text{-}OH][H^+]) \quad (5.2)$$

$$K_2 = [BDCH^{2+}]/([BDC^+][H^+]) \quad (5.3)$$

Equation 5.4 describes the relationship of the $[BDC]_{total}$ to the three species available in solution. Add equations 5.2 and 5.3 into 5.4, the equation 5.1 can be achieved.

$$[BDC]_{total} = [BDC\text{-}OH] + [BDC^+] + [BDCH^{2+}] \quad (5.4)$$

The pK_{a1} value has therefore increased from 4.12 to 6.46 (with ΔpK_{a1} of around 2.3), and pK_{a2} has decreased from 5.48 to 3.96 (with ΔpK_{a2} of around -1.5) by complexation of CB[7]. After addition of CB[7] into the colorless BDC-OH solution at pH 6 to 7, the major (almost the only) species, BDC-OH, has been mostly converted to visibly blue colored BDC^+ (Figure 5.8).

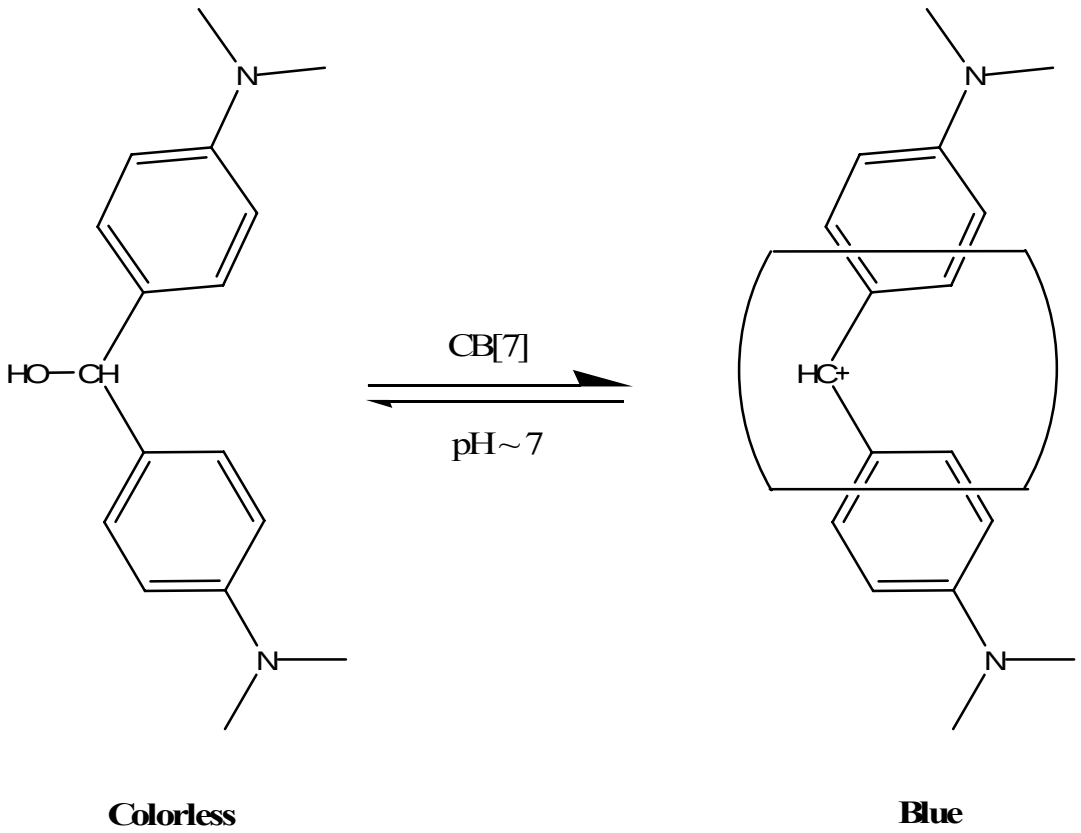

Figure 5.8 A schematic diagram of the conversion of BDC-OH to a carbonium ion BDC^+ upon the addition of CB[7] to a BDC-OH aqueous solution at pH 7.

In the absence of CB[7] at around pH 7, as previously discussed, the major (almost the only) species is BDC-OH. The addition of CB[7] drives the equilibrium dramatically to the formation of BDC^+ (with a new pK_a value of 6.46 in the presence of CB[7]), the second equilibrium to produce $BDCH^{2+}$ does not exist in this pH range (as $BDCH^{2+}$ has a pK_a of 3.96 in the presence of CB[7]) (Figure 5.8). The mechanism for the CB[7]-complexation induced visible color change of BDC-OH may be, therefore, a simple equilibrium shift caused by CB[7] complexation. The equilibrium shift (and pK_a

shift) is presumably driven by stabilization of carbonium cation upon complexation with CB[7]. As discussed in previous chapters, CB[*n*] host molecules have demonstrated their versatility in stabilizing various cationic guest molecules and we have demonstrated that CB[*n*] molecules have stabilized cationic guest molecules such as (*E*)-FcMPE$^+$, and have also shifted both the ground-state and excited state pK_a values of protonated aromatic amines through complexation induced stabilization of the cationic protonated form (ammonium). It is, therefore, not surprising that the carbonium ion BDC$^+$ is promoted in the equilibrium through host complexation-induced stabilization.

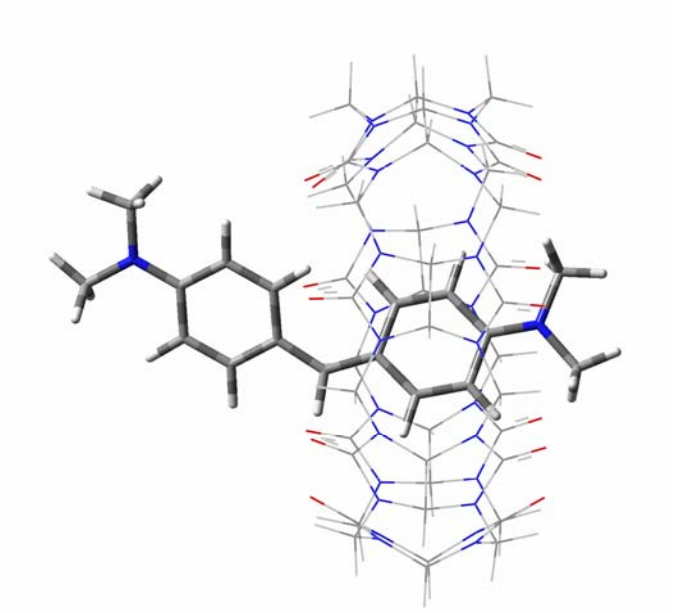

Figure 5.9 Energy-minimized structure of the BDC$^+$@CB[7] inclusion complex.

In the previous section, the ESI-MS spectrum revealed that the complex between BDC-OH and CB[7] actually exists in the form of BDC$^+$@CB[7], and ^{1}H NMR

spectroscopy has supported the inclusion complex formation with mainly the aromatic rings included in the cavity of CB[7]. An *ab initio* calculation for the major binding mode (Figure 5.9) of the structure of the complex clearly supports the 1:1 complex formation between BDC^+ and CB[7]. The complexed BDC^+ is, therefore, stabilized by CB[7] through hydrophobic interactions (aromatic ring with the hydrophobic cavity), dipole-cation interaction (carbonyl portals and the positive charge on carbonium) and probably hydrogen bonding as well (between carbonium-H and carbonyl portal oxygens).

The ^{1}H NMR spectrum of the complex (Figure 5.3, top spectrum) seems inconsistent with the energy-minimized structure (with only one of the two benzene ring included) here, as there are not separate sets of proton resonances for aromatic rings upon guest complexation (predicted from the complexed structure). This may be explained by a fast exchange rate of the CB[7] complexation over the two aromatic rings (although the total complexation-decomplexation rate is slow on ^{1}H NMR timescale), as the two aromatic rings have equal opportunity to be encapsulated by CB[7]. CB[7], therefore, is probably shuttling between two aromatic rings in the complexed form. This study has also provided us with the first example of the ability of CB[7] to stabilize a carbocation, and has further expanded the range of cationic guest molecules that CB[7] can encapsulate and stabilize.

5.3.2 Purple to Blue Switch of Pinacyanol Chloride

In addition to the significant color change of the BDC-OH dye molecules caused by

CB[7] complexation, a dramatic visible color change of another guest dye molecule, pinacyanol chloride (PC), has been observed upon complexation with CB[7].

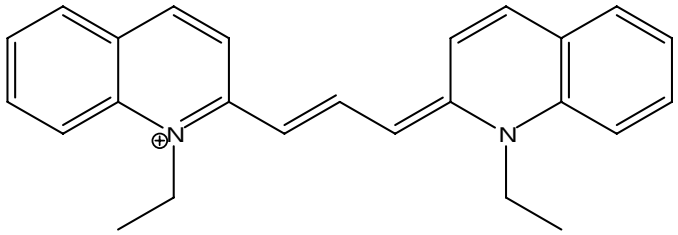

Figure 5.10 The structure of pinacyanol chloride.

The full name of pinacyanol chloride (PC) is 1,1'-diethyl-2,2'-carbocyanine chloride (Figure 5.10) and it is a cationic dye in the class of symmetric (through resonance) cyanine dye molecules. Because of its amphiphilic nature, it is soluble and finds applications in a wide range of solvents including water and chloroform.[11] One of the most significant features of the PC dye molecules is its self-aggregation, especially in aqueous solution.[12] At low concentrations, the aggregates of PC mainly stay in the form of dimers and trimers,[11,13] whereas at higher concentrations, a polyaggregate is formed with extremely low absorbance intensity at multiple lower wavelengths, and this phenomenon has been referred to as metachromasia.[14,15] In aqueous solution, the monomer of PC has an absorbance band centered at 600 nm (α band), while the absorbance of the dimer has a blue-shifted band (β band) with a maximum at 546 nm, and the trimer has a more blue-shifted maximum at 522 nm (γ band). This special feature has enabled PC to be intensively employed as a spectrometric tool to determine critical

micelle concentrations.[11,16,17]

It has been reported that the addition of a polymer to aqueous solutions of PC changes its purple color (mainly caused by the absorbance of its dimer) to a colorless solution (polyaggregate) through the formation of weak absorbing PC polyaggregates association by ion-ion interactions.[14] Attempts to induce more monomer formation (by dissociating the dimers, trimers and polyaggregates) through supramolecular host-gust interactions, however, have not been reported.

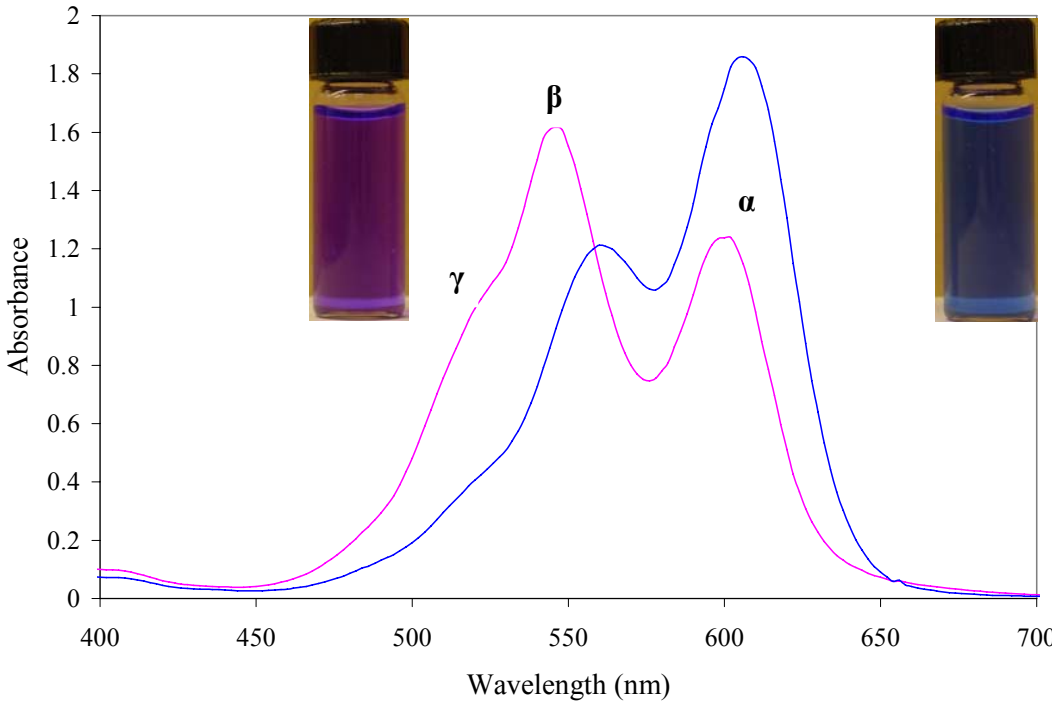

Figure 5.11 UV-visible absorbance spectrum of PC (25 μM) in aqueous solution in the absence (purple line) and in the presence (blue line) of 30 μM CB[7]. **Insert**: Digital images of 25 μM PC aqueous solution without (purple) and with (blue) 30 μM CB[7] under room light.

Cucurbit[7]uril has again been selected from the CB[*n*] family for this task because of its superior water solubility. The addition of CB[7] to aqueous solutions of PC results in a significant visible purple to blue color switch (inset pictures in Figure 5.11). Figure 5.11 shows the absorbance spectra of an aqueous solution of PC in the absence and in the presence of about 1.2 equivalents of CB[7]. It clearly reveals that in the absence of CB[7] (purple line), the most intensive absorbance band is the β band (dimer). In the presence of 1.2 equivalents of CB[7], the α band (monomer) absorbance becomes the most intensive band, whereas both the β (dimer) and γ (trimer) bands are decreased significantly.

It is also worth noting that the addition of CB[7] has noticeably red-shifted the β band maximum from 546 nm to 560 nm and moderately shifted the α band maximum from 600 nm to 606 nm (Figure 5.12), presumably attributed to the nonpolar environment that the CB[7] cavity provides. Both the red-shift of the absorbance bands, and the absorbance increase of α band and the simultaneous absorbance decreases of both the β and γ bands result in a visible purple to blue color switch of PC upon complexation of CB[7]. Figure 5.12 shows the smooth changes of both absorbance intensity and bands maxima of PC upon gradual addition of CB[7]. After the addition of 1.8 equivalents of CB[7], the absorbance changes reached a new equilibrium, and further addition of CB[7] gave little change in the absorbance. Apparently, the addition of CB[7] does not convert all of the aggregates to monomers, although the equilibrium is shifted to form more monomers

from aggregates.

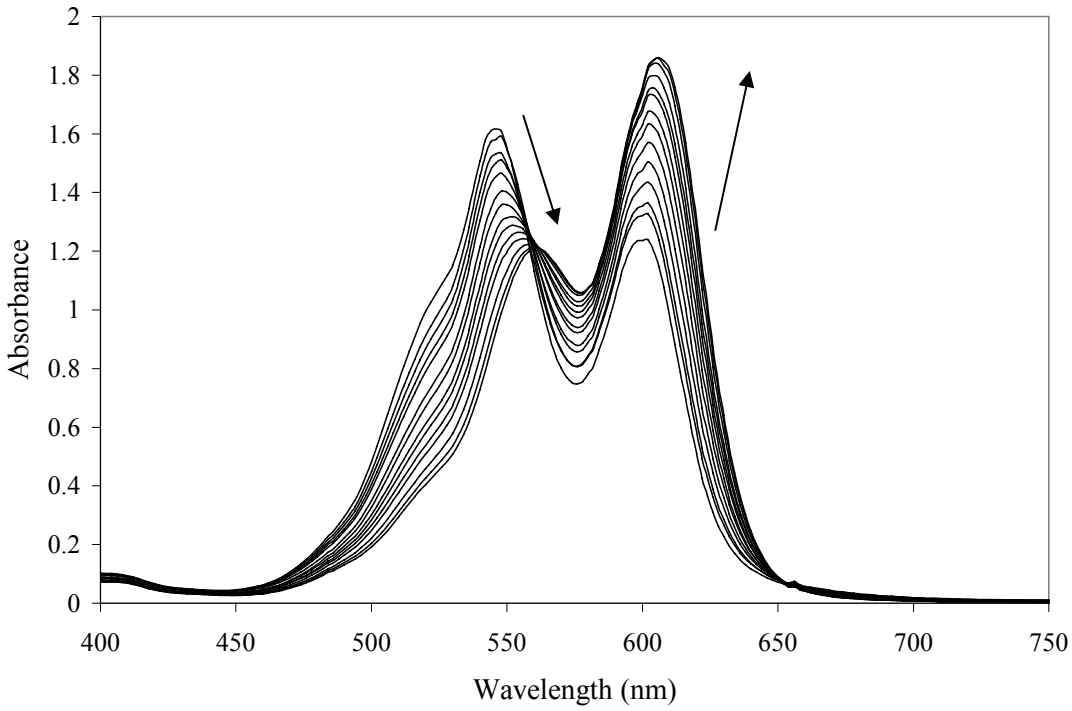

Figure 5.12 UV-visible absorption spectra of PC (25μM) in aqueous solution in the absence and in the presence of various amounts of CB[7] (0.1:1, 0.2:1, 0.3:1, 0.4:1, 0.5:1, 0.6:1, 0.7:1, 0.8:1, 0.9:1, 1:1, 1.1:1, 1.2:1, 1.4:1, 1.6:1 and 1.8:1 ratios of CB[7]:PC).

It has been clearly demonstrated that visible color change of PC is a result of aggregates to monomer conversion upon an addition of CB[7]. The nature of the interaction between CB[7] and PC, however, remains unclear. The ESI-MS spectrum of a mixture of CB[7] and PC gives a relatively strong singly charged peak at *m/z* = 1515 ($(PC\text{-}Cl)^{+}$@CB[7]) and a weak doubly charged peak at *m/z* = 1340 ($(PC\text{-}Cl+H)^{2+}$@$CB[7]_2$), which reveals the presence of both 1:1 and 2:1 host-guest

complexes comprised of CB[7] and PC guest dye molecules. The ^{1}H NMR spectra (Figure 5.13) of the free and bound PC (with only 0.25 equivalents of CB[7]) shows that upon complexation, almost all guest proton resonances become broader and are slightly shifted upfield. This tells us that there might be multiple CB[7] binding sites on the guest PC molecule (considering the structure of the PC molecule), and a few binding modes may be possible. The broad resonances of bound PC protons indicate that fast exchange of complexation/decomplexation of PC molecules by CB[7] in ^{1}H NMR timescale is likely.

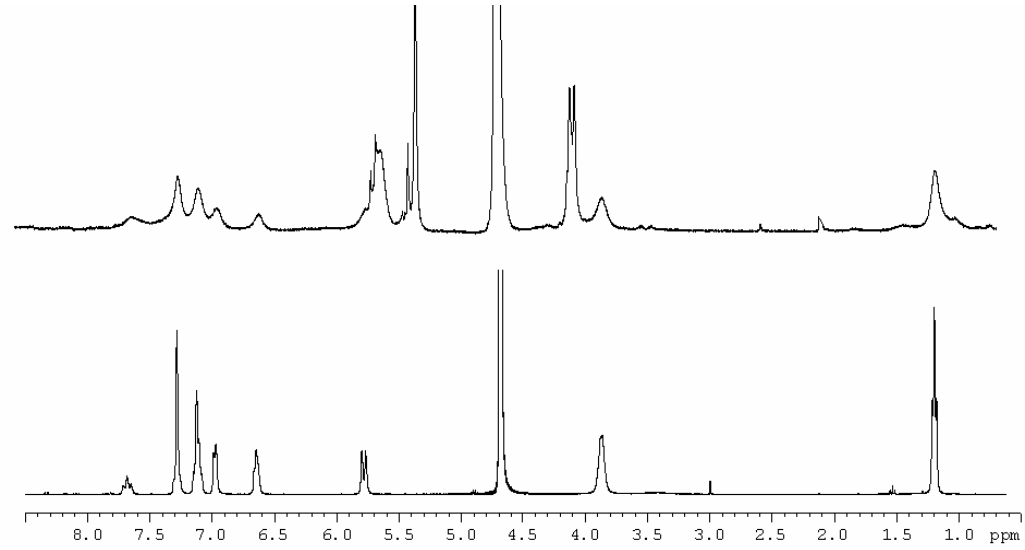

Figure 5.13 ^{1}H NMR spectra of the free PC guest (bottom) and bound PC with 0.25 equiv CB[7] (top) in D_2O (400 MHz)**.**

Whether there are one or two CB[7] host molecules that are complexed with one guest PC molecule and no matter what the binding mode might be, the aggregates (dimer,

trimer and polyaggregates) tend to be broken into monomers by CB[7] complexation, as shown by the absorbance spectra of PC titrated with CB[7] (Figure 5.12). As CB[7] might bind the ethyl group of PC to form 1:1 or 2:1 host-guest complexes, the PC molecules can still aggregate (but aggregates formation becomes more difficult) together through π-π or π-cation interactions of the aromatic rings. Not all of the aggregates, therefore, are broken into monomers even after the addition of excess CB[7].

In this example, we have demonstrated chromotropic character of CB[7] with cyanine dye molecules to modify or significantly change the visible color of guest dye molecules through mediating the monomer/aggregate equilibrium.

5.4 Conclusion

The two examples discussed in this chapter have illustrated that the CB[*n*] host molecules have the potential to modify the absorbance spectra and to dramatically change the visible colors of guest dye molecules. The visible color change of guest dye molecules upon complexation with CB[7] demonstrated herein has established a model for a visible color switch regulated by complexation-decomplexation of CB[*n*] host molecules, and may find applications in chemical sensing and/or bio-labeling.

References

(1) Szejtli, J. *Cyclodextrins and Their Inclusion Complexes*; Akademiai Kiado: Budapest, 1982.

(2) Buvari, A.; Kajtar, M.; Barcza, L. *J. Chem. Soc. Perkin Trans. 2* **1988**, 1687.

(3) Buvari, A.; Barcza, L. *J. Incl. Phenom. Mol. Recog. Chem.* **1989**, *7*, 313.

(4) Kuwabara, T.; Takamura, M.; Matsushita, A.; Ikeda, H.; Nakamura, A.; Ueno, A.; Toda, F. *J. Org. Chem.* **1998**, *63*, 8729.

(5) Kuwabara, T.; Nakajima, H.; Nanasawa, M.; Ueno, A. *Anal. Chem.* **1999**, *71*, 2844.

(6) Ong, W.; Gomez-Kaifer, M.; Kaifer, A. E. *Org. Lett.* **2002**, *4*, 1791.

(7) Kim, H. J.; Jeon, W. S.; Ko, Y. H.; Kim, K. *Proc. Natl. Acad. Sci. USA* **2002**, *99*, 5007.

(8) Day, A.; Arnold, A. P.; Blanch, R. J.; Snushall, B. *J. Org. Chem.* **2001**, *66*, 8094.

(9) Rankin, M. A.; Wagner, B. D. *Supramol. Chem.* **2004**, *16*, 513.

(10) Humphries, B. A.; Rohrbach, M. S.; Brookhart, M. S.; Harrison, J. H. *Bioorg. Chem.* **1974**, *3*, 163.

(11) Sabate, R.; Gallardo, M.; Estelrich, J. *J. Colloid Interfac. Sci.* **2001**, *233*, 205.

(12) West, W.; Pearce, S. *J. Phys. Chem.* **1965**, *69*, 1894.

(13) Merrill, R. C.; Spencer, R. W. *J. Am. Chem. Soc.* **1950**, *72*, 2894.

(14) Mitra, A.; Nath, R. K.; Chakraborty, A. K. *Ind. J. Biochem. Biophys.* **1992**, *29*, 411.

(15) Kostarelos, K.; Luckham, P. F.; Tadros, T. T. *J. Colloid Interfac. Sci.* **1997**, *191*, 341.

(16) Corrin, M. L.; Klevens, H. B.; Harkins, W. D. *J. Chem. Phys.* **1946**, *14*, 480.

(17) Corrin, M. L.; Harkins, W. D. *J. Am. Chem. Soc.* **1947**, *69*, 679.

Chapter 6

CONCLUSIONS AND SUGGESTIONS FOR FUTURE WORK

6.1 Conclusions

The thesis research has been focused on the development of new supramolecular host-guest complexes based on CB[*n*], and in particular on the investigations of the altered chemical reactivity and spectroscopic properties of aromatic guest molecules induced by CB[*n*] complexation.

We have demonstrated that the chemical reactivity, especially photoreactivity, of selected aromatic guest molecules has been altered upon their complexation with CB[*n*] host molecules. It has been illustrated that the [4+4] photodimerization of protonated 2-aminopyridine within a 2:1 guest-host complex with CB[7] is highly stereoselective, producing exclusively the *anti*-*trans*-DADAT^{2+} isomer and protecting the dimer from thermal rearomatization. This result, for the first time, has demonstrated the potential

application of CB[7] in mediating stereoselective photodimerizations of small aromatic molecules in aqueous solution. We have investigated the CB[7] mediated photoreactions of protonated *trans*-1,2-bis(4-pyridyl)ethylene [(*E*)-$BPEH^{2+}$] and its N-alkylated derivatives to demonstrate the potential of CB[7] to control the outcome of a photoreaction, specifically to direct a photoreaction to proceed through a selective route. Upon complexation by CB[7], the (*E*)-H_2BPE^{2+} guest molecule selectively favors photoisomerization over the otherwise dominant photohydration reaction in aqueous solution. CB[7] has also been demonstrated to have the ability to eliminate the photoinstability of (*E*)-1-ferrocenyl-2-(1-methyl-4-pyridinium)ethylene in aqueous solution by supramolecular encapsulation of the ferrocenylethylene portion of the included guest. Moreover, the inclusion of the ferrocene in the CB[7] cavity significantly reduces the complex's electron-transfer reactivity. In the same fashion, CB[7] might be able to regulate the reactivity and stability of other ferrocene derivatives through the strong complexation between CB[7] and the ferrocene moiety and/or reactive substituent groups, and may find applications in stabilizing and storing unstable chemical species.

In addition to the changes in the photoreactivity of these guest molecules caused by CB[*n*] complexation, the reactivity (H/D exchange rate) of the C(2)-proton of carbon acids guest molecules upon complexation with CB[7] hosts has been affected. A series of cationic imidazolium and thiazolium carbon acids have exhibited strong complexation with CB[7]. The C(2)-H/D exchange rates are inhibited and the acidity of these carbon

acids are decreased upon their complexation with CB[7]. The resultant pK_a shifts of these carbon acids has been related to multipoint C–H···O=C hydrogen bonding with the host molecules. This guest-host complexation has the potential to be employed in controlling the reactivity/stability of a range of imidazolium and thiazolium carbon acids, which are often employed as N-heterocyclic carbene precursors in catalytic organic and organometallic chemistry.

It has also been demonstrated that spectroscopic properties of complexed guest molecules can be altered by CB[*n*] complexation. The emission color switch of protonated aromatic amines such as protonated 2-aminoanthracene, upon complexation with CB[7], has been observed. The mechanism for such color switch has been proposed to be mainly the result of a decrease in the excited state acidity of the protonated aromatic amines caused by CB[7] complexation. The emission intensity decrease/increase of acridizinium molecules, upon sequential addition with CB[8]/CB[7] has been demonstrated. This is the first example of the employment of different sized CB[*n*] hosts to control fluorescence intensity as the result of different binding stoichiometries between the cyclic hosts and the fluorophore guests. These examples of fluorescence switches (both emission color switch and off/on switch) may have potential applications as supramolecular-controlled fluorescent switches and chemical sensors.

The UV-visible absorbance spectra of guest dye molecules may also be altered by CB[*n*] complexation. We have observed a significant visible color switch from nearly colorless to deep blue in the BDC-OH dye molecules upon complexation with CB[7] at

neutral pH. This has been shown to be a result of a shift in the BDC-OH/BDC^+ equilibrium (to produce more blue colored BDC^+ cations), caused by CB[7] complexation and stabilization of BDC^+. We have also discovered a dramatic visible purple to blue color change of another guest dye molecule, pinacyanol chloride (PC), upon complexation with CB[7], which is attributed to the dissociation of PC aggregates upon CB[7] complexation. These examples for visible color switches triggered by CB[*n*] host molecules have the potential to be developed into other visible color molecular switches regulated by complexation-decomplexation of host molecules, which may find applications in chemical sensing.

In summary, through our research we have expanded the variety CB[*n*] host-guest complexes that have been investigated and have demonstrated that the chemical reactivity and/or spectroscopic properties of many aromatic guest molecules have been significantly altered. The examples we have demonstrated in this thesis may lead to further expansions in the applications of CB[*n*] host molecules in catalysis, molecular sensing and molecular machine/switch construction.

6.2 Suggestions for Future Research

The investigations of fluorescent color switch of protonated aromatic amines and fluorescence off/on switch of acridizinium, caused by CB[*n*] complexation, could be further expanded to a competitive complexation study by fluorescence spectrometry. In such a study, the complexation of nonfluorescent guest molecules with CB[7] and/or

CB[8] could be observed and studied by fluorescence spectroscopy. In the case of blue emission host-guest complexes based on CB[7] and protonated 2-aminoanthracene (2-AAH$^+$), an addition of nonfluorescent guest molecules (a competitive guest of 2-AAH$^+$ for CB[7]) can competitively replace 2-AAH$^+$ in the cavity of CB[7] and the emission of the solution would switch back to green emission (free 2-AAH$^+$ released in solution). In the case of nonfluorescent host-guest complexes based on CB[8] and acridizinium salts, competitive guest molecules (which bind strongly to CB[8]) can result in the release of the acridizinium guest molecules from the cavity of CB[8], such that the emission of acridizinium cation is turned on (fluorescent "light-up" switch). The 1,3-bis(4,5-dihydro-1*H*-imidazol-2-yl)adamantane dication (BIAD^{2+}) has been tested before in the case of the acridizinium@CB[8] complexes. A large number of nonfluorescent guest molecules for CB[7] and CB[8] could be investigated in these two systems by employing fluorescence spectroscopy. The different fluorescence outputs upon the addition of different nonfluorescent guest molecules may be employed to differentiate the analytes (nonfluorescent guests), and such a study may find applications in the design of fluorescent detectors or sensor of nonfluorescent molecules.

The research project of CB[*n*] complexation mediated UV-visible absorbance spectra changes of included guest dye molecules could be expanded to a biologically important dye molecule, a retinylideneiminium cation (visual pigment in rhodopsin[1]), to build up a biomimic rhodopsin model in which the CB[7] host molecule can mimic a hydrophobic pocket of a rhodopsin protein. In a preliminary experiment, the all-*trans*

N,N-dimethylretinylideneiminium cation (DMRI) (Figure 6.1) has been synthesized according to a literature method.[2] The addition of CB[7] to an aqueous solution of DMRI resulted in a large red shift of the absorbance maximum from 444 to 470 nm ($\Delta\lambda_{max}$ = 26 nm) of this retinylideneiminium salt, induced by CB[7] complexation (Figure 6.2).

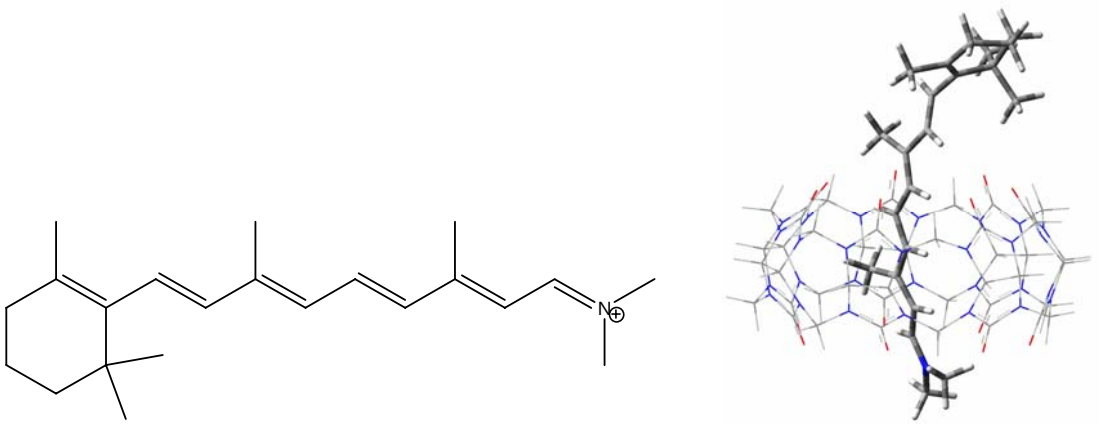

Figure 6.1 The structure of the all-*trans* N,N-dimethylretinylideneiminium cation (**left**) and the energy-minimized structure of the CB[7] host-guest complex of the all-*trans* N,N-dimethylretinylideneiminium cation (**right**).

The *ab initio* structure calculations supported the conclusion that the CB[7] is complexed to the linear cationic iminium portion through hydrophobic and cation-dipole interactions (Figure 6.1). Previous reports have shown that the cyclohexene portion of the guest may be encapsulated in the hydrophobic cavity of β-cyclodextrin, inducing a

moderate blue shift in λ_{max}.[3] In a comparative study, β-cyclodextrin complexation has induced a significant blue shift in λ_{max} from 444 to 384 nm ($\Delta\lambda_{max}$ = 60 nm) (Figure 6.2). The different binding site preferences of the two hydrophobic host molecules on this retinylideneiminium cation thus exhibit different effects on the λ_{max} shift, which may provide a better understanding to the physiochemical aspect of the visual pigment, although the mechanism of such absorbance shifts haven't been clearly understood.

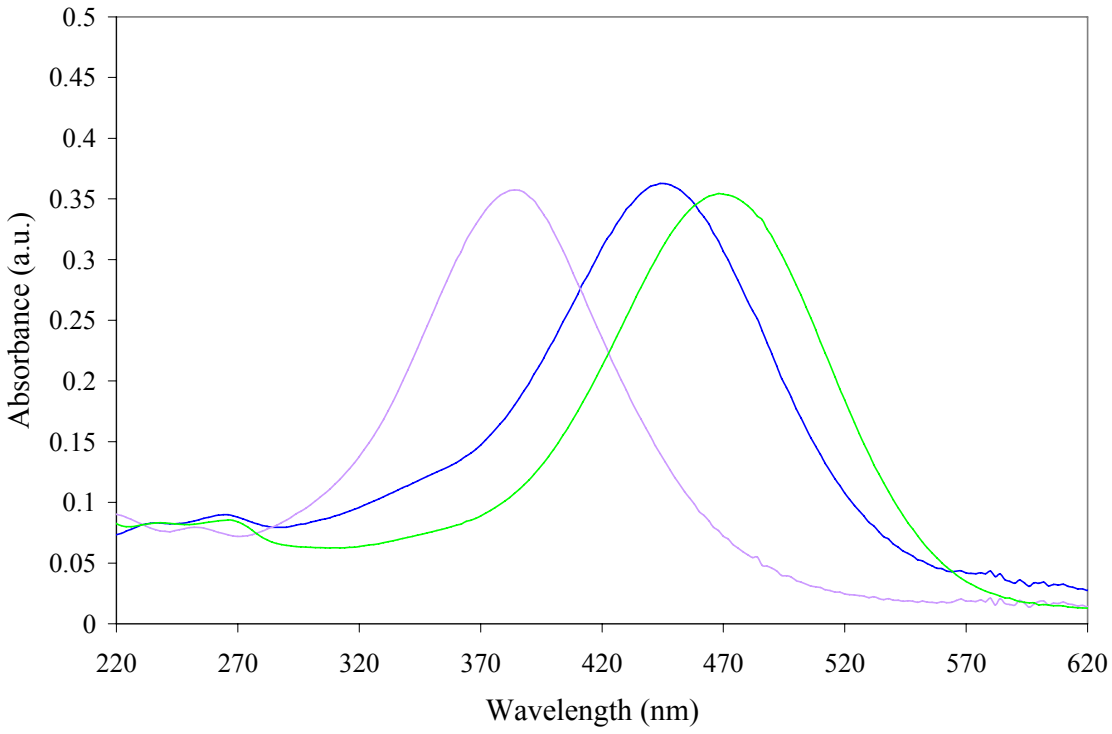

Figure 6.2 The absorbance spectra of DMRI (20 μM) in the absence of 100μM CB[7] or β-CD (blue line), in the presence of CB[7] (green line), and in the presence of 1 mM β-CD (purple line).

In order to confirm these preliminary results and to further test the effect of CB[*n*] complexation on the absorbance spectra of retinylideneiminium salts, a number of other retinylideneiminium salts could be synthesized, and their complexation with CB[7] and β-CD, the effect of the complexation on the UV-visible absorbance spectra, and the effect of CB[7] complexation on the *trans-cis* photoisomerization should be investigated.

References

(1) Bownds, D. *Nature* **1967**, *216*, 1178.

(2) Childs, R. F.; Shaw, G. S. *J. Am. Chem. Soc.* **1988**, *110*, 3013.

(3) Tabushi, I.; Kuroda, Y.; Shimokawa, K. *J. Am. Chem. Soc.* **1979**, *101*, 4759.